ENHANCED CONCEPTUAL SITE MODEL FOR THE LOWER BASIN COEUR D'ALENE RIVER

Technical Memorandum Addendum D-3—

Processes of Sediment and Lead Transport, Erosion, and Deposition

PREPARED FOR

United States Environmental Protection Agency
Region X
Seattle, Washington

PREPARED BY

ch2m

EPA CONTRACT NO. EP-W-06-021
Task Order 85

ES052009001PDX 382081.TA.09.02.02 02-27-14 ih

AUGUST 2016

Processes of Sediment and Lead Transport, Erosion, and Deposition

Lower Basin of the Coeur d'Alene River (OU3)

PREPARED FOR:	U.S. Environmental Protection Agency, Region 10
PREPARED BY:	CH2M
DATE:	August 26, 2016
EPA CONTRACT NO:	EP-W-06-021
TASK ORDER NO:	85
DCN:	0085-02000

This addendum is a supplement to the series of technical memorandums that make up the Enhanced Conceptual Site Model (ECSM) for the Lower Basin of the Coeur d'Alene River (Lower Basin) (CH2M HILL, 2010a). This and other addendums provide new data, analyses, interpretations, and other information that have become available since publication of the initial ECSM documents in August 2010. The addendums update and expand the ECSM, allowing it to remain current and functional as data collection, analysis, modeling, and other investigations proceed. These addendums are grouped under the specific ECSM technical memorandum topics defined in the original ECSM.

The specific purpose of Addendum D-3 is to provide an update to *Technical Memorandum D – Hydraulics and Sediment Transport.* The addendum covers sediment transport, lead transport, floodplain sedimentation rates and processes, bank erosion rates and processes, and current trends in the transport and storage of sediment and lead in the Lower Basin. This addendum is meant to provide a consolidated resource covering the most important data, analyses, and interpretations relating to sediment and lead transport, storage, and remobilization in the Lower Basin.

Due to the size and complexity of this topic, this addendum deviates from the typical style of a technical memorandum and is reformatted in a report style for greater accessibility.

Table of Contents

Table of Contents ..... **i**

Executive Summary **ES-1**
Primary Findings ES-1
Key Remaining Uncertainties and Data Gaps ES-2

1 Introduction **1-1**

2 Overview and Background **2-1**
2.1 Previous Work 2-1

3 Contaminated Sediment Transport **3-1**
3.1 Data Sources and Methods 3-1
3.2 Suspended Sediment Concentrations and Rating Curves 3-2
3.3 Changes in Rating Curve over Time 3-4
3.4 Other Controls on Bulk Sediment Transport Rates 3-5
3.4.1 Event Hysteresis for Historic Data 3-5
3.4.2 Hysteresis in the April 2013 High-Flow Event 3-6
3.4.3 Seasonal Hysteresis 3-7
3.4.4 Impact of Lake Level 3-9
3.5 Sediment Concentrations by Size Fraction 3-10
3.5.1 Suspended Sand 3-10
3.5.2 Suspended Fines 3-11
3.6 Sediment Fluxes 3-12
3.6.1 Approach 3-12
3.6.2 Flow Records 3-13
3.6.3 Differences from the ECSM Sediment Flux Calculation 3-13
3.6.4 Annual Sediment Fluxes 3-15
3.6.5 Sensitivity Analysis of Annual Sediment Fluxes 3-15
3.6.6 Interpretation of Differences in Annual Sediment Fluxes between Stations 3-20
3.6.7 Frequency, Magnitude, and Duration of Sediment Loads 3-20
3.6.8 Relative Amounts of Sand and Fines in Suspension 3-21
3.6.9 Sediment Flux during Individual Events 3-22
3.6.10 Summary of Sediment Transport Observations 3-24

4 Lead Transport **4-1**
4.1 Data Sources 4-1
4.2 Lead Concentrations 4-2
4.2.1 Differences in Bulk Lead Concentration among Locations 4-3
4.2.2 Relationship between Grain Size and Lead Concentration in Suspended Sediment 4-4
4.3 Lead Fluxes 4-5
4.3.1 Approach to Computing Lead Fluxes 4-5
4.3.2 Annual Bulk Lead Fluxes 4-6
4.3.3 Lead Budget in the Gravel-Bed Reach: Confluence to Cataldo 4-6
4.3.4 Lead Budget in the Sand-Bed Reach: Cataldo to Harrison 4-6
4.3.5 Influence of Flow Magnitude and Frequency on Bulk Lead Transport 4-7
4.3.6 Grain Size and Lead Transport 4-8
4.3.7 Summary of Lead Transport Observations 4-10

5 Sediment and Lead Erosion from the Floodplain 5-1
5.1 Floodplain Surface Erosion 5-1
5.2 Bank Erosion 5-2

6 Sediment and Lead Entering the Floodplain 6-1
6.1 Sedimentation Rates from Floodplain Cores 6-1
6.1.1 Data Sources and Methodology 6-1
6.1.2 Revised Estimate of Sediment and Lead Deposition Based on Floodplain Core Data Originally Compiled by Bookstrom et al. (2004) 6-2
6.2 Floodplain Sedimentation Modeling 6-4
6.2.1 Approach 6-4
6.2.2 Results 6-5
6.2.3 Temporal Patterns in Sediment and Lead Deposition in the Floodplain 6-7
6.2.4 Spatial Patterns in Sediment and Lead Deposition in the Floodplain 6-7

7 Sediment and Lead in Storage in the Lower Basin 7-1
7.1 Floodplain Storage 7-1
7.2 Channel Bed Storage 7-3
7.2.1 Estimation of Sediment and Lead Mass in the RI/FS as Computed by Bookstrom et al. (2001) 7-3
7.2.2 Estimation of Contaminated Sediment Mass and Lead Mass Based on Riverbed Mapping and Coring in 2012 and 2013 7-4
7.3 Sediment and Lead Budgets of the Lower Basin 7-6

8 References 8-1

Executive Summary

Technical Memorandum (TM) Addendum D-3 addresses sediment and lead transport processes in the Lower Basin of the Coeur d'Alene River. It is structured around the sediment budget of the Lower Basin, and considers sediment transport, bank erosion, floodplain sedimentation, and riverbed erosion, as well as developing best estimates of contaminated sediment and lead inventories. The estimated annualized sediment and lead budgets for the Lower Basin are presented in Exhibit 65. The key findings associated with the specific elements of the budgets ('sources' and 'sinks' of sediment and lead) are summarized below in this summary, and extensive discussions, analyses and interpretations of each of the sediment budget components are provided in the main body of the document. The approximate sediment budget values presented in the report are based on limited data and simplifying assumptions which result in significant uncertainties, but the relative amounts and approximate magnitudes are useful for informing managers about the processes that transport, erode, and deposit sediment and lead in the system. Key uncertainties and/or remaining data gaps are also summarized below.

Primary Findings

- The suspended sediment concentration (SSC) at four stations that record sediment transport in the Lower Basin primarily depends on discharge, except at low flows in which little sediment transport occurs. There is an observed discharge threshold of about 3,000 cfs in the Coeur d'Alene River, above which SSC correlates with discharge. Data were sufficient to develop sediment rating curves for bulk SSC, as well as separate rating curves for sand and fines (silt and clay) at stations measuring sediment both into and out of the Lower Basin (Cataldo and Harrison, respectively), as well as on the two main tributaries (North and South Forks of the Coeur d'Alene River). The largest amount of unexplained variability is associated with the fines ratings curve at Harrison (R^2=0.63), indicating more complex supply and transport mechanisms associated with mobilization of fines in the Lower Basin that are not represented by using discharge as the predictor of sediment transport. A subsequent analysis of sediment fluxes at Harrison using a multiple regression rating curve, which also accounts for the influence of lake level, lowered the residuals between predicted and observed sediment transport and reduced the estimated annual sediment transport rate out of the Lower Basin by about 25 percent.
- The sediment balance of the Lower Basin is negative, as measured over a recent 25 year period (1988-2013). That is, there is significantly more sediment transported out of the Lower Basin (at Harrison) than into it (at Cataldo). On average, about 50,000 metric tons [MT]/year[1] moves past Harrison relative to about 30,000 MT/year coming in at Cataldo.
- The lead concentration in suspended sediment (in milligrams [mg] of lead per kilogram [kg] sediment) also increases markedly (>50%) in the downstream direction. This implies that erosion between Cataldo and Harrison is mobilizing more highly contaminated sediment than is currently entering from upstream. With both sediment and lead concentrations increasing in the downstream direction, the lead load (MT/year) increases at a greater rate (in percentage terms) than the concentration of sediment or lead individually.
- A large but poorly constrained amount of sediment enters the floodplain between Cataldo and Harrison. A simple floodplain sedimentation model produced an estimate that about 25,000 MT/year of sediment, on average, entered the floodplain over the 25 year period of record.

[1] The value 50,000 MT/yr as the average annual sediment flux at Harrison is a revised estimate from the original estimate of 67,000 MT/yr reported in section 3.6.4. The revised estimate is based on a multiple regression model that includes as a variable the lake level of Coeur d'Alene Lake as well as discharge. The details of the revised calculation are provided in Attachment C.

- Based on flux differentials at Cataldo and Harrison, and accounting for estimates of sediment loss to the floodplain, an average of at least 40,000 MT/year of sediment is eroded from the Lower Basin.
- Conservatively, bank erosion in the Lower Basin is estimated to account for no more than 5,000 MT/year of sediment, a small percentage of the sediment deficit.
- Net erosion of the riverbed is inferred to be the primary source of the sediment deficit. The total amount of bed erosion, back calculated from the other elements of the sediment budget, and applied evenly across the riverbed, is equivalent to an erosion rate of 0.5 to several cm/year. This direction and general magnitude of riverbed erosion is generally corroborated by the limited data available from long term repeat cross sections in the river (CH2M HILL, 2014c).
- Over the 25 year period of record, an estimated 850,000 MT more sediment left the Lower Basin than entered it, most of this during years with high flows. This sediment deficit consists of similar proportions of fines and sand. The sand deficit may come from either modern (post-mining) deposits, legacy sand deposits, or both. In contrast, the large amount of fines eroding from the riverbed must be primarily sourced from legacy deposits, which contain substantially elevated levels of lead. Thus, a large fraction of the sediment and lead source in the Lower Basin is attributed to the erosion of legacy deposits of fines, which must be exposed at or near the riverbed surface.
- There are both seasonal and event-scale hysteresis patterns, observed at Harrison but not at Cataldo, in the transport of sand and fine fractions of sediment. In the seasonal hysteresis pattern, greater quantities of sand and especially fines are transported during winter compared with spring floods. Although seasonality in sediment supply may play a role in this pattern, the most likely cause of the hysteresis pattern is thought to be the influence of the changing level of Coeur d'Alene Lake and the resulting backwater influence. Winter floods occur when the lake level is substantially lower, leading to steeper river gradients and higher shear stresses that may increase bed erosion of exposed legacy tailings. Backwater effects may also lead to conditions that result in accumulation of fines and lead in the riverbed during summer months.

Key Remaining Uncertainties and Data Gaps

1. Estimates of ***system-wide modern floodplain sedimentation rates*** are poorly constrained. A simple deposition model, based on flood flow estimates to discrete floodplain units, combined with sediment rating curves and trapping efficiencies in the floodplain, yielded deposition estimates 6 to 7 times lower than estimates based on measurements in cores of sediment thickness above to the 1980 Mt. St. Helens ash layer. The uncertainty in this term affects the estimated sediment and lead mass balance, specifically the estimated amount of bed erosion that occurs between Cataldo and Harrison, which is back-calculated from the other elements in the sediment budget. The rate and spatial pattern of long-term channel lowering will be constrained with additional high resolution repeat bathymetric data collected in 2016. Additionally, floodplain sampling is also being planned to improve the empirical database on floodplain deposition rates.
2. The ***total amount of contaminated sediment and lead stored in the channel bed*** is poorly constrained. The composition and structure of sediment in the uppermost 1.5 m of the channel bed is relatively well known from an extensive and coordinated coring effort, to be presented in an upcoming report. However, there is limited information on the total thickness of contaminated sediment in those areas where cores did not encounter native material – including dune fields, planar bed mobile sediment areas, and rough-textured areas of the bed; these areas are where the thickest deposits are believed to reside.
3. There is no clear correlation between bulk lead concentration on sediment and SSC or discharge in the data set available for this study. A weak correlation was seen between the lead

concentration on sediment at Harrison and lake level at Coeur d'Alene Lake. Therefore ***average lead concentrations were used to estimate lead fluxes***. Lead concentrations increase between Cataldo and Harrison, but concentrations at Harrison are highly variable due to differences in the sediment sources in different floods, and this variability increases the uncertainty associated with the estimates of lead erosion. Additional evidence are needed to better understand the relationship between particulate lead, SSC, discharge.

4. The rate and spatial pattern of long-term channel downcutting are poorly constrained because of the absence and relatively low resolution of repeat bathymetric data.

1 Introduction

This addendum is a supplement to the series of technical memorandums that make up the Enhanced Conceptual Site Model (ECSM) for the Lower Basin of the Coeur d'Alene River (Lower Basin) (CH2M HILL, 2010a). This and other addendums provide new data, analyses, interpretations, and other information that have become available since publication of the initial ECSM documents in August 2010. The addendums update and expand the ECSM, allowing it to remain current and functional as data collection, analysis, modeling, and other investigations proceed. These addendums are grouped under the specific ECSM technical memorandum topics defined in the original ECSM.

The specific purpose of Addendum D-3 is to provide an update to *Technical Memorandum D – Hydraulics and Sediment Transport.* Addendum D-3 summarizes data, analyses, and interpretations related to the transport, storage, and remobilization of contaminated sediment and lead in the Lower Basin system. The addendum was prepared for two primary reasons: (1) to improve the understanding of the processes and rates of sediment and lead transport, erosion, and deposition in the Lower Basin system, to support the evolving conceptual site model (CSM) and guide decision- making in the Lower Basin; and (2) to provide data and analyses that will be used in the development and calibration of a 2-D sediment and morphological model, under development at the time of this writing using the software MIKE 21C; this is referred to as the sediment transport model in this report. The addendum includes updated data sets, available modeling results, and interpretations of the nature of sediment and lead dynamics in the system. The addendum is current as of its writing, but data collection and analyses are ongoing, so it is anticipated that certain sections of this addendum need to be further updated as new findings become available in the future.

The addendum covers sediment transport, lead transport, floodplain sedimentation rates and processes, bank erosion rates and processes, and current trends in the transport and storage of sediment and lead in the Lower Basin.

This addendum is meant to provide a consolidated resource covering the most important data, analyses, and interpretations relating to sediment and lead transport, storage, and remobilization in the Lower Basin. Although not typical for a technical memorandum, the following table of contents is intended to simplify locating specific topics within this large addendum:

2 Overview and Background

Large quantities of sediment are stored in the riverbed and floodplain of the Lower Basin of the Coeur d'Alene River, a 20,000 acre low gradient complex of channels, lakes, and marshes in the seasonal backwater area of Coeur d'Alene Lake. Nearly all this active fluvial zone (Exhibit 1) contains elevated concentrations of lead and other heavy metals that pose risks to people and wildlife. Sediment and associated metals (notably lead, a primary source of risk) are continually eroded, transported, and re-deposited in complex patterns across this active fluvial system, mostly during floods. An overall understanding of the processes of sediment and lead transport and storage, and estimates of the absolute and relative rates of these processes, in this system is necessary to inform the evaluation and selection of effective remedial actions, to prevent recontamination, and to develop reliable modeling tools.

A simplified conceptual model of sediment transport, erosion, and deposition processes and storage reservoirs in the Lower Basin has been developed (Exhibit 2). This addendum is organized around the sediment transport and exchange processes depicted in this simplified conceptual model, as follows:

- Section 3 covers in-channel transport of contaminated sediment.
- Section 4 covers transport of lead associated with contaminated sediment.
- Section 5 covers sediment and lead erosion from the floodplain (primarily due to bank collapse).
- Section 6 covers sediment and lead deposition into the floodplain.
- Section 7 uses existing data to estimate the mass of sediment and lead currently stored in the channel bed and floodplain.
- Section 8 summarizes and interprets the annual average sediment and lead "budgets" based on the transport and exchange processes in Sections 3 through 6.

2.1 Previous Work

Initial efforts to inventory the area, volume, and lead content of lead-containing sediments in the Lower Basin were conducted by Bookstrom et al. (2001). Later Bookstrom et al. (2004) built on this work by reanalyzing hundreds of cores from the floodplain, and computing estimates of the rates of sediment and lead accumulation outside the river channel. That analysis was based in part on the core data compiled by Box et al. (2001) and earlier contaminant mapping (Bookstrom et al., 1999).

Other studies used suspended sediment data collected by USGS to compute short- and long-term sediment and metals fluxes through the channel. These studies include reports by Clark and Woods (2001), Box et al. (2005), and Berenbrock and Tranmer (2008). In addition, modeling studies (e.g., Borden and Goodwin, 2001; Borden et al., 2004; Donato, 2006) have included sediment transport calculations for the purpose of trying to better understand the movement of lead through the Lower Basin. These studies are summarized in the Hydraulics and Sediment Transport Technical Memorandum (TM D) of the initial ECSM (CH2M HILL, 2010a). More recently, Clark and Mebane (2014) collected data from 18 streamflow gaging and water quality monitoring sites throughout the Coeur d'Alene and Spokane River basins and used the data to estimate flow-weighted mean concentrations and total annual loads of lead and other constituents (cadmium, zinc, phosphorous and nitrogen) for water years 2009 through 2013. These and other studies and their data are used and cited throughout the text of the current report where they are discussed.

This addendum update is intended to (1) compile all the pre-existing data on sediment and lead transport and storage processes in the Lower Basin, (2) combine them with more recent data and new

analyses that were done to fill the data gaps specified in the ECSM, and (3) provide new interpretations based on the combined data sets and analyses.

3 Contaminated Sediment Transport

Sediment transport, in this context, refers to the movement of particles by hydraulic forces within the main channel. For the Lower Basin, CH2M HILL assumes that sediment fluxes, and particularly fluxes of sediment-bound lead, are dominated by suspended sediment, and for the purpose of this report, assumes that bed load sediment is of secondary importance. Typically, bed load, which moves along the bottom of the river by rolling sliding, or saltating, tends to be less than 10 percent of the total long-term sediment flux in large low-gradient, sand-bed rivers (Dunne and Leopold, 1978). The bed load movement associated with the translation of dune forms during a flood amounts to less than 5 percent of the suspended load, as evidenced by repeat high-resolution bathymetry collected during a flood in 2012 (to be summarized in forthcoming TM Addendum E-6 about riverbed characterization [CH2M HILL, pending publication]). This small contribution is assumed to account for a minor portion of the total load, and its total contribution is small compared with the amount of uncertainty in the suspended sediment transport estimates described in this section. In addition, finer particles, which travel as suspended load, typically contain higher levels of contamination than coarser particles that compose bed load. This operating assumption is confirmed by data from many rivers, including sediments in the Lower Basin (Bookstrom et al., 2004; CH2M HILL, 2010a). Therefore, this addendum focuses on the dominant suspended load, and bed load transport of contaminated sediment is assumed to be small.

The suspended sediment load is typically subdivided into two distinctive parts. There is an important distinction between the *wash load*, which is well-mixed in the flow column and does not generally deposit in the bed; and the *bed material suspended load*, which is carried in suspension but can be deposited in the riverbed. With some exceptions, generally in the Coeur d'Alene River (and in most other non-tidal rivers), the wash load is mostly composed of silt and clay, and the bed material suspended load consists of fine and very fine sand grains. Thus, the distinction between wash load and the bed material suspended load of the river can be approximated by the transport of particles smaller than and larger than 0.0625 millimeter (mm), which separates sand and silt size fractions.

3.1 Data Sources and Methods

Two separate but related suspended sediment sampling programs operate in the Lower Basin: the U.S. Geological Survey (USGS) monitoring program and suspended sediment samples collected by CH2M HILL since 2010. Clark and Mebane (2014) describe the history of USGS gaging in the Upper and Lower Basins, and of the Coeur d'Alene River Basin Environmental Monitoring Plan (BEMP) program. Water quality monitoring by the USGS dates back to 1970 at Enaville (Exhibit 3), but suspended sediment data are sparse before the 1990s. Some samples were collected in the early 1990s, but the bulk of the data have been collected since 2004 with the start of the BEMP program. USGS sampling data are available for download from the National Water Information System (NWIS) database (http://waterdata.usgs.gov/nwis).

In addition to the USGS samples, CH2M HILL has also collected high-flow samples for the U.S. Environmental Protection Agency (EPA), following USGS methods, since Water Year (WY) 2010. This sampling focused primarily on sampling near the peak of flows at specific locations in the Upper and Lower Basins. Suspended sediment sampling at each Lower Basin location was conducted with a crane-operated isokinetic depth-integrated sampler (D-96) following USGS methods for equal discharge or equal increment sampling (Radtke, et al., 1999). Additional information regarding sampling methods and data quality assurance can be found in WY summary reports of the BEMP sediment program (CH2M HILL, 2010b, 2011a, 2011b, 2013a, 2013b, 2015a).

In addition to bulk suspended sediment measurements (milligrams per liter [mg/L]), USGS sediment sampling typically reports the percent, by mass, of the total sediment sample consisting of grains finer than 63 micron (µm) diameter, corresponding to the classification break between silt and sand particles, following the commonly-used phi scale for grain size (Wentworth, 1922). Similarly, when sufficient mass

is available, BEMP samples are sieved and, in addition to the total suspended sediment concentration (SSC), the proportions of sediment smaller than 63 µm (silts and clays), between 63 and 250 µm (very fine and fine sands), and larger than 250 µm (medium sands and larger) are also measured (CH2M, 2012a).

In order to determine the mass of sediment by grain size, sufficient volume of the sample must be obtained to allow accurate sieving of the sample. Of 473 USGS samples, 355 contain information on the percentage of the "fines" fraction (silt and clay). Of 34 CH2M HILL BEMP samples, 27 had sufficient mass to allow determination of the relative amount of fines in the sample mass.

A quality check of the suspended sediment data for the BEMP samples through WY 2012 was conducted for the five stations shown in Exhibit 3 by reviewing laboratory reports and checking the raw laboratory data reports. In this review, 3 of the 27 BEMP grain size subsamples had unresolved laboratory data quality issues; the grain size data for these samples were excluded from use in subsequent analyses (bulk SSC values were not affected). For an additional 7 BEMP samples, laboratory sample mass measurements indicated that the sieving procedure resulted in a loss of more than 10 percent of the sample mass, leading to questionable grain size fractionation data (again, bulk SSC values were not affected). Because these 7 samples do not appear to be outliers, and they did not importantly affect the rating curve parameters, the data from these samples were retained for developing the regressions, as it was determined that they increased the size of the data set without biasing it.

The SSC, grain size, and lead concentrations from both the USGS and CH2M HILL BEMP samples are compiled in Attachment A, and Exhibit 3 is a summary of the hydrologic and sediment data available for these stations.

In addition to the bridge sampling data set, CH2M HILL in 2012 conducted a trial investigation of sediment transport measurements using new technology, known as Laser In-Situ Scattering and Transmissivity (LISST). A LISST device was used on a boat during an overbank flood to try to measure vertical, lateral, and downstream patterns in suspended sediment and grain size from a boat during flood stage. That investigation was considered as a proof of concept of a new technology in the Lower Basin, and not meant to systematically measure sediment for creating a sediment budget. The effort yielded data useful and relevant enough to develop a high-flow boat flood sampling program using LISST, in which similar data will be collected in future high-flow events. At the time of completion of this report, however, subsequent LISST sampling had not been conducted due to the lack of flows that exceeded the threshold to trigger a sampling event. Thus, as the results of the first LISST sampling event are primarily viewed as a validation of the technology, and because new and more extensive and systematic data will be collected in the future, they are not reported in detail here. Instead, the general approach, data, and findings of the 2012 LISST sampling effort are summarized in Attachment B.

3.2 Suspended Sediment Concentrations and Rating Curves

Total (bulk) SSC plotted against instantaneous discharge at the time of sample collection, for the sampling stations in the Lower Basin, is shown in Exhibit 4A. There is a clear correlation between SSC and discharge at higher flows. However, there is a poorer correlation at low discharge rates, and simple power law regression lines fitted to Cataldo and Harrison tend to overestimate SSC at low flows and underestimate them for high flows.[2]

There appears to be a threshold discharge for each site on the Coeur d'Alene River at which suspended sediment transport shifts from a low-flow regime (characterized by low SSC, uncorrelated with

[2] Sediment rating curves are commonly computed using a power law regression equation, which would appear as straight lines on a log-log plot. This regression tends to fit suspended sediment data better than other regression models, and is simple. Alternate regression models were evaluated to see if they improve the quality of the fit to this data set, particularly to the high-flow data, but they did not. As a result the power law regression was used for this sediment budget.

discharge) to a sediment transport regime in which SSC increases as discharge increases. Because of the large number of seasonally-defined samples collected by the USGS during low-load/low-flow periods, much of the data represent periods with little sediment transport. In order to prevent the large amount of data from periods with small amounts of sediment transport from exerting strong leverage on the regression, and thus biasing the overall sediment transport calculation, a threshold discharge was selected for each site, below which no sediment transport is assumed to occur; regressions were computed using only data from above these threshold discharges. Based on visual observation of the data set, experimentation with the calculations, and general knowledge of flow frequency and magnitude at the sites, a threshold discharge of 1,000 cubic feet per second (cfs) was selected for Pinehurst, and 3,000 cfs was selected as the threshold discharge for all other sites. Above these threshold discharges, SSC clearly increases with discharge for all five sites (Exhibit 4B), while below it there is low SSC and no correlation with discharge (Exhibit 4C). The threshold discharge set for Pinehurst (1,000 cfs) is exceeded about 15 percent of the time, and the threshold discharge at Enaville of 3,000 cfs is exceeded about 20 percent of the time, with the threshold discharge of 3,000 cfs exceeded about 25 percent of the time at Cataldo (CH2M HILL, 2010a, Technical Memorandum C—Hydrology, Exhibit 20). The flow record was not long enough to allow a similar exceedance curve at Harrison.

Clark and Mebane (2014) identified the same qualitative threshold in measurements of the concentration of trace metals in water samples. Their filtered and unfiltered water samples are different from the filtered sediment samples in the current analysis. However, they also noted that dissolved and total concentrations of trace metals increased with increasing discharge, but that "at streamflows of about 3,000 ft3/s or less, dissolved and total concentrations of cadmium and zinc in the CDR near Harrison are essentially the same" (Clark and Mebane, 2014). This observation further supports the use of a 3,000 cfs threshold value as a minimum flow for measureable sediment transport.

A box-and-whisker plot illustrating the variability of SSC measurements above and below the threshold discharges at four locations is shown in Exhibit 4D (insufficient data were available to create separate box-and-whisker plots for the Rose Lake station). These plots clearly show that median, maximum, and total variability in SSCs are much smaller during the low-flow regime compared with the high-flow regime—supporting the hypothesis that there is a threshold discharge below which meaningful sediment transport does not occur.

For the Harrison data set, excluding the lower flow samples improves the R^2 regression between total SSC and discharge; but more importantly, this approach qualitatively improves the way in which the regression characterizes the data[3]. By excluding data collected at flows below the threshold discharges, the regression lines at Harrison and at Cataldo diverge as flows increase, predicting higher SSC at Harrison than Cataldo at high flows. In other words, the Harrison regression equation has the largest exponent, indicating that incremental flow increases sediment flux more at the Harrison location than at the other locations. Thus, the data show that, at higher discharges, sediment is being eroded downstream of Cataldo and upstream of Harrison, and that the magnitude of this erosion increases at high flows.

The regression coefficients and exponents used in the sediment transport model are summarized in Exhibit 5. These, along with the discharge hydrographs, are the primary controls on the sediment fluxes computed for the sediment budget. Because of their importance and high level of uncertainty associated with them, a sensitivity analysis was performed to evaluate the sensitivity of the long-term sediment flux estimates to (1) the selected threshold discharge value, (2) the parameters of the power law rating curve, and (3) the form of the sediment rating curve equation. In addition, a separate

[3] The R^2 value for Cataldo gage data does not improve by excluding data points below the threshold, but the regression line does steepen so that it comes closer to passing through the cluster of high-flow data points, which is more important than passing through the center of the data at low flows.

calculation was done to confirm that flows less than the threshold discharge of 3,000 cfs do not carry significant amounts of sediment over the long term. This sensitivity analysis is described in detail in Section 3.6.5.

Although the amount of variability around the regression lines is large, they do not appear to be biased. Biased regressions would be detected as residuals (the difference between the measured and predicted SSC) that are correlated with discharge. Exhibit 6 plots the regression residuals against discharge for all the stations, and shows that there is significant deviation from the predicted values. This simply reflects the large amount of scatter in the data, as is the case for all sediment transport data. No strong correlations are present between the residuals and discharge values. This is demonstrated in Exhibit 6B, in which regressions fitted to the residuals have both low slopes and low R^2, suggesting that while the data scatter is large, there is little evidence for a systematic bias in the power law regression equation that is fit to the data.

3.3 Changes in Rating Curve over Time

Changes in sediment rating curves over time can indicate changes in system dynamics, such as the availability of sediment over time, or changes in the particle size distribution, or changes in hydraulic characteristics of the channel. Using fixed rating curves for suspended sediment, such as those described above, to compute long-term fluxes assumes that the sediment supply has not changed over the time period for which the data were collected. Therefore, the data were evaluated to try to identify whether any long-term changes to the rating curves could be observed in the data. The two purposes of this evaluation are to better understand changes in the system over time, and to test the validity of using fixed rating curves to compute the long-term sediment loads.

SSC data were organized by time interval (1980s, 1990s, 2000 through 2005, and 2006 through 2013) at the Cataldo and Harrison sites (Exhibit 7). All the data points below the threshold discharge value of 3,000 cfs are excluded from these graphs to focus on sediment transport characteristics at high flows. No depth-integrated sediment samples were collected at flows above 10,000 cfs during the 1980s and 1990s, making evaluation of time trends in sediment transport rates difficult. The U.S. Geological Survey collected several samples and reported SSC values from the 1995 and 1996 floods (Box et al., 2005; see p. 11 of that report), but those samples are not comparable to the data in Exhibit 4 because they did not follow the same sampling procedure. The samples shown in Exhibit 4 represent the flow-weighted mean SSC based on depth-integrated sampling across the river; the samples from the 1995 and 1996 floods were grab samples collected at the surface, with a Ziploc® bag, from the shoreline. The USGS samples reported by Box et al. (2005), while useful for characterizing the geochemistry as done in that report, should not be mixed with the USGS and BEMP samples for statistical analyses such as rating curves. Although this analysis is limited by the relatively small amount of high-flow data available from the 1980s and 1990s, there are no obvious indications that rating curves have shifted between the earlier data (red and blue symbols in Exhibit 7) and the more recent data (green and yellow symbols).

A significant change in the rating curves likely occurred following 1968, when direct mine waste discharges into streams in the Upper Basin were stopped. However, no data prior to 1968 are available to document this change. Following this reduction in the upstream sediment supply, it is believed that the river began to erode into deposits in the riverbed that had been laid down during the period of mine waste discharges (CH2M HILL, 2014c). Over time, as these deposits were eroded, it may be expected that the rating curve at the Harrison gaging station may have gradually shifted downwards, implying reducing sediment supply over time, as these legacy sediments were eroded away. In summary, the data in Exhibit 7 do not show evidence of a shift in the rating curve since the 1980s, and the lack of such a signal is attributed to one or both of two factors: (1) there are no high flow data from 1980s and 1990s that would allow the detection of such a change (Exhibit 7); and (2) erosion of legacy deposits might not

have sufficiently depleted the legacy sediment inventory enough to cause a reduction in the sediment load.

3.4 Other Controls on Bulk Sediment Transport Rates

As seen above, SSC at each site depends primarily on discharge, which explains as much as 80 percent of the variability in the SSC data at a station (as shown by R^2 values in Exhibit 5). However, even for a given discharge at a particular station, the sediment concentration may still vary by an order of magnitude (Exhibit 4), depending on a number of secondary conditions and factors. This section investigates some of the factors controlling sediment transport rates other than instantaneous discharge.

While discharge is the primary control on sediment transport rates at a given location, many secondary factors may contribute to scatter in the data set. These include: seasonality, presence or absence of snowpack, intensity of rainfall, the occurrence of prior recent flood events, the shape of the hydrograph, local land disturbances, water level in Coeur d'Alene Lake, and the timing of sediment sampling relative to the hydrograph (i.e., was sample collected during the on rising or falling limb).

3.4.1 Event Hysteresis for Historic Data

In hydrological systems, the term hysteresis functionally describes processes that are dependent on past conditions. For example, SSCs are commonly higher during the rising limb than the falling limb of floods; the early portion of flows may begin to transport easily-mobilized sediment that had been deposited in the falling stages of the previous event, or the first rainfall in a storm may deliver the most mobile sediment to the river in the early stages of the event. Alternatively, sediment may move through a system more slowly than water, so its delivery at a defined point may lag in time, resulting in higher sediment concentrations on the falling limb than the rising limb for the same discharge.

To test for event hysteresis in SSCs, each suspended sediment sample (catalogued in Attachment A) was classified as occurring on the rising, falling, peak, or steady limb of the hydrograph, based on the slope of the hydrograph over 3 days bracketing the sample (day before, day of, and day after the sample). If the absolute value of the hydrograph slope exceeded about 400 cfs per day (a somewhat arbitrary value chosen based on inspection of the data), and was rising both before and after the sample was collected, the sample was classified as a rising limb sample; with the reverse for falling limb samples. If the flow on the day of the sample was greater than both the previous and subsequent days, the sample was classified as a peak flow measurement. If flow changed less than 400 cfs per day throughout the 3-day period, or if flows fluctuated at relatively low discharges, the corresponding sample was considered to be a "steady flow" measurement. Using these as general guidelines, the flow data for the period associated with each sample was examined individually and assigned to one of the four categories.

If hysteresis patterns related to the timing of sampling on the hydrograph are a clear first order effect on sediment concentration, then a grouping of similar symbols in the plot would be expected. For example, the SSC of the rising limb samples would systematically lie above those collected on the falling limb for similar discharge. Total SSC was plotted against discharge for each of five stations (for samples above threshold discharge) (Exhibit 8). No hysteresis grouping of data is apparent at any of the stations. Although the steady flow samples tend to characterize conditions at lower discharges, and the peak flows characterize higher discharges, there does not seem to be a segregation of points along the Y-axis, such that one set tends to have a systematically higher or lower SSC for a given discharge. In general, for a given discharge at a given station, the scatter for the different symbols overlap, rather than segregate. When the suspended sediment data are compiled in this way, it appears that hysteresis due to the time of sampling, relative to the peak of hydrographs, is not a *primary* control on sediment concentration in the Lower Basin. Any patterns related to event hysteresis are lost within the scatter of combining data from a range of events over many years, and the primary control over several decades appears to be the relationship between SSC and instantaneous discharge.

3.4.2 Hysteresis in the April 2013 High-Flow Event

Although no clear patterns of event hysteresis are evident when comparing data from all the samples collected on the rising versus the falling limb of the hydrograph, a different conclusion may emerge when data are considered from just a single high-flow event. During WY 2013, CH2M HILL planned a near-continuous sampling program aimed at identifying temporal patterns of sediment transport within floods (CH2M HILL, 2013c). No significant high-flow events occurred during the winter, and the spring snowmelt in April 2013 yielded only one moderately high-flow event. During the rising, peak, and falling stages of that event, sampling teams were stationed at the Cataldo and Harrison bridge locations, and suspended sediment samples were collected from the center of the bridge at intervals of about 1 to 3 hours over several days (during daylight hours). For each sample, a crane-operated, depth-integrating sampler located at the center of the bridge was repeatedly lowered and raised through the water column at a constant rate until a 5-gallon sample was collected. This volume was considered the minimum required to reliably estimate the SSC, the proportion of silt and sand in the suspended load, and the concentration of lead in the bulk sample, and required lowering and raising the sampler about 20 times over a period of about an hour [4]. The time series of sediment concentration measured this way at the Harrison and Cataldo gages is shown in Exhibit 9, along with the hydrographs at both stations. For comparison, the yellow diamond symbols in the Exhibit 9 graphs indicate the results for the BEMP samples (depth and width-integrated SSC measurements) collected near the flow peak at each of these sites. Gaps occur in the record because of the inability to safely sample at nighttime, limitations of equipment, and limitations of personnel, who were simultaneously conducting BEMP sampling.

Exhibit 9 generally shows a pattern of SSC rising and then falling at both stations, following the shape of the hydrograph. The gap in the data during the peak of flow at the Cataldo gage prevents knowing clearly whether peaks in sediment concentration and flow occurred simultaneously. However, it appears that sediment concentration peaked about a day before the flow peak at the Harrison gage (Exhibit 9B), and that sediment concentration was already declining by the time of the flow peak.

When the suspended sediment data are plotted against discharge at the time of sampling, a clearer "clockwise" pattern of hysteresis is evident, with higher sediment concentration on the rising than the falling limb of the hydrograph (Exhibit 10A). The same pattern of hysteresis is apparent in the sand and fines data as well (Exhibits 10B and 10C). This sort of "clockwise" pattern of hysteresis is the most common pattern of hysteresis seen in rivers (e.g., Leopold, Wolman, and Miller, 1964; Beschta, 1987; and Glysson, 1987), and reflects the phenomenon of more sediment being mobilized during the early part of the flow than the later part of the flow. This pattern is not apparent in the Cataldo data, indicating that changes at Harrison must be dependent on factors within the river between Cataldo and Harrison (both supply and transport capacity) rather than changes in sediment supply from upstream, which includes North Fork, South Fork, and the gravel bed reach upstream of Cataldo.

One explanation for the clockwise hysteresis at Harrison is that it may be attributed to changes in the level of Coeur d'Alene Lake during the course of the 2013 flow event (Exhibit 9C). The lake level was low (2,126 feet) at the beginning of the flood on the rising limb, increased to 2,130 feet at the time of the flow peak at Harrison, and then receded to 2,128 feet and stayed at that elevation during the falling limb. Thus, the base level was at least 2 feet higher during the falling limb of the flood than it was during the rising limb (Exhibit 9C). The lower base level on the rising limb would have contributed to steeper water surface slope, and, therefore, increased transport capacity on the rising limb compared with the falling limb.

[4] These samples were not collected using the standard USGS-based BEMP equal discharge approach of sampling at five different verticals across the section; thus, these center-of-bridge data were not combined with the other BEMP and USGS data to develop rating curves or other analyses in this addendum. Instead, these data are only used to evaluate relative hysteresis and time trends.

Another interpretation of the clockwise hysteresis is that more mobile sediment was available on the bed of the river prior to the arrival of the flood (perhaps deposited by receding waters of an earlier flood, or accumulation of sediment during low-flow periods between floods), and was removed during the earlier part of the flow. The April 2013 high flow was the first and only significant flow event in WY 2013, so it had been nearly a full year since the previous significant flow. Mobile sediment could have accumulated on the riverbed over the year by a variety of processes, including temporary deposition of sediment in scour holes at the end of the last flood, slumping or gradual movement of sediment along steep side slopes adjacent to scour holes, gradual erosion of riverbanks, and other processes.

The hysteresis observed at Harrison during the April 2013 event (Exhibit 10A) can probably be attributed to both causes because the sediment supply and transport capacity are both likely to have been higher during the early part, rather than the later part, of the flood event.

In summary, no hysteresis patterns are apparent when comparing the samples collected on the rising and falling limbs of many floods. However, in at least one recent event, there appears to be a clockwise hysteresis pattern for that particular event. The pattern is observable at Harrison, but not at Cataldo. Therefore, the rate of transport of sediment and lead past Harrison can depend on fluctuations in lake level, on the time between significant flood events, and other factors in the Lower Basin, and not only on the flow rate. These factors likely contribute to much of the scatter shown in Exhibit 4.

Although event hysteresis appears to be factor affecting sediment dynamics in the Lower Basin, it is not accounted for in the sediment budget discussed in following sections of this addendum. Sufficient data are not available to develop an empirical model of event hysteresis patterns for events between 1987 and 2012. Additionally, although event-scale hysteresis is apparent in the Lower Basin (Exhibit 10), the primary controls on sediment fluxes are location and instantaneous discharge. As measured by the R^2 values of the regressions in Exhibit 5 (0.78 for both Cataldo and Harrison), instantaneous discharge explains about 80 percent of the variability in the SSC (Exhibit 5).

3.4.3 Seasonal Hysteresis

Hysteresis due to changes in sediment supply and the transport capacity of rivers can also occur seasonally (for examples, refer to Topping et al., 2000; Hudson, 2003; and Gellis, 2013). In the Coeur d'Alene River, typical types of high flows include those driven by storm-generated rainfall, and those driven by snowmelt or rain-on-snow events. Commonly, rain-driven events occur in the winter and snowmelt events occur in the spring. To examine potential seasonal hysteresis effects, suspended sediment data collected at flows above the threshold discharge (i.e., 3,000 cfs) were organized by the season in which they were collected. "Winter" samples were those collected between November and March, and "spring" samples those between April and June. The data were plotted against discharge at the Cataldo and Harrison stations (Exhibit 11A and 11B).

No clear difference in SSC between samples collected in the winter and the spring at the Cataldo gage, at the upstream end of the Lower Basin, is apparent in Exhibit 11A. At Harrison, however, the data do appear to segregate by season (Exhibit 11B), showing that the bulk SSC for winter samples is substantially higher than for spring samples collected at similar flow rates. The difference between winter and spring sediment concentrations is more pronounced for higher flows (above about 10,000 cfs).

The pattern in seasonal sediment concentration at the Harrison gaging station may be examined further by separately analyzing the different grain size components of the sediment load. Exhibit 11C shows that the pattern of higher SSC in winter events is not as pronounced for sand (particles larger than 63 μm diameter) as it is for bulk SSC. In contrast, the distinction is much stronger for fine-grained sediment (silt and clay particles smaller than 63 μm): Exhibit 11D shows a strong divergence at higher flows, with concentrations of fines increasing exponentially with discharge in the winter, but not in the spring.

Clark and Mebane (2014) also observed that winter and early spring high streamflows in the Coeur d'Alene River transported more sediment and associated trace metals into Coeur d'Alene Lake and could be more important than late spring snowmelt runoff:

> It seems that winter and early spring high streamflows in the CDR could be more important than spring snowmelt runoff in transporting sediment and associated trace metals into Coeur d'Alene Lake. Each year, sediments and associated trace metals accumulated and stored during the previous year are scoured and flushed from the river bottom during early, high-streamflow events of the following year. Snowmelt-runoff periods later in spring do not seem to scour and transport the same quantity of sediment and trace metals to the lake.

Thus, available data show the following seasonal patterns in sediment transport:

- Transport of sediment is generally higher in the winter than spring events at Harrison.
- This pattern is not apparent at Cataldo.
- The pattern is more pronounced for fines than for sand-sized sediment.

The occurrence of seasonal hysteresis at Harrison and not at Cataldo suggests that additional sediment is being mobilized in winter-type events somewhere between the two gages. One or more of the following three factors could contribute to seasonal hysteresis, in which winter events transport more sediment than spring floods:

1. ***Transport capacity hysteresis***: Winter floods may generate higher shear stresses than floods with similar flows during the spring as a result of base level control. During winter months, the level of Coeur d'Alene Lake is lower due to removal of flow controls at the dam, and high flows during the winter and spring commonly raise lake levels. In the spring, the backwater effect of the rising lake level may reduce the shear stress available to mobilize sediment from the bed of the river by reducing the water surface gradient.

2. ***Sediment supply hysteresis:*** Mobile sediment may be deposited on the riverbed and side slopes during low-flow periods between floods (summer and fall), and then be remobilized during the first flood(s) of the wet season (winter). Multiple mechanisms could contribute to making mobile sediment available during the low flow periods, including bank collapse (CH2M HILL, 2013d) and submerged gravity flows from the steeper channel margin side slopes and the steep slopes leading into scour holes (Exhibit 12). Sediment may also accumulate during the spring and summer months in the widespread accumulations of aquatic vegetation that grow seasonally in dense patches along the side slopes and breaks down or is washed out in the first (winter) floods. Deposition of sediment produced by these processes during the low flow period is enhanced by the very low flow velocities throughout the Lower Basin caused by high lake levels from summer through the fall. Sediment supplied by multiple processes during low flows would then available to become mobilized by the first high flows of the year, which deplete this mobile sediment before spring snowmelt occurs.

3. ***Climate-caused hysteresis:*** A third possible cause for seasonal hysteresis is the difference in the type of factors generating winter flood events compared with spring. Winter events are driven by storm rainfall, or rain-on-snow processes, sometimes enhanced by reduced infiltration due to frozen or saturated ground, and tend to generate "flashier" hydrographs and more hillslope erosion. In contrast, spring high flows due to seasonal snowmelt generally create longer and more gradual hydrographs. Since spring floods are generated by atmospheric heating rather than rainfall, runoff events are not accompanied by widespread hillslope erosion that occurs during winter events.

While all three of these processes occur in the Lower Basin, their relative importance in causing the observed seasonal hysteresis pattern is not presently known. Of the three, it is believed that the most important is the lake level effect (as per explanation 1 above). The sediment supply explanation

(explanation 2) is thought to be less important than lake level influence in generating seasonal hysteresis because sediment concentrations and transport rates are low (Exhibit 4C) during low-flow periods when depositional conditions are likely. Flows less than 3,000 cfs contribute an estimated 4.8 percent of the sediment load at both Cataldo and Harrison, assuming an average low-flow SSC based on data at each station (Section 3.2). In addition, according to the sediment budget discussed in Section 8, bank erosion and other low-flow sediment contributions are small compared with the amount of sediment that is eroded during floods. Of the three possible causes of hysteresis, the climate explanation (explanation 3) is judged to be the least important because the hysteresis pattern is seen at Harrison but not Cataldo, indicating that hillside erosion during winter months is not a major factor.

3.4.4 Impact of Lake Level

The elevation of Coeur d'Alene Lake is the base level controlling the water surface slope in the Coeur d'Alene River. Water surface slope directly influences the shear stress, which in turn controls the sediment transport capacity. Lake levels for the sediment samples collected in the Lower Basin ranged from 2,121.78 to 2,133.76 feet above sea level, a difference of nearly 12 feet. As the Coeur d'Alene River is a low-gradient river, fluctuating lake level is expected to exert an influence on sediment transport. While the quantitative implications of this influence may best be addressed with a hydraulic model, the empirical data on sediment transport provide first order observations on this phenomenon.

If a lake-level influence on sediment transport were to exist, the influence would be expected to be greatest at the downstream-most gage (Harrison) - less at Rose Lake and with little or no effect at Cataldo. No lake-level effect would be expected at Pinehurst or Enaville on the North and South Forks, because these stations are well upstream of the lake backwater effect.

The potential effect of lake level was investigated by determining the lake level corresponding to each suspended sediment sample in the database. Lake level data are available for Coeur d'Alene Lake (at Coeur d'Alene) from the USGS NWIS database (http://waterdata.usgs.gov/nwis; station 12415500). The data were grouped into five categories of very low lake level (< 2,125 feet) through very high lake level (> 2,132 feet) for evaluation.

Exhibit 13 compares total, sand, and fines SSCs for low, medium, and high lake levels, at Harrison (Exhibits 13A through C) and at Cataldo (Exhibits 13D through F). The plots indicate that, at both stations, discharge exerts a stronger control on sediment concentration than lake level. Lake level has no apparent influence on SSCs at Cataldo. At Harrison, however, some influence may be evident; generally, in Exhibit 13A, SSC measured during events with low lake levels are greater than those measured at high lake levels.

As noted in Section 3.4.3 above, one explanation for the higher SSC at lower lake levels is that lower lake levels translate to higher shear stresses at the same discharge. Although this effect would be expected more in the sand fraction, Exhibit 13 indicates that fines, rather than sands, are higher at low lake levels, especially at flows above about 10,000 cfs (Exhibits 13B and 13C). At least two possible, potentially complimentary explanations may account for this observation.

This first explanation is that older, fine-grained sediments in the riverbed are being eroded. As flow and shear stress increase during sediment transporting flood events, the surface sand may be mobilized, and the underlying fine-grained layer begins to erode. The higher shear stresses exerted at low lake levels may cause more erosion of the consolidated deposits of fine-grained, highly contaminated sediment that are present in the bed. Once eroded by high shear stresses, these fines would contribute to the fine grained wash load that is measured at the Harrison gage. This hypothesis is supported by the observation (presented in Section 4) that the lead concentration on fines increases in the downstream direction, implying that the fines that enter the flow in the Lower Basin are predominantly coming from older, more highly contaminated deposits. Another line of evidence is the observation (also presented in Section 4) that there is a slight but measurable inverse relationship between the elevation of Coeur

d'Alene Lake and the lead concentration in sediment at Harrison – implying that, as lake level decreases, more of the older, more highly contaminated deposits are being eroded.

The second explanation is that fines are deposited in the Lower Basin during the summer months, when flows are low and lake levels high, and mobilized by the first floods of the following water year, which are winter floods that occur when lake levels are low. Accumulations of fines between high-flow events, possibly due to deposition of the sediment entering from upstream during low flow periods, bank collapse during summer low flows, and subaqueous mass wasting of the steeper parts of the riverbed (Exhibit 12), could account for some of the higher fines transport rates during winter (low lake level) compared with spring (higher lake level) flows.

In summary, there appears to be a noticeable difference between the transport rates of fines at Harrison at low and high lake levels. For a given discharge above about 10,000 cfs, sediment concentrations (especially fines) are greater during floods occurring when the lake level is low. This pattern is apparent at Harrison (leaving the Lower Basin), but not at Cataldo (entering the Lower Basin). Because lake level is lower during winter floods than it is during spring floods, it is difficult to separate the hydraulic impacts from the seasonal sediment supply impacts. The explanation for the differences in winter and spring events may involve multiple mechanisms, some of which (hydraulic impacts) are predictable with the sediment transport model that is currently being developed, and others (sediment supply impacts) that are not possible to represent in the model. As discussed in Section 3.4.3, the downstream increase in lead concentration on sediment suggests that a primary source of the fines mobilized between Cataldo and Harrison is remobilization of legacy fine-grained, highly contaminated deposits.

3.5 Sediment Concentrations by Size Fraction

Sediment of different particle sizes have different characteristics with respect to their sources, transport mechanisms, and chemical characteristics. In general, fine sediment (defined here as silt and clay particles smaller than 63 µm) behave as wash load; they are relatively well mixed in the water column at most flows, are transported in suspension, and do not interact with the riverbed. In contrast, sand-size sediment (larger than 63 µm) tends to concentrate near the bottom of the water column and continuously exchanges with sand on the riverbed.

It is common for finer sediments typically to have higher concentrations of contaminants such as heavy metals due to their higher surface area-to-volume ratio, and natural chemical affinities of clay minerals to sorb contaminants from the water column. In the case of the Coeur d'Alene River, sediment with the highest lead concentrations typically has grain size distributions dominated by silt, not sand or clay (Bookstrom et al., 2004, and CH2M HILL, 2012b—unpublished data to be provided in the forthcoming TM Addendum E-6 about riverbed characterization [CH2M HILL, in review]). This is believed to be due to the fact that the source of contamination is mechanically-reduced ore, and, therefore, the sediment particles contain heavy metals, as opposed to the metals being adsorbed onto the particles as is commonly the case in other rivers. Because of the different behavior and chemical characteristics of fines and sands, this section describes how available data are used to develop separate rating curves for the two size fractions. EPA is currently investigating a limited number of sediment samples from the channel bed to evaluate the relationships between grain size, lead concentration, particle density, and particle settling rate.

3.5.1 Suspended Sand

The data set for suspended sand is summarized in Exhibit 14. Suspended sand concentration (> 63 µm) is plotted against discharge for five sampling sites in the Lower Basin for a period of record extending back to 1986 (Exhibit 14A). As with the bulk SSC data, there is no apparent correlation between suspended sand concentration and discharge at low flows, below the threshold discharge (Exhibit 14C). At higher

flows, sand concentration increases with discharge at all stations (Exhibit 14B). The regression equations for suspended sand follow the same pattern observed with bulk SSC; the regression exponent for suspended sand at Harrison is high compared with the other regressions (Exhibit 5), indicating that the sand concentration increases rapidly with discharge (as sand is mobilized from the bed). At Harrison, the rating curve exponent for sand (3.3) is larger than for bulk SSC (2.6), indicating that as discharge increases, the proportion of sand in suspension increases relative to the proportion of fines. This could reflect that fines are the dominant fraction at lower flows, and/or that more sand than fines is being mobilized as flows increase.

This pattern is not observed at Cataldo, where the regression exponent for sand (1.2) is *less than* that for bulk SSC (1.4), indicating that the proportion of sand in suspension remains nearly steady at all flows above threshold discharge. This difference is explainable by the different availability of mobile sand at the two locations: upstream of the Cataldo gage, the bed material is dominantly gravel, so there is no plentiful source of sand as flow strength increases – thus, sand transport is supply-limited. Between Cataldo and Harrison the bed is dominantly composed of sand, so as discharge increases, sand recruited from bed erosion contributes an increasing proportion of the sediment flux.

An alternative explanation for the increase in the proportion of sand in the suspended load with increasing discharge is that some fines are preferentially lost to the floodplain, especially as flows increase above flood stage. However, losses to the floodplain could only be a partial, secondary explanation for the downstream change in grain size, because the total amount of sediment increases significantly downstream. The primary explanation for the higher proportion of sand downstream, therefore, must be an increase in the availability of sediment from the riverbed.

3.5.2 Suspended Fines

Data representing suspended sediment concentrations of “fine” fractions (< 63 µm) for the five sampling sites in the Lower Basin are shown in Exhibit 15. As with the total SSC and suspended sand concentration plots, there is a clear correlation between flow and fines concentration above the discharge thresholds for each site (Exhibit 15B), but there is no apparent correlation at low flows (Exhibit 15C), supporting the working hypothesis that there is a threshold below which no significant sediment transport occurs.

Regression exponents for the Harrison, Pinehurst, and Enaville locations are all similar (2.1 to 2.2; Exhibit 5) indicating that fine sediment in suspension at these locations increases with discharge at approximately the same rate. This is different from the rating curves for suspended sand and bulk SSC, which both increase more rapidly with discharge at Harrison. The fine fraction regression exponent for Cataldo is less than the other locations (1.5), indicating that the concentration of fines in suspension increases at a lesser rate than the other locations. The explanation for this difference is not obvious, because the Cataldo rating curve should generally combine contributions of sediments measured at Enaville and Pinehurst, only 8 river miles upstream on the two main tributaries.

One possible explanation for why the rating curve exponent for fines would decrease between the confluence and Cataldo, and then increase between Cataldo and Harrison, is loss of fines at high flows to floodplain deposition between the confluence and the Cataldo gage. As the combined flows from the North and South Forks increase, a correspondingly larger amount of flow enters the floodplain between the confluence and Cataldo. Flow entering the floodplain typically contains a higher proportion of fines than sand, because sand tends to be more concentrated within the channel, near the bottom of the water column. Unlike the reach downstream of Cataldo, the riverbed upstream is gravel, and fines lost to the floodplain are not replaced by fines eroded from the bed.

3.6 Sediment Fluxes

Sediment flux refers to the volume or mass of sediment transported past a location in the channel over a fixed amount of time. Suspended sediment flux estimates can be made by multiplying the measured or computed sediment concentration by the flux of water past that point (for example, in tons per hour), and then summing the fluxes of the hydrograph for the period of interest. In this analysis, the time frame of interest is the 25-year period from 1987 through 2012. This is a period for which flow data either existed, or, in the case of the Harrison gage before 2004, could be modeled as explained in Section 3.6.2. This period is inferred to be long enough to provide a general indication of the long-term average sediment fluxes, year-to-year variability in sediment fluxes, and difference in sediment fluxes between different stations.

3.6.1 Approach

Empirically-based calculations of suspended sediment transport in rivers are typically made by first defining a relationship between river discharge and SSC (a "rating curve"), then multiplying the computed sediment concentration by discharge measured at a gaging station, and summing these values over the time period of interest to compute the cumulative sediment flux:

$$Q_{sed} = \sum_{t=0}^{t_{end}} Q \times SSC(Q) \times \Delta t \times a \qquad (1)$$

where Q_{sed} is the sediment flux over the time period of interest (between time t = 0 to t = end); Q is the water discharge in units of volume/time; *SSC(Q)* is the mass concentration of suspended sediment (SSC) computed for the corresponding discharge; Δt is the time interval for which the suspended sediment flux is being estimated (often 1 day, but in this calculation, 1 hour); and a is a constant to account for unit conversions (a conversion factor of 0.00010194 was used to calculate suspended sediment flux in metric tons/hour from a SSC in mg/L, with discharge in cfs). The resulting computed suspended sediment flux is presented in terms of the mass of sediment over the specified time interval (in this case, metric tons of sediment per hour[5]). The annual sediment fluxes at each station were computed by summing the hourly fluxes over each WY (which runs from October 1 to September 30) in the 25-year time period of record between 1987 and 2012. To estimate a sediment budget, suspended sediment and discharge data are required for the upstream and downstream ends of a clearly defined river reach between two stations.

A central part of the calculation and a primary source of uncertainty in a sediment budget is the predicted relationship between sediment concentration and discharge, *SSC(Q)* in Equation 1 above. The relationship between SSC and Q is typically computed using an empirical regression between the flow and sediment concentration for a particular location, referred to as a sediment rating curve (e.g., Leopold, Wolman, and Miller, 1964). To define the rating curve, a sufficient number of suspended sediment samples over a range of flows is required. Overall, SSC increases with discharge because the instantaneous water discharge is a proxy for all the erosion and sediment transport processes occurring in a watershed. As shown in Sections 3.2 through 3.5 above, while there are many controls on sediment transport in the Lower Basin, the primary influences on SSC are the instantaneous water discharge and location within the Lower Basin. Above a threshold discharge of about 3,000 cfs (and 1,000 cfs at Pinehurst on the South Fork), SSC increases with discharge at all stations (Exhibit 4). For a given discharge, SSCs are highest at the downstream station near Harrison, and lower upstream at Cataldo. The magnitude of the difference between the sediment concentration at Cataldo and at Harrison increases as discharge increases, suggesting that high flows result in net erosion of sediment between

[5] Note that for the current addendum (D-3, Processes of Sediment and Lead Transport, Erosion, and Deposition) suspended sediment mass flux is presented in metric tons (1 metric ton = 1,000 kilograms). Fluxes from other reports, if not already reported in metric tons, are converted in this addendum to metric tons for consistency and ease of comparison.

these two points. When data collected below the threshold discharge are excluded, regression equations between SSC and water discharge explain about 70 to 80 percent of the data scatter, as measured by the r^2 values in Exhibit 4B. Superimposed on these first order controls on sediment transport are several secondary factors that also influence sediment transport, including event hysteresis (Section 3.4.2), seasonal hysteresis (Section 3.4.3) and hysteresis due to fluctuating lake level (Section 3.4.4).

These secondary influences exert measureable control on transport rates in the Lower Basin, and understanding them helps inform the conceptual site model. However, for the purposes of computing a long-term sediment budget, accounting for these secondary effects would present computational problems and could overextend the available data set. Therefore, the secondary effects are not accounted for in the sediment flux calculations (in which the fixed rating curves summarized in Exhibit 5 are applied to the historical record of flows at Harrison, Cataldo, Pinehurst, and Enaville) to compute the hourly sediment fluxes over a 25-year period (WYs 1987 to 2012). The impact of the uncertainties related to the sediment rating curve are evaluated in Section 3.6.4, which quantifies the sensitivity of the sediment yield estimates to both the form and parameters of the rating curve.

3.6.2 Flow Records

Where possible, measured flow data were used with the suspended sediment rating curves (Exhibit 5) to compute sediment fluxes. The Enaville, Pinehurst, and Cataldo sites have long periods of record, dating from 1911, 1987, and 1911, respectively (Exhibit 3). The shortest gage record is at Harrison, which began measuring flow using an acoustic Doppler velocity meter (ADVM) in March 2004[6]. At the Harrison gage, both flow and WSE data are available from 2004 to present; water surface elevation (WSE) and discharge measurements are available from 1991 associated with sediment sampling, but a continuous record is not available.

CH2M HILL extended the length of the hydrologic record for Harrison (to allow computation of a longer-term sediment budget) by calculating flow using a calibrated one-dimensional (1D) model for the Lower Basin (CH2M HILL, 2013d) with flow data from the Cataldo, Pinehurst, and Enaville gages, and WSE data for Coeur d'Alene Lake (a USGS lake level gage dates to 1904). The regression analysis and other computations used to extend the Harrison flow record are described in detail in a separate document (CH2M HILL, 2014a). In summary, a multi-variate regression was developed to relate WSE at the downstream boundary of the 1D model at Highway 97 to concurrent and time-lagged measurements of (1) the elevation at the Coeur d'Alene Lake gage and (2) the flow at Cataldo. This regression was then used along with the history of Cataldo flow and Coeur d'Alene Lake level between 1987 to 2004 to predict flow at Harrison, providing a synthetic flow history at the lower boundary of the 1D model (the Highway 97 bridge) for the period 1987 to 2004. Thus, simulated discharges were used to represent the Harrison flow record from 1987 to 2004, and measured discharges were used from 2004 to 2012. The upstream boundary conditions for the model were measured inflows from the North Fork and South Fork of the Coeur d'Alene River.

For all five sampling stations (Enaville, Pinehurst, Cataldo, Rose Lake, and Harrison), the sediment flux was computed on an hourly time step. Annual fluxes were computed by summing the hourly fluxes over each WY, from October 1 (of the previous year) to September 30.

3.6.3 Differences from the ECSM Sediment Flux Calculation

This section documents the differences between the present sediment flux estimates and previous estimates. Previous calculations of sediment flux, documented in the initial ECSM (CH2M HILL, 2010a, in Technical Memorandum D – Hydraulics and Sediment Transport), applied sediment rating curves

[6] A typical rating curve relating discharge to water surface elevation is not possible at Harrison because of the influence of Coeur d'Alene Lake on water surface elevation, so discharge values require direct measurement of water velocity using ADVM. Discharge is computed using an index velocity method (Levesque and Oberg, 2012).

developed by Berenbrock and Tranmer (2008) to the entire period of record for the Pinehurst, Enaville, and Cataldo gages, for the period from 1988 through 2008, as explained below. There are several substantial differences between the current calculation outlined here and the previous one, which lead to different conclusions about the sediment and lead budgets. Differences in the approach are discussed below, and differences in findings are summarized in Section 3.6.8.

1. In the initial (2010) ECSM calculation, flow at the Harrison gage was assumed to be equal to flow at Cataldo, to extend the short gage record at Harrison. This assumption was acknowledged in the ECSM to be problematic, because flows are known to be significantly attenuated between Cataldo and Harrison; however, it was done because at the time there were less than four years of data from the Harrison gage. Since the gage record at Harrison now has additional years of data, and because these additional data have provided a clearer idea of the changes in flow that occur between the two gages, actual discharges measured at the Harrison gage are used to represent flows there from 2005 through 2012. Additionally, as discussed above and detailed in a separate report (CH2M HILL, 2014a) the Harrison flow record was extended for the period 1987 through 2004 using a 1D model to generate a flow record based on water surface elevations from the Harrison gage. Thus, the current sediment flux calculations cover the time period WY 1987 to 2012, and in this calculation the Harrison flow record is based on data collected at Harrison, rather than using the flows at Cataldo.

2. The initial (2010) ECSM calculations did not include a separate sediment rating curve for the Cataldo gage – only for Pinehurst, Enaville, and Harrison (Berenbrock and Tranmer, 2008). The current calculations of sediment fluxes include a data analysis for the mainstem Coeur d'Alene River at Cataldo based on a new rating curve derived from data collected at that sampling station (Exhibit 5). As described above, there is a clear difference between the rating curves at Cataldo and at Harrison that can have important impacts on the results of the sediment and lead budgets.

3. The present calculation makes use of a much larger data set (the data in Attachment A) for computing the rating curves than was previously used. The 2010 ECSM calculations used rating curves presented by Berenbrock and Tranmer (2008), which were computed from regressions on only a subset of the available data - namely, the 1999 to 2000 data set of Clark and Woods (2001), plus new data collected by the USGS between 2000 and 2005. The data used to compute the rating curves in the current analysis (Exhibits 4, 14, and 15) includes all the available USGS sediment data dating as far back as 1980 at Enaville, 1986 at Cataldo, 1989 at Pinehurst, and 1993 at Harrison. In addition, the current analysis includes the more recent BEMP data collected since 2008, which has focused primarily on high-flow measurements during the past 5 years. Thus, the current rating curves include far more high-flow data and are assumed to better represent sediment transport at higher flows, which dominate the long-term sediment budget.

4. The rating curve approach used here, in which all sediment data below the threshold discharge are eliminated, is new. This is an important improvement because the large number of samples collected at low flow exerts a strong leverage on the regression equation, reducing the slope and causing under-prediction of sediment transport rates at higher flows. The current rating curve approach better represents reality, in which sediment transport increases quickly only beyond a threshold discharge level. The regression equations computed in this way pass through the center of the data clouds at high flows, rather than below them.

5. In the current approach separate regression equations were developed for suspended fines, sands, and total SSC. These are used to estimate bulk sediment fluxes at each location as well as fluxes for sand and silt/clay particle fractions. This approach was taken to allow evaluation of the relative amount of lead transport that is associated with fines and sand, because these two size fractions are transported by different mechanisms, may be stored in the system in different locations, and contain different amounts of contamination. However, use of three separate regression equations for each gaging station results in some minor inconsistencies, because estimates for suspended sand

and silt/clay do not necessarily add up to the regression equation estimate for total SSC. The size-specific sediment flux results are used to evaluate relative sediment transport rates and better understand the role of the two different types of sediment in transporting lead, and in the overall system behavior. However, the total sediment flux calculations are derived from the bulk suspended sediment rating curves, rather than from summing the two size fractions. This is because the regressions for bulk SSC are based on more data than the regressions for the two size fractions (and are therefore presumably more representative).

3.6.4 Annual Sediment Fluxes

Annual sediment fluxes were computed for each gaging location for the period of WY 1987 through WY 2012 (Exhibits 16 and 17)[7]. The data show that computed sediment fluxes at Harrison are greater than at Cataldo during all but three of the low-flow years (years when peak flows did not exceed 15,000 cfs). The greater sediment fluxes at Harrison than Cataldo during all but the lowest flow years likely reflects the process of sediment being mobilized in the Lower Basin during high flows, which typically show much higher annual sediment loads in the years they occur. In years when significant high flows do not occur on the mainstem, relatively higher (and flashier) flows may occur in the North Fork or South Fork Coeur d'Alene River, but these might be attenuated downstream, and little sediment is mobilized within the Lower Basin. On average, over the period of record, sediment flux at Harrison is more than twice that at Cataldo (approximately 67,000 metric tons per year [tpy] to 32,000 tpy). This difference amounts to an average annual sediment deficit of about 35,000 metric tons, but the deficit is much greater during years with higher flows (Exhibit 18). The differential between Harrison and Cataldo indicates that in both WY 1996 and WY 1997 a net of about 100,000 metric tons was eroded from the Lower Basin; in 2008, the total was over 200,000 metric tons. This higher net erosion computed for years with longer and higher flood flows is the result of the diverging sediment rating curves for the upstream (Cataldo) and downstream (Harrison) stations (Exhibit 4B), which reflect the greater amount of sediment that is mobilized from the bed as flows increase beyond about 10,000 to 15,000 cfs.

3.6.5 Sensitivity Analysis of Annual Sediment Fluxes

Even in the simplest situations, sediment transport calculations are characterized by a high degree of uncertainty. In most sediment budgets, including this one, the largest source of uncertainty is associated with scatter—of as much as an order of magnitude—in the SSC for a given discharge. This is expected of suspended sediment data from any river—even in the Coeur d'Alene River, for which there is more high quality suspended sediment data than most rivers of similar size, and for which the rating curve for high flows (above 3,000 cfs) at Harrison is significant (R^2 of 0.78 for bulk sediment, R^2 of 0.79 for sand, and R^2 of 0.63 for fines) (Exhibits 4, 14, and 15). Therefore, a sensitivity analysis was performed to characterize the uncertainty of the sediment transport calculations. Another purpose of the sensitivity analysis was to further test the working hypothesis of the conceptual site model that the river is eroding sediment and lead between the Cataldo and Harrison stations.

The primary source of uncertainty associated with estimates of sediment and lead fluxes at each station is the sediment rating curve used to compute the long-term flux (Exhibit 4). As is normally the case, SSC increases with Q because the instantaneous water discharge is a proxy for all the erosion and sediment transport processes occurring in a watershed. The relationship between SSC and *Q* is typically computed using an empirical regression, which usually takes the form of a power law ($SSC = aQ^b$) (e.g., Leopold, Wolman, and Miller, 1964). The rating curves in Exhibit 4 are based on more high quality suspended sediment data, and more data at high flows, than are typically available for most rivers. As a result, the

[7] Since this report was written, revised sediment flux estimates were made for the Harrison gage and the revised results are presented in Attachment C. To begin to account for the influence of lake level fluctuation on sediment transport (see Section 3.4.4), the revised calculation uses a multiple regression model that predicts the SSC from both discharge and lake level, as opposed to a single regression (discharge only). As shown in Attachment C, the revised estimate of the sediment flux at Harrison is about 25 percent lower than the estimates in Exhibits 16 and 17.

R^2 values for the rating curves are generally quite high: 0.78 at both Harrison and Cataldo (Exhibit 4B). Even so, suspended sediment data always contain a large amount of scatter around the rating curve, because sediment transport processes depend on many factors, and a sensitivity analysis of the rating curves is needed to better convey the level of certainty of the conclusions and interpretations of the sediment budget presented in this addendum.

The sensitivity analysis was conducted by changing the rating curves in a variety of ways, then carrying the calculation described above through the 25-year hydrologic record, and computing the long-term average annual sediment flux for each set of assumptions. This approach provides a general sense of the range of estimates of sediment flux for a variety of assumptions about the rating curves. Three separate types of rating curve sensitivity analyses were performed:

1. Sensitivity to definition of the "threshold" discharge (see Section 3.2).
2. Sensitivity to power-law regression exponents.
3. Sensitivity to the choice of the power-law regression model. In this analysis, two different forms of the regression equation—linear regression and a two-variable regression that included both discharge and stage—were used instead of a power law.

These three categories of sensitivity analysis are discussed separately below.

Sensitivity to Varying Threshold Discharge

The USGS data set contains a large number of samples collected at low flows (summer and fall, when dissolved metals data are important), when comparatively little sediment transport occurs. The disproportionately greater number of these low-flow data exerts more leverage on the regression equations than the sparser data collected at high flow, which are more important to the sediment budget. As a result, power-law regressions fit to the entire data set tended to under-predict sediment concentrations at higher flows. To offset this bias, a "threshold discharge" was chosen (Section 3.2), and data below this threshold were excluded from the regression. Data collected at flows less than this discharge were eliminated before performing the rating curve regression, and as a result, the regression lines fit the high-flow data better in a qualitative sense (Exhibit 4). In the calculation described above, a value of 3,000 cfs was chosen as the threshold discharge at Cataldo and Harrison (also at Enaville; the threshold value of 1,000 cfs was chosen for Pinehurst on the smaller South Fork Coeur d'Alene River). A sensitivity analysis was performed to evaluate the importance of the choice of threshold discharge on the rating curves and long-term sediment fluxes.

Separate sediment rating curves were developed assuming threshold discharges of 1,000 cfs, 2,000 cfs, and 5,000 cfs, and the calculations were carried through to the sediment flux estimates (Exhibit 19). The results show that as the threshold discharge increases, so too does the exponent (steepness) of the sediment rating curve for both the Harrison and Cataldo gages. Excluding more low-flow samples from the regression tends to "flatten" the rating curve, increasing the influence of high-flow measurements. Of the four threshold discharges tested (1,000, 2,000, 3,000, and 5,000), the rating curves developed using the 3,000 cfs threshold had the highest R^2 values (0.78 at both Cataldo and Harrison), and increasing or decreasing the threshold tended to reduce the quality of the curve fits.

Varying the threshold discharge had a relatively minor effect on the computed average annual sediment fluxes; they remained between 29,800 and 33,600 metric tons per year at Cataldo, and between 57,800 and 66,700 metric tons per year at Harrison (Exhibit 20). The computed average erosion rate for the Lower Basin (transport at Harrison minus transport at Cataldo) was greatest for the 5,000 cfs discharge threshold and lowest for the 1,000 cfs discharge threshold; however, varying the threshold discharge throughout this range has a relatively small impact (maximum of about 13 percent) on the computed sediment deficit. As shown below, other uncertainties – especially the influence of fluctuating lake level on high flow transport rates (Attachment C) – and the fluxes of sediment to the floodplain (Section 6) –

are much larger sources of uncertainty in the computed sediment budget than the sediment fluxes at flows below the threshold discharge.

A separate calculation examined the impact of ignoring the flows below threshold discharge in the long-term sediment transport calculation. Flows below 3,000 cfs occur about 75 percent of the time at Cataldo (CH2M HILL, 2010); a flow duration curve was not computed for the Harrison gage due to insufficient record length, but the low-flow part of the flow duration curve is probably comparable to Cataldo. In this calculation, the best fit regression for the calculation with a 3,000 cfs threshold was used to compute the SSC in flows above the threshold discharge. For flows below the threshold, an average SSC was used, which was the average of all the SSC measurements collected below threshold discharge (Exhibit 4C); the average was about 2 mg/L at Cataldo and 4 mg/L at Harrison. The calculation showed that the impact on the computed sediment flux of including flows below the threshold discharge is small, changing the long-term and annual fluxes less than 5 percent at both Cataldo and Harrison.

Sensitivity to Power-Law Regression Exponents

The power-law equation ($SSC = aQ^b$) has two parameters, a constant *a* and an exponent *b*, which define the position and slope, respectively, of the rating curve. Of the two parameters in the model, the rating curve exponent *b*, which determines the rate at which sediment concentration increases as discharge increases, has the greatest impact on computed sediment transport rates, especially at high discharges, and therefore this parameter has a dominant effect on the long-term sediment fluxes. Although the original power-law regressions with discharge explain nearly 80 percent of the variation in SSC (i.e., the coefficient of determination, R^2, is 0.78 for both Cataldo and Harrison), there is still a substantial amount of scatter around the regression lines (Exhibit 4B). This scatter reflects differences between events in storm type, lake level, statistical sampling errors, and other factors, and is typical for suspended sediment field data.

To evaluate the effects of the uncertainty of the rating curve exponent *b* on the long-term sediment budget, the SSC was fixed at the threshold discharge, and reasonable “upper-bound” and “lower-bound” exponents were chosen for the Cataldo and Harrison stations (Exhibit 21). The upper-bound exponent was chosen for each gage so that the rating curve passed through or above the few high-discharge samples in the data set; and the lower-bound exponents passed below nearly all the data points for samples collected at moderate and larger flows (10,000 cfs) (the data and bounding curves are shown on both logarithmic and linear scale graphs in Exhibit 21). Any regression model that passes above all the data points would, in effect, assume that every flood event was an intense winter rainstorm occurring during periods of low lake level—the conditions associated with the samples having the highest SSC, as discussed in the previous sections. Meanwhile, the lower-bound regression model would essentially require that all the sediment-generating flows are associated with conditions that minimize the amount of sediment movement.

For the purpose of this analysis, the maximum SSC for the upper-bound rating curve at Harrison was limited to 1,000 mg/L. If such a limit was not imposed on the calculation, it would estimate unreasonably high SSC at high discharges—for example, at flows of 35,000 cfs, the equation would predict sediment concentrations approximately an order of magnitude higher than any that have actually been measured. The limiting value of 1,000 mg/L is believed to be a conservative upper limit to sediment concentrations that occurred during the 25-year sediment budget period. This value is roughly 50 percent higher than the two highest measured SSC values at Harrison (611 and 658 mg/L), which were both collected on January 18, 2011, by the USGS and CH2M HILL, respectively, at flows of approximately 20,000 cfs. Those SSC values were unusually high (the next highest measured SSC was 368 mg/L), and both were measured at Harrison during an overbank flow at a time when the lake level was low; therefore, the erosive energy of that flow was about as high as can be expected to occur under present conditions. (Sediment concentrations may have exceeded this value during the period of

heaviest mine tailings discharges, but the period being evaluated in the present calculation is WY 1987 through WY 2012, well after cessation of direct discharge of mine waste in 1968.)

Even with this imposed upper limit on SSC, the upper-bound regression exponent overestimates sediment transport rates at Harrison because it assumes that SSC is 1,000 milligrams per kilogram (mg/kg) at all flows above 22,000 cfs. This is likely an unreasonably high value, because 1,000 mg/L significantly exceeds even the unusually high measurements made in January 2011 when flow was overbank and lake levels were unusually low. More typically at high flows at Harrison, sediment concentrations likely remain less than 500 mg/L. Nevertheless, this set of assumptions would clearly provide an upper bound on long-term sediment fluxes.

The results of the sensitivity analysis of the rating curve exponents show that the predicted annual average sediment flux at Cataldo would vary from 19,800 metric tons per year for the "low-bound" rating curve to 53,500 metric tons per year for the upper bound. These values bracket the best-fit regression estimate of 32,400 metric tons per year (Exhibit 22). At Harrison, the range is from 33,200 to 142,700 metric tons per year, compared with the original best-fit estimate of 66,700 metric tons per year. The estimated sediment deficit (difference between Harrison and Cataldo) would be 13,400 metric tons per year for the lower-bound equations and 89,200 metric tons per year for the upper-bound values.

The difference between the upper and lower bounds at Cataldo is a factor of 2.7, well within the maximum range of uncertainty for typical sediment transport models (e.g., Gomez and Church, 1989). The upper-bound sediment flux estimate at Harrison is 4.3 times the lower-bound estimate. However, using the upper-bound rating curve exponent at Harrison is unreasonably high, for the reasons explained above. Based on this, the most likely sediment flux at Harrison is probably closer to the lower bound (33,000 tons per year) than the upper bound (144,000 tons per year). Thus, the annual flux is likely to be reasonably close to the value computed using the best-fit power-law regression.

This analysis supports the overall conclusion that the fluxes at Harrison are higher than at Cataldo. The sediment flux ratio computed for Harrison relative to Cataldo is 1.7 times using the lower-bound exponent, 2.1 using the best-fit exponent, and 2.7 using the upper-bound values. The best-fit estimate at Harrison (67,000 metric tons per year) is higher than the upper-bounding sediment flux estimate at Cataldo (53,000 metric tons per year). Although the upper-bound estimate at Cataldo is higher than the lower-bound estimate at Harrison (33,000 metric tons per year), it is extremely unlikely that both these values are close to the actual average sediment fluxes over the 25-year period.

Sensitivity to Varying Regression Models

Sediment rating curves are commonly developed using empirically-fit power-law ($SSC = aQ^b$) regressions because of their simplicity and statistical goodness-of-fit to paired measurements of SSC and Q. However, there is no theoretical reason, based on physical processes, that sediment rating curves need to follow a power-law regression. To assess the consequences of choosing a power-law model to estimate sediment transport rates, a linear regression model was used to estimate SSC instead of a power law:

$$SSC(Q) = aQ + b \qquad (2)$$

A linear regression model was considered for this comparison because it is the simplest form of a regression model.

The linear regression model had lower R^2 values than the power-law regression model (0.76 and 0.54 at Cataldo and Harrison, respectively). At Cataldo, the linear model and power-law model produce similar predictions over the range of discharges recorded at that gage (Exhibit 23) because the exponent in the

power-law model is fairly close to 1 (1.4). By contrast, at Harrison, the power-law exponent *b* was much higher than 1 (2.6), and, thus, the linear and power-law models diverge at higher flows, with the linear model predicting much lower sediment concentrations than the power-law model. For the Harrison gage data, the coefficient of determination, R^2, is lower for the linear model (0.54) than for the power-law model (0.78). At Cataldo, the average annual sediment flux computed using the linear model (37,000 metric tons per year) is about 15 percent higher than the flux computed with the power-law model. At Harrison, the linear model predicts a transport rate of 97,000 metric tons per year, about 50 percent higher than using the power-law model. This appears to be primarily due to the linear model: While it predicts lower SSC than the power-law model at flood flows above 20,000 cfs, it predicts higher SSC during more frequent moderate flows between about 5,000 and 20,000 cfs (Exhibit 23C).

An exponential regression also fit the data well statistically, but was not considered because it produced unreasonably high estimates of SSC at high discharges: in excess of 5,000 mg/L when the flow is 30,000 cfs at Harrison; nearly an order of magnitude greater than any measured SSC.

Conclusions of Sensitivity Analysis

The sensitivity analysis was conducted by comparing the average annual sediment fluxes from the original power-law rating curve calculations with values derived by using different threshold discharges, bounding values for the power-law exponent, and with a linear regression model (Exhibit 24). Based on these comparisons, the following observations can be made:

- Varying the threshold discharge before performing the regressions has a relatively small impact on the computed sediment yields over 25 years.
- Using the lower and upper bounds for power-law regression exponents makes a significant difference to the sediment yields. In particular, using an upper bounding value for the regression exponent at Harrison leads to unreasonably high predictions of SSC at high flows. Even if the SSC is capped at a maximum value of 1,000 mg/kg, as was done for the calculation shown here, the computed sediment fluxes at Harrison (143,000 metric tons per year), and the predicted erosion rates based on this estimate appear to be unreasonably high.
- Using a linear regression rather than a power-law regression results in a small difference (+15 percent) to the sediment yields at Cataldo, and a moderate difference (+50 percent) at Harrison. The sediment fluxes for the linear model are higher because the model overpredicts SSC for moderate flows between 5,000 and 20,000 cfs.
- For all reasonable scenarios, the computed sediment transport rate at Harrison is greater than at Cataldo, implying that erosion is occurring between the two stations.
- Although the amount of erosion or deposition in the riverbed is expected to vary widely in time and space, for all reasonable scenarios, the magnitude of erosion between the two gages equates to a spatially averaged rate between a half centimeter and several centimeters per year.

In summary, the predicted sediment fluxes are sensitive to the assumptions made in creating the sediment rating curves, but not unusually or unexpectedly so. The sensitivity analysis shows that changing the form of the rating curves would produce differences in the computed annual sediment fluxes on the order of less than 50 percent, and would not produce order-of-magnitude differences in the sediment fluxes, which is sometimes the case in sediment transport studies. This sensitivity analysis strengthens the primary conclusion of the analysis that transport rates are significantly higher at Harrison than at Cataldo, meaning that the reach between these points is eroding at a rate on the order of tens of thousands of metric tons per year.

3.6.6 Interpretation of Differences in Annual Sediment Fluxes between Stations

While it is clear from these calculations that the divergence in the sediment rating curves at higher flows leads to *net* erosion (sediment deficit) during wetter years (Exhibit 16), it is important to note that the amount of sediment eroded from the bed cannot be calculated simply from the difference in sediment flux between Cataldo and Harrison. This is because other sources and sinks of sediment also exist between the two gaging stations. To estimate the amount of riverbed erosion, estimates of these other sources and sinks - especially the amount of sediment eroded from and deposited in the floodplain - are needed. These estimates - and specifically floodplain estimates - have been quantified using field data and modeling described later in this addendum (Sections 5 and 6). However, evaluation of the annual sediment balances between stations provides some additional understanding of the importance of bed and floodplain exchanges in this system, as described below.

Exhibit 18 plots the annual net sediment storage in the system, computed at the gaging stations, against the annual peak flow at Harrison, providing an imperfect but simple proxy for the size of floods in a given year in the Coeur d'Alene River. This evaluation examines the differences in sediment fluxes between Lower Basin stations to determine how much sediment is gained or lost by reach. The comparison in Exhibit 18 shows a difference between the Cataldo Reach—the first 8 miles below the confluence of the North and South Forks—and the flatter 29-mile-long Lower Basin segment, between Cataldo and Harrison. As flows increase, the magnitude of the net sediment storage between the gages increases in both reaches, but in opposite directions (positive above Cataldo, negative below). For example, in 1996, there was a net loss (deposition) of about 100,000 metric tons of sediment between the confluence and Cataldo, but a net gain (erosion) of about the same amount between Cataldo and Harrison. The prediction of a large amount of floodplain deposition above Cataldo is consistent with the extensive and damaging overbank flooding and sedimentation that was observed there during the 1996 flood (Box et. al, 2005). During years when flows did not exceed about 15,000 cfs at Harrison, there is relatively little net erosion or deposition. However, during years when flows exceeded this level, net erosion (negative deposition) below Cataldo increases markedly with flow, while net deposition increases above Cataldo.

The pattern shown in Exhibit 18 appears to reflect a difference in sediment and lead dynamics in these two reaches, generally above and below the grade break at Cataldo. In the gravel-bed reach between the confluence and Cataldo, positive net storage suggests that sediment is lost to the floodplain during periods of high flow. In contrast, although floodplain deposition is assumed to occur during high-flow years in the reach between Cataldo and Harrison, the overall trend is net *erosion*, presumably because floodplain deposition is less than the erosion of sediment from the sand-dominated riverbed. The reach between the confluence and Cataldo is gravel-bedded, so there is little opportunity for additional mobilization of this bed material to offset sediment entering the floodplain.

3.6.7 Frequency, Magnitude, and Duration of Sediment Loads

Although higher flows move more sediment than lower flows, they also occur less frequently. It is common in studies such as this to try to identify an "effective discharge"- that is, the range of flows that, over the long term, transport the greatest amount of sediment when both frequency of flows and magnitude of sediment transport are considered (e.g., Wolman and Miller, 1960; Nash, 1994). Developing a better understanding of the most representative effective discharge with regard to sediment and lead transport can help provide a context for managing contaminated sediment.

The importance of frequency and magnitude of flooding on sediment discharges was evaluated by first grouping hourly flow data from each of the four stations (Pinehurst, Enaville, Cataldo, and Harrison) over the 25-year period of record (1987 to 2012). The data were grouped into "bins" as follows: flows below the 3,000 cfs threshold discharge; flows between 3,000 and 5,000 cfs; a separate bin for each 5,000 cfs interval from 5,000 cfs to 30,000 cfs; and a bin for flows greater than 30,000 cfs. Sediment

transported by flows within each bin was summed to compute the total amount of sediment transported for each range of flows, thereby incorporating both the magnitude and the frequency of sediment transport for flows in each flow "bin" (Exhibit 25). The number of equivalent days of flow within each bin (computed by dividing the number of hours of flow in the bin by 24), is also shown in Exhibit 25.

Flood stage flow at Cataldo is approximately 20,000 cfs. Floods of this magnitude, which are accompanied by overbank flooding, occur on average about every 2 years. While flows of this magnitude or greater represent only about 0.5 percent of the period of record, they transport about 30 percent of the sediment at Cataldo (and about 20 percent at Harrison); these relatively infrequent events thus contribute a disproportionately large amount of the total sediment flux. Flows below 20,000 cfs but associated with the rising and falling limbs of floods represent an even larger portion of each flood hydrograph than the peak periods, and convey a larger portion of the sediment load than flows above the 20,000 cfs flood threshold. At Harrison, because of flow attenuation in the Lower Basin, peak flows over 20,000 cfs are less common, and so a greater proportion of total flux occurs in flows less than 20,000 cfs. Over the 25-year period of record on the Coeur d'Alene River, flows in the 5,000 – 20,000 cfs range account for approximately 78 percent, or 1.3 million metric tons, of sediment passing Harrison, and about 62 percent, or 510,000 metric tons, of the sediment flux at Cataldo.

The recurrence intervals of flows responsible for varying levels of sediment transport were further evaluated by creating a set of frequency/magnitude/duration curves, analogous to curves typically developed for assessing flow duration and frequency (Exhibit 26). The analysis was performed using the Hydrologic Engineering Center's HEC-SSP software (version 2.0) (USACE, 2010), a statistical software package that is based on Bulletin 17B, "Guidelines for Determining Flood Flow Frequency" (Interagency Advisory Committee on Water Data, 1982). However, instead of evaluating flood flows, the time series of sediment fluxes (derived from combining the flow and sediment rating curves) was input to the software package. The resulting plots (Exhibit 26) convey the magnitudes of sediment transport for different recurrence intervals.

These curves allow direct comparison of sediment fluxes during different types of floods at different locations. They show that although fluxes at Harrison may be similar to Enaville and Cataldo for short periods (Exhibit 26A), there is increasing separation between the fluxes over longer periods, with fluxes at Harrison exceeding all locations for 3 days or longer. Exhibit 26 further demonstrates that sediment fluxes at Cataldo and Harrison diverge at higher recurrence intervals, indicating that large floods account for most of the sediment erosion in the Lower Basin.

3.6.8 Relative Amounts of Sand and Fines in Suspension

Suspended sediment includes *wash load* (for practical purposes in this river, silt and clay particles smaller than 63 μm diameter) and *bed material suspended load* (very fine through medium sand between 63 and 500 μm). The sand particles of the bed material suspended load can settle more readily, and can be re-deposited in the bed, whereas the smaller wash load particles tend to stay in suspension once mobilized because the settling velocity of silt and clay is too slow to allow significant quantities to settle against upward mixing of a flowing water column in the channel. The silt and clay fraction may deposit in the floodplain, or interact with the bed in localized areas where eddies or still water occurs, but does so to a lesser extent than heavier sand particles. Additionally, it may be possible for fines to settle out in certain times of the year when a combination of low discharges and high lake level creates nearly still water conditions throughout much of the Lower Basin, such as during the summer and fall period. However, under current conditions very little sediment is present in the flow at those times; as estimated in Section 3.6.5, flows below the threshold discharge of 3,000 cfs carry less than 5 percent of the long term sediment load. Wash load can, however, deposit in the shallow and slow flow areas on the floodplain.

The total sediment flux for the Coeur d'Alene River was computed using the bulk sediment rating curves for each station and the discharge record of the gages (Exhibit 4). Similarly, the flux of sand (bed material load) and fine (wash load) fractions were also computed using the rating curve regressions for the corresponding grain size fractions (Exhibits 14 and 15). Because the different components were computed with different regression equations, the fluxes of sand and fines do not sum exactly to the total sediment flux, but are close enough to compare the relative proportions in the sediment load.

The computed total sediment flux and fluxes for the two size fractions were computed for the primary gaging stations (Exhibit 27). Fines are the dominant fraction at Pinehurst and Enaville (the two major tributaries), and at Cataldo at the upstream portion of the Lower Basin). At Harrison, which represents the downstream boundary of the Lower Basin, the relative proportions of fines and sand fluctuate from year to year, with a higher proportion of sand being moved during years with higher flow.

The relative proportion of sand in the suspended sediment load (including both wash load and suspended bed material load) is summarized in Exhibit 28. Most of the sediment flux is dominated by fines at Enaville, Pinehurst, and Cataldo, with the sand proportion of the sediment flux relatively constant at about 20 to 30 percent. In contrast, the proportion of sand in suspension at Harrison varies greatly, ranging from 13 percent in 1992 to 50 percent in 1996, and corresponds closely with the peak flow. This is likely an indication of higher rates of sand mobilization at higher flow rates in the Lower Basin. The transport of fine-grained sediment also increases in wet years, but not as much as sand. Thus, while both fines and sand are mobilized at high flows in the Lower Basin, more sand is mobilized than fines as flows increase. In higher flow years, sand accounts for about half of the sediment flux at Harrison.

The cumulative amount and relative proportions of sand and fines in the Lower Basin "sediment deficit" (that is, the net amount of material mobilized between Cataldo and Harrison) is summarized in Exhibit 29. The approach described above yields an estimate of about 850,000 tons more sediment leaving the Lower Basin than entering it between 1987 and 2012. Although fines comprise about two-thirds to three-fourths of the sediment *flux* at upstream stations during most years (Exhibit 28), fines account for just under half of the sediment *deficit* in the Lower Basin (Exhibit 29). This is almost certainly attributable to a net erosion of sand from the riverbed between Cataldo and Harrison. However, the fact that nearly 400,000 metric tons of fines were also mobilized in this period (Exhibit 29), combined with the understanding (detailed in Section 5.2 below) that bank erosion is a comparatively slow process, together imply that a substantial quantity of erodible, wash load-sized sediment is also present in the riverbed. Since, under current conditions, the interpretation is that wash load evidently does not deposit in significant quantities in the bed once it is mobilized, it is apparent that it must be present as erodible legacy deposits in the bed.

3.6.9 Sediment Flux during Individual Events

Suspended sediment transport at the scale of *individual flood events* in the Lower Basin was investigated by reviewing four discrete events during the 25-year period of record. Exhibit 30 shows the measured hydrographs and the associated "sedigraphs" computed from the rating curves for each of the stations. All the events involved overbank flow and transported significant amounts of sediment, but each had distinctly different hydrographs as follows:

- High peak flow event
- Long-duration spring snowmelt event
- Large (but more typical) shorter-duration winter flood event
- Larger, shorter-duration spring flood

For comparing the sizes of the events, all four panels in Exhibit 30 have the same vertical and horizontal scales. Details of these events are provided as follows:

1. The event with the highest peak flow for the 25-year period of record was in February 1996 (Exhibit 30A), with peak flows at Cataldo estimated at 70,000 cfs (at the USGS gage) and 34,000 cfs at Harrison (by the modeling approach described above). This was a major flood as measured by peak flow, but was relatively short-lived. Nevertheless, the lake level of Coeur d'Alene Lake quickly rose 10 feet in 4 days, from 2,125 at the beginning of the event to 2,135 feet following the flow peak at Harrison. As shown by the difference in peak flows at Cataldo and Harrison, the hydrograph was greatly attenuated in the Lower Basin.
2. The longest sustained runoff event in the period of record was a spring snowmelt flow in May 2008 (Exhibit 30B), in which flows remained high for several weeks. Lake level was relatively high (2,129 feet) at the beginning of the event (May 15), and rose relatively slowly to 2,133 feet over the course of a week. Flows were only slightly attenuated between the Cataldo gage (peak flow of 32,000 cfs) and the Harrison gage (29,000 cfs) in this event.
3. A "peaky" winter storm event occurred in January 2011, in which flows were significantly attenuated by the floodplain between Cataldo (33,000 cfs) and Harrison (19,000 cfs) (Exhibit 30C). Lake level at the beginning of the event was low (2,125 feet) and rose to 2,131 feet in two days.
4. A large but not extreme spring flood in April 2002; this event was relatively short-lived for a spring event, and was characterized by a moderate amount of flood attenuation between Cataldo (38,000 cfs) and Harrison (26,300 cfs) (Exhibit 30D). Lake levels during this event were similar to those of the 2008 snowmelt event, with relatively high (2,129 feet) lake levels at the beginning of the event, rising to about 2,133 feet at the time of the flow peak at Harrison.

Hourly estimates of total suspended sediment transport, suspended sand transport, and suspended fine sediment transport ("sedigraphs") were computed for each gaging station for each flood event. Exhibit 30 shows the measured hydrographs and computed bulk sedigraphs for the Enaville, Pinehurst, Cataldo, and Harrison gages for the four events. For comparison, the exhibit also shows the instantaneous suspended sediment flux estimated from measured sediment concentrations at the Cataldo and Harrison gages during the 2008 and 2011 events.

Additional discussion of the characteristics of these events follows.

1996 Event: Water discharge (based on gage data) and computed sediment fluxes (computed using rating curves) during the February 1996 major flood event are shown in Exhibit 30A. The 1996 flood produced the highest peak flows in the 25-year period between 1988 and 2012, and the second highest peak flows ever recorded at Cataldo (the historic peak was in 1974). The 1996 event resulted from heavy snowfall over saturated and partially frozen ground, followed by warm subtropical wind and rain that melted the snowpack and caused flooding throughout the Pacific Northwest region. This sequence of events caused a rapid rise in river levels at Cataldo beginning on February 7 and peaking on February 9, followed by a relatively quick falling limb, and flows receded to below 20,000 cfs at Cataldo by February 11. As a result of the relatively low flows preceding the flood, the level of Coeur d'Alene Lake was low before the flood and quickly rose 10 feet in 4 days, from 2,125 at the beginning of the event to 2,135 feet following the flow peak at Harrison. The high flows and low lake levels during the rising limb of the hydrograph resulted in widespread flooding, but the short peak allowed substantial attenuation of the hydrograph between Cataldo (peak flow about 70,000 cfs), and Harrison (about 34,000 cfs, estimated by hydraulic model results) (Exhibit 30A). The calculated sediment flux decreased between the confluence and Cataldo, from about 162,000 metric tons to about 61,000 metric tons, with much of the difference assumed to be deposited on the floodplain in the gravel-bed reach, consistent with the reports of floodplain sedimentation there (Box et al. 2005) (though some of the difference may be due to measurement and calculation errors). In contrast, the estimated sediment flux between Cataldo and Harrison *increased* by a factor of about 2, presumably from recruitment of sediment from the sandy riverbed below Cataldo (Exhibit 30A).

2008 Event: In contrast to the rapid rise and fall of the 1996 event, the sustained spring flood in May 2008 showed a very different profile; although peak flows were much lower at Cataldo in 2008 compared with 1996 (about 32,000 cfs versus 70,000 cfs), peak flows at Harrison were nearly the same (29,000 cfs in 2008 compared with 32,000 cfs in 1996) (Exhibit 30B). Additionally, flows exceeded 20,000 cfs for more than a week at both Cataldo and Harrison. These sustained flows allowed the floodplain lakes and marshes to fill, greatly reducing the ability of the floodplain to attenuate flood flow later in the event. The amount of sediment transported past Harrison during the May 2008 event is estimated to have been more than 260,000 metric tons (including 220,000 metric tons in a two week period); this is about four times the average *annual* sediment load at that station, and more sediment than was transported in any other full year in the 25-year period of record. Significantly, the sediment flux increased by a factor of about 5 between Cataldo and Harrison, indicating extensive net erosion in the Lower Basin. Overall, although the quantity of sediment entering the Lower Basin at Cataldo was lower in 2008 than 1996 (42,000 metric tons to 61,000 metric tons), the 2008 event transported almost twice as much sediment at Harrison than the 1996 event, despite having a lower peak flow.

Other Events: While the 1996 and 2008 events represent the two most significant floods in the 25-year period, Exhibits 30C and 30D illustrate examples of water and sediment fluxes in more typical winter and spring flood events, respectively. In general, these events (January 2011 and April 2002) show patterns similar to the larger events of 1996 and 2008.

The January (winter) 2011 event had a flow peak close to 33,000 cfs at Cataldo, but the flood lasted only about two to three days, and was greatly attenuated at Harrison (with peak flow below 20,000 cfs). Sediment flux increased by a factor of about two between the two stations: from 16,000 to 35,000 metric tons (Exhibit 30). In contrast, the April (spring) 2002 event (Exhibit 30D) peaked at close to 38,000 cfs at Cataldo, and the flood was less strongly attenuated; peak flow at Harrison was about 26,500 cfs. Sediment loads for the April 2002 event were somewhat higher at Cataldo than the 2011 event (23,000 metric tons compared with 16,000 tons for the January 2011 event - a 44 percent increase), but significantly greater at Harrison (59,000 metric tons compared with 35,000 metric tons, a 69 percent increase). Thus, flood events associated with longer duration flows and less attenuation, typical of spring events, may be able recruit and transport more sediment.

The comparison between the hydrographs and sedigraphs in the 1996 (winter storm), 2002 (snowmelt), 2008 (snowmelt) and 2011 (winter storm) flood events demonstrates important differences in the sediment dynamics between the two types of events. During shorter duration floods generated by winter storms - which commonly begin when lake level is low – more water, sediment, and lead are delivered to the floodplain, and downstream flow is greatly attenuated. In contrast, spring snowmelt events, which are characterized by sustained high flows at high lake levels, are not attenuated between Cataldo and Harrison. Because of the lack of downstream attenuation and longer duration of high flows, snowmelt floods have the potential to mobilize greater quantities of contaminated sediment from the riverbed.

3.6.10 Summary of Sediment Transport Observations

Observations about Sediment Transport Characteristics

- Significant sediment transport appears to occur at all stations only above a threshold discharge. This threshold is about 3,000 cfs in the North Fork (Enaville gage) and in the Lower Coeur d'Alene River (Cataldo and Harrison), and about 1,000 cfs in the South Fork of the Coeur d'Alene River (Pinehurst). Below these thresholds, SSCs are very low and not correlated with flow rates; above these thresholds, sediment concentrations increase with discharge.

- Sediment concentrations increase at different rates with discharge above the threshold discharges. Differences in the station-specific sediment concentration rating curves reflect differing availability of sediment and different potential for sediment storage in the floodplain.
- The much steeper slope of the rating curve for suspended sand at Harrison compared with the other stations implies significant bed erosion between Cataldo and Harrison at higher flows.
- No trends in sediment transport over the last several decades are evident based on changes in rating curves over time between the 1980s and 2012. However, this may be due to limited data availability from the earlier part of the record.
- The evidence for hysteresis throughout flood events – referring to sediment concentration varying systematically over time independent of instantaneous flow – is ambiguous. No obvious differences in rating curves are apparent when decades of SSC measurements are segregated by rising, falling, and peak portions of flood hydrographs. However, evidence for a hysteresis pattern at Harrison was observed in a single, moderately high-flow event in April 2013, in which sediment concentrations were higher in the earlier portion of the flow event than in the later portion of the event. The hysteresis pattern was particularly clear for sand-sized sediment. This hysteresis pattern was not observed at the Cataldo gaging station during the same event.
- The data also show some evidence for a seasonal hysteresis pattern at the Harrison gaging station, in which sediment concentrations are generally higher during winter than spring events, particularly for fine-grained sediment (Exhibit 11D). This pattern could be partly attributable to erosion of easily-mobilized sediment that is available in the bed during the earlier winter floods. Bank collapse and slumping of submerged side slopes around scour holes during the summer season could both produce fine-grained sediment during low flows, which would be evacuated by winter floods. This supply of easily eroded sediment could be mostly gone in the Lower Basin when spring flows occur. In addition, lake level is also an important contributor to seasonal hysteresis: in general, lake levels are lower at the start of winter flood events and higher at the beginning of spring snowmelt. Lower lake levels may contribute to higher instantaneous sediment transport rates (and therefore SSC) in winter than spring events.
- Water level in Coeur d'Alene Lake has a substantial impact on instantaneous sediment transport rates at Harrison, but not at Cataldo. For a given discharge above about 10,000 cfs, fines concentrations at Harrison are higher when the lake level is low than when Coeur d'Alene Lake is at higher stands. The explanation for this effect likely relates to increased gradient and shear stresses at lower lake levels.

There are important and complex differences between winter and spring events that relate to sediment and contaminant erosion and deposition. During shorter duration floods typically generated by winter storms—which commonly begin when lake level is low—more water, sediment, and lead are delivered to the floodplain, and downstream flow is greatly attenuated. In contrast, spring snowmelt events, which are characterized by sustained high flows at high lake levels, are not attenuated between Cataldo and Harrison. Because of the lack of downstream attenuation and longer duration of high flows, snowmelt floods have the potential to mobilize greater quantities of contaminated sediment from the riverbed.

Observations about Annual and Long-Term Sediment Fluxes

- The sand bed portion of the Lower Basin between Cataldo and Harrison experienced a net loss (erosion) of sediment every year over the 25 years of record. Based on the rating curves and hydrographs, the net sediment storage change in the 28-mile reach was about -35,000 metric tons/year (negative indicating a deficit). Annual deficits ranged from -2,600 to -281,000 metric tons.

- The size of the annual sediment deficit between Cataldo and Harrison increases with the size and duration of flood flows over a given WY. This indicates that at high flows, the recruitment of bed material within the Lower Basin exceeds the amount of sediment deposited in the floodplain.
- The data suggest that, in contrast to the reach between Cataldo and Harrison, there is a net *gain* of sediment (positive storage, or net deposition) between the confluence of the North and South forks (measured by the sum of fluxes at the Pinehurst and Enaville gages) and the Cataldo gage, about 5 miles downstream. The net annual gain of sediment in this reach averages about +8,000 metric tons over the 25-year analysis period. However, the computed difference ranged from -6,000 metric tons to +101,000 metric tons, with most of the deposition occurring during large floods (for example, 2008, 2002, 1996). In other years, the net difference is typically within a few thousand metric tons – a relatively small difference that may be within the range of uncertainty for the data.
- As noted above, the magnitude of net sediment deposition within the reach between the confluence and Cataldo increases with the magnitude and duration of high flows. Furthermore, the deposited sediment is dominated by fines, as inferred by the differences in fluxes for fines at the confluence and at Cataldo. This pattern indicates that sedimentation in the floodplain in that reach exceeds sediment erosion from the riverbed. Floodplain deposition exceeding bed erosion is consistent with what would be expected for the dominantly gravel bed character of the reach, which limits the availability of sand for erosion from the riverbed. Presumably, net sediment losses in the gravel reach during the lower flow years are mostly attributable to bank erosion, minor erosion from the bottom of sand bottom pools, or data uncertainty.
- Floodplain storage of sediment also occurs downstream of Cataldo, but this is not reflected in the calculated net flux relative to Harrison because it is offset by the large amount of sediment mobilized from the riverbed (i.e., a large amount of floodplain deposition occurs but it is masked by the larger amount of bed erosion that occurs). Floodplain deposition in the Lower Basin is discussed further in Section 6 of this addendum, where results of a simplified floodplain sedimentation model are discussed.
- Contributions of flow and sediment from the North and South forks follow the same general patterns as documented in the original ECSM (CH2M HILL, 2010a). The contribution of sediment from the South Fork is in the range of about 10 and 20 percent of the total flux at Harrison; the contribution from the North Fork varies greatly, from less than 30 percent to almost 90 percent of the Harrison sediment flux.
- The proportion of sand in the suspended load generally remains between 20 to 35 percent at Pinehurst, Cataldo and Enaville. At Harrison, however, the percent of sand varies from less than 15 percent to about 50 percent. Higher in the basin, the proportion of sand decreases with increasing flood flows, but at Harrison, the proportion of sand *increases* with increasing flows. This is interpreted as an indication that the supply of sediment at high flows at the upper stations is dominated by wash load (originating from runoff and bank erosion), whereas the sediment supply at Harrison at high flows is dominated by erosion of the sand bed between Cataldo and Harrison. A possible but less likely cause of this pattern may be preferential loss of fines to the floodplain during large flood years, increasing the proportion of sand in suspension at Harrison.
- The differences in sediment fluxes between the spring and winter events illustrate the importance of floodplain storage of water and sediment in modulating flooding and sediment fluxes in the Lower Basin. The shorter-lived February 1996 and January 2011 winter events were significantly attenuated by water entering floodplain, resulting in a large amount of floodplain deposition of sediment. In the 2002 and 2008 spring events, sustained flows early in the event, and higher lake levels compared with the two winter floods, limited the ability of the floodplain to absorb more water during peak flows, allowing floods to translate through the system with little attenuation,

preventing storage of large amounts of sediment in the floodplain, and resulting in more significant erosion of sediment from the riverbed during the snowmelt floods.

- Current data indicate that the Lower Basin is net erosional during floods, based on a sediment deficit between the Cataldo and Harrison gages. This finding is different from that in the previous ECSM document (CH2M HILL, 2010a) which suggested that high-flow events result in net deposition in the floodplain in the Lower Basin. The previous analysis, however, probably underestimated sediment loads at Harrison at high flows because it did not incorporate high-flow sediment data from Harrison. The BEMP monitoring program over the past several years, aimed at measuring high flows, began to fill data gaps and shows that much more sediment is transported past Harrison than Cataldo, especially at higher flows (Exhibit 4). The conclusions of this report are the result of several years of additional high flow and suspended sediment data at Harrison, which has allowed the development of separate sediment rating curves for Cataldo and Harrison. Additionally, the use of gaged and modeled flow data at Harrison allows a more reliable and longer term evaluation. The sediment budget in this report therefore supersedes the conflicting earlier one.
- Following the completion of this addendum, CH2M HILL conducted additional analysis of sediment and lead fluxes at Harrison based on the interpretations summarized above (Attachment C). This analysis used a multiple regression rating curve that predicted SSC as a function of the level of Coeur d'Alene Lake at the time of measurement, as well as discharge (Q). Accounting for the lake level in the rating curve, in addition to Q, reduces the residuals between predicted and observed SSC, especially for samples collected at higher flows. The revised estimate of the average annual sediment transport rate at Harrison is 25 percent lower using the multiple regression rating curve than estimates currently cited in this section (about 50,000 MT/yr vs. 67,000 MT/yr). Similarly, the revised sediment deficits and computed riverbed lowering rates are also lower by the same amount (25 percent) compared with those cited here. Because the revised approach reduces the residuals between predicted and observed sediment transport, and is based on physical processes as understood by the current conceptual site model, the revised estimates of the sediment and lead fluxes in Attachment C are considered more representative than those shown in the body and exhibits cited in Sections 3 and 4 of the current addendum. However, rather than updating all the exhibits and text of the addendum (the values of which will soon be further improved by the sediment transport model), the revised analysis is provided as Attachment C.

4 Lead Transport

This section uses lead concentration data from suspended sediment samples in the Lower Basin examine the variability of lead on suspended sediment and to quantify longer-term lead transport in the Lower Basin. Lead transport within the Lower Basin is mostly associated with fluvial transport of lead-containing sediment. Therefore, estimations of lead transport are computed by combining lead concentration data with the suspended sediment transport calculations presented in Section 3 of this addendum. The movement of dissolved lead, assumed to account for less than 10 percent of the total lead load, is not addressed by this analysis.

4.1 Data Sources

Sediment concentration, grain size, and lead data in the Coeur d'Alene River were measured in the context of two separate but related monitoring programs: a USGS water quality monitoring program and a CH2M HILL monitoring program, being conducted for EPA, which focuses on sediment. Both the USGS water quality and CH2M HILL sediment monitoring programs measure the concentrations of sediment, lead, and other metals in water samples collected from the river. The data from the two programs through WY 2013 are compiled in Attachment A. Both sampling programs used standard USGS sampling equipment and procedures for sediment sampling, using isokinetic samplers to collect depth and width-integrated samples at bridges to provide a representative flow-weighted average sample of the river water. However, the objectives of the sampling programs were different, and therefore some sampling program and laboratory procedures varied in notable ways.

The USGS data set (downloaded from the NWIS online data base http://waterdata.usgs.gov/nwis, on a variety of dates over several years) contains data on lead concentrations from several hundred depth-integrated water samples collected since 1993. This sampling was conducted at seasonal intervals, including high flows in winter and spring, and low flows in the summer and fall. The purpose of the USGS program was primarily water quality monitoring. Lead measurements were conducted on the water samples (filtered and unfiltered), not on the sediment directly; the suspended sediment concentration (in milligrams per liter) was measured separately. Sample volumes collected for water quality sampling were insufficient to provide enough solid material to perform particle size distribution testing and metals analysis directly on the sediments themselves, and this was not the objective of that program. However, the lead concentration on sediment (in milligrams lead per kilograms of sediment) can be back-calculated by dividing the difference in the lead concentration between the unfiltered and filtered samples by the suspended sediment concentration. This estimation of the lead concentration on the suspended sediment thus incorporates error from all three measurements (unfiltered lead concentration, filtered lead concentration, and suspended sediment concentration). Additionally, the SSCs in samples from summer and fall flow conditions, which include a majority of the samples, were uniformly very low, and so of limited value for evaluating sediment and lead transport, which occurs primarily during high-flow conditions. As shown in Section 3.6.5, flows below 3,000 cfs transport less than 5 percent of the sediment load at Cataldo and Harrison, despite the fact that such flows occur about 75 percent of time (CH2M HILL, 2010).

In contrast to the USGS water quality program, the purpose of suspended sediment sampling conducted by CH2M HILL was to measure metals in suspended sediment directly, especially at high-flow conditions, and to measure metals in discrete particle size classes to support the calculations presented here and related sediment transport modeling. Large volumes of water (20 gallons) were necessary to obtain enough sediment material to analyze for particle size distribution and metals content by size class. CH2M HILL's BEMP suspended sediment sampling program began in 2010 (USGS collected samples for BEMP in 2008 and 2009), and sampling was focused exclusively on high flows, so the total number of samples in the data set is considerably smaller than the USGS data set (Attachment A). Since 2010, CH2M HILL sampled one to three events per year. For these samples, lead concentration is measured on

bulk suspended sediment, plus the sand-sized fraction of the sample (> 63 μm) and the silt and clay portion of the sample (< 63 μm) separately (Exhibit 31).

For this evaluation, an attempt was made to expand this relatively small data base by normalizing the USGS data to allow comparison of lead concentration measurements from the two data sets, by subtracting the filtered lead values from the unfiltered values in the USGS data and assuming all the lead in the USGS samples resides on the sediment. The two data sets are compared in Exhibit 32, which shows that there is considerably more scatter in the lead concentrations in the USGS data, especially for the samples with very low SSC (less than about 10 mg/L). To convert the data from the USGS samples, which report lead in water, to an estimate of lead concentration on sediment, it is necessary to divide the lead measured in the water sample by the SSC—thus incorporating uncertainties in both the SSC and lead measurements into the answer. In samples with low SSC, the lead concentration in water samples is also low, and the percentage measurement uncertainty for both SSC and lead concentrations are both likely to be high. The higher uncertainty possibly accounts for much of the scatter seen in the USGS data for low SSC. In those samples, the lead content is very low, and a large fraction of the lead that is present is in the dissolved phase (Clark and Mebane, 2014). When the percentage of lead in the dissolved phase is computed from the USGS data and plotted against discharge, the data show that a large percentage of lead may be in dissolved phase at low flows, up to a discharge of about 3,000 to 5,000 cfs. At higher flows, the percentage of lead in the dissolved phase drops rapidly as the amount of SSC increases from near zero to non-negligible sediment transport, and particulate lead accounts for nearly all the lead in water samples. Thus at higher SSC, the lead concentration on sediment from the USGS water quality samples is similar to the lead concentrations on sediment from the BEMP samples (Exhibit 32). This drop in the percentage of dissolved lead, and the convergence of the USGS and BEMP data is consistent with the threshold discharge of about 3,000 cfs for mobilizing sediment in flows as discussed in Section 3.2 above.

The BEMP samples measure lead on sediment directly, without the necessary conversion that magnifies uncertainty in the USGS water quality samples. Thus, for the purposes of the calculations and analysis in this section, the BEMP data are considered to be more reliable, and CH2M interprets that at least some of the USGS data do not accurately represent the lead concentration on sediment. As it is unclear which of the USGS samples should be included and which excluded in the analysis of lead concentration on sediment, and the two data sets generally converge at higher flows, which dominate the sediment and lead budgets, the current analysis relies on the more limited data set of direct measurements of lead on sediment from the BEMP samples[8] (Exhibit 31).

4.2 Lead Concentrations

Data for lead concentrations in suspended sediment from BEMP sampling in the Lower Basin are summarized in Exhibit 33. Between 2008 and 2013, 38 suspended sediment samples were collected at five stations in the Lower Basin (samples collected in the Upper Basin are reported separately) at relatively high flows, and the sediments in these samples were analyzed for lead and other heavy metals. Of these, sample masses were adequate for the analysis of 27 sieved fine fraction (< 63 μm) and 21 sand fraction (63 – 25 μm) subsamples. The lowest bulk lead concentration was 122 mg/kg for a sample collected at Enaville on the North Fork, and the highest bulk lead concentration was 4,900 mg/kg for a sample collected near the flood peak in January 2011 at Harrison (this sample had an anomalously high SSC as well, as shown in the sedigraph for this event in Exhibit 30C). The highest lead concentration measured for any of the samples was 6,280 mg/kg, from the fine fraction portion of the January 2011 sample at Harrison that had the highest bulk lead concentration.

[8] Although the analysis of lead only uses data from the smaller BEMP data set, the analysis of sediment transport discussed in Section 3 includes SSC measurements of both the USGS and BEMP data sets compiled in Attachment A.

4.2.1 Differences in Bulk Lead Concentration among Locations

Measured bulk lead concentrations in suspended sediment are plotted as a function of discharge and SSC in Exhibit 33. There is no clear indication of an overall correlation between bulk lead concentration and SSC or discharge. However, the data are grouped by location, as illustrated in Exhibit 33B. Bulk lead concentrations in suspended sediment are lowest at Enaville on the North Fork (average 204 mg/kg) and highest at Harrison (average 3,727 mg/kg), with intermediate concentrations at Cataldo (average 1,054 mg/kg) and Rose Lake (average 2,638 mg/kg). Concentrations at Pinehurst (average 2,431 mg/kg) are diluted by the larger flow and sediment load from the North Fork.

Lead concentrations in sediment from the South Fork (Pinehurst) are an order of magnitude higher than those in the North Fork (Enaville). Mixing of sediment from these two sources results in intermediate lead concentrations at Cataldo. Concentrations then increase through the Lower Basin, rising between Cataldo (RM 163) and Rose Lake (RM 153), and between Rose Lake and Harrison (RM 134) (Exhibit 33B). At Harrison, there is a weak but discernable negative correlation between the lead concentration and lake level (Exhibit 33C). The observation that lead concentrations may increase at lower lake levels provides evidence supporting the hypothesis (discussed in Section 3.4.4) that low lake levels, by creating steeper water slopes and therefore higher shear stresses, contribute to the erosion of legacy contaminated sediment.

This general downstream increase in lead concentration is substantiated by a different set of data collected from a boat during a single flood in April 2012 (Exhibit 34). Sampling conducted during that event collected point-integrated “grab” samples, using a sampler that could be manually triggered to collect a sample of ambient water and sediment at a known depth. These 10 gallon grab samples were collected 1.5 meters (m) above the bed—judged to be high enough to only capture the suspended load but low enough to obtain enough sample material for metals analysis. These samples were filtered on board, with recovered sediment submitted to a laboratory for metals analysis. The grab samples in the 2012 event were supplemented profiles of SSC and particle size distribution LISST (Attachment B), collected from the same boat.

Data from the April 2012 grab sampling indicate a downstream increase in lead concentration in suspended sediment for each of the sampling days (Exhibit 34). A comparison between lead levels in suspended sediment with those in the riverbed corroborates this interpretation: the bed surface sediment samples (Ponar samples from 2010 and 2011) generally have higher bulk lead concentrations than does the suspended sediment at Cataldo, but the concentrations of the bed material and suspended load become more similar in the downstream direction (Exhibit 35). This pattern suggests that the lead concentration in the suspended load increases downstream due to sustained exchange and mixing of sediment between the bed material and the suspended load.

Variability in lead concentrations measured in sediment particles[9] also shows distinctive differences among measuring stations. Lead concentrations in sediment remain within a relatively narrow range at the Enaville station (typically between 100 and 400 mg/kg), Pinehurst station (1,500 to 3,000 mg/kg), and Cataldo station (800 to 1,400 mg/kg). The lead concentration on sediment is both higher and more variable at Harrison, where lead concentrations range from 1,550 mg/kg to nearly 5,000 mg/kg. The explanation for the greater variability is the wide range of lead concentrations in sediments in the Lower Basin, which is believed to be the source of much of the sediment at Harrison. Some flows mobilize large quantities of riverbed sediment in the Lower Basin, which contains sediments with lead concentrations varying from less than 100 mg/kg to as much as 60,000 mg/kg. Other flows do not mobilize as much sediment in the Lower Basin, and the lead concentrations reflect more predominantly the concentrations on sediments entering the Lower Basin from the North Fork and the South Fork.

[9] Referring to samples analyzed by the BEMP program, which measured the lead content of filtered sediment samples, and not the USGS water quality samples, which are discussed in the next paragraph.

The conclusions in this section are based on the relatively small number of BEMP sediment samples collected during high flows (Exhibit 31). For those samples collected at high flows, there was sufficient sediment in the flow that the sample could be filtered and enough material recovered to perform a direct lead assay directly on sediment. The USGS water quality monitoring program, which has collected a much larger number of water samples from the same stations, collects water at regular and irregular intervals, focused especially on lower flow period when dissolved constituents are highest. That program measured lead and SSC in the water samples, from which an estimate of the lead concentration on sediment can be back-calculated. Using the back-calculated water quality data to estimate lead on sediment produced lead concentrations with much higher uncertainty and variability than the BEMP data. The uncertainty and variability in those data, with the back-calculation procedure, made it difficult to discern some of the trends discussed above. Although the conclusions described in this section are based primarily on the direct lead-in-sediment BEMP measurements, none of the conclusions are refuted (and some are supported) by the larger database of USGS water quality samples as reported in Clark and Mebane (2014) and earlier USGS reports.

4.2.2 Relationship between Grain Size and Lead Concentration in Suspended Sediment

Fine grained sediments in many river systems contain higher concentrations of contaminants and heavy metals compared with coarser sediment particles (e.g., Salomons and Förstner, 1983). A combination of factors contribute to this pattern, including higher surface area-to-volume ratio of fine-grained sediments, and higher cation-exchange capacity of many clay minerals that comprise a portion of the fine fraction. However, sediment in the Coeur d'Alene River system does not fit neatly in this characterization. The bulk lead content of suspended sediment does not show a clear correlation with the percent fines in suspension at most locations, though there is a weak positive relationship between bulk lead and percent fines at Harrison (Exhibit 36). Similarly, at most sites there is little difference in lead concentration between the sand and fines subfractions of the suspended load, though suspended fines at Harrison generally contain higher lead concentrations than sand (Exhibit 37). At Pinehurst, there may be a slight tendency for higher lead concentrations in sand than in the fine fraction (Exhibit 37).

A significant portion of the sediment, and nearly all the lead in mobile sediment in the Lower Basin, is attributable to mine tailings. This source accounts for a key distinction in the relationship between particle size and lead concentration; while in many rivers contaminants are adsorbed onto particle surfaces and therefore the constituent concentration increases with the surface-area-to-volume ratio, particles in Coeur d'Alene River sediment contain lead within the mineral structure of the sediment, often as the ore mineral lead sulfide (galena, or PbS), or as lead oxides. Based on limited data, this appears to be the most common form of lead in particles of all sizes in the Lower Basin, and it appears to be especially true for fine particles of silt and very fine sand, because these size classes reflect the texture that ore was physically ground to during ore processing (CH2M HILL, unpublished data, 2013e). Particles that were ground more finely during the milling process would not be expected to have a greater mass concentration of the contaminant. However, waste material discharged to the river contained particles of galena ore and ore rock in a particular size range, and it is this history, rather than any grain size affinity, that appears to account for observable correlations between lead content and grain size. Thus, although lead is commonly associated with fine-grained sediment in this system, the contaminant concentration of a particular sedimentary deposit depends more on the history and origin of this sediment than its grain size distribution. Moore et al. (1989) found that the traditional relationship between metal content and grain size also did not apply to floodplain sediments in the metals-contaminated Clark Fork River in Montana; they similarly suggested that typical grain size-metals concentration relations should not be applied a priori to sediments contaminated by mine and mill wastes. The distinction is important for understanding the data relating lead and grain size in this system.

Lead concentrations in silt/clay particles in suspension are consistently higher than concentrations associated with sand-sized particles at Harrison (Exhibit 38), but this is not the case at the other sampling stations. As discussed in Section 3.6, suspended sediment transport rates increase in the downstream direction from Cataldo to Harrison, and that divergence increases at higher flows; increasing discharges mobilize both sand and fines from the riverbed in the Lower Basin. Sand in the Lower Basin clearly contributes to the increase in the sediment load between Cataldo and Harrison, as elaborated in Section 3.6.6 (Exhibit 30). However, compared with sands in the active layer of the bed, fine-grained deposits in the bed of the Coeur d'Alene River contain more concentrated deposits of legacy mine tailings, and these are characterized by both high fractions of silt/clay-sized particles (a result of the milling process), as well as high lead concentrations (EPA, 2001). Thus, while there is likely no preferential affinity of lead for fines, there is a mechanism explaining why finer sediments would tend to have higher lead content at Harrison. Erosion of legacy tailings deposits within the bed in the Lower Basin contributes higher lead concentrations associated with fines in suspension at Harrison.

4.3 Lead Fluxes

This section combines sediment fluxes computed in Section 3.6 with lead concentrations in suspended sediments (Section 4.2) to evaluate the magnitude, frequency, and spatial patterns of lead transport in the Lower Basin.

4.3.1 Approach to Computing Lead Fluxes

The sediment flux calculations in Section 3.6 used regression equations to estimate the SSCs (bulk, sand, or silt/clay fraction) corresponding to a given discharge at each sampling location in the Lower Basin. The hourly sediment flux (metric tons per hour) was computed as the regression-based estimate of SSC multiplied by the measured discharge. Similarly, the lead flux can be computed by multiplying the sediment flux by the corresponding concentration of lead in suspended sediment.

Exhibit 33 shows that lead concentrations do not correlate with discharge or SSC; rather, the primary control on lead concentration is location within the Lower Basin. Based on these observations, the average lead concentration for bulk, sand and silt/clay fractions at each station were used to estimate the daily lead flux associated with each fraction:

$$Pb_{flux(i)} = Q \times SSC(i) \times Pb_{conc(i)} \times 1.0194 \times 10^{-4} \qquad (3)$$

where $Pb_{flux(i)}$ is the lead flux of size fraction *i, (*bulk, sand, or silt/clay fraction) in metric tons per hour, Q is the mean daily discharge in cfs, SSC(*i)* is the SSC of size fraction in milligrams per liter (mg/L), Pb_{conc} (*i*) is the average lead concentration in sediment in each size class fraction in mg/kg, and the 1.02×10^{-4} constant is a conversion factor to compute the lead flux estimate in metric tons/hour. Average lead concentrations for the bulk, sand and silt/clay fractions are based on the data in Exhibit 31.

Lead fluxes were estimated for the same period of record described in Section 3.6 (WY 1987 through WY 2012), addressing Enaville (North Fork Coeur d'Alene River), Pinehurst (South Fork Coeur d'Alene River), Cataldo and Harrison. An insufficient number of sediment samples (n=3), and limited discharge data, prevented computation of lead fluxes at Rose Lake.

Estimates of lead fluxes are subject to the same limitations as those described for suspended sediment (Sections 3.2 and 3.5). In addition, the following assumptions apply to the calculations of lead fluxes:

- Bulk lead concentrations in sediment are assumed to vary only by location, and are assumed to not vary with other factors such as discharge, or over time due to land use changes. For purposes of estimation, a single average lead concentration is assumed to be representative of a location over the range of discharges at that location.
- Separate averages are used to compute lead concentrations for bulk, sand and silt/clay fractions. Fewer samples are available to estimate lead concentrations for grain size subfractions than for bulk

samples, and this results in greater uncertainty associated with lead estimates for sand and silt/clay fractions, compared with the bulk lead estimates.

4.3.2 Annual Bulk Lead Fluxes

Computed annual lead fluxes for the 25-year period of record are summarized in Exhibit 38. These values show that lead fluxes are about an order of magnitude higher at Harrison than at Cataldo and Pinehurst, and nearly two orders of magnitude higher than at Enaville. This difference reflects both the higher suspended sediment fluxes (Exhibit 16) and the higher lead concentrations at Harrison (Exhibit 33). Annual time series graphs (Exhibit 39) show that the lead flux *into* the Lower Basin was by far the highest in 1996 (at Enaville, Pinehurst, and Cataldo gages), but the flux *out* of the Lower Basin at Harrison was greatest in 2008, a year that was dominated by a sustained spring flood. Lead flux results are similar to sediment flux results, in that the difference in flux between Harrison and Cataldo is greatest in the highest flow years (Exhibit 40), suggesting that net erosion of lead from the riverbed is greatest during sustained spring floods.

4.3.3 Lead Budget in the Gravel-Bed Reach: Confluence to Cataldo

Differences between the annual lead fluxes at different locations define the lead budget of the Lower Basin (Exhibit 40). The lead flux at Cataldo is close but not identical to the combined flux of lead from Enaville (North Fork) and Pinehurst (South Fork) (Exhibit 38). Over the 25-year period of record, the calculated lead flux is, on average, about 4.5 metric tons per year higher at Cataldo than for the combined North and South Fork stations. The differences are likely within the range of uncertainty of measurements, but may also reflect the influence of actual processes, as outlined below.

In most years, and particularly those without significant flooding, the computed combined Enaville/Pinehurst lead flux is less than at Cataldo, implying that some lead is being mobilized within that reach during lower flows. Presumably this lead would derive from bank erosion, rather than bed erosion, since the bed in that reach is composed primarily of gravel and cobble, and the fine-grained banks are tall and unstable with high concentrations of lead, with clear evidence (in the form of collapsed soil blocks) that erosion of tailings-rich banks occur in that reach. During the four years with the highest flows (1996, 1997, 2008, and 2012), however, lead flux from the North and South Fork Coeur d'Alene River *exceeded* the flux at Cataldo, suggesting that a detectable amount of lead may be lost to the floodplain between the confluence and Cataldo during larger floods. While the difference between the combined lead fluxes of the North and South Fork and the flux at Cataldo are small enough to be within the range of uncertainty, these interpretations are supported by the data and may be helpful for understanding the lead balance at a qualitative level.

4.3.4 Lead Budget in the Sand-Bed Reach: Cataldo to Harrison

The annual average bulk lead flux at Harrison (1987 to 2012) was approximately 250 metric tons, compared with 34 tons at Cataldo, 23 tons at Pinehurst, and 6 tons at Enaville (Exhibit 38). Thus the average annual net erosion rate of lead is about 215 metric tons between Cataldo and Harrison. However, the annual net erosion rate values over that time varied greatly, from 6 tons in 1992 to nearly 1,000 tons in 2008, depending on the number, size, and type of floods that occurred (Exhibit 40).

The *net* annual erosion of lead (not accounting for exchange processes with the floodplain between Cataldo and Harrison) is closely tied to the magnitude and duration of high-flow events. There is a close correlation between net lead loss and the annual peak discharge at Harrison (used here as a proxy for both the magnitude and duration of high flows) (Exhibit 40B). Thus, the calculations using rating curves imply that most of the net erosion of lead occurs during high magnitude flood events, rather than during years with moderate flows but no large floods.

Overall, the lead budget values suggest that most of the lead transported in the Lower Basin originates within the sand-bed reach of the river. Notably, about seven times as much lead is transported past

Harrison than Cataldo, whereas for sediment the difference is only about a factor of two. Put another way, contributions from the Upper Basin account for less than 12 percent of the approximately 250 metric tons/year of lead transported out of the Lower Basin. Note also that these results refer to the *net* increase in lead flux; the amount of sediment mobilized from the bed is assumed to be greater than these numbers suggest, because a percentage of sediment and lead eroded from the bed is transported to and deposited in the floodplains, and therefore is not accounted for in the flux leaving the basin at Harrison. (Section 7 of this addendum discusses estimates of the amount of sediment and lead entering and depositing in the floodplain, and the overall sediment and lead budget summary attempts to address holistically the amount of sediment and lead eroded and deposited in both the bed and floodplain.)

In summary, the lead flux leaving the Lower Basin is nearly an order of magnitude greater than that entering it. The average annual net loss of lead from the Lower Basin over the 25-year period of record is about 215 metric tons per year. The amount and proportion of net lead loss generally increases with the size of the flows in a given year, despite the fact that during floods some of the material mobilized enters floodplain storage and is not transported out of the Lower Basin, and thus not reflected in the lead flux at Harrison. Upstream of Cataldo, where the riverbed is dominated by gravel and cobble, bank erosion may supply a small but detectable amount of lead during dry years. In years with sustained flooding, however, floodplain storage of lead in this reach may offset lead mobilized by bank erosion, potentially accounting for as much as about 15 tons (as in 2008).

4.3.5 Influence of Flow Magnitude and Frequency on Bulk Lead Transport

As noted above, the long term lead flux is disproportionately influenced by large and sustained flooding. About two-thirds of the lead leaving the Lower Basin is estimated to have occurred during about a quarter of the water years (1996, 1997, 2002, 2008, 2011, and 2012) over the 25-year period of record (Exhibit 38). The calculated annual lead flux is a function of flow magnitude (which influences the SSC) and flow duration - specifically the number of hours above discharge values where the most sediment and lead transport occur; although higher flows move more lead per hour, they occur less frequently and for shorter durations.

These factors were assessed by evaluating the total annual lead flux contributed by flows of different frequencies and magnitude at Cataldo and Harrison (Exhibit 41). The values were calculated by binning hourly flows into 5,000 cfs intervals, and then summing the lead transport occurring within each bin for each year. The height of each column segment in Exhibit 41 indicates the amount of lead transported by flows within the specified range.

In typical years, most of the lead transport occurs at moderate flow rates, between 5,000 and 20,000 cfs, at both Cataldo and Harrison. This is because, in part, these discharges occur during the rising and falling limbs of a given flood hydrograph (including floods with higher peaks), and flows at these levels tend to persist longer than briefer periods of peak or near-peak flows. Flood stage flow (about 19,500 cfs at Cataldo), occurs on average only about once every 2 years, so flows in the 5,000 to 15,000 cfs range are much more common.

The amount of lead transported at Cataldo and Harrison is typically proportional to the magnitude of an event: a large flood will yield proportionately more lead at both Cataldo and Harrison compared with other flood events. However, there are notable exceptions to this pattern. While the 1996 flood—a flashy, winter event—showed the highest annual lead flux of the 25-year period of record at Cataldo, the 2008 sustained spring runoff event produced the highest lead flux at Harrison based on the rating

curve. Nonetheless, both these two events were the in the top four flux values in the period of record at both sites[10].

In the 1996 flood, more than half the lead transport at Cataldo occurred while flows exceeded 30,000 cfs, a period of less than 2 days, indicating an exponential increase in lead transport at very high-flow rates. The pattern at Harrison is similar, though the peak flow rates are generally lower because of flood attenuation due to water storage in off-channel areas, and peak discharges for a given event are generally lower at Harrison than at Cataldo. At both locations, the floods with the greatest lead flux were in 1996, 1997, 2002, 2008, 2011, and 2012.

The magnitude and frequency of lead transport is shown differently in Exhibit 42, with total and proportional lead fluxes by flow rate indicated for four stations in the Lower Basin, showing the amount of lead transported by varying flows over the 25-year flow record, computed using the rating curve, average lead concentration, and the 25-year flow history for each station. Exhibit 42A shows the magnitude of the computed total lead flux at Harrison is much higher than the other stations, and dominated by flows less than 20,000 cfs. Exhibit 42B shows lead fluxes by flow rate, normalized to show differences in the dominant discharge for lead. At Harrison, 77 percent of the lead flux occurs at moderate flows between 5,000 and 20,000 cfs. At Cataldo, however, flows in this range account for about 61 percent of the lead transport, and a larger portion of lead is transported at high flows. This is interpreted to reflect the role of floodplain attenuation of flows between Cataldo and Harrison, so that there are fewer days of flow exceeding 20,000 cfs at Harrison.

In summary, evaluation of the magnitude and frequency of lead transport indicates that lead transport at all flows is almost an order of magnitude higher at Harrison than Cataldo, due both to higher sediment loads and higher lead concentrations of the sediment. This is attributable to several factors, including:

- Higher sediment concentrations at Harrison as a result of erosion off the sand/silt bed. A steeper exponent in the rating curve at Harrison compared with Cataldo implies that sediment transport increases more quickly with discharge at Harrison.
- Higher lead content in sediment at Harrison, due to its origin in the riverbed (representing older, more contaminated deposits).
- The duration of elevated flow is longer at Harrison than Cataldo, because of floodplain attenuation of flashier flows upstream. While instantaneous peak flows at Harrison are typically lower than at Cataldo, high-flow rates persist longer, resulting in longer durations of sediment-transporting flows.

Although instantaneous lead transport at high flows is exponentially greater than low flows at both Cataldo and Harrison, very high flows comprise a relatively small proportion of total flow duration (the duration of a given flow is longer if the peak flow is higher than that flow; for example, a peak of 25,000 cfs means that flows must rise and fall through lower flow ranges, increasing the amount of time flows are within the range from 15,000 to 20,000 cfs).

4.3.6 Grain Size and Lead Transport

The relative and absolute amount of transported lead associated with several particle size ranges were calculated. As a practical approximation, the fine grained fraction generally moves as wash load and once mobilized, flows out of the system or enters the floodplain, and has limited interaction with the riverbed. In contrast, sand is continuously exchanged with particles in the riverbed and is less likely to enter the floodplain. Understanding the relative contribution of these different sediment fractions to

[10] These calculations are based on predictions of SSC from rating curves, applied to measured hydrographs, and not on measurements collected in specific events. By far, the highest measured SSC and Pb concentrations were observed in the January 2011 event (Attachment A).

lead transport will help in evaluations of the relative effectiveness of different strategies to manage lead transport in this system.

The sand fraction proportion of the total lead flux is shown in Exhibit 43. (As with the sediment transport calculations, the sum of the sand and fines fractions lead fluxes do not exactly equal the total lead flux, because the calculations were made using rating curves derived from different data). Lead transport calculations as a function of discharge using the sediment rating curves for fines and sand (Exhibits 14 and 15) along with the average lead concentration on each fraction (Exhibit 31) show that less than half the lead load is present in sand (meaning the majority is in fines). The proportion of lead in sand versus fines varies as a function of location and flow (Exhibit 43). The proportion of lead associated with sand (abbreviated "PLS" for ease of discussion) is usually highest in the South Fork at Pinehurst, where sand carries approximately 35 to 40 percent of the lead. At Cataldo, the annual PLS is less variable as a function of flow compared with the other stations, and is typically in the 25 to 30 percent range. At Harrison, however, which has the highest lead load, the partitioning of lead between sand and fines depends strongly on the flow, with the PLS increasing to about 50 percent of the total lead load during high-flow (and high sediment transport) water years, such as 1996 and 2008 (Exhibit 43A).

There is a strong positive relationship between instantaneous flow and the PLS at Harrison, but the relationship is negative for the Pinehurst and Cataldo (Exhibit 43B), implying that wash load exceeds mobilization of sand from the bed during larger floods. This may be because the bed is dominated by gravel above Cataldo, limiting the amount of sand that can be mobilized from the bed as flows increase. The nearly constant PLS at Enaville (~25 percent) reflects the partitioning of the more naturally-occurring lead content between sand and fines in this system.

Variability in the PLS is important for understanding the dynamics of lead in the Lower Basin. As noted previously, the lead flux at Harrison is an order of magnitude greater than at Cataldo, indicating that most the lead originates within the Lower Basin. Although the annual PLS at Harrison varies from nearly 10 to 40 percent over a 25-year period of record, the long-term lead load is dominated by conditions during the higher flow years, averaging about 30 percent PLS.

Based on these calculations, the wash load fraction (consisting of fines) carries about 23 tons per year of lead into the Lower Basin (at Cataldo), and about 186 tons per year out of the Lower Basin (at Harrison). Thus, it can be inferred that mobilization of fines within the Lower Basin generates most (163 tons of 250 tons per year total, or 65 percent) of the lead eroded out of this system. A cumulative plot of the net "lead deficit" (total lead leaving minus entering) shows that over 25 years, the deficit was approximately 1,700 tons of lead associated with sand, and 4,200 tons associated with fines (Exhibit 44). As these calculations are based on multiplying the sediment fluxes by an average lead concentration, which itself has uncertainty associated with it, the uncertainty associated with these values is expected to be greater than for the sediment flux estimates, as discussed in Section 3.6.5. Nonetheless, the general patterns and approximate order of magnitude of the lead fluxes help to understand the primary sources, sinks, and exchanges of lead in the Lower Basin.

Bank erosion supplies a relatively small proportion of sediment mobilized in the Lower Basin (as discussed by CH2M HILL [2014b] and in Section 5.2); therefore, most of the lead in the system appears to originate from erosion of silt- and clay-sized sediment from the dominantly sandy riverbed. The implication of this finding appears to be that the wash-load-sized contaminated sediment that represents most of the mobile contamination (a) must have been emplaced by a different process or at a time when it was possible for large amounts of silt and clay to deposit in the riverbed; and (b) once mobilized, this portion of the lead load will not re-enter storage in the riverbed – it will only deposit in off-channel areas or enter Coeur d'Alene Lake.

This conclusion is further supported later in this addendum through the comparison of the different parts of the sediment budget, but additional data from riverbed sampling and coring may be necessary to further strengthen this finding and its possible implications.

4.3.7 Summary of Lead Transport Observations

- Lead transport out of the Lower Basin system at Harrison (an estimated 250 metric tons per year) is on average almost an order of magnitude greater than the amount of lead that enters the system at Cataldo (34 tons per year). In the 25-year period from 1987 to 2012, an estimated 6,250 metric tons of lead left the Lower Basin at Harrison, compared to less than 900 metric tons that entered at Cataldo (Exhibit 44). These are considered approximate order-of-magnitude estimates, and subject to the same uncertainties as the sediment transport estimates discussed in Section 3.6.5. However, the general patterns and relative amounts of lead transport and erosion are believed to be reasonable.
- According to these calculations, the North Fork delivers about 6 metric tons of lead annually to the Lower Basin, and the South Fork about four times this amount (23.5 metric tons per year). Combined, these contributions of lead from the Upper Basin are a relatively small component of the 250 metric tons per year of lead leaving the Lower Basin. Most of the mobile lead in the Lower Basin is inferred to originate from erosion of the bed between Cataldo and Harrison.
- The computed annual average lead deficit (net erosion) between Cataldo and Harrison was about 215 metric tons per year—a net loss of 5,400 metric tons between 1987 and 2012 (Exhibit 44). The annual deficits varied from a minimum of 6 metric tons in 1992 to a maximum of 980 metric tons in 2008 (a range of more than two orders of magnitude). These are net values, and do not account for exchange processes within the Lower Basin such as storage in and erosion from the floodplain.
- The amount of lead in storage between the confluence of the North and South Fork Coeur d'Alene Rivers and the Cataldo gaging station, 8 miles downstream (known as the Cataldo, "Gravel Bed," or "Braided" Reach), appears to be nearly in balance (with a difference of 5 metric tons per year on average, within the range of uncertainty in the calculations). However, larger year-to-year differences exist, and may be attributable to exchanges with the floodplain in this reach. The data suggest that the lead balance is negative (erosional) during drier years, and positive (depositional) during wetter years. An interpretation of this pattern is that the Cataldo Reach supplies, on average, about 5 to 15 metric tons per year of lead, primarily from bank erosion, while in flood years, this is offset by lead that deposits in the floodplain.
- The bulk of lead transport in the Lower Basin occurs during years with larger and more frequent high flows; more than two thirds of the lead flux at Harrison over the 25-year period occurred during six water years (1996, 1997, 2002, 2008, 2011 and 2012).
- Although most of the lead transport occurs during wetter WYs, the bulk of lead transport is not only concentrated at peak flows. An analysis of the frequency and magnitude of lead-transporting flows (Exhibit 42) showed that at Harrison, almost 80 percent of the lead transport occurred at flows between 5,000 and 20,000 cfs, incorporating the rising and falling limbs of larger flood events.
- About 70 percent of the lead flux at Harrison is carried on silt and clay-sized particles (fine-grained wash load), and the remainder is on sand (suspended bed material) (Exhibit 43A). The sand, once mobilized, continually interacts with the bed material as it gradually moves downstream, and can be redeposited in the riverbed. In contrast, the lead associated with wash load is unlikely to re-enter storage in the riverbed. Wash load, once mobilized, is generally deposited in significant quantities only outside the channel, or is transported out of the system into Coeur d'Alene Lake.
- The net lead deficit of between the Cataldo and Harrison gages averages about 163 tons per year, and about 70 percent of this deficit is associated with fine-grained wash load. Most of this lead is inferred to derive from erosion of the riverbed, since bank erosion is a comparatively slow process, and proportionally a small source, in this river system (Section 5.2). Therefore, the majority of lead in this system is inferred to derive from erosion of wash load-sized sediment from the riverbed.

Since the wash load does not deposit in the riverbed in large quantities during most flow conditions, it is interpreted that the primary source of lead in the system comes from legacy fine-grained, highly contaminated deposits that are believed to have been emplaced when it was possible for large amounts of silt and clay to deposit in the riverbed (under conditions different from those existing in the present system).

5 Sediment and Lead Erosion from the Floodplain

The fate of lead in the Lower Basin depends primarily on the transport, deposition, and remobilization of sediment in a variety of temporary storage elements, including the floodplain (Exhibit 2). Sections 3 and 4 provided an extensive evaluation of the transport of sediment through the river channel. Sections 5 and 6 consider sediment exchanges with the floodplain; this section discusses and quantifies the amount of sediment and lead erosion from the floodplain.

Sediment and lead may be mobilized from temporary storage in the floodplain by two primary mechanisms: surface erosion of the floodplain by overbank floods, and bank erosion. This section provides estimates of the rates of erosion of both sediment and lead from the floodplain, which is believed to primarily occur through bank erosion. Bank erosion rate estimates are based on data and analysis documented in a separate study of riverbank characteristics and erosion rates (CH2M HILL, 2014a).

5.1 Floodplain Surface Erosion

Erosion of sediment from the floodplain surface is not considered to be a first-order contributor to the overall sediment and lead budget and was not quantified. Field data and observations, and hydraulic modeling, do not indicate that erosion from the floodplain surface would be likely to erode sediment in significant quantities from the floodplain into the active channel. If this process were an important mechanism for eroding the floodplain, the floodplain surface would contain scour marks, potholes, and other evidence of active scour and sediment removal. Widespread evidence of these characteristics is generally lacking.

The following additional considerations further suggest that floodplain surface erosion is a process of limited importance in the Lower Basin:

- Even at the relatively small number of well-defined locations where the hydraulic model shows significant amounts of water exit the channel (CH2M HILL, 2013d)—including at Swan Lake (River Mile 141.5), near Medimont at River Mile 143.7, Strobl Marsh at River Mile 147.8, and near Black Rock Slough at River Mile 151.7—there are not strong physical indications of significant and widespread floodplain erosion. For example, at the entrance to Strobl Marsh, where the hydraulic model and observations showed a large fraction of water was exiting the channel, intact grass cover and a lack of mobile sediment immediately after a flood show that little sediment was eroded or deposited at that location during the flood (Exhibit 45A).
- Overbank shear stresses are generally low throughout most of the floodplain, based on modeled and observed conditions. Even if most of the floodplain area is inundated during floods, much of this area consists of slow-moving or standing water, rather than swift flows (Exhibit 45B). These are depositional, rather than erosional areas.
- The surface of the floodplain is, in most areas, vegetated with low brush and wetland vegetation, preventing substantial surface erosion from occurring (while providing evidence that widespread surface erosion does not occur).
- The amount of time in which floodplain scour is possible is short compared with other processes such as sediment transport in the channel and bank erosion. Floodplain surface erosion is a process that can occur only over a few days every several years, and, even then, may only occur during the rising limbs of hydrographs, in limited distinct locations, when and where flow is actively entering the floodplain.
- Any sediment that is eroded from the exposed floodplain surface is likely to be redeposited in the off-channel lakes and wetlands, such as within Strobl Marsh or Killarney Lake. Thus, most of the sediment that is mobilized by this process never actually enters the main channel

Thus, while it may occur locally, floodplain surface erosion is not considered to be a first-order influence on the sediment budget, so it is not quantified as part of the sediment budget.

5.2 Bank Erosion

Lateral bank erosion is perhaps the most visible mechanism for lead mobilization in the Lower Basin (Exhibit 46). Observations and measurements of bank characteristics and erosion rates are documented in detail in a separate report (CH2M HILL, 2014b) and summarized here as follows.

The river is bounded in many places by vertical cut banks with collapsing segments consisting of sediments that contain mine waste. The banks have a consistent layering (stratigraphy) that reflects changes in the mode of delivery of contaminant mine tailings over time during the period of mine waste discharges. Bank erosion and remobilization of this material can occur when over-steepened vertical banks are undercut and collapse. These bank collapses produce coherent blocks, which remain in place for an extended period of time, gradually eroding and supplying sediment and lead to the flow (Exhibit 47).

The visibility and accessibility of eroding banks has contributed to a focus on measuring and mitigating bank erosion over recent decades. Several previous studies have reported on the rates of bank erosion in the Lower Basin (Wetzel, 1994; Flagor, 2002; Box, 2003; Kootenai-Shoshone Soil and Water Conservation District [KSSWD], 2009; and unpublished data summarized by Bookstrom et al., 2004). CH2M HILL also conducted studies and field work to characterize the composition and stratigraphy of the exposed bank material throughout the Lower Basin, and monitored erosion rates using repeat surveys with a terrestrial LiDAR instrument. The results of these studies are discussed in detail in a separate ECSM addendum (CH2M HILL, 2014b).

Estimates of the linear rate of bank erosion in the Lower Basin are based on a compilation and assessment of the available data, which include opportunistic measurements (summarized by Bookstrom et al., 2004), bank erosion pins monitored over 3 years (KSSWD, 2009), and 3 years of LiDAR surveys of five sections of vertically eroding bank, each about 100 m long (CH2M HILL, 2014a). The average rate from the Bookstrom et al. (2004) compilation was about 9 centimeters per year (cm/yr), with a median value of 5.1 cm/yr. The mean and median values from the erosion pins were 10 cm/yr and 2 cm/yr, respectively. The LiDAR bank scanning results ranged from 1 cm/yr to 11 cm/yr, with an average erosion rate of 4 cm/yr. Based on these values, a value of 8 cm/yr was chosen from these to represent the average annual erosion rate of the eroding sections of the riverbanks. This value applies to areas similar to those that were measured, and does not apply to heavily vegetated or artificially protected sections of bank. The rate of 8 cm/yr for eroding banks is considered conservative, tending toward the high end of the measured erosion rates.

An average annual erosion rate of 8 cm/yr equates to an average bank line migration rate of 8 meters in 100 years, or less than one tenth of a channel width per century. This is a very slow migration rate for an unregulated river in the mountainous western U.S., especially as the last century coincided with the period of active mine waste discharges. Nevertheless, the estimated short term bank retreat rates of 8 cm/yr, carried out over a time scale of decades, is consistent with what is known about historic channel bank line positions. Comparisons of historical maps and air photos with the current channel alignment, from the late 1800s to present, show the migration of channel banks of the Lower Coeur d'Alene River below the Cataldo dredge pool to be barely detectable (CH2M HILL, 2013f).

Additional parameters required to compute the mass of sediment and lead attributable to bank erosion between Cataldo and Harrison are summarized in Exhibit 48 and described in more detail in the bank characterization report (CH2M HILL, 2014b). The length of total bank line between the Cataldo and Harrison gages is about 93 kilometers (including both shore lines). A significant proportion of this bank line is armored with riprap, and is not actively eroding. Other portions of the bank line are heavily

vegetated and gently sloping, and are not prone to active erosion. A maximum of 37 percent of the total bank line is estimated to be actively eroding (CH2M HILL, 2014b). Estimates of the average height of the banks (1.85 m) and the thickness of the contaminated deposits exposed in the banks (1.18 m) are based on stratigraphic measurements and sampling at 17 bank exposures between Cataldo and Harrison (CH2M HILL, 2014b). The dry bulk density of bank material is estimated to be 1.51 grams per cubic centimeter (Bookstrom et al., 2001). The thickness-weighted average lead concentration of the contaminated portion of the banks was approximately 6,500 mg/kg (CH2M HILL, 2014b).

Based on these parameters, the approximate mass of sediment mobilized by bank erosion each year in the Lower Basin is around 8,000 metric tons per year. Of this amount, about 40 percent is estimated to be uncontaminated, pre-tailings sediment. By these calculations, erosion of riverbanks contribute about 4,900 metric tons per year of contaminated sediment, containing about 32 metric tons of lead (Exhibit 48).

6 Sediment and Lead Entering the Floodplain

During flooding events, lead-rich sediments can enter the floodplain through tie channels connecting off-channel lakes with the main channel or via overbank flow. These sediments may be deposited in low-velocity areas of the floodplain, defined here as the hydraulically-complex series of lateral lakes, sloughs, marshes, wetlands, and natural levees with varying degrees of connectivity to the river. Contaminated sediment is present in approximately 73 percent (61 square kilometers [km^2]) of the Lower Basin valley floor (Bookstrom et al., 2004).

At the time this addendum was prepared, little new field data on floodplain deposition rates had been obtained since the late 1990s.[11] The most comprehensive data currently available on floodplain deposition of sediment and lead is compiled in the 2004 USGS report, *Baseline and Historic Depositional Rates and Lead Concentrations, Floodplain Sediments, Lower Coeur d'Alene River, Idaho* (Bookstrom et al., 2004). That report computed sediment deposition rates and average lead concentrations based on the volcanic ash layer (from the 1980 Mt. St. Helens eruption) observed in some of the floodplain cores by several studies in the 1990s, and combined these estimates with geomorphic maps of depositional environments to estimate sediment and lead deposition rates throughout the Lower Basin floodplain.

The coring data, while informative, are limited in spatial extent and resolution, and extrapolating point data across the 80 km^2 floodplain area introduces considerable uncertainty into estimates. In an effort to develop more representative spatially-detailed and accurate estimates of floodplain sedimentation, a 1-D hydraulic model of the Lower Basin (CH2M HILL, 2013d) was used in combination with sediment rating curves (discussed in Section 3 of this addendum) and simple assumptions about particle settling and trapping efficiency to provide an independent estimate of the magnitude, and spatial and temporal patterns, of deposition of lead and sediment in the floodplain. The assumptions, uncertainties, and results of this simplified floodplain sediment deposition model are discussed in detail in a separate report (CH2M HILL, 2015b), and are briefly summarized below in the context of the sediment and lead budgets.

6.1 Sedimentation Rates from Floodplain Cores

6.1.1 Data Sources and Methodology

Bookstrom et al. (2004) compiled sediment core data from six separate studies conducted between 1991 and 1998, which included 125 core locations outside of the main channel bed (Bender, 1991; Rabbi, 1994; Hoffman, 1995; Horowitz et al., 1995; Fousek, 1996; and Box et al., 2001). The combined data were compiled from studies that included coring locations based on random selection, as well as on stratified and systematic sampling strategies in focused locations. A "depositional setting" was assigned by Bookstrom et al. (2004) to each core location, based on previous mapping of geomorphic environments in the floodplain (Exhibit 49). Depositional settings were classified as riverbank, upland, palustrine (i.e., wetland), lacustrine-littoral (i.e., shallow areas of lateral lakes), or lacustrine-limnetic (i.e., deeper areas of lateral lakes).

Most sediment core data included regular depth intervals with lead concentrations based on the analysis of sediment in the respective interval. Where present, the depths of two chronological reference markers were noted for each core: the Mt. St. Helens ash layer (1980) and the base of contaminated sediment (assumed to represent a time horizon around 1900). For example, sediments above the Mt. St. Helens layer in a core would be assigned to a time-stratigraphic interval "1980 to XXXX

[11] CH2M HILL, as part of the BEMP program, placed some tiles in the floodplain to capture recently deposited sediment, primarily for the purpose of monitoring time trends in the metals content in suspended sediment, and also has measured the thickness of deposition on those tiles. The deposition rates have been on the order of zero to several centimeters per overbank flood event (CH2M HILL, 2011a, 2011b, 2013a, 2013b); however, the program was not designed to measure sedimentation rates throughout the floodplain at the time and spatial scales considered in this analysis, and therefore those data are not used in this sediment budget analysis.

(year-of-core-collection)" representing the most recent (modern-era) sedimentation rates, and the lead concentration in this material. Deposition rates for individual time-stratigraphic intervals were determined by dividing the sediment depth to the ash by the time elapsed between 1980 and the date of sample collection. Exhibit 50 catalogs the locations and associated modern-era sediment deposition rates based on this method of calculation.

The resulting data were also grouped by the geomorphic environment in which each core was collected, and a median deposition rate and lead concentration was calculated for each depositional setting as mapped by Bookstrom et al. (2004) (Exhibit 51). Bookstrom et al. (2004) recommended using a median (rather than mean) deposition rates, lead concentrations, etc.as a conservative indicator of central tendency for computing contaminated sediment volumes, because the median is less sensitive to extreme and outlying values.

6.1.2 Revised Estimate of Sediment and Lead Deposition Based on Floodplain Core Data Originally Compiled by Bookstrom et al. (2004)

Bookstrom et al. (2004) estimated that 15 times more contaminated sediment was released in the Upper Basin and deposited in the Lower Basin during the pre-modern era (1900-1980) than during the modern-era interval (1980-2013). However, they concluded:

> During episodes of high discharge, lead-rich sediments will continue to be mobilized from large secondary sources on the bed, banks, and natural levees of the river, and will continue to be deposited on the floodplain during frequent floods. Floodplain deposition of lead-rich sediments will continue for centuries unless major secondary sources are removed or stabilized. It is therefore important to design, sequence, implement, and maintain remediation in ways that will limit recontamination.

CH2M HILL reviewed and updated the evaluation of deposition rates by Bookstrom et al. (2004) by making some modifications to assumptions, reach breaks, and study boundaries, but using the same data. One modification was to include all of the cores containing the Mt. St. Helens ash layer (n = 125; Bookstrom et al., 2004), whereas Bookstrom et al. (2004) had used data only from "paired" cores (n = 48)—locations where the cores contained markers for both the modern era (above the ash layer) and the mining era (below ash layer). Whereas the Bookstrom et al. (2004) estimates were made for comparing modern- and mining-era deposition rates and lead concentrations, CH2M HILL's calculation focuses on the modern-day sediment and lead budgets, and so can use data from all the cores containing the ash. This increases the size of the data set used to estimate deposition rates and lead concentrations since 1980 (Exhibit 50).

The CH2M HILL calculations also applied deposition rates over a different area than those used in the original analysis, so that the results would be consistent with the sediment budget being developed as part of this addendum. The rates of sediment mass deposition were determined by multiplying the representative median deposition rate by the sediment bulk density for each depositional unit (Balistrieri et al., 2000 and summarized by Bookstrom et al., 2001), and by the geomorphic area corresponding to each unit. Bookstrom et al. (2004) computed the area of the various geomorphic units (Exhibit 49) in the entire Lower Basin. In contrast, CH2M HILL focused on the area between the Cataldo and Harrison gages (see dashed lines in Exhibit 1) and did not include the entire valley upstream and downstream of those boundaries. Bookstrom et al. (2004) used the median lead concentration for each map unit type to calculate the mass of lead and the amount of lead deposited for each map unit. The total deposition rate of lead on the floodplain was determined by summing the rates of lead deposition for every depositional environment.

Bookstrom et al. (2004) calculated that modern-era annual floodplain deposition was about 194,000 tons of sediment and 500 tons of lead. CH2M HILL's estimates of floodplain deposition, using more points from the same data set, showed somewhat lower annual deposition rates of approximately 156,000 metric tons of sediment and 499 metric tons of lead between the Cataldo and Harrison gages

(Exhibit 51). Although the computed value of deposited lead is nearly identical in the two evaluations, CH2M HILL's analysis only includes deposition between the Cataldo and Harrison gages, and the values generally reflect higher lead concentrations, lower deposition rates, and smaller floodplain areas than those used by Bookstrom et al. (2004).

Recent updates to the sediment budget have resulted in an annual average sediment flux of 67,000 metric tons per year at Harrison (Section 3.0, Exhibit 17)[12]. Even though floodplain sedimentation is known to be an important term in the sediment budget, it is unlikely, though not impossible, that more than twice as much sediment (156,000 metric tons, Figure 51) would enter the floodplain each year than be transported through the river channel past Harrison. According to the calculations in Section 3, only about 22 percent of the total sediment load at Harrison is carried during flows greater than 20,000 cfs, when widespread floodplain flow occurs. Thus, either the sediment flux estimates are too low, or the core-based floodplain sedimentation estimates are too high.

Both the extrapolation of the Bookstrom et al. (2004) cores and the CH2M HILL sediment transport calculations in Section 3 yield values that are considered to contain high levels of uncertainty, but for different reasons. The rating curve calculation contains a high level of uncertainty due to hysteresis, regression uncertainty, and measurement errors. The large amount of scatter in the rating curves at Cataldo and at Harrison (Exhibit 4) imply a large degree of uncertainty in the sediment flux estimates, even though the rating curves are based on relatively large data sets and have strong correlation coefficients (R^2 +~ 0.8). A sensitivity analysis (Section 3.6.5) indicated that an upper bounding estimate of the sediment flux at Harrison of about 143,000 metric tons per year, based on a rating curve that intersected the uppermost SSC measurements, was likely a significant overestimate of the flux because it led to high SSC estimates well beyond the range of measured data. Thus, even if the rating curves underestimated the sediment fluxes, a realistic upper bounding value for the flux is substantially less than 143,000 metric tons per year.

The uncertainties in the core-based deposition rate estimates are caused by the small number of cores relative to the large floodplain area, the order-of-magnitude spatial variability in deposition rates, the relatively high measurement uncertainty in individual cores, and likely sampling and preservation bias. The Box et al. (2001) data used by Bookstrom et al. (2004) to compute sedimentation rates were compiled from a variety of studies that were conducted for differing purposes. As noted by A. Bookstrom (USGS, written communication, 2016), two of the most important specific uncertainties in the coring data include preservation and sampling bias, that would tend to overestimate sedimentation rates based on the data set used:

1. Measurement sites are biased toward sites with high sedimentation rates, because the Mt. St. Helens ash layer is better preserved in natural levees or in highly connected lateral lakes with higher deposition rates. A subset of the Bookstrom et al. (2004) data indicates a clear pattern of diminishing deposition depths with increasing distance from the river (Exhibit 52), but nearly all the samples were collected close to the river.
2. Property access constraints caused a bias toward sampling sites with higher than typical deposition rates, because sampling occurred mostly on public land. Public land is more widespread north of the river, where sedimentation rates are relatively high, and less sampling occurred on private land south of the river, where deposition rates are expected to be lower due to the presence of the former railroad alignment (and present bike path) that prevents flood water from inundating as much land on the south side of the river.

[12] Note that the sediment transport rate at Harrison has since been revised lower than the value of 67,000 metric tons per year as cited here, to 50,000 metric tons per year (see Attachment C for full explanation). The revised sediment transport rate calculation therefore increases the discrepancy between the floodplain deposition rates estimated by Bookstrom et al. (2004) and the computed sediment transport rates. The floodplain deposition rate derived from the cores is a factor of 3 greater than the revised sediment transport rate at Harrison.

The data set compiled and analyzed by Box et al. (2001) and Bookstrom et al. (2004) remain the best available direct data on floodplain deposition rates available for the Lower Basin, though the core-based estimates of floodplain sedimentation are thought to be high due to the low data density, high spatial variability of floodplain environments, and apparent preservation and sampling bias, Until more data are collected to more systematically estimate this term in the sediment budget, the high level of uncertainty associated with floodplain deposition estimates will remain.

To provide an alternative estimate of basin-wide floodplain deposition rates using existing data and resources, an alternate approach was developed to calculate the sedimentation rates. Section 6.2 summarizes the development of a simple 1D floodplain sediment deposition model, based on modeled hydraulics, suspended sediment rating curves, and sedimentation estimates, for this purpose.

6.2 Floodplain Sedimentation Modeling

An independent estimate of floodplain sediment deposition was developed using results from a calibrated 1D hydraulic model (CH2M HILL, 2015b). Unlike the analysis of the coring data, which provides an average sedimentation rate since 1980, the modeling approach provides estimates of both the spatial and temporal distribution of sedimentation rates for a 25 year period (WYs 1988 to 2012, consistent with the time frame used for the sediment and lead transport analyses in Sections 3 and 4). The methods and results from this analysis are summarized below, and are described in greater detail in a separate technical memorandum (CH2M HILL, 2015b).

The general 1D sedimentation estimation approach was to calculate sediment fluxes into hydraulic floodplain "units" used by the 1D model and apply a trapping efficiency (TE) for each unit, describing the proportion of the sediment flux estimated to settle and remain in the floodplain. Both the sediment influx and the TE vary spatially (among floodplain units, due to their geometry and hydraulic characteristics) and temporally (due to the time series of overbank flow during the 25-year period considered).

6.2.1 Approach

The floodplain is represented in the 1D model as two distinct non-channel model element types: "off-channel storage areas," consisting of lakes, marshes, and other large storage elements, and "overbank flow areas," representing near-bank floodplain flow path areas that are in the model as a subset of the total cross section flow. The hydraulics of these types of areas are different, and floodplain sedimentation processes are distinct, justifying the different treatments. The floodplain sedimentation modeling approaches are described in greater detail in a separate technical memorandum focusing on floodplain sedimentation modeling (CH2M HILL, 2015b). The two approaches are briefly summarized here, focusing on the modeling results in the context of the sediment budget.

The portions of the floodplain modeled as off-channel storage areas and as overbank flow areas are shown in Exhibit 53. Off-channel storage areas are labeled by the storage area identification number used in the model, and overbank flow areas are labeled by the approximate river mile and channel location (channel left [L] or channel right [R]). In-text descriptions of specific areas use the area name, where available, and the area identification number in brackets.

Sediment flux, TE, and sediment trapped were calculated using a time series of 1D hydraulic model results, consisting of 6-hour steps for off-channel storage areas and 12-hour steps for overbank flow areas. Sediment flux into each unit was computed as the product of flow entering the floodplain and the suspended sediment concentration. SSC was based on the total river flow, as modeled locally, and on the bulk SSC rating curve (e.g., Exhibit 4B) for the station nearest each off-channel storage area or overbank flow area.

The TE for the off-channel storage area model elements was calculated using the modified Churchill reservoir TE equation (Roberts, 1982, modification of Churchill, 1948), an empirical equation that relates TE to reservoir geometry (length and volume) and reservoir inflow. The original Churchill equation was based on reservoirs containing mostly silt-size sediments and thus may over-predict TE if sediments are highly colloidal, and may under-predict TE for coarser-grained sediments.

The TE for the overbank flow areas was computed by estimating the ratio of the vertical distance a particle will fall over a given flow path to the average depth of water across the overbank flow area.) The necessary parameters for water depth, velocity, and flow path length in each overbank flow area were derived from 1D model results, and based on a single cross section that was selected to be representative of the flow area; therefore, these calculations contain some subjectivity and uncertainty.

This modeling approach includes a number of assumptions, approximations, and uncertainties. Ten separate sources of uncertainty in the sedimentation analysis were identified and selected for quantitative sensitivity analysis, and are summarized in Exhibit 54. While the quantitative sensitivity analysis was not extended to the full basin and the various sources are not additive, a reasonable estimate of overall uncertainty is +/- 50 percent, with a greater chance that the basin-wide average of sedimentation is an overestimate than an underestimate. These uncertainties and limitations are outlined in more detail in the separate technical memorandum focusing on floodplain sedimentation modeling (CH2M HILL, 2015b).

6.2.2 Results

The 1D floodplain sediment deposition model predicts that, on average, floodplain deposition accounts for about 24,000 metric tons per year of sediment (12,000 to 36,000 metric tons per year of sediment when considering uncertainty) and 68 metric tons per year of lead entering the floodplain. These values are roughly 4 times lower than the core-based estimates (100,000 metric tons per year) modified[13] from analysis by Bookstrom et al. (2004 and CH2M HILL).

Trapping efficiency for the floodplain units is shown in Exhibit 55. Results are presented for the 25-year period of record as well as for 1996 and 2008, years noted for large winter and spring floods, respectively. As expected, TE is highest in floodplain areas with low flow (and velocity), and is lowest in areas with higher floodplain flow. Thus, areas that experience large overbank through-flows, such as the Killarney Lake system (Strobl Marsh [1257], Killarney Lake [1261 & 1260] and Moffit Slough [1259]), and the Swan Lake system (Swan Lake [1265], Blue Marsh [1239], and Blue Lake [1240]), have the lowest TE, with predictions that between 10 and 50 percent of the sediment entering will be deposited. In contrast, the model predicts that most of the sediment entering low-flow areas such as Cave, Thompson, and Medicine Lakes will remain (TE > 80 percent). These lakes exchange water predominantly through limited, confined access points such as a tie channel, and TE is expected to be higher because these areas fill during the rising stage of floods, and remain full for days during high water, so the residence time of particles in those areas is longer.

It should be noted that Blessing Slough (the area in the right floodplain connecting Moffit Slough [1259] and Swan Lake [1265]) has hydraulics more similar to a channel than a floodplain; it carries large flow volume and has a small cross sectional area and thus TE and sedimentation rates were not evaluated for this unit using the same assumptions as the overbank flow areas.

The mass of sediment deposition for each floodplain unit was computed as the product of sediment flux and TE for individual time steps, and then summed over each water year or averaged for the entire 25-year period (Exhibit 56). As noted before, the majority of floodplain sediment influx occurs during floods. The floodplain sedimentation values are much higher during high-flow years than during average years (Exhibit 56), despite those high-flow years having lower TE.

[13] Floodplain deposition values were modified from Bookstrom et al. (2004) as described in Section 6.1.2 and Exhibit 43 of this addendum.

The mass of sediment deposited in each unit was also normalized by area to provide an average deposition depth (Exhibit 57). Average sedimentation rates from USGS core samples (Bookstrom et al., 2004) and BEMP sediment tiles (e.g., CH2M HILL, 2011a, 2011b, 2013a, 2013b) are shown in Exhibit 58 for comparison. These depositional thicknesses assume an average inundation area, determined from 1D hydraulic model results; the 2D model currently in development may help refine the predictions of sediment deposition thicknesses. BEMP sediment tile data shown in Exhibit 58 were obtained for WYs 2011, 2012, and 2013, but are compared with average modeled deposition rates from a 25-year period of record.

Overall average sedimentation rates predicted by the model are highest in Blue Marsh (1239) and in the overbank area 163_L (near the Cataldo gage), with predicted average rates above 10 mm/year. These areas have high-flow sediment influx rates, and high sedimentation mass relative to their depositional areas.

Comparison with Estimates Based on Coring Data

Overall, the best estimates of sediment deposition rates using the 1D model are lower than those estimated from modified USGS core analysis. However, considering the uncertainty of both the 1D sedimentation deposition model and the core-based estimate, the two methods show some agreement, with overlapping result ranges (12,000 to 36,000 metric tons per year based on sedimentation deposition model and 25,000 to 207,000 metric tons per year based on modified core analysis).

A number of reasons, some discussed in the previous section (Section 6.1.2), may account for the modeled sediment deposition rate being lower than the sedimentation rate derived from the cores. As discussed above, the limited number of cores had to be assumed to represent large floodplain areas, propagation of small errors in measurement, along with sampling bias and preservation bias may have contributed to estimated sedimentation rates higher than average for a given unit type. Alternately, it is possible that the modeling under-predicts sedimentation rates, due to uncertainties discussed in a separate report (CH2M HILL, 2015b) and summarized in Section 6.2.1 and Exhibit 52, which relate to underestimation of flow and/or sediment flux into the floodplain, or underestimation of trapping efficiencies. However, though the sedimentation model is known to have a high level of uncertainty due to many possible factors, there is no known reason why the multiple sources of model uncertainty should all tend towards under-prediction of the actual rates.

Values for average annual sedimentation rates, shown graphically in Exhibits 55 through 57, are provided in tabular form in Exhibit 58. This exhibit also shows a conversion of sediment mass to mass of lead, using bulk sediment lead concentrations (using the average lead concentration in suspended sediment at the gaging station closest to each off-channel storage element or overbank flow area). As discussed in Section 4.2, the lead concentration on sediment can vary, especially at Harrison; therefore, the predicted values of lead mass entering the floodplain contain an additional element of uncertainty, and, therefore, the lead estimates are considered more uncertain than those for sediment.

Overall, the model estimates floodplain deposition of about 24,000 metric tons per year of sediment and 68 metric tons per year of lead in the Lower Basin. As noted previously, these estimates are roughly 7 to 8 times lower than those derived from the coring data. When considering uncertainty of both the sedimentation deposition model and the core-based estimate, the two methods show some agreement with overlapping result ranges (12,000 to 36,000 metric tons per year based on sedimentation deposition model and 25,000 to 207,000 metric tons per year based on modified core analysis). Similarly, when considering the comparison of individual core sedimentation rates and model-derived rates (Exhibit 58, Panel C), patterns of agreement arise, such as absolute core depths in Swan Lake and the observation that cores in Swan Lake have some of the highest measured deposition rates.

The core analysis and model-based sedimentation analysis are fundamentally different. For example, the modeled predictions include estimates of the amount of water and sediment that enter the

floodplain and from this calculate average deposition over large areas, whereas the coring data provide point estimates at widely spaced intervals that are then used to extrapolate deposition rates over large areas. Keeping in mind their individual strengths and uncertainties, both the USGS core estimate and the model-based sedimentation estimate can be used to guide decisions regarding additional sampling, pilot testing, and related evaluations until the more reliable sediment transport model is completed (scheduled for 2016).

6.2.3 Temporal Patterns in Sediment and Lead Deposition in the Floodplain

Floodplain sediment deposition occurs primarily when flow overtops bank lines, although exchange also occurs through tie channels into the off-channel storage reservoirs at flows below bankfull (approximately 20,000 cfs in the Lower Basin) (CH2M HILL, 2010a). Thus, the largest sediment fluxes to the floodplain occur during high-flow years and high-flow events (as can be observed in Exhibit 52 where the greatest core depths are observed in samples collected after the large 1996 event). Panels A and B of Exhibits 55 through 57 show the TE, deposition mass, and deposition rate results for the high-flow years of 1996 and 2008, while Panel C in each exhibit shows the 25-year average values. The data from 1996 and 2008 WYs combined account for nearly 40 percent of the total sediment deposited during the 25-year modeled period (WYs 1988 to 2012) on the Lower Basin floodplain.

Exhibit 59 shows the annual, spatially averaged TE, along with the predicted annual sediment mass deposition for the Lower Basin. The model predicts a higher rate of floodplain sedimentation in WY 1996 than in 2008. This finding contrasts with sediment and lead fluxes for the river, which were dominated by WY 2008 (e.g., Exhibit 16). The difference, however, is consistent with and complementary to the explanations presented in Section 3.6: in 1996, exchange with the floodplain from the channel was significant, and had the effect of attenuating peak flow at Harrison, whereas in 2008 the sustained flow reduced off-channel attenuation during a larger portion of the flood cycle, with longer and higher flows at Harrison compared with 1996. Thus, it would be expected that an event routing large volumes of floodwater out of the channel for a longer period would result in the greatest amounts of floodplain sediment deposition.

Floodplain sedimentation is driven by the largest flood events. The highest estimated floodplain sedimentation rates occurred in 1996, 1997, 2002, 2008, 2011, and 2012, with these 6 years accounting for 78 percent of the total mass deposited over 25 years. In other words, the short periods of overbank flooding during one quarter of the WYs account for three quarters of the sediment deposition in the floodplain. In contrast, the same 6 years account for only 66 percent of the 25-year total sediment flux at Harrison.

6.2.4 Spatial Patterns in Sediment and Lead Deposition in the Floodplain

Modeled sediment deposition results indicate that there is considerable variability by area (Exhibit 60A). The largest estimated mass of sediment is deposited in the off-channel storage areas of the Killarney Lake system (Strobl Marsh [1257], Killarney Lake [1261 & 1260], and Moffitt Slough [1259]), and in Swan Lake (1265). These two complexes, the Killarney Lake and Swan Lake flow systems, are estimated to receive about 6,000 metric tons or more of sediment per year, accounting for more than half the total off-channel deposition in the Lower Basin.

During high-flow years, a large amount of sediment is also deposited in floodplain overbank flow areas 160_R and 163_L (Exhibit 57B), near the Cataldo Mission and Cataldo, respectively. Of the 48 off-channel and overbank deposition areas shown in Exhibit 60, 5 have an annual average deposition rate of more than 1,000 metric tons per year, accounting for two thirds (67 percent) of the floodplain deposition of sediment and lead; and the top 11 have an annual deposition of more than 500 metric tons per year, accounting for 82 percent of the floodplain deposition of sediment and lead.

7 Sediment and Lead in Storage in the Lower Basin

Sediment and lead are primarily stored within two types of reservoirs in the Lower Basin: the floodplain and the channel bed. The floodplain is here defined as the land adjacent to the river channel where out-of-channel flows have historically or could deposit contaminated sediment—this includes lakes, marshes, and occasionally flooded areas. The channel bed storage reservoir is defined as the historic sediment underneath the low-flow wetted perimeter of the channel when Coeur d'Alene Lake is at the elevated summer pool elevation. For the purposes of volume calculations and the sediment budget, the upstream and downstream boundaries of the floodplain and channel are defined by the locations of the Cataldo and Harrison USGS river gages, respectively.

Over the past several decades, the compositions of the bed and floodplain have been investigated with a variety of means. This section compiles information from previous and ongoing studies to develop a provisional estimate of the mass of contaminated sediment and lead currently stored in the Lower Basin. While a substantial amount of data has been collected to characterize different aspects of sediments in the riverbed and floodplain, estimates of the inventory of contaminated sediment and lead in the channel and floodplain are not well constrained. The sediment and lead mass inventories reported on this section are considered provisional because the estimates use extrapolations of decades-old data, or of newer data and analyses that were unpublished and considered provisional at the time this addendum was completed.

The floodplain inventories are derived from data published by Bookstrom et al. (2001), Box et al. (2001), and Bookstrom et al., (2004). The primary data used to compute the channel bed sediment and lead inventories, along with the computational methods to arrive at these values, will be fully documented in the forthcoming TM Addendum E-6 about riverbed characterization (CH2M HILL, pending publication), and are only summarized below.

The estimates of sediment and lead masses described in this section are based on data, but they are considered provisional; these estimates are expected to improve with the additional data that will likely be collected in the future. Estimates provided here are intended to generally constrain the estimates for the purposes of the sediment budget—they are not intended to be used for costing or planning purposes.

7.1 Floodplain Storage

For the purpose of the sediment budget, the floodplain reservoir of sediment is assumed to be the contaminated portion of the floodplain between the Cataldo and Harrison gaging stations (Exhibit 1). The floodplain, for purposes of this evaluation, includes all the lakes, marshes, and upland (normally dry areas that are occasionally flooded by the river) bounded by the valley walls. Lead-rich sediments (following previous convention, sediment containing at least 1,000 mg/kg of lead) cover the surface of about 60 km^2 of the 84 km^2 (21,000 acres) of the valley floor (Bookstrom et al., 2004).[14]

As observed by Bookstrom et al. (2004), the rate of floodplain deposition was high during the peak mining era, and decreased measurably after cessation of direct discharge of tailings in 1968. The amount of contaminated sediment in the floodplain remains, generally speaking, poorly constrained because of the diversity of environments in the large floodplain, and because most previous studies focused on more detailed local measurements. There has not yet been a systematic and widespread coring effort aimed at creating a system-wide inventory of sediment and lead in the Coeur d'Alene River floodplain. Bookstrom et al. (2004) compiled all the field data available at that time, and used the compiled coring

[14] The floodplain as studied by Bookstrom et al. (2004) extended from the confluence of the North and South Forks of the Coeur d'Alene River near Enaville to the mouth of the river at Coeur d'Alene Lake near Harrison. The spatial extent considered here is smaller than that. To develop sediment and lead inventories corresponding to the sediment budget in the rest of this addendum, the upstream and downstream boundaries of the river are defined as straight lines across the valley floor crossing through the USGS gages at Cataldo and Harrison, respectively.

data set to produce their estimates. The data set primarily uses data from floodplain coring studies that were carried out by multiple groups in the 1990s. A subset of these coring data (specifically, those cores in which the Mt. St. Helens ash layer was identified) was used in Section 6.1 to estimate the modern day rate of floodplain deposition, and the data set is discussed in more detail in that section. However, the data set for computing sediment inventory is greater than for computing the sedimentation rate because the inventory estimates can also include data from cores that did not contain the Mt. St. Helens ash layer.

The current estimate of the amount of contaminated sediment and lead stored on the Coeur d'Alene floodplain is based on data presented by Bookstrom et al. (2004), and uses the same approach, but has been modified here in two ways: (1) the boundaries were changed to reflect the geographic limits of the sediment budget (see Footnote 13) and (2) the estimates of Bookstrom et al. (2004) were projected to 2013 for consistency with the time span considered in the sediment budget.

The calculation of sediment inventory follows Bookstrom et al. (2004)'s stratigraphic approach, in which two separate stratigraphic intervals were considered: 1903 (assumed) to 1980 (pre-modern), and 1980 to 1993 (date of many of the cores), separated in many of the cores by the Mt. St. Helens ash layer. Bookstrom et al. (2004) assumed that the base of the contaminated sediment in cores represents a time horizon of approximately 1903, coincident with initial reports of historic mining deposits reaching the Lower Basin. The volumetric sediment deposition rates for the 1903–1980 interval was computed by dividing the thickness of the pre-modern layer by 73 years. Likewise, the modern (post-1980) deposition rate was computed as the thickness of sediment above the ash layer divided by the time between 1980 and the core sampling date. Bookstrom et al. (2004) multiplied the median deposition rate for both the pre-1980 and post-1980 (modern) periods for each of the mapped depositional units (Exhibit 49). For the purpose of the present study, the sediment inventory was modified by adding an additional volume of sediment equivalent to 20 more years of the modern deposition rate, to represent the time period between 1993 and 2013 (Exhibit 51; rows under the subtitle "Calculation of Mass of Contaminated Sediment").

Using this approach, the total volume of contaminated sediment stored in the floodplain as of 2013 was estimated to be 17 million cubic meters (m^3); or 19.2 million metric tons (assuming the area-weighted median bulk density of floodplain sediment is 1.13 metric tons/m^3; Bookstrom et al., 2001). Using the median lead concentrations for each depositional unit within the floodplain, and within each of the two stratigraphic units (i.e., 1903–1980, and 1980–2013), the total amount of lead stored in the floodplain between Cataldo and Harrison gages was estimated to be 111,000 metric tons (Exhibit 51). Lead and sediment estimates from the 1903 to 1980 layer contain about 90 percent of the sediment (15.3 million tons) and lead (105,000 tons) in the floodplain, with only 10 percent estimated to have been deposited since 1980.

The values shown in Exhibit 51 for the floodplain sediment inventories are considered to be very approximate, and, in particular, could be overestimates of the actual amounts of contaminated sediment in the floodplain. As discussed in detail in Section 6.2 and a separate report (CH2M HILL, 2015b), there is an apparent discrepancy between the sedimentation rates based on cores and sedimentation rates derived from a prediction based on suspended sediment data, flow history, and a 1D hydraulic model. Though Bookstrom et al. (2004) used the best available data and a sound and logical approach to compute the sediment inventories, the floodplain coring data set is limited compared with the size of the Lower Basin, and the data sets were not collected following the same procedures, or using a systematic sampling plan in order to create a system-wide sediment inventory. The 125 cores used to compute the sediment inventory in Exhibit 51 is based, on average, on one data point per 168 acres of floodplain area. In addition, the majority of those points where data are available are concentrated in a few areas of highest interest to those studies, such as near-channel areas where sedimentation rates are highest.

Given the high degree of data uncertainty in these floodplain sediment inventories, the floodplain storage mass estimates in Exhibit 51 should not be used for any costing or engineering design purposes.

7.2 Channel Bed Storage

A number of efforts have been devoted over several decades to characterizing sediment in the Lower Basin riverbed. Much of this work was done in the 1990s and compiled and presented by Bookstrom et al. (2001), Box et al. (2001), and EPA (2001), and used by EPA in the development of the RI/FS (USEPA, 2001). To fill gaps in this data set, extensive field data collection and analysis activities were performed by CH2M HILL for EPA during numerous data collection activities between 2012 and 2015. The new data and analyses will be presented in detail in the forthcoming TM Addendum E-6 about riverbed characterization (CH2M HILL, pending publication). However, because a subset of those findings are necessary to close the sediment budget, the channel bed sediment inventory results are provided prior to providing a complete explanation of how they were developed. The full justification of these findings is left for the upcoming riverbed report.

This section first summarizes the channel bed storage estimates from the USGS data set from the 1990s, and then provides the provisional results of the newer study.

7.2.1 Estimation of Sediment and Lead Mass in the RI/FS as Computed by Bookstrom et al. (2001)

The Coeur d'Alene River remedial investigation/feasibility study (RI/FS) (EPA, 2001) included a preliminary estimation of the mass of contaminated sediment in the Lower Basin based on coring, mapping, and geophysics conducted in the 1990s, and subsequently analyzed by Bookstrom et al. (2001) (Exhibit 61). Bookstrom et al. (2001) subdivided the river into six contiguous "Estimation Units," (Exhibit 62) establishing a single constant thickness of mining-era sediments for each unit, based on a combination of coring and ground penetrating radar (GPR) soundings of the riverbed. The coring determined thicknesses based on the presence or absence of lead above background levels in cores. The cores were collected in 1994, 1995, and 1997 using a variety of methods (and bracketed the large 1996 flood). GPR soundings (330) were conducted along five transects near each of the coring transects. The details of the GPR data analysis are apparently not documented, but Bookstrom et al. (2001) provide mean and median thicknesses for each "Estimation Unit," based on a combination of coring and GPR data. The estimated thicknesses of contaminated sediment varied from 0 to 8.4 m, with some of the thicker values in the upstream areas just downstream of the Cataldo dredge pool (Exhibit 62). Bookstrom et al. (2001) concluded that the median thickness of contaminated sediment decreased in the downstream direction, from about 3.8 m in Estimation Unit R-2 (between Cataldo and Rose Lake) to 1.62 m in R-6 (near Harrison) (Exhibit 61). (Estimation Unit R-1 included the highly disturbed portion of the river at the former dredge pool).

Bookstrom et al. (2001) used these estimates of contaminant thicknesses, estimates of the channel bed area and of the channel sediment dry density (assumed to be 1.61 metric tons per m^3) to compute that 17.54 million metric tons of contaminated sediment were stored in the riverbed. Of that amount, Unit R-6 is mostly downstream of the Harrison gage. The estimated mass of contaminated sediment in units R-1 through R-5, which closely approximates the sediment budget boundary shown in Exhibit 1, is about 16 million metric tons (Exhibit 61). The estimate of the amount of contaminated sediment in the RI/FS (EPA, 2001) provided slightly different values based on different reach breaks, but were also based on the analyses by Bookstrom et al. (2001), and likewise provides an estimate of the amount of contaminated sediment in the riverbed of approximately 16 million metric tons.

Bookstrom et al. (2001) computed the amount of lead stored within this sediment by estimating typical values of lead concentration in riverbed sediments. They note that lead concentrations in contaminated sediments vary greatly throughout the Lower Basin, but generally increase with age of the deposit, so

early post-mining sediments are generally more contaminated than more recently deposited sediments. At a given location, there is therefore likely to be a range of lead concentration in the vertical stratigraphy, with more highly contaminated sediments underlying less contaminated deposits.

Bookstrom et al. (2001) reported mean and median values of "thickness-weighted average" lead concentrations in the riverbed for each of the six Estimation Units (Exhibit 61). These concentrations varied between 2,300 and 2,400 mg/kg (median and mean, respectively) in the vicinity of the Cataldo dredge pool, to 9,000 to 10,000 mg/kg in Estimation Unit R-4, between Killarney Lake and Medimont. Bookstrom et al. (2001) estimated an overall thickness-weighted mean concentration of 7,100 mg/kg for the Lower Basin riverbed sediments. Using these estimates and estimates of the total mass of contaminated sediment in the riverbed, they developed a median-based estimate of 129,000 metric tons of lead stored in the river channel between Estimation Units R-1 through R-6. For consistency with the boundaries of the current sediment budget, the total lead mass in the channel bed in Estimation Units R-1 through R-5 by Bookstrom et al. (2001) is recomputed here as 117,000 metric tons of lead (Exhibit 61).

7.2.2 Estimation of Contaminated Sediment Mass and Lead Mass Based on Riverbed Mapping and Coring in 2012 and 2013

Additional riverbed coring was undertaken by CH2M HILL in 2012 and 2013 to supplement the cores collected in the 1990s. The additional coring was conducted to improve and update understanding of the extent of riverbed contamination, constrain the estimates of contaminated sediment and of lead, and help parameterize a two-dimensional (2D) sediment transport model being developed for the Lower Basin. As mentioned above, this current addendum only summarizes these studies, pending more complete discussion in the forthcoming TM Addendum E-6 about riverbed characterization (CH2H HILL, pending publication).

In 2012, about 70 cores of riverbanks and the riverbed were collected along eight transects between the Dudley Scour Hole and Harrison (River Mile 158.3 to River Mile 133.5) (Exhibit 62), using a vibracore device, with three of these transects including terrestrial coring in the riverbank and floodplain. Like the investigations performed in the 1990s (Bookstrom et al. 2001), the 2012 cores were collected in transects, with most at relatively straight stretches of the river in areas where the bed is dominated by dunes. Some transect locations were chosen to complement transects from earlier studies. The stratigraphy in each core was evaluated in the field using geologic indicators and a field X-ray fluorescence (XRF) instrument. The field XRF provided measurements of lead concentrations in the core and was useful for delineating stratigraphic boundaries and identifying the transition from contaminated and uncontaminated sediment. The 2012 vibracore transects confirmed Bookstrom et al. (2004)'s contention that lead appears to increase with depth below the riverbed surface to a sharp buried horizon below which is "native" sediment (defined as sediment with background levels of lead). Some of the 2012 cores found deposits of very highly contaminated sediment, with as much as 7 percent lead by mass (70,000 mg/kg) as far downstream as Harrison, and other cores found native sediment exposed at the surface. That effort demonstrated that the stratigraphy of the riverbed does not vary smoothly downstream, but can vary drastically between locations in close proximity to one another.

Following the 2012 coring effort, additional investigations of the riverbed sediment were undertaken using multibeam bathymetry, geomorphic mapping and more laboratory investigations. This work culminated in an extensive riverbed coring effort conducted in September 2013, in which 315 shallow vibracores, and 19 deep sonic drilling cores were collected from the riverbed (Exhibit 62). The primary purpose of the 2013 vibracore data collection was to characterize the horizontal and vertical distribution of grain size, lead, and contaminant thickness with an adequate resolution to create a continuous three dimensional representation of the upper 2 m of the riverbed, which is required as input for a 2D sediment transport model currently being developed by CH2M HILL.

Instead of conducting coring on a grid-like sampling pattern or along a set of spaced transects, the sampling approach for the 2013 shallow vibracore effort was based on the hypothesis that relatively similar geomorphic environments will contain similar stratigraphy. Based on this hypothesis, a geomorphic map of the riverbed was created using high-resolution bathymetry, which delineated the spatial distribution of dunes, planar bed areas, scour holes, side slopes, and other recurrent geomorphic features in the bed (Exhibit 63). Based on this mapping, a stratified coring plan was developed to sample the sediment characteristics of the upper (approximately 2 m) of the riverbed, covering the range of bedform environments and providing adequate spatial upstream-to-downstream coverage. Unlike the previous coring efforts that focused primarily in dune areas, the 2013 coring was planned to sample all the different geomorphic environments. However, the 2013 shallow coring effort emphasized characterization of the upper 2 m of the riverbed, because the primary purpose was parameterization of the sediment transport model. Thus, most of the 2013 vibracores did not penetrate to the depth of native sediment.

In addition, sonic drilling cores were also collected in 2013 at 19 locations, along 4 transects (Exhibit 62). The drilling method was needed to advance coring equipment beyond the relatively shallow limits of the vibracore equipment in the Coeur d'Alene riverbed, and allowed a high degree of accuracy in documenting the depth intervals of cores and sediment characteristics, including documentation of the native sediment horizon. These cores, relative to previous cores along the same transects, provide more accurate indication of contaminant profiles at depth and of the total depth of contaminated sediment. The sonic drilling cores were limited, however, to a half mile segment of the Dudley Reach dominated by dunes.

Based on the mapping and vibracoring results from 2013, estimates of the total amount of contaminated sediment present in the riverbed were recalculated, based on bedform area, and where possible, maximum depth of contamination (forthcoming TM Addendum E-6, CH2M HILL, pending publication). Where native sediment was not encountered (primarily within areas where dunes and planar sand beds predominate), a range of thicknesses between 6 feet and 15 feet was used to estimate the volume of contaminated sediment. The resulting sediment mass computed this way was estimated at 4 to 8 million m^3, or 6 to 13 million metric tons[15], depending on the assumed thicknesses of sediments in the dune and planar bed areas (Exhibit 64). Because many of the cores did not reach the base of contamination, the actual thickness of the non-sampled sediments is not well known; however, based on the thickness of contaminated sediment in sonic cores collected in dunes, which were typically 12 to 16 feet thick, it is more likely that the total volume is closer to the upper end of the range than the lower end. Assuming typical lead concentration of 5,000 mg/kg, the contaminated riverbed sediment would contain between 30,000 and 65,000 tons of lead, a value that is considered to be an underestimate,[16]

These approximate and provisional estimates of sediment and lead inventory in the channel are provided for the purpose of comparison with other elements of the sediment budget. However, due to insufficient data, the values are not well known and are subject to revisions. These values should not be used for any specific planning purposes.

---

[15] These values are considered highly provisional but are provided for the purpose of completing the sediment budget and not to be used for planning purposes. Refer to forthcoming TM Addendum E-6 about riverbed characterization (CH2M HILL, pending publication) for updated estimates of the channel bed sediment and lead masses.

[16] This value is a rough estimate, and likely an underestimate. The range of concentrations in the bed vary from less than 10 mg/kg to nearly 70,000 mg/kg, and, thus, using a single representative value is subject to substantial error. Additionally, most of the more highly contaminated sediment is more deeply buried, below the 2 m sampling depth of the 2013 cores. For simplicity here, for the purpose of the inventory calculation, an approximate average value of 5,000 mg/kg (0.5 percent by mass) of lead on sediment was used as a "round number" that is approximately representative of the depth-weighted average value for the upper 2 m of sampled sediments. Since most of the most highly contaminated sediment is unsampled, this number, and, therefore, the estimate of the lead inventory, is probably an underestimate.

7.3 Sediment and Lead Budgets of the Lower Basin

A sediment budget is a systematic accounting of sediment transport, deposition, mobilization, and storage in a drainage basin or other clearly defined portion of a landscape (Dietrich et al., 1982; Reid and Dunne, 1996). Sediment budgets of rivers attempt to quantify and explain the processes of erosion, transport, and storage as well as the masses of temporary and permanent reservoirs in which sediment is stored**.** The simplified conceptual model of the sediment budget of the Lower Basin is illustrated in Exhibit 2. The preceding sections addressed the component processes of a sediment budget for the Lower Basin, and this section combines this information to summarize the sediment and lead budgets of the Lower Basin.

One of the primary purposes of developing an overall sediment and lead budget is to provide a framework for understanding and comparing the absolute and relative importance of different processes. Sediment budgets are used in resource assessments in which land managers need to anticipate the erosion or deposition response to potential changes in hillslope or channel processes (Reid and Dunne, 1996). For example, in the Lower Basin, understanding the relative proportion of bank erosion and sediment transport rates can help understanding of the potential impact of remedial measures on the transport of contaminated sediment and lead downstream. Similarly, a sediment budget can help inform understanding of the role of floodplain deposition in storing sediment and lead.

Based on the data analyses, modeling, and evaluations presented in Sections 1 through 7, Exhibit 65 compiles the estimated annualized sediment and lead budgets for the Lower Basin. These values are necessarily approximations, based on limited data representing different time periods, a large number of simplifying assumptions, and a high level of uncertainty. However, the updated budget reasonably represents the approximate magnitude and relative importance of the different components of sediment and lead dynamics in this system.

For ease of evaluation, the sediment and lead transport processes are subdivided into (a) sediment and lead "sources," which mobilize sediment in the active system and include influx from upstream, erosion of the bed, and erosion of the banks; and (b) sediment and lead "sinks," where mobilized sediment and lead are deposited—mobilized materials either enter the floodplain, or exit the system and enter Coeur d'Alene Lake (Exhibit 66).

An estimated 31 million metric tons of contaminated sediment are present in the Lower Basin between Cataldo and Harrison, containing around 170,000 metric tons of lead (Exhibit 65). Although more contaminated sediment and lead are stored in the floodplain than the channel, the channel accounts for the largest source of ***mobile*** lead and contaminated sediment: on average, about 50,000 metric tons of contaminated sediment containing 250 tons of lead is estimated to erode from the riverbed annually. By comparison, only about 5,000 tons of sediment containing around 30 tons of lead are supplied by bank erosion. Inflows from the Upper Basin at Cataldo account for about 30,000 metric tons per year of contaminated sediment, but due to the lower lead concentrations in sediment entering from the Upper Basin, these sediments contain only around 30 tons of lead. About 25,000 tons of sediment containing about 70 tons of lead enter the floodplain each year[17], and around 70,000 tons of sediment and 250 tons of lead enter Coeur d'Alene Lake (Exhibits 65 and 66).

In general terms, the riverbed is the source of most of the sediment and lead moving in the system; by comparison, contributions from the riverbanks and inflow from the Upper Basin are relatively minor. As a result of the sediment deficit between Cataldo and Harrison, the river appears to be gradually eroding through legacy deposits of contaminated sediment stored in the bed. The sediment deficit in between Cataldo and Harrison, along with the other sediment budget components, would imply that riverbed is

[17] Estimate is based on simplified 1D floodplain sedimentation model (CH2M HILL, 2015b); the estimate based on floodplain cores is much higher than this, as discussed in Section 6.

degrading at a rate of roughly one to several centimeters per year (net, averaged over the entire channel; erosion is not evenly distributed) (CH2M HILL, 2014c). Once mobilized, most of the contaminated sediment that is eroded from the riverbed enters Coeur d'Alene Lake, but a substantial fraction (about 20 percent) also enters the floodplain and is deposited there (Exhibit 66).

The proportional contributions of sediment and lead to the overall budget vary (Exhibit 66), reflecting the legacy of contaminant supply and storage in the system. For example, although about 35 percent of mobile *sediment* in the Lower Basin enters from the North and South Forks, this influx accounts for only 11 percent of the *lead*. Conversely, whereas erosion of the riverbed in the Lower Basin supplies about 60 percent of the sediment mass, this erosion accounts for nearly 80 percent of the lead (probably more, as the lead concentration assumed for the channel sediments is probably an underestimate as explained in Footnote 15). This reflects the higher concentrations of lead in riverbed sediment compared with sediment that enters the system at Cataldo.

In summary, contaminated sediments from earlier mining operations remain stored in the riverbed, and erosion of these legacy deposits continue to be the primary source of lead in the system. More highly contaminated sediments are generally stored beneath the surface. Thus, continued net degradation indicated by the sediment budget and supported by long-term monitoring data (CH2M HILL, 2014c) suggest that, without intervention, the riverbed could increase as a source of lead over time (Exhibits 65 and 66).

8 References

Balistrieri, L.S., Box, S.E., Ikramuddin, Mohammed, Horowitz, A.J., and Elrick, K.A. 2000. *A Study of Porewater in Water Saturated Sediments of Levee Banks and Marshes in the Lower Coeur d'Alene River Valley, Idaho; Sampling, Analytical Methods, and Results*. U.S. Geological Survey Open-File Report 00-126, 62 p.

Bender, C.F. 1991. *Investigation of the Chemical Composition and Distribution of Mining Wastes in Killarney Lake, Coeur d'Alene Area, Northern Idaho*. M.S. Thesis, University of Idaho. Moscow, Idaho.

Berenbrock, C. and A. Tranmer. 2008. *Simulation of Flow, Sediment Transport, and Sediment Mobility of the Lower Coeur d'Alene River, Idaho*. Scientific Investigations Report 2008–5093. U.S. Geological Survey. Reston, Virginia.

Beschta, R.L., 1987. "Conceptual Models of Sediment Transport in Streams." In: Thorne, C.R., Bathurst, J.C., Hey, R.D. (Eds.), *Sediment Transport in Gravel-bed Rivers*. Wiley, New York, pp. 387-419

Bookstrom, A.A., Box, S.E., Campbell, J.K., Foster, K.I., and Jackson, B.L. 2001. *Lead-rich Sediments, Coeur d'Alene River valley, Idaho; Area, Volume, Tonnage, and Lead Content*. U.S. Geological Survey Open File Report OF 01-140, 44 p.

Bookstrom, A.A., Box, S.E., Fousek, R.S., Wallis, J.C., Kayser, H.Z., and Jackson, B.L. 2004. *Baseline and Historic Depositional Rates and Lead Concentrations, Floodplain Sediments, Lower Coeur d'Alene River, Idaho*. U.S. Geological Survey Open-File Report OF 2004-1211.

Bookstrom, A.A., Box, S.E., Jackson, B.L., Brandt, T.R., Derkey, P.D., and Munts, S.R. 1999. *Digital Map of Surficial Geology, Wetlands, and Deepwater Habitats, Coeur d'Alene River valley, Idaho*: U.S. Geological Survey Open-File Report 99-548,121 p.

Borden, C. and P. Goodwin. 2001. *Simulation of Flow and Sediment in the Lower Coeur d'Alene River: A Demonstration*. University of Idaho, Ecohydraulics Research Group.

Borden, C., P. Goodwin, L. Mink, and J. Liou. 2004. *Simulation of Flow and Sediment in the Lower Coeur d'Alene River, Phase Two of the Demonstration*. University of Idaho Ecohydraulics Research Group and DHI. Boise, Idaho.

Box, S.E., Bookstrom, A.A., Ikramuddin, Mohammed, and Lindsay, James. 2001. *Geochemical Analyses of Soils and Sediments, Coeur d'Alene Drainage Basin, Idaho; Sampling, Analytical Methods and Results*. U.S. Geological Survey Open-File Report 01–139, 230 p.

Box, S.E. 2003. Informal notes prepared by S. E. Box (USGS) for a Field Trip to the Lower Basin.

Box, S.E., A.A. Bookstrom, and M. Ikramuddin. 2005. *Stream-Sediment Geochemistry in Mining-Impacted Streams: Sediment Mobilized by Floods in the Coeur d'Alene-Spokane River System, Idaho and Washington*. Scientific Investigations Report 2005-5011. U.S. Geological Survey. Reston, Virginia.

CH2M HILL. 2010a. *Enhanced Conceptual Site Model for the Lower Basin of the Coeur d'Alene River*. Technical Memorandum Series. Prepared for U.S. Environmental Protection Agency. August.

CH2M HILL. 2010b. *Quality Assurance Project Plan, Coeur d'Alene Basin Environmental Monitoring Plan*. Prepared for U.S. Environmental Protection Agency. April.

CH2M HILL. 2011a. *WY2010 BEMP Sediment Sampling Data Summary*. Coeur d'Alene River Basin Environmental Monitoring Plan Operable Unit 3. Prepared for U.S. Environmental Protection Agency. April.

CH2M HILL. 2011b. *WY2011 BEMP Sediment Sampling Data Summary*. Coeur d'Alene River Basin Environmental Monitoring Plan Operable Unit 3. Prepared for U.S. Environmental Protection Agency. December.

CH2M HILL. 2012a. *Sampling Plan Alteration Form for the QAPP Addendum.* Coeur d'Alene Basin Environmental Monitoring Plan. Prepared for U.S. Environmental Protection Agency. April.

CH2M HILL. 2012b. Grain size and metals data from combined coring and bed surface sampling, as analyzed in 2012. Unpublished data.

CH2M HILL. 2013a. *WY2012 BEMP Sediment Sampling Data Summary*. Coeur d'Alene River Basin Environmental Monitoring Plan Operable Unit 3. Prepared for U.S. Environmental Protection Agency. March.

CH2M HILL. 2013b. *WY2013 BEMP Sediment Sampling Data Summary.* Coeur d'Alene River Basin Environmental Monitoring Plan Operable Unit 3. Prepared for U.S. Environmental Protection Agency. November.

CH2M HILL. 2013c. *Sample Plan Alteration Form (SPAF), Bridge Sampling, Lower Basin Coeur d'Alene River Focused Suspended Sediment Investigation* (April 2012 QAPP). Prepared for U.S. Environmental Protection Agency. March.

CH2M HILL. 2013d. *Model Development Report for 1D Hydraulic Model, Lower Basin of the Coeur d'Alene River (OU3).* Prepared for U.S. Environmental Protection Agency. June.

CH2M HILL. 2013e. X-Ray diffraction/clay mineralogy results from ten riverbed surface and subsurface samples and interpretation with respect to grain size and lead content. Analyses conducted in 2012 and in 2013. Unpublished data.

CH2M HILL. 2013f. *Documentation and Interpretation of Historical Channel Changes, Lower Basin of the Coeur d'Alene River (OU3)*. Draft Technical Memorandum Addendum E-4. Prepared for U.S. Environmental Protection Agency. November.

CH2M HILL. 2014a. *Development of Synthetic Water Surface Elevation Data Near Harrison Using a Multi-variate Regression Technique*. Technical Memorandum Addendum C-2. Prepared for U.S. Environmental Protection Agency. January.

CH2M HILL. 2014b. *Riverbank Characteristics, Erosion Rates, and Lead Contribution, Lower Basin of the Coeur d'Alene River (OU3)*. Draft Technical Memorandum Addendum E-1. Prepared for U.S. Environmental Protection Agency. December. Minor revisions submitted to EPA on October 30, 2015.

CH2M HILL. 2014c. *Aggradation and Degradation of the Coeur d'Alene River, Lower Basin of the Coeur d'Alene River (OU3)*. Draft Technical Memorandum Addendum E-2. Prepared for U.S. Environmental Protection Agency. January.

CH2M HILL. 2015a. *WY2014 BEMP Sediment Sampling Data Summary*. Coeur d'Alene River Basin Environmental Monitoring Plan Operable Unit 3. Prepared for U.S. Environmental Protection Agency. February.

CH2M HILL. 2015b. *Floodplain Sedimentation Rates Developed from One-Dimensional Model Results, Lower Basin of the Coeur d'Alene River (OU3).* Draft Technical Memorandum Addendum E-5. Prepared for U.S. Environmental Protection Agency. July.

CH2M HILL. In review. *Riverbed Characterization, Lower Basin of the Coeur d'Alene River (OU3).* Technical Memorandum Addendum E-6. Prepared for U.S. Environmental Protection Agency.

Churchill, M.A., 1948. *Discussion of Analysis and Use of Reservoir Sedimentation Data.* pp. 139-140. Proceedings of Federal Interagency Sedimentation Conference, Denver, Colorado, United States Bureau of Reclamation.

Clark, G.M. and P.F. Woods. 2001. *Transport of Suspended Solids and Bedload Sediment at Eight Stations in Coeur d'Alene River Basin, Idaho*. U.S. Geological Survey Open-File Report 00-472.

Clark, G.M. and C.A. Mebane. 2014. *Sources, Transport, and Trends for Trace Metals and Nutrients, Coeur d'Alene and Spokane River Basins, Idaho, 1990-2013.* U.S. Geological Survey Scientific Investigations Report 2014-5204. 62 p.

Dietrich, W. E.; Dunne, T.; Humphrey, N. F.; Reid, L.M. 1982. *Construction of Sediment Budgets for Drainage Basins.* In: Sediment Budgets and Routing in Forested Drainage Basins: Proceedings of the Symposium; 31 May – 1 June 1982, Oregon. Gen. Tech. Rep. PNW-141. Portland, Oregon: Pacific Northwest Forest and Range Experiment Station, Forest Service, U.S. Department of Agriculture; 1982: 5-23.

Donato, Mary M. 2006. *Annual Trace-Metal Load Estimates and Flow-Weighted Concentrations of Cadmium, Lead, and Zinc in the Spokane River Basin, Idaho and Washington, 1999-2004*. Scientific Investigations Report 2006-5188. U.S. Geological Survey. Reston, Virginia.

Dunne, T., & Leopold, L. B. 1978. *Water in Environmental Planning*. W.H. Freeman: San Francisco, California. 818 p.

EPA. See U.S. Environmental Protection Agency.

Flagor, R. 2002. *Coeur d'Alene River Bank Erosion Survey 2002: Coeur d'Alene, Idah*o. U.S. Natural Resources Conservation Service, Kootenai-Shoshone Soil and Water Conservation District. 12 p.

Fousek, R.S. 1996. *Trace-Element Distributions in the Sediments of the Flood Plain and River Banks of the South Fork and Coeur d'Alene Rivers, Shoshone and Kootenai Counties, Idaho*. Auburn, Alabama, Auburn University, M.S. thesis, 333 p.

Gellis, A.C. 2013. "Factors Influencing Storm-Generated Suspended-Sediment Concentrations and Loads in Four Basins of Contrasting Land Use, Humid-Tropical Puerto Rico." *Catena,* Vol. 104, May 2013, pp. 39-57.

Glysson, G.D. 1987. *Sediment-Transport Curves*. U.S. Geological Survey Open-File Report 87-218. 47 p.

Gomez, B., and Church, M. 1989. "An assessment of Bed Load Sediment Transport Formulae for Gravel Bed Rivers." *Water Resources Research*, 25(6). 1161-1186.

Hoffman, M.L. 1995. *Characterization of Heavy Metal Contamination in Two Lateral Lakes of the Coeur d'Alene River Valley, Northern Idaho.* M.S. Thesis, University of Idaho. Moscow, Idaho. 76 p.

Horowitz, A. J., Elrick, K.A., Robbins, J. A., and Cook, R. B. 1995. "Effect of Mining and Related Activities on the Sediment - Trace Element Geochemistry of Lake Coeur d'Alene, Idaho, USA; Part II, Subsurface Sediments." *Hydrological Processes*, v. 9, pp. 35-54.

Hudson, P.H. 2003. "Event Sequence and Sediment Exhaustion in the lower Panuco Basin, Mexico." *Catena*, Vol. 52, pp. 57-76.

Interagency Advisory Committee on Water Data. 1982. *Guidelines for Determining Flood-Flow Frequency*. Bulletin 17B of the Hydrology Subcommittee, Office of Water Data Coordination, U.S. Geological Survey, Reston, Va., 183 p., http://water.usgs.gov/osw/bulletin17b/bulletin_17B.html.

Kootenai-Shoshone Soil and Water Conservation District (KSSWCD), in Cooperation with Idaho Department of Environmental Quality. 2009. *Lower Coeur d'Alene Riverbank Stabilization Prioritization*. 57 p.

Leopold, L.B., M.G. Wolman, and J.P. Miller. 1964. *Fluvial Processes in Geomorphology*. W.H. Freeman: San Francisco, California. 522 p.

Levesque, V.A., and Oberg, K.A. 2012. Computing Discharge Using the Index Velocity Method: U.S. Geological Survey Techniques and Methods, Book 3 Chapter A23, 148 p. [Also available at http://pubs.usgs.gov/tm/3a23/.]

Moore, J.N., Brook, E.J., and Johns, C. 1989. "Grain Size Partitioning of Metals in Contaminated, Coarse-Grained River Floodplain Sediment: Clark Fork River, Montana, U.S.A." *Environmental Geology and Water Sciences*, Vol. 14, No. 2, pp. 107-115.

Nash, D.B. 1994. "Effective Sediment-Transporting Discharge from Magnitude-Frequency Analysis." *Journal of Geology*, Vol. 102, No. 1 (Jan., 1994), pp. 79-95.

Rabbi, F. 1994. *Trace Element Geochemistry of Bottom Sediments and Waters from the Lateral Lakes of Coeur d'Alene River, Kootenai County, North Idaho.* Ph.D. Dissertation, University of Idaho. Moscow, Idaho. 256 p.

Radtke, D. B., Jacob Gibs, and R. T. Iwatsubo. 1999. *National Field Manual for the Collection of Water-Quality Data: Processing of Water Samples*. USGS–TWRI book 9, chap. A4. 156 pp. 9-A5.

Reid, L.M. and Dunne, T., 1996. Rapid Evaluation of Sediment Budgets. Catena. Reiskirchen, Germany.Roberts, C.P.R. 1982. *Flow Profile Calculations, HYDRO 82*. University of Pretoria, South Africa.

Salomons, W. and Förstner, U. 1983. *Metals in the Hydrocycle*. Springer. Berlin.

Topping, T.J., Rubin, D.M., and Vierra, L.E. 2000. "Colorado River Sediment Transport: 1. Natural Sediment Supply Limitation and the Influence of Glen Canyon Dam." *Water Resources Research*, Vol. 36, No. 2, pp. 515-542.

U.S. Army Corps of Engineers (USACE). 2010. *HEC-SSP Statistical Software Package Users Manual*. Version 2.0. U.S. Army Corps of Engineers, Hydraulic Engineering Center, Davis, California.

U.S. Environmental Protection Agency (EPA). 1998. *Sediment Contamination in the Lower Coeur d'Alene Basin: Geophysical and Sediment Coring Investigation in the River Channel, Lateral Lakes, and Floodplains: Bunker Hill Facility Basin Wide RI-FS Data Report. Volume 1 and Volume 2*. Prepared for the U.S. Environmental Protection Agency by URS Greiner, Inc., and CH2M HILL.

U.S. Environmental Protection Agency (EPA). 2001. *Final (Revision 2) Remedial Investigation Report, Remedial Investigation Report for the Coeur d'Alene Basin Remedial Investigation/Feasibility Study*. Prepared for U.S. Environmental Protection Agency by URS Greiner, Inc., and CH2M HILL. September.

U.S. Environmental Protection Agency (EPA). 2004. *Basin Environmental Monitoring Plan – Bunker Hill Mining and Metallurgical Complex Operable Unit 3*. March.

U.S. Geological Survey (USGS). National Water Information System. http://waterdata.usgs.gov/nwis

Wentworth, C. K. 1922. "A Scale of Grade and Class Terms for Clastic Sediments." *Journal of Geology*, Vol. 30, p. 377-392.

Wetzel, M. 1994. *Geology Report: Coeur d'Alene River Cooperative River Basin Study*. Boise, Idaho, U.S. Soil Conservation Service. 69 p.

Wolman, M. G., and Miller, J P. 1960. “Magnitude and Frequency of Forces in Geomorphic Processes.” *Journal of Geology*, Vol. 68, No 1.

Exhibits

1 Location Map, Lower Coeur d'Alene River
2 Components of Sediment and Lead Budgets
3 Summary of Available Data for Selected USGS Gaging Stations
4 Bulk Suspended Sediment Concentration Measurements from USGS and CH2M HILL Sampling Programs
5 Summary of Regression Parameters for Bulk Suspended Sediment Concentration and Size Fractions
6 Residuals from Suspended Sediment Rating Curves Plotted against Discharge
7 Evaluation of Decadal Changes in Sediment Rating Curves
8 Comparison of Sediment Concentrations from Rising and Falling Portion of Hydrographs
9 Center of Bridge Sediment Samples during the April 2013 High-Flow Event
10 Patterns of Event Hysteresis, April 2013 Event
11 Patterns of Seasonal Hysteresis
12 High Resolution Bathymetry Showing Steep Side Slopes along Channel Banks and Adjacent to Scour Holes
13 Impact of Coeur d'Alene Lake Level on Suspended Sediment Concentration
14 Suspended Sediment Concentration Measurements (Sand Fraction) from USGS and CH2M HILL Sampling Programs
15 Suspended Sediment Concentration Measurements (Fines Fraction) from USGS and CH2M HILL Sampling Programs
16 Computed Annual Sediment Fluxes at Five Locations in Lower Basin
17 Computed Sediment Fluxes, by Water Year, for Lower Basin Gaging Stations
18 Net Sediment Deposition and Erosion between Gaged Locations
19 Effect of Changing the Threshold Discharge on Computed Rating Curves
20 Sensitivity of Average Annual Sediment Flux and Net Sediment Deficit to the Assumed Threshold Discharge
21 Estimating the Upper and Lower Bounding Exponents for Sediment Rating Curves at Cataldo and Harrison Gages
22 Sensitivity of Average Annual Sediment Flux to the Rating Curve Exponent
23 Comparison of Linear and Power-Law Regression with Data from Harrison and Cataldo
24 Summary of Sensitivity of Average Sediment Fluxes to Rating Curve Regression Models

25 Frequency and Magnitude of Sediment Fluxes at Harrison and Cataldo
26 Frequency/Magnitude/Duration Plots for Sediment Transport in the Lower Basin
27 Annual Sediment Fluxes By Grain Size
28 Computed Sand Proportion of Annual Sediment Flux at Four Gaging Stations
29 Sand and Fines Contributions to the Net Sediment Deficit between Cataldo and Harrison
30 Flow and Sediment Transport in Four High-Flow Events
31 Measurements of Lead in Suspended Sediment
32 Comparison of Bulk Lead on Sediment between USGS and BEMP Samples
33 Lead Concentration on Suspended Sediment
34 Downstream Distribution of Bulk Lead Concentration on Suspended Sediment in the April 2012 Flood Event
35 Downstream Distribution of Bulk Lead Concentration in Recent Suspended Sediment, Depositional Sediment, and Riverbed Surface Samples
36 Relationship between Bulk Lead Concentration and Percent Fines in Suspended Sediment
37 Lead Concentrations in Different Sample Subfractions of Suspended Sediment Samples
38 Computed Lead Fluxes, by Water Year, for Lower Basin Gaging Stations
39 Annual Lead Fluxes Associated with Sediment at Four Stations in Lower Basin
40 Annual Net Lead Erosion in the Lower Basin
41 Lead Fluxes Contributed by Flows of Different Magnitude and Frequency
42 Relative Proportion of Lead Transported by Different Size Flows
43 Sand and Fines Contribution to Annual Lead Transport
44 Sand and Fines Contributions to the Net Lead Deficit between Cataldo and Harrison
45 Evidence that Floodplain Surface Erosion is not a Primary Process Moving Sediment in the Lower Basin
46 Photograph of Bank Erosion of Tailings-Rich Sediment in Lower Basin
47 Process of Bank Erosion and Lead Release in the Lower Basin
48 Summary of Calculation of Sediment and Lead Contributed by Bank Erosion in the Lower Basin
49 Coring Locations and Mapping by Bookstrom et al. (2004)
50 Average Annual Sedimentation in USGS Cores
51 Table Summarizing Results of Sediment and Lead Deposition in Floodplain
52 Average Annual Sedimentation Rate in USGS Cores Versus Distance From the River
53 1D Model Areas Used for Sedimentation Analysis
54 Uncertainty Analysis Summary
55 Floodplain Sediment Trapping Efficiency
56 Floodplain Sedimentation Mass
57 Floodplain Sedimentation Rate
58 Average Annual Sedimentation
59 Floodplain Sedimentation by Water Year for the Entire Lower Basin
60 Annual Sediment Deposition in Lower Basin Floodplain (from CH2M HILL, 2014)
61 Estimation of Mass of Contaminated Channel Bed Sediment by Bookstrom et al. (2001)
62 Locations of 2012 Coring Transects and 2013 Shallow Vibracores
63 Example of Geomorphic Mapping and Coring (Triangles) Used in 2013 Shallow Vibracore Investigation
64 Estimate of the Volumes and Masses of Contaminated Sediment in the Riverbed Based on Geomorphic Mapping and 2013 Shallow Vibracore Sampling
65 Sediment and Lead Budgets for the Lower Basin (Cataldo to Harrison Gages)
66 Relative Sources and Sinks of Contaminated Sediment in the Lower Basin

Gravel-Bed Reach:
Confluence to Cataldo

Cataldo Reach

Dudley Reach

Sand-Bed Reach:
Cataldo to Harrison

Killarney Reach

Springston Reach

Cataldo Bridge

Enaville (North Fork)
USGS Gage

Cataldo USGS Gage

Pinehurst (South Fork)
USGS Gage

Rose Lake USGS Gage

Rose Lake
Bridge

Interstate 90
Bridge

Harrison USGS Gage

Springston
Bridge

Highway 97
Bridge

Thompson Lake
Blue Lake
Harrison Slough
Anderson Lake
Harrison
Delta
Killarney
Lake
Rose
Lake
Bull Run
Lake
Swan Lake
Cave Lake
Medicine
Lake
Black Lake
CATALDO
HARRISON

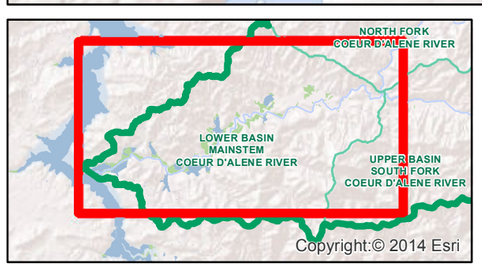

LEGEND

USGS Gages

Symbology Maintained throughout Report

- Cataldo
- Rose Lake
- Harrison
- Pinehurst (South Fork)
- Enaville (North Fork)

- Spatial Extent of Sediment and Lead Budgets in this Report
- Reach Divide
- Trail of the Coeur d'Alenes
- River Mile Marker
- Major Roads
- Waterbody
- Marsh or Slough

N

0 0.5 1 2 Miles

Exhibit 1. **Location Map**
Lower Coeur d'Alene River
Processes of Sediment and Lead Transport, Erosion, and Deposition
Lower Basin of the Coeur d'Alene River (OU3)

ch2m

\\PDXFPP01\PROJ\USEPA\382081BUNKERHILL\LOWERBASIN\GIS\MAPFILES\2013\UPDATED_ECSM\SED_PB_BUDGET\EX1_GAGINGSTATIONS.MXD GGEE 12/1/2015 8:53:08 AM

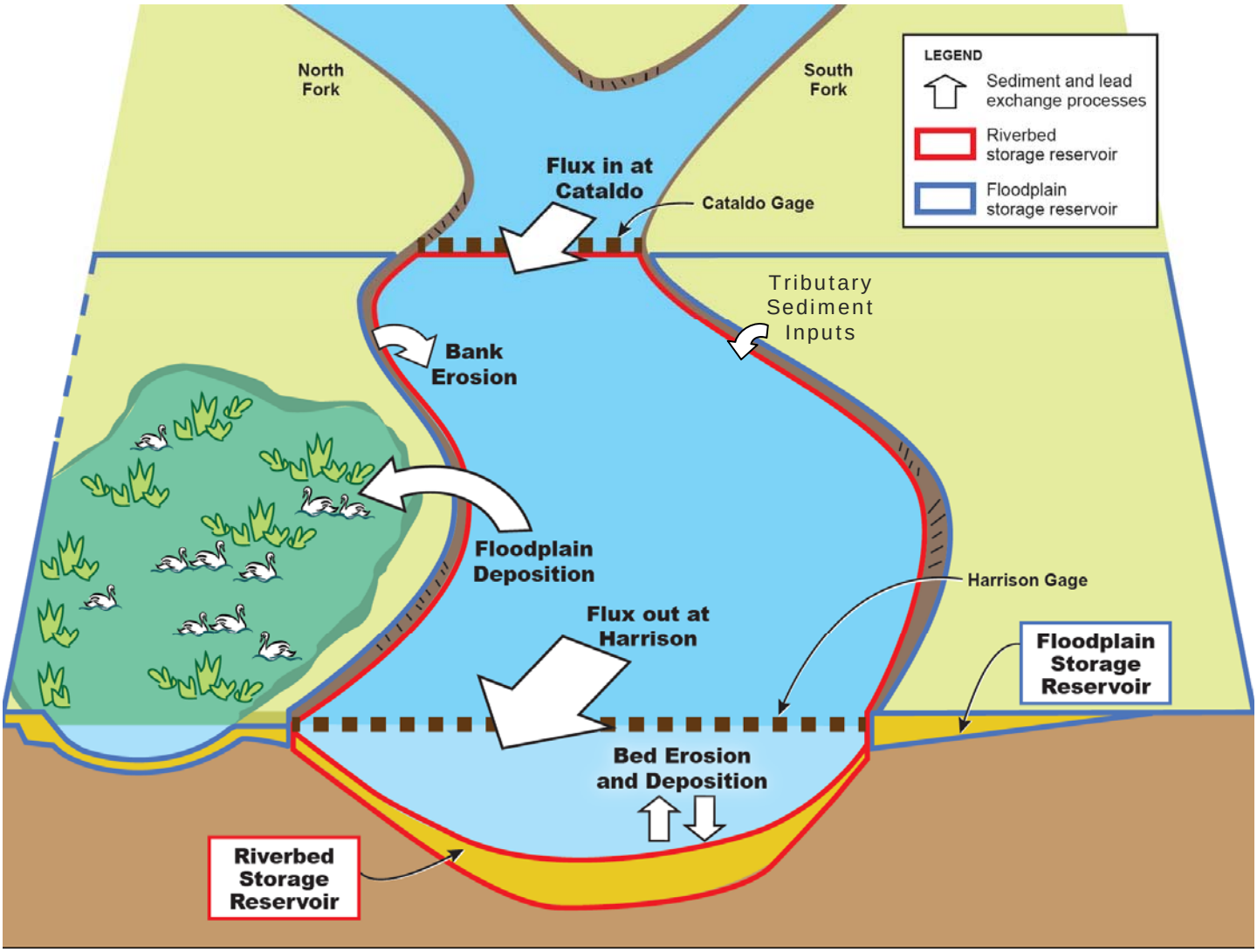

Note:
Tributary sediment inputs are assumed to be small compared with the other components of the sediment budget. No data or analyses were done to try to constrain tributary sediment inputs.

Exhibit 2. **Components of Sediment and Lead Budgets**
Processes of Sediment and Lead Transport, Erosion, and Deposition
Lower Basin Coeur d'Alene River (OU3)

Exhibit 3. **Summary of Available Data for Selected USGS Gaging Stations**
Processes of Sediment and Lead Transport, Erosion, and Deposition
Lower Basin Coeur d'Alene River (OU3)

	Station				
Parameter	**Harrison**	**Rose Lake**	**Cataldo**	**Pinehurst (S. Fork)**	**Enaville (N.Fork)**
Flow Data					
Period of record	2004 – 2012	1994 - 1994	1911 – 2012	1988 – 2012	1912 – 2012
Historical Average Peak Flow (cfs)	15,091	--	22,354	4,339	18,364
SSC Data					
Number of SSC samples	107	15	83	186	139
Dates of SSC samples	1993, 1994, 2002-2012	1994, 1999, 2011-2012	1986-1994, 2002-2012	1989-2012	1980, 1989-2012
Number of BEMP samples	11	4	9	8	7
Average bulk lead of BEMP samples (mg/Kg)	3,727	2,638	1,054	2,431	204

Notes:
Complete dataset located in Attachment A.
cfs = cubic feet per second
mg/Kg = milligrams per Kilogram

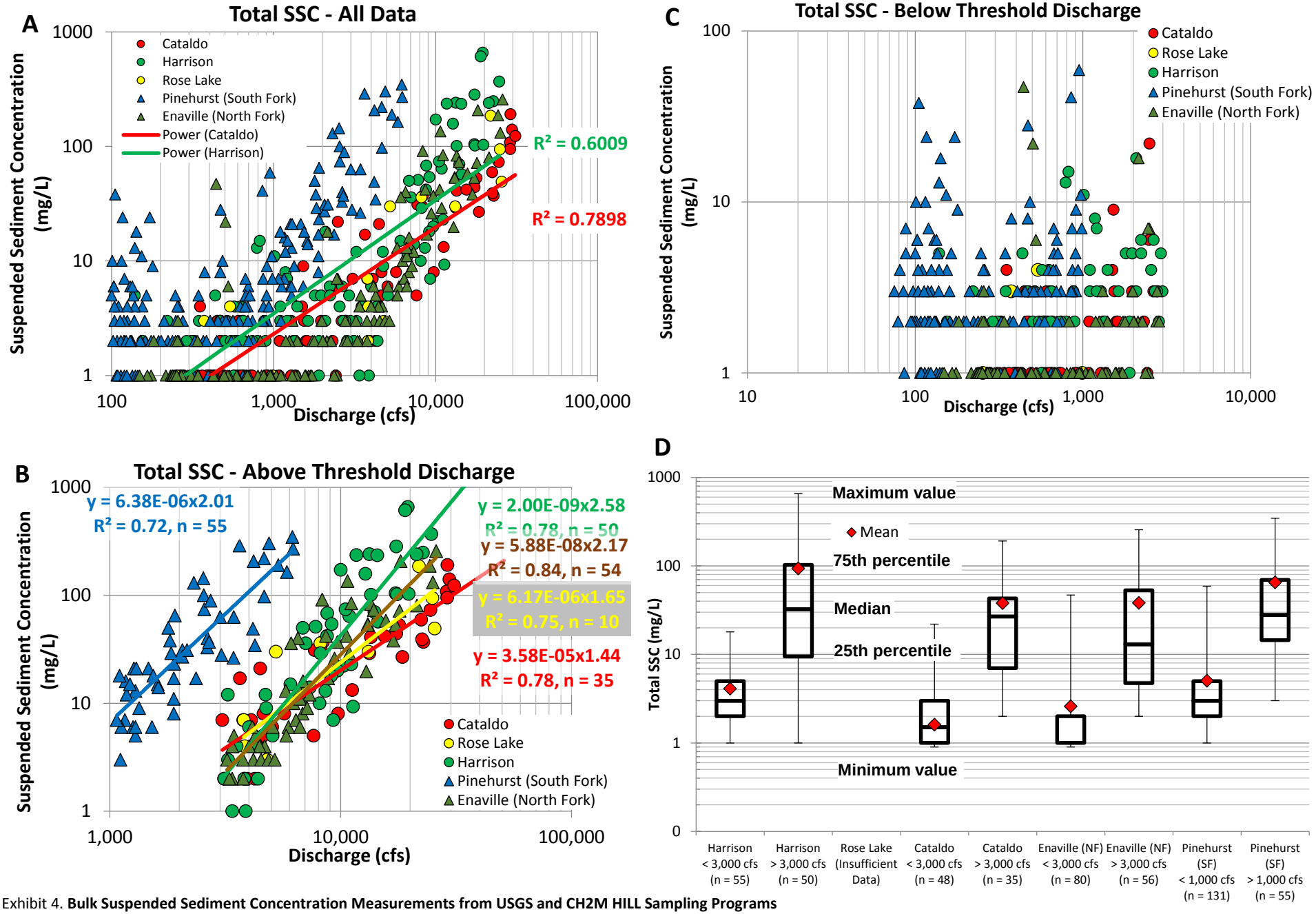

Exhibit 4. **Bulk Suspended Sediment Concentration Measurements from USGS and CH2M HILL Sampling Programs**
Processes of Sediment and Lead Transport, Erosion, and Deposition
Lower Basin Coeur d'Alene River (OU3)

Exhibit 5. **Summary of Regression Parameters for Bulk Suspended Sediment Concentration and Size Fractions**
Processes of Sediment and Lead Transport, Erosion, and Deposition
Lower Basin Coeur d'Alene River (OU3)

REGRESSION PARAMETERS AND LEAD CONCENTRATIONS FOR COMPUTING SEDIMENT AND LEAD BUDGETS

$SSC_i = a*Q^b$

Station	Threshold Discharge (cfs)	Total SSC				Suspended sand				Suspended fines			
		a	b	n	r^2	a	b	n	r^2	a	b	n	r^2
Cataldo	3,000	3.6E-05	1.4	50	0.78	7.0E-05	1.2	33	0.52	1.5E-05	1.5	33	0.81
Rose Lake	3,000	6.2E-06	1.6	14	0.75			3				3	
Harrison	3,000	2.0E-09	2.6	35	0.78	6.9E-13	3.3	43	0.79	1.0E-07	2.1	43	0.63
Pinehurst (S. Fork)	1,000	6.4E-06	2.0	55	0.72	9.7E-06	1.8	38	0.65	9.3E-07	2.2	40	0.77
Enaville (N.Fork)	3,000	5.9E-08	2.2	56	0.84	1.6E-08	2.1	44	0.75	8.4E-08	2.1	47	0.82

Notes:
Regression equations computed using samples collected during flows above threshold discharge (see text for explanation).

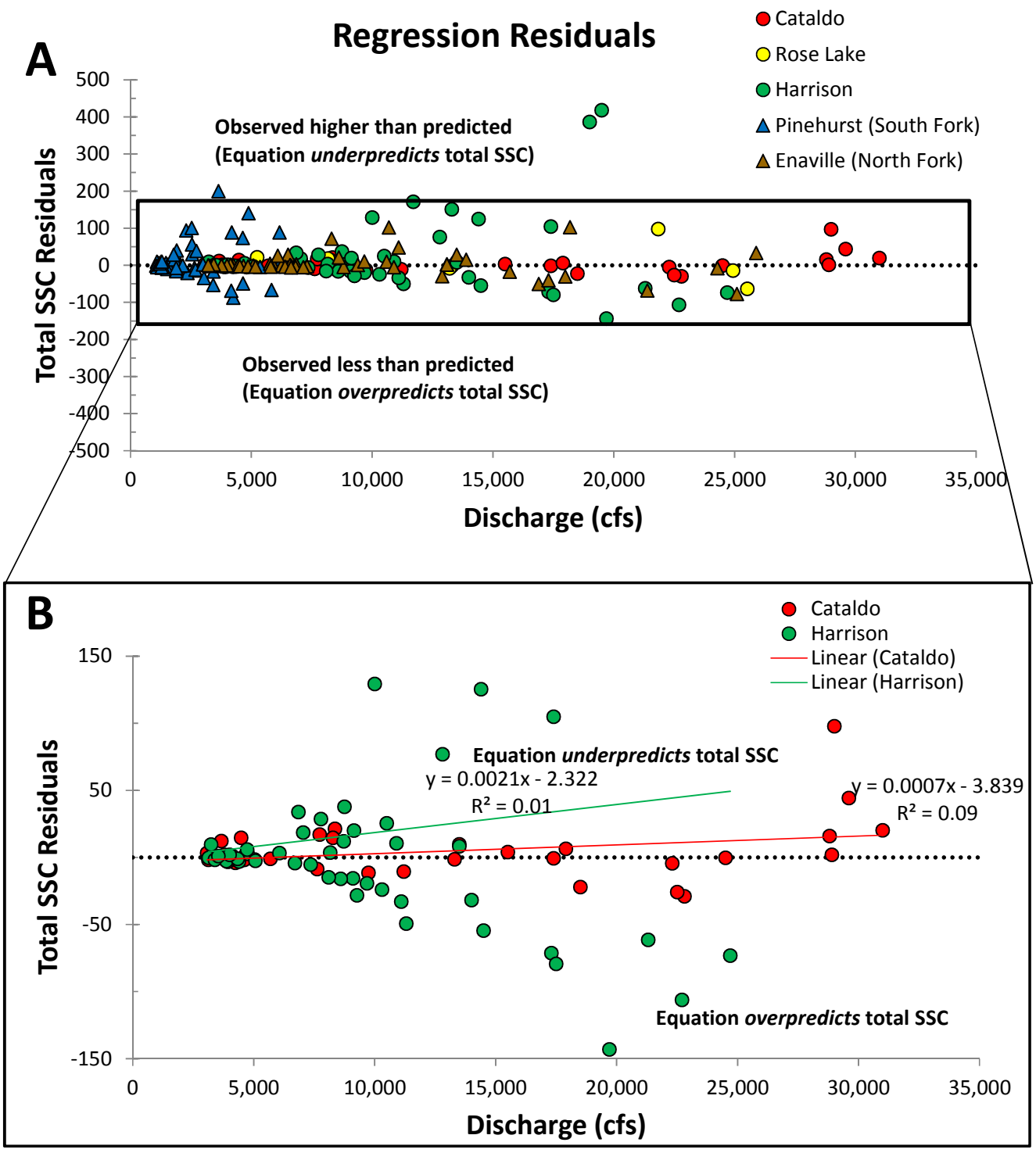

Exhibit 6. **Residuals from Suspended Sediment Rating Curves Plotted against Discharge**
Processes of Sediment and Lead Transport, Erosion, and Deposition
Lower Basin Coeur d'Alene River (OU3)

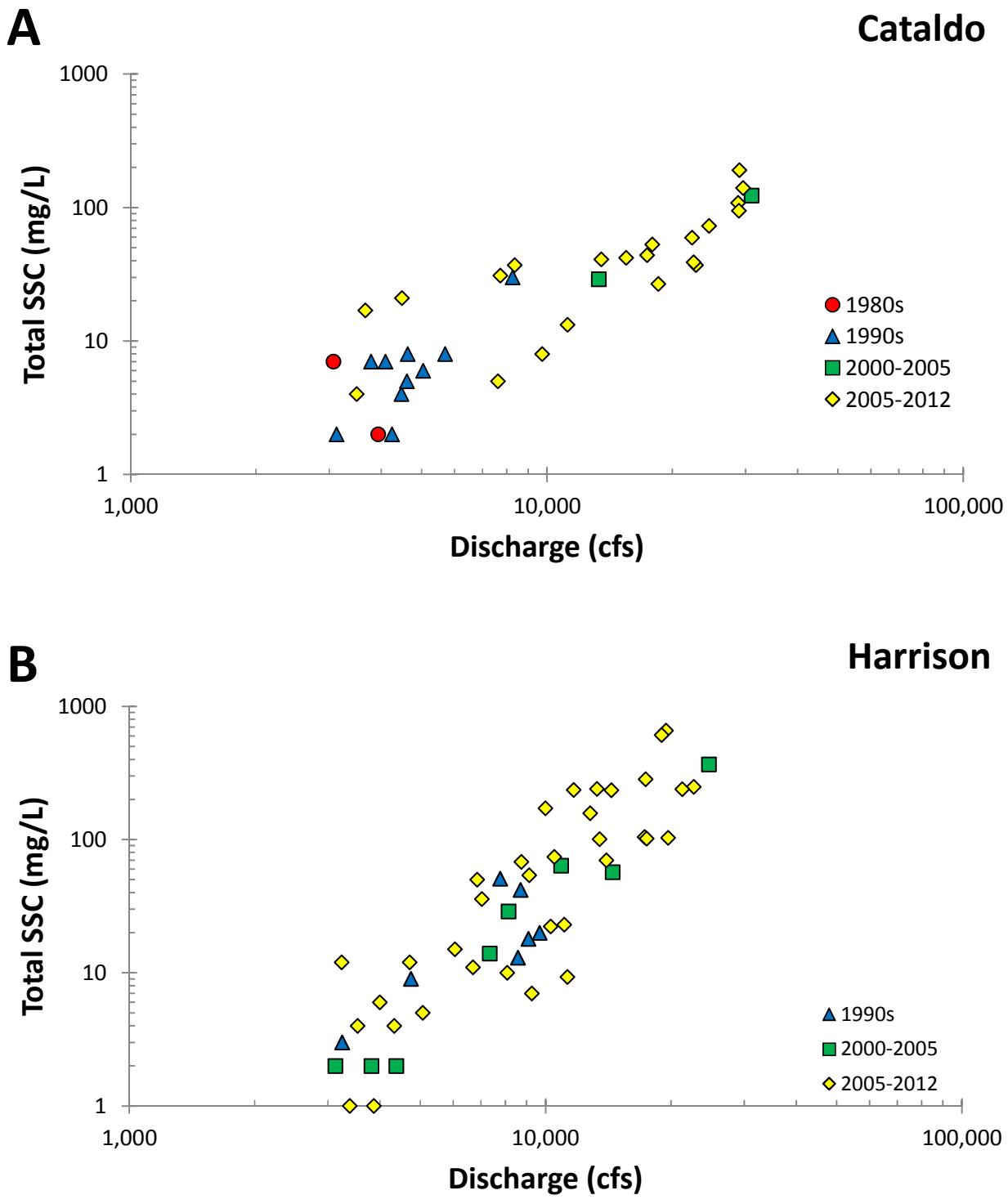

Exhibit 7. **Evaluation of Decadal Changes in Sediment Rating Curves**
Processes of Sediment and Lead Transport, Erosion, and Deposition
Lower Basin Coeur d'Alene River (OU3)

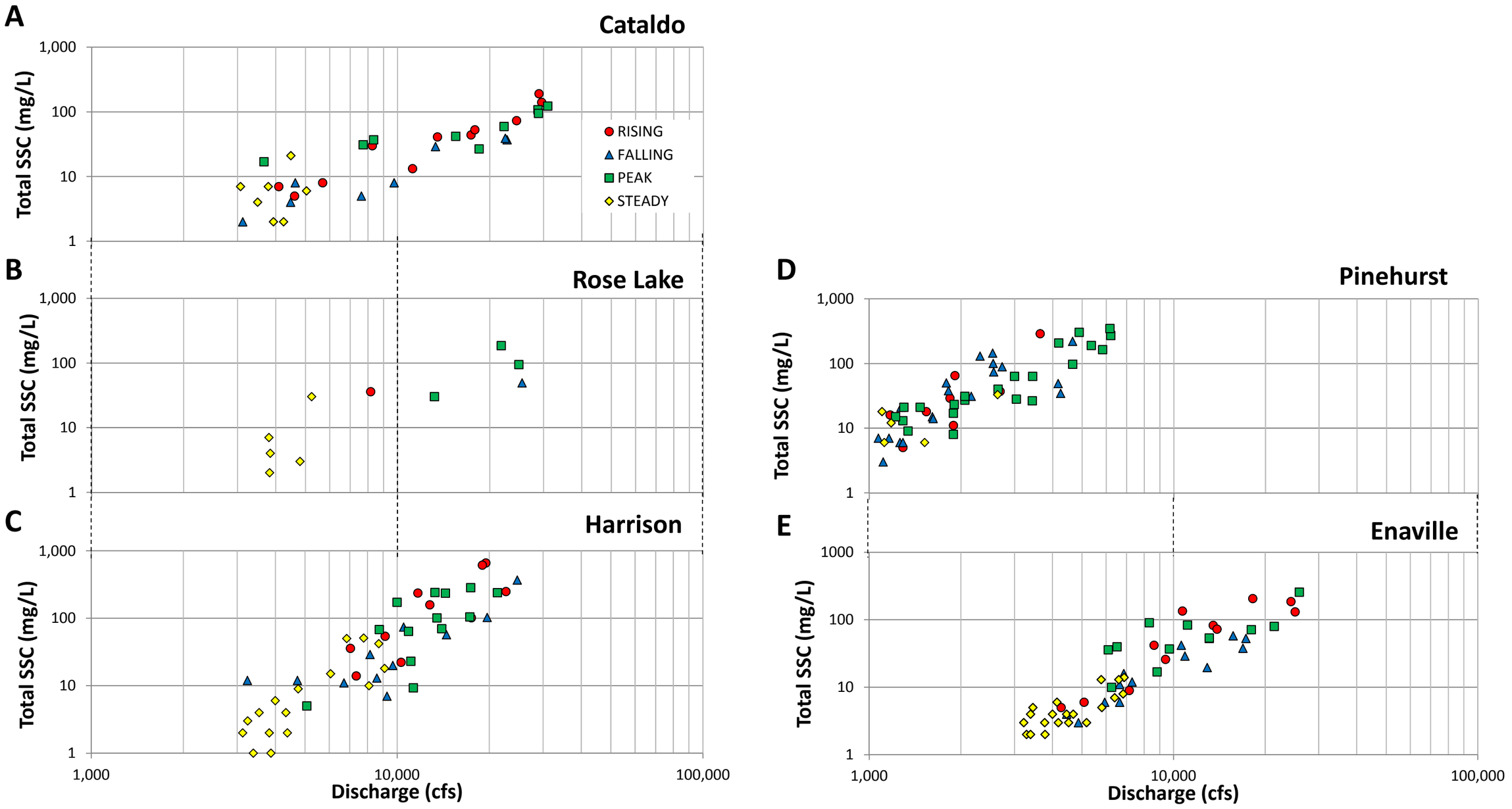

Exhibit 8. **Comparison of Sediment Concentrations from Rising and Falling Portion of Hydrographs**
Processes of Sediment and Lead Transport, Erosion, and Deposition
Lower Basin Coeur d'Alene River (OU3)

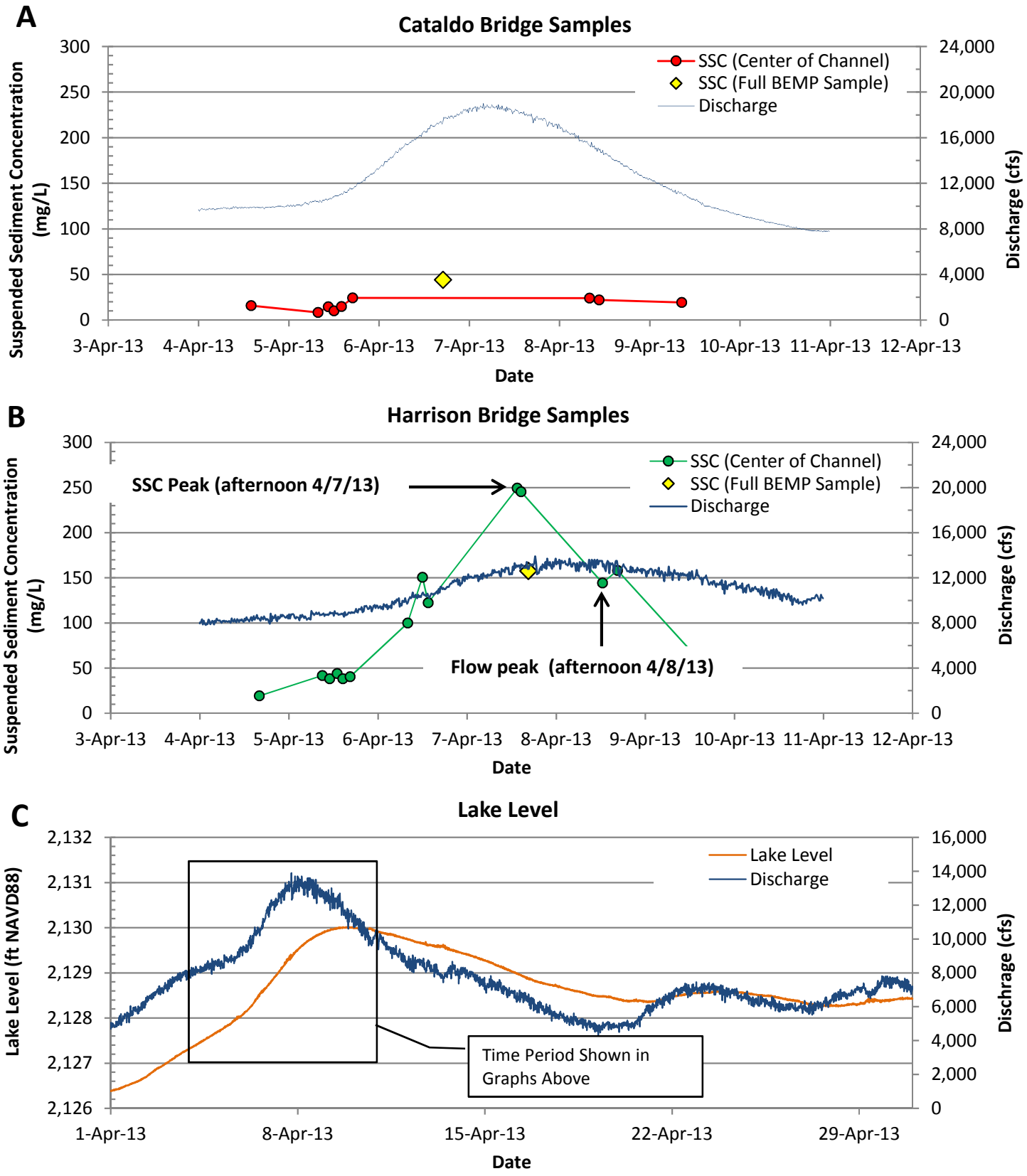

Exhibit 9. **Center of Bridge Sediment Samples during the April 2013 High Flow Event**
Processes of Sediment and Lead Transport, Erosion, and Deposition
Lower Basin Coeur d'Alene River (OU3)

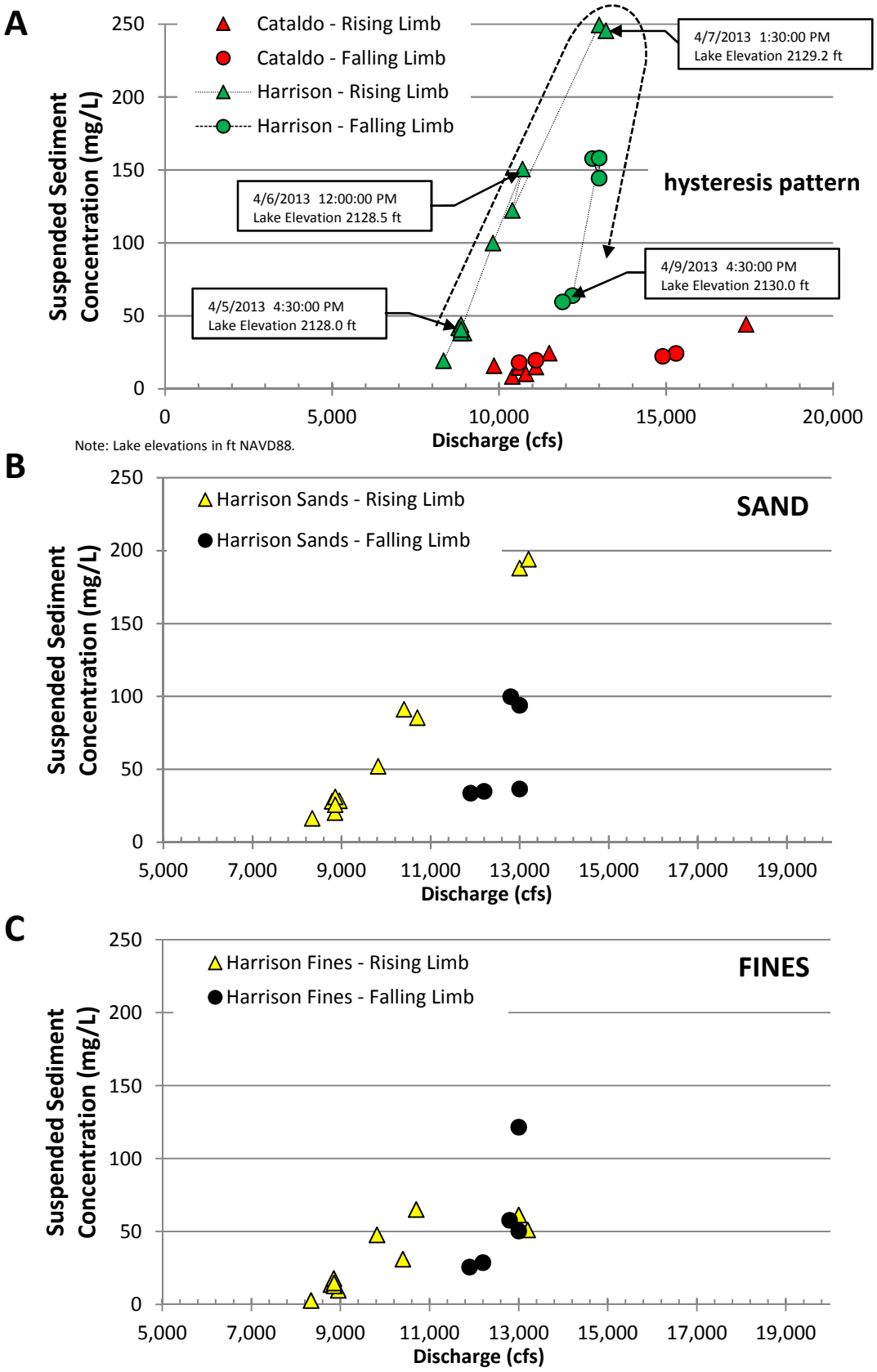

Exhibit 10. **Patterns of Event Hysteresis, April 2013 Event**
Processes of Sediment and Lead Transport, Erosion, and Deposition
Lower Basin Coeur d'Alene River (OU3)

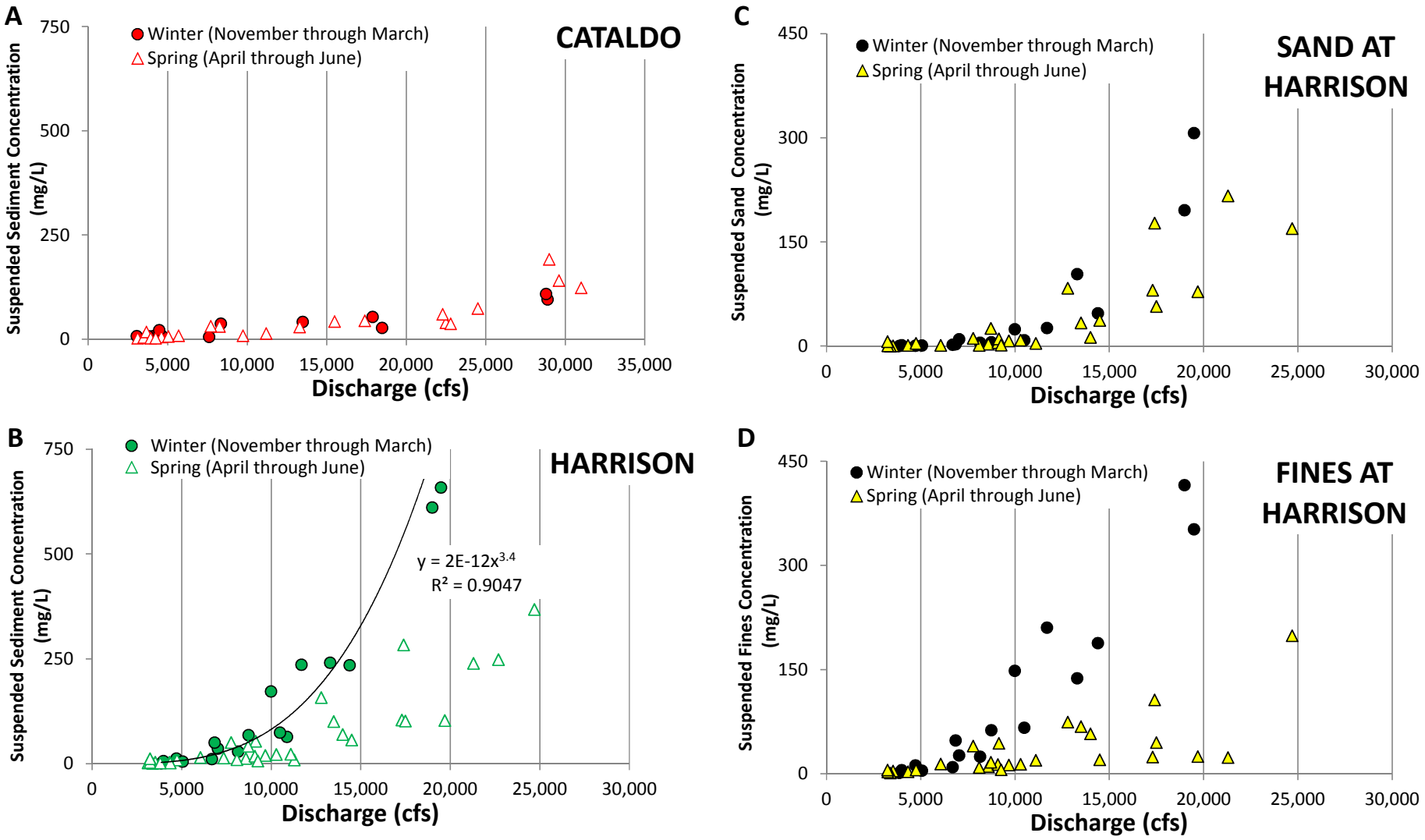

Exhibit 11. **Patterns of Seasonal Hysteresis**
Processes of Sediment and Lead Transport, Erosion, and Deposition
Lower Basin Coeur d'Alene River (OU3)

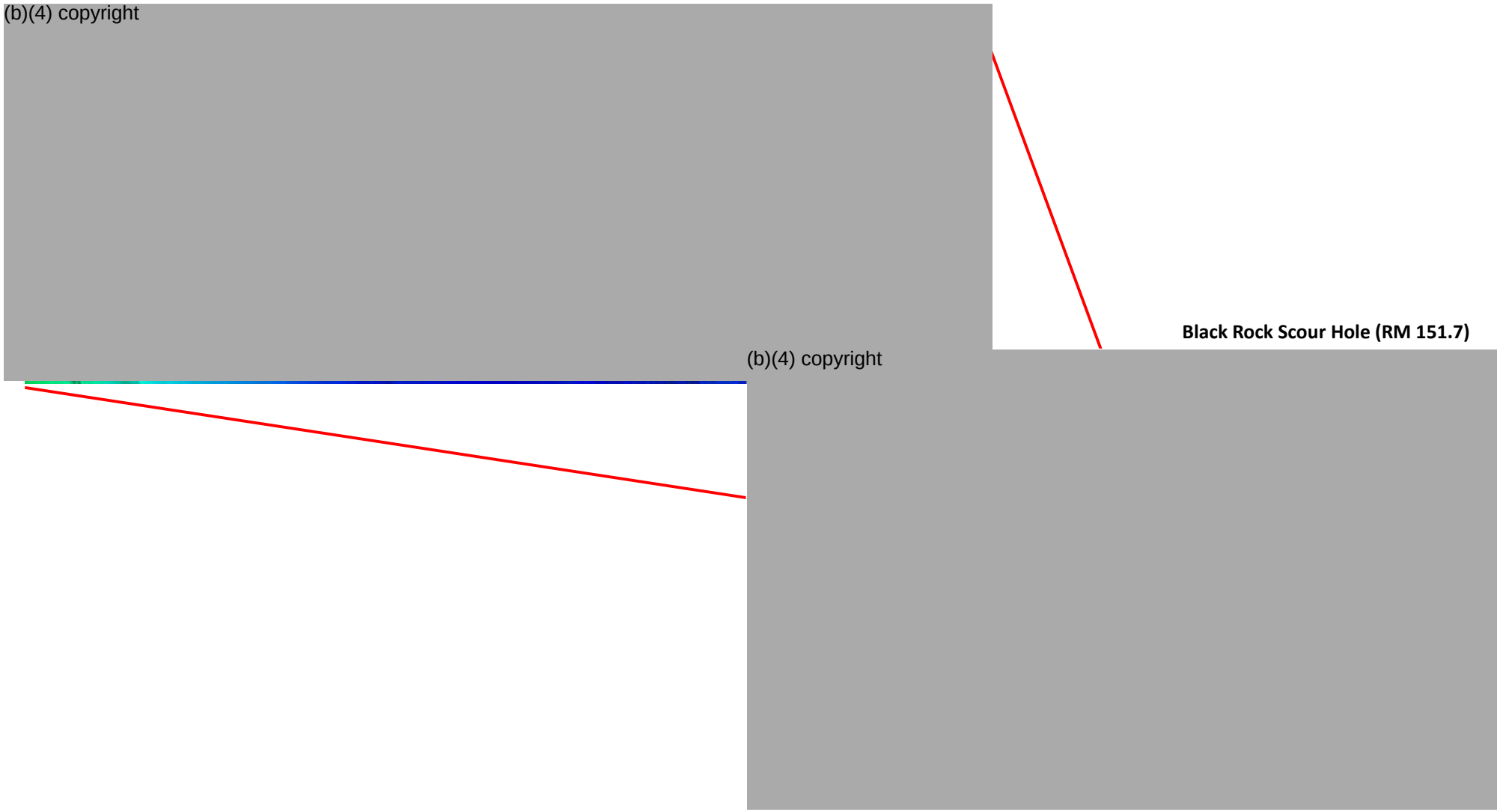

Exhibit 12. **High Resolution Bathymetry Showing Steep Side Slopes along Channel Banks and Adjacent to Scour Holes**
Processes of Sediment and Lead Transport, Erosion, and Deposition
Lower Basin Coeur d'Alene River (OU3)

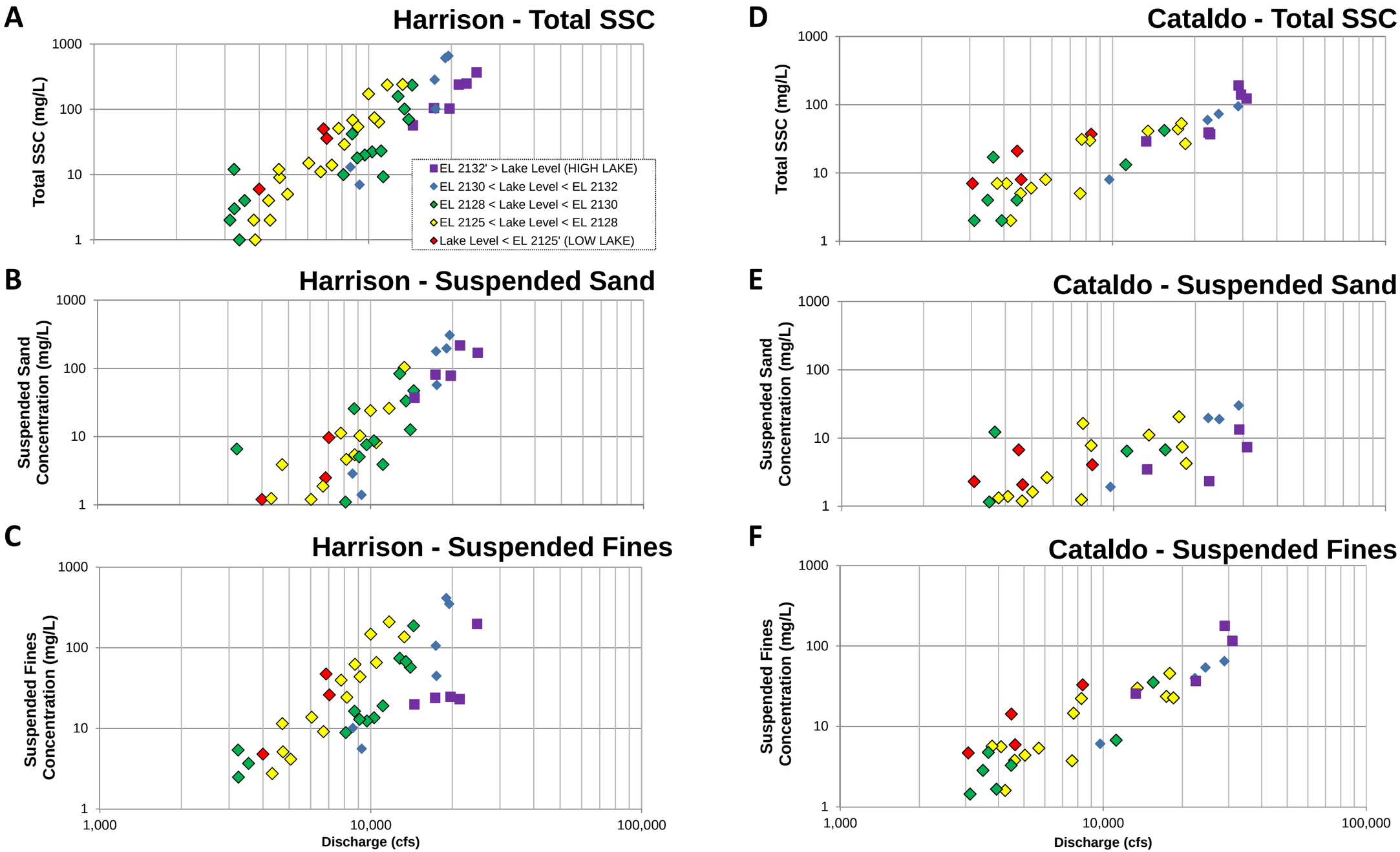

Exhibit 13. **Impact of Coeur d'Alene Lake Level on Suspended Sediment Concentration**
Processes of Sediment and Lead Transport, Erosion, and Deposition
Lower Basin Coeur d'Alene River (OU3)

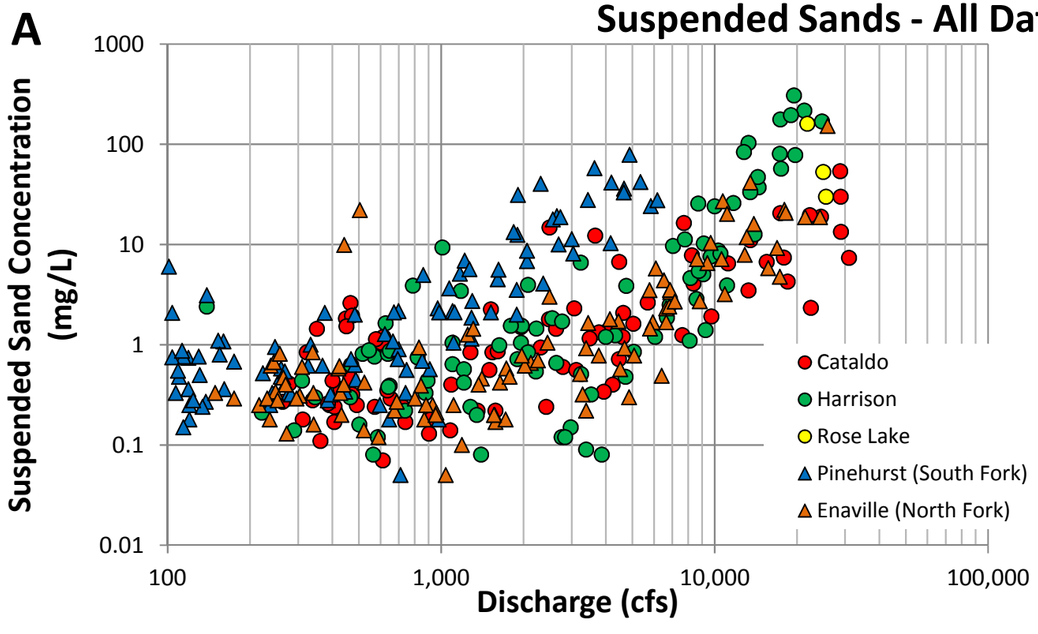

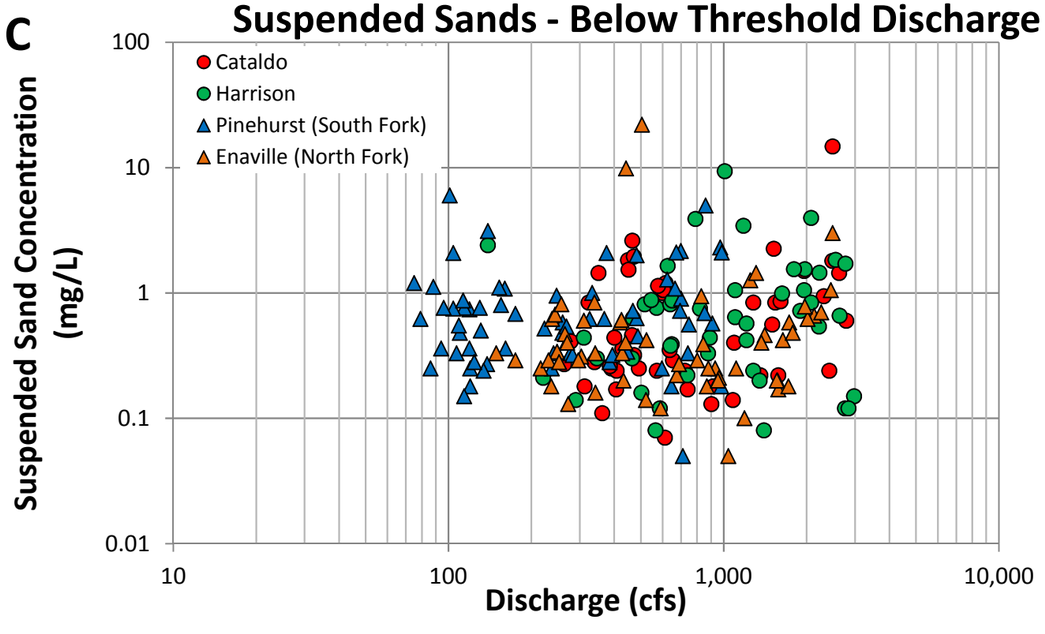

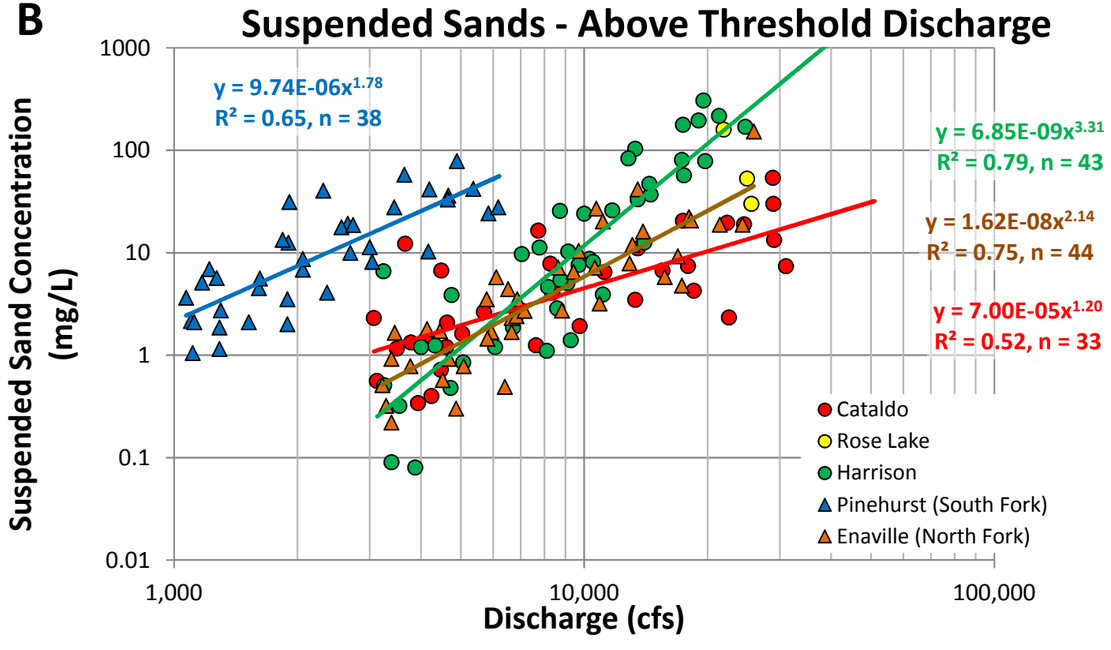

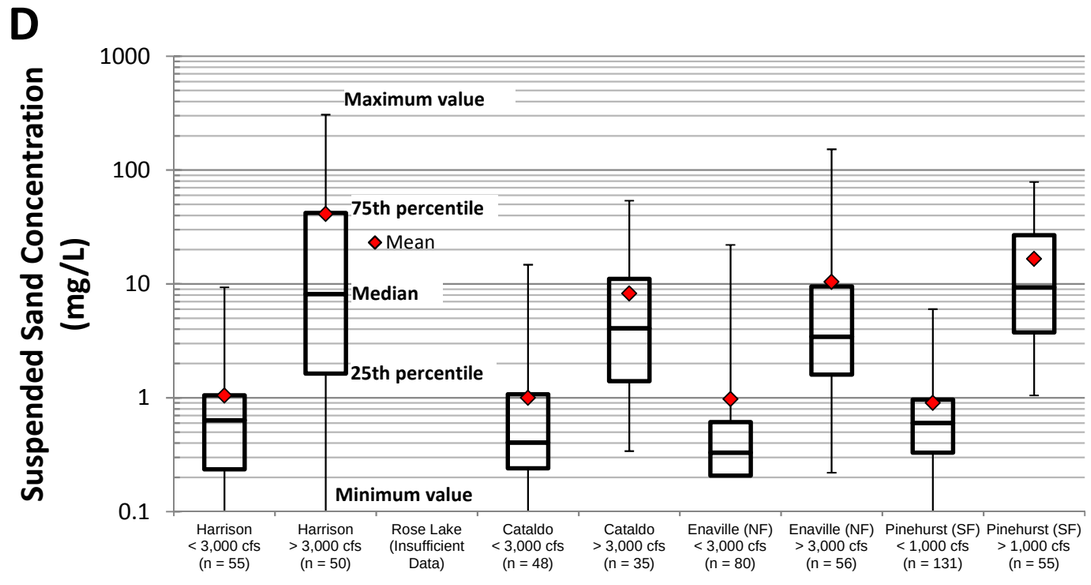

Exhibit 14. **Suspended Sediment Concentration Measurements (Sand Fraction) from USGS and CH2M HILL Sampling Programs**
Processes of Sediment and Lead Transport, Erosion, and Deposition
Lower Basin Coeur d'Alene River (OU3)

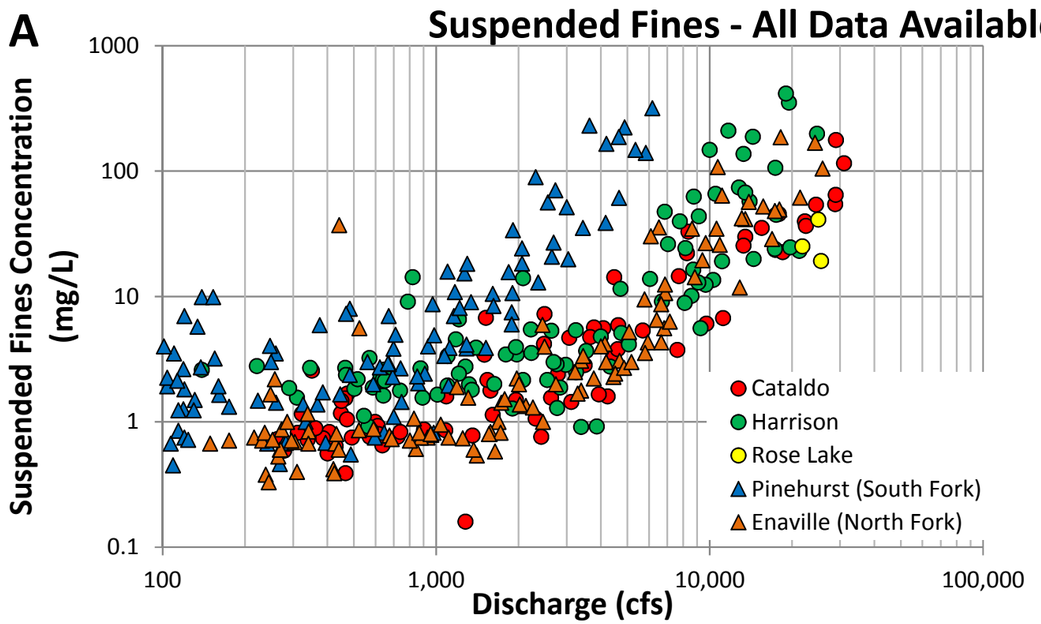

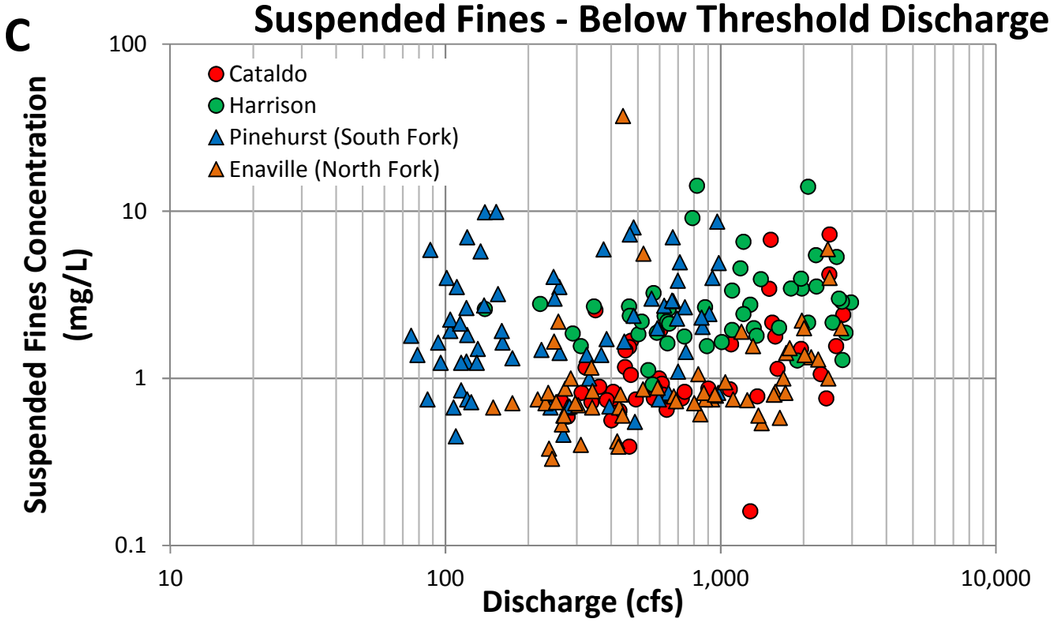

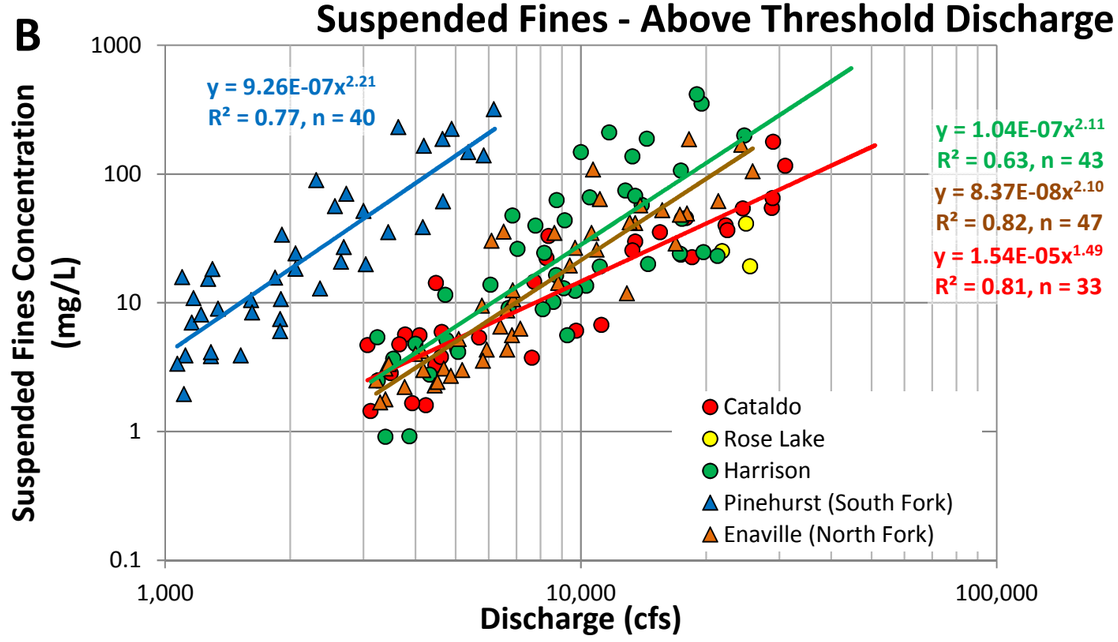

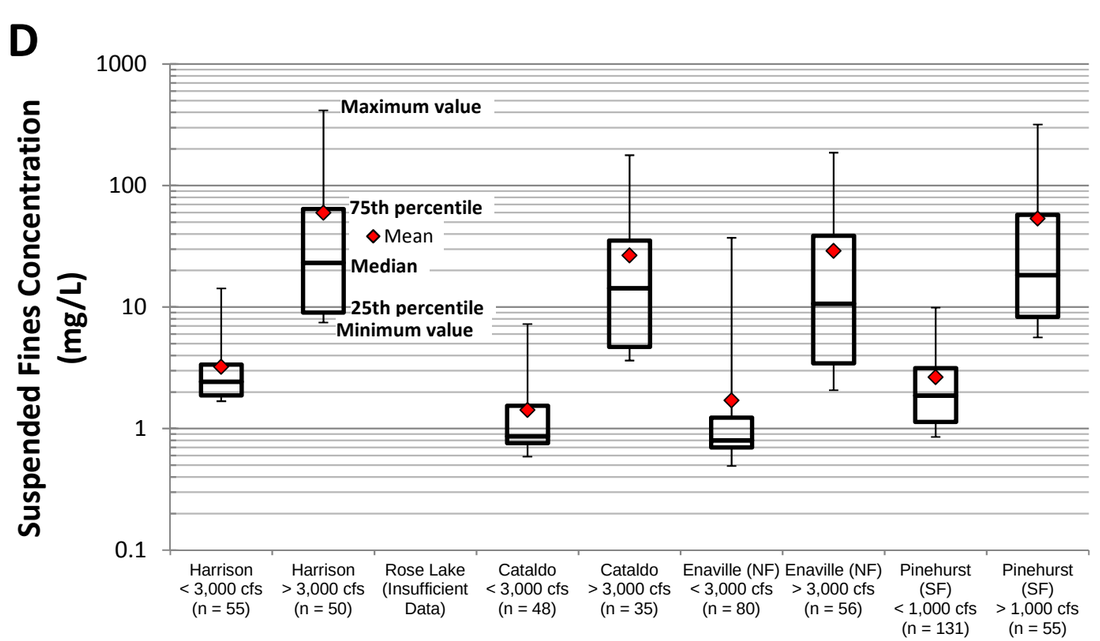

Exhibit 15. **Suspended Sediment Concentration Measurements (Fines Fraction) from USGS and CH2M HILL Sampling Programs**
Processes of Sediment and Lead Transport, Erosion, and Deposition
Lower Basin Coeur d'Alene River (OU3)

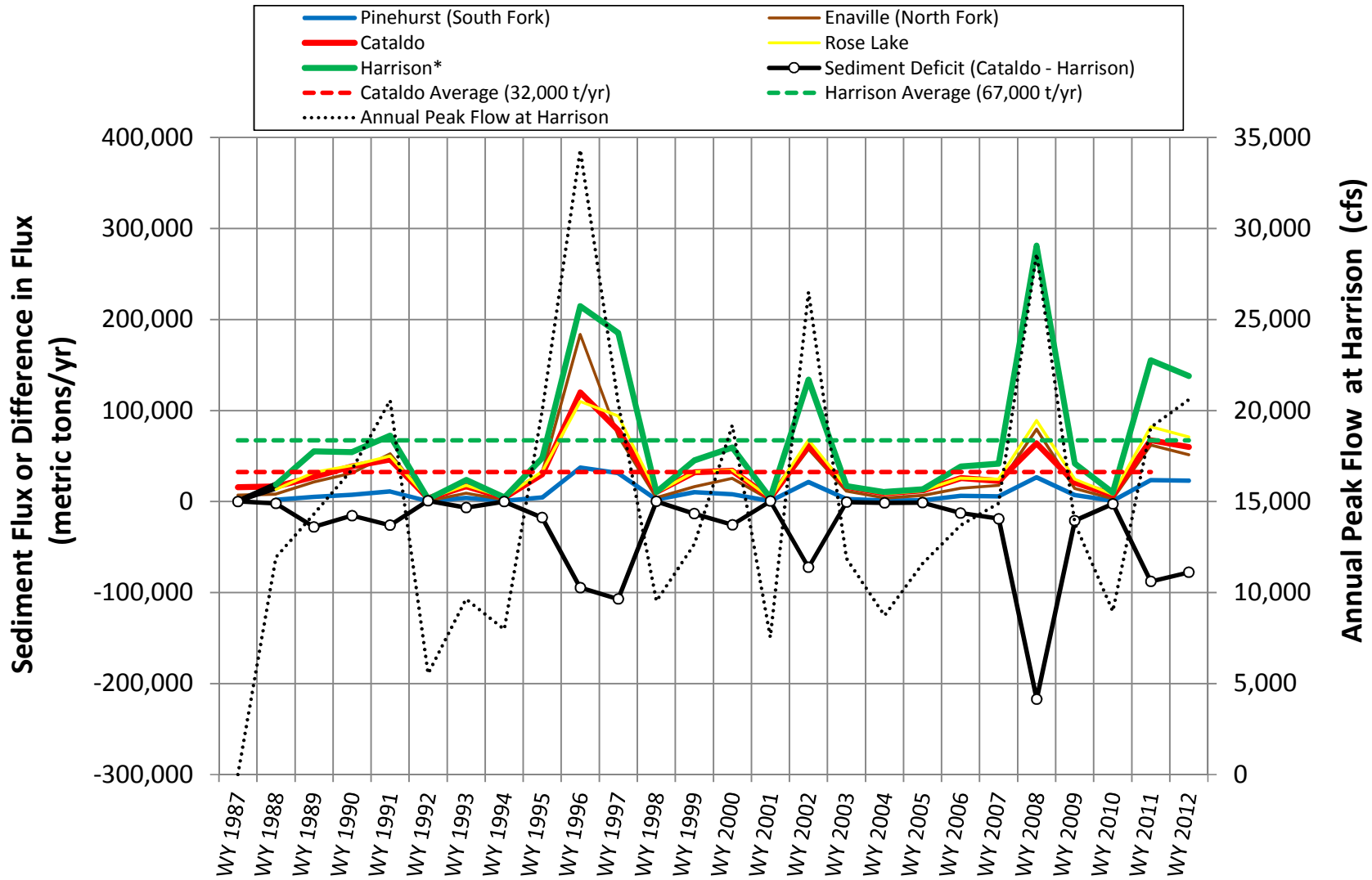

Notes: Harrison flows prior to 2004 are based on calibrated 1-D model, as explained in text.

* A revised time series of predicted annual sediment fluxes for Harrison is available based on a multiple regression equation approach. See Attachment C.

Exhibit 16. **Computed Annual Sediment Fluxes at Five Locations in Lower Basin**

Processes of Sediment and Lead Transport, Erosion, and Deposition

Lower Basin Coeur d'Alene River (OU3)

Exhibit 17. **Computed Sediment Fluxes, by Water Year, for Lower Basin Gaging Stations**

Processes of Sediment and Lead Transport, Erosion, and Deposition

Lower Basin Coeur d'Alene River (OU3)

Water Year	Total Sediment Flux, by Water Year (metric tons)						Peak Flow at Cataldo (cfs)	Peak Flow at Harrison (cfs)
	Pinehurst	Enaville	Cataldo	Rose Lake	Harrison[1,3]	Cataldo *minus* Harrison[2]		
WY 1987	-	7,003	15,737	-	-	-	14,300	-
WY 1988	1,804	8,206	16,329	13,442	18,582	-2,253	17,000	11,948
WY 1989	4,833	21,405	27,167	32,103	55,077	-27,910	17,700	14,314
WY 1990	7,288	31,121	38,640	39,602	54,232	-15,592	28,300	16,750
WY 1991	10,994	52,332	46,145	49,814	72,164	-26,018	33,700	20,551
WY 1992	286	824	3,473	3,187	2,629	843	7,090	5,543
WY 1993	3,857	9,021	16,722	17,562	23,540	-6,818	11,500	9,633
WY 1994	649	1,858	4,302	4,589	4,491	-189	9,238	7,977
WY 1995	4,267	31,534	30,057	33,222	47,732	-17,675	32,400	20,014
WY 1996	37,214	183,438	119,822	109,847	214,468	-94,646	69,898	34,322
WY 1997	31,272	71,948	78,232	93,905	185,347	-107,115	26,400	20,425
WY 1998	1,995	4,158	10,551	9,721	10,404	147	14,300	9,523
WY 1999	10,277	16,321	31,926	32,491	45,280	-13,354	17,300	12,656
WY 2000	7,750	25,483	33,710	34,423	59,367	-25,657	28,900	19,192
WY 2001	438	1,709	4,122	3,815	3,709	412	11,000	7,547
WY 2002	21,243	57,459	61,469	67,657	133,799	-72,330	37,600	26,509
WY 2003	2,791	11,211	16,171	15,528	16,989	-818	23,700	11,872
WY 2004	808	3,913	8,874	8,590	10,492	-1,618	9,820	8,740
WY 2005	1,260	6,683	12,163	11,767	13,383	-1,220	20,200	11,600
WY 2006	5,994	14,330	25,702	25,587	38,351	-12,649	20,600	13,700
WY 2007	5,521	17,646	22,460	24,378	41,499	-19,039	24,200	14,900
WY 2008	26,573	79,437	63,780	88,845	281,002	-217,222	31,900	28,600
WY 2009	7,119	14,135	20,796	24,482	41,856	-21,059	19,700	13,800
WY 2010	787	2,897	7,164	7,858	9,752	-2,588	9,160	8,970
WY 2011	23,363	61,806	67,249	82,053	155,102	-87,854	32,900	19,074
WY 2012	22,833	51,125	60,010	70,766	137,792	-77,782	28,900	20,600
Average	**9,649**	**30,269**	**32,414**	**36,209**	**67,082**	**34,667**		

Notes:

[1] Computed using Harrison flows prior to 2004 that are based on calibrated 1-D model, as explained in text.

[2] Average differential computed as the difference between 25-yr sediment flux average Harrison and Cataldo.

[3] A revised time series of predicted annual sediment and lead fluxes for Harrison is available based on a multiple regression equation approach. See Attachment C.

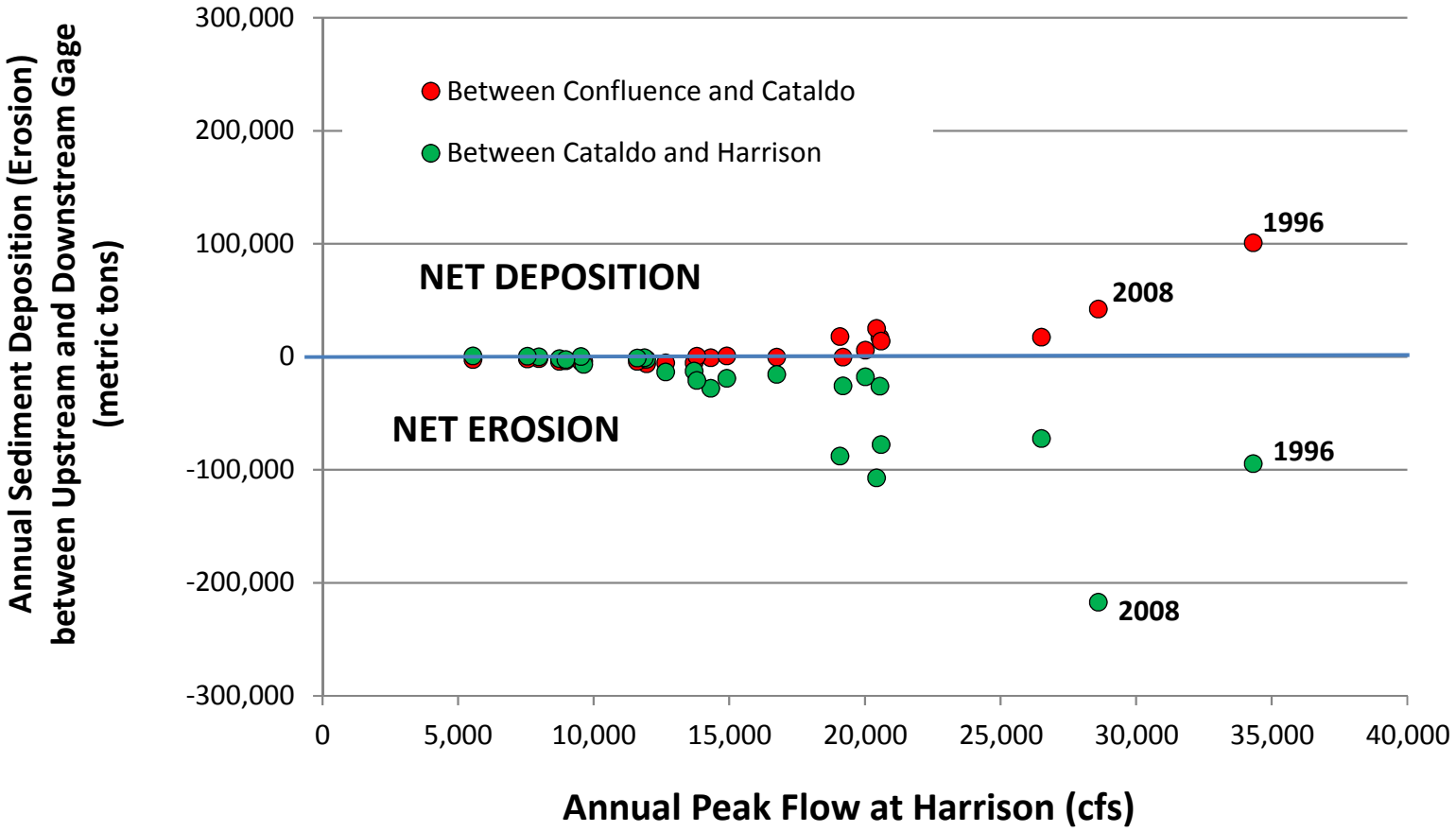

Note: Each data point shown on this graph represents the difference in computed sediment flux between two stations for a given water year, based on integrating the sediment rating curves over the 15-minute flow record at each station for the year.

Exhibit 18. **Net Sediment Deposition and Erosion between Gaged Locations**

Processes of Sediment and Lead Transport, Erosion, and Deposition

Lower Basin Coeur d'Alene River (OU3)

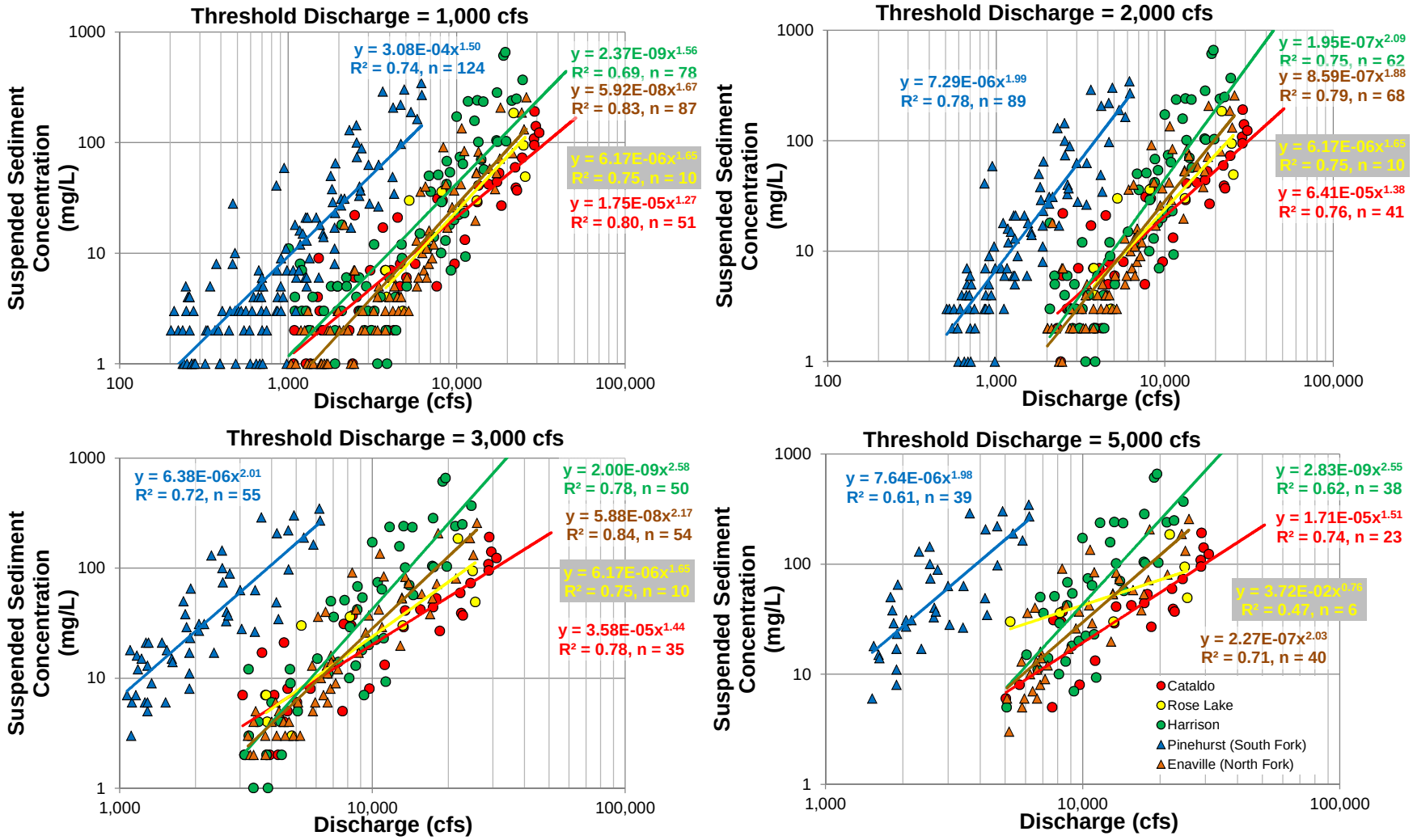

Exhibit 19. **Effect of Changing the Threshold Discharge on Computed Rating Curves**
Processes of Sediment and Lead Transport, Erosion and Deposition
Lower Basin Coeur d'Alene River (OU3)

Exhibit 20. **Sensitivity of Average Annual Sediment Flux and Net Sediment Deficit[1] to the Assumed Threshold Discharge**
Processes of Sediment and Lead Transport, Erosion, and Deposition
Lower Basin Coeur d'Alene River (OU3)

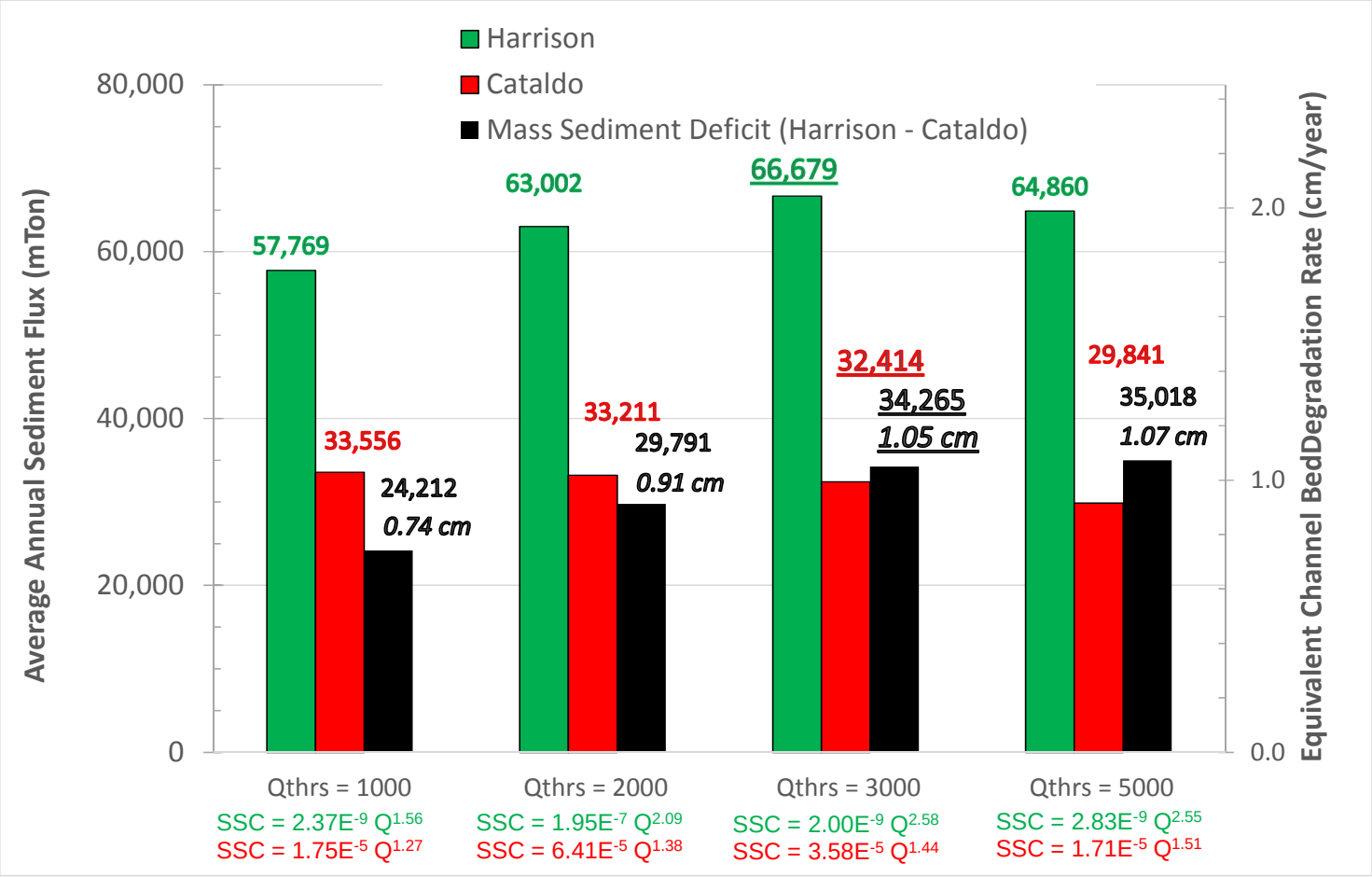

Note:

1. Vertical axis on the left shows sediment mass transport rates and the mass sediment deficit (net erosion) between the Cataldo and Harrison. Right axis is scaled to show the equivalent average aggradation/degradation of the bed. The right axis was computed by dividing the volumetric sediment deficit by the area of the riverbed, where the volume deficit is mass deficit times riverbed bulk density (1.5 metric tons/m^3). The equations on the bottom of the graph are the regression equations from Exhibit 19.

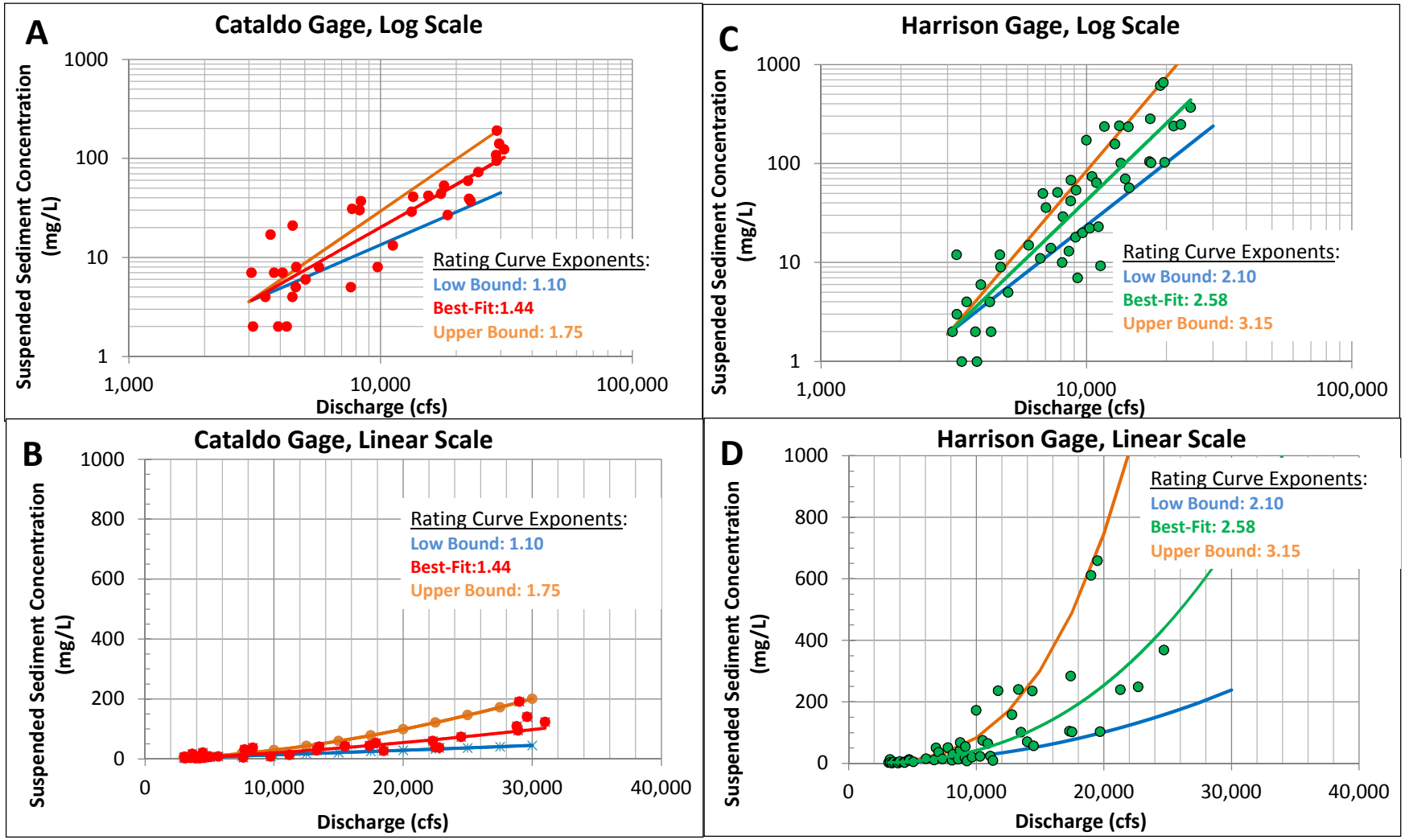

Exhibit 21. **Estimating the Upper and Lower Bounding Exponents for Sediment Rating Curves at Cataldo and Harrison Gages**
Processes of Sediment and Lead Transport, Erosion and Deposition
Lower Basin Coeur d'Alene River (OU3)

Exhibit 22. **Sensitivity of Average Annual Sediment Flux to the Rating Curve Exponent**
Processes of Sediment and Lead Transport, Erosion and Deposition
Lower Basin Coeur d'Alene River (OU3)

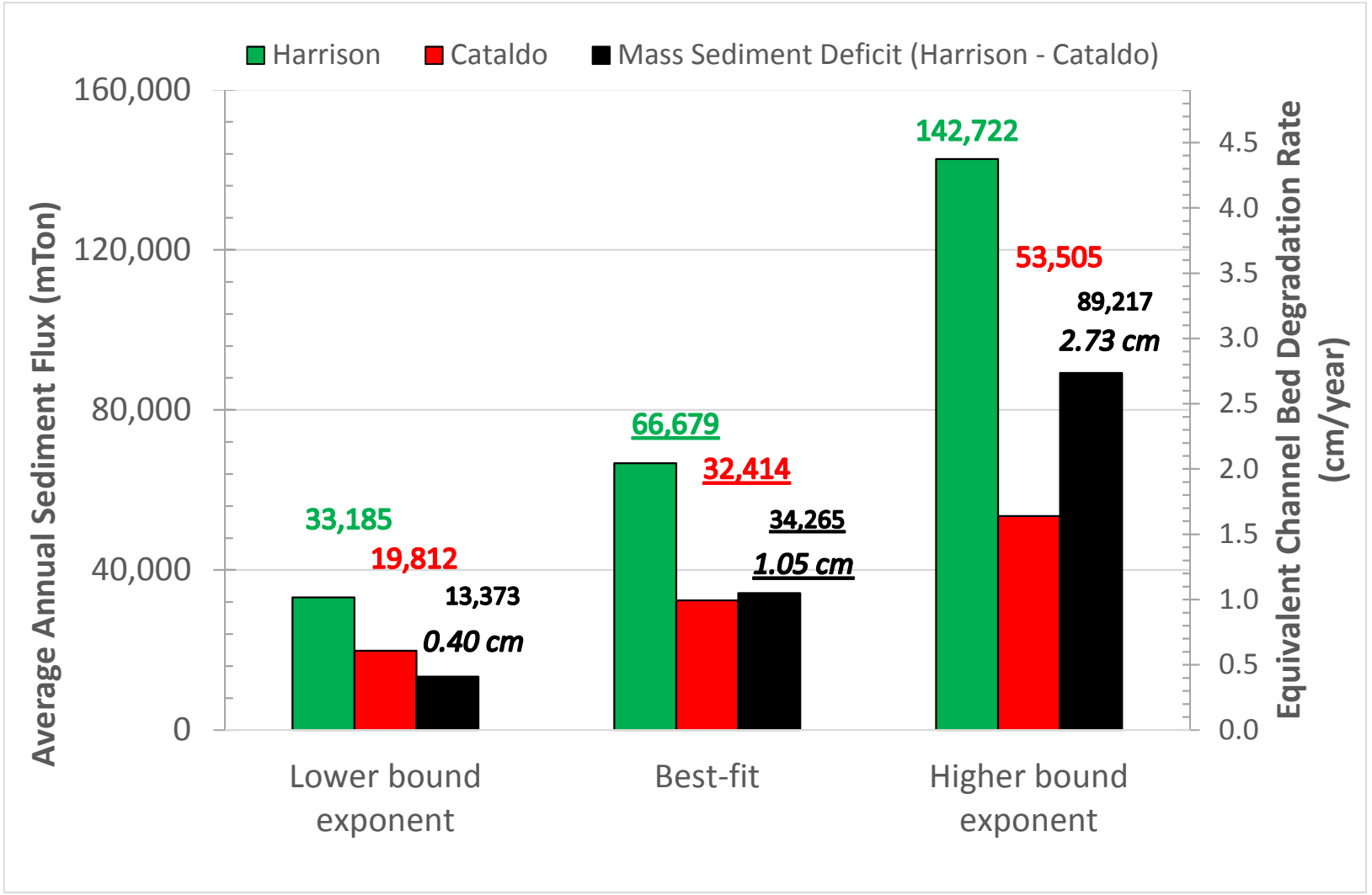

Exhibit 23. **Comparison of Linear and Power Law Regressions with Data from Harrison and Cataldo**
Processes of Sediment and Lead Transport, Erosion, and Deposition
Lower Basin Coeur d'Alene River (OU3)

Log-log plots

Linear plots

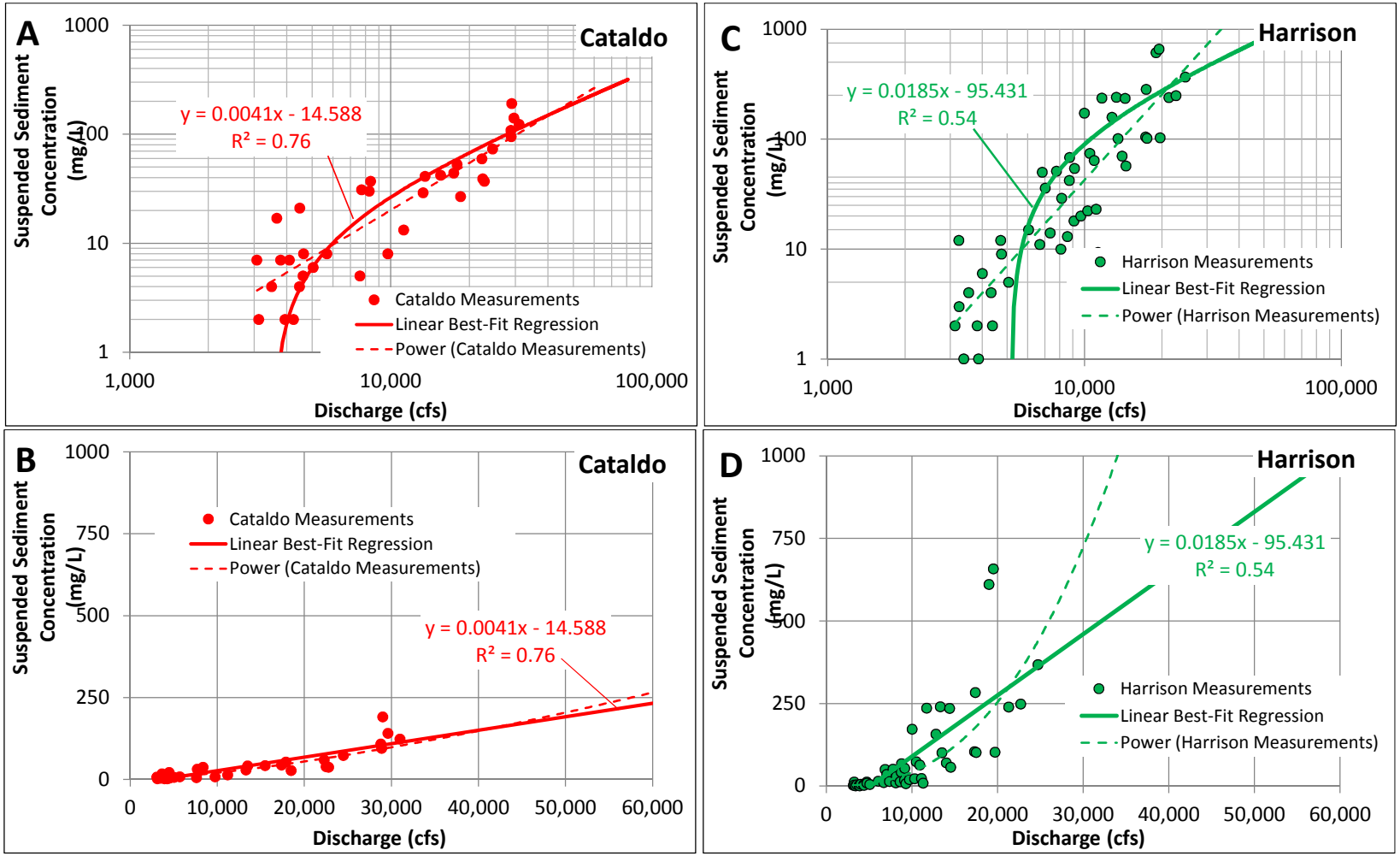

Exhibit 24. **Summary of Sensitivity of Average Sediment Fluxes to Rating Curve Regression Models**
Processes of Sediment and Lead Transport, Erosion and Deposition
Lower Basin Coeur d'Alene River (OU3)

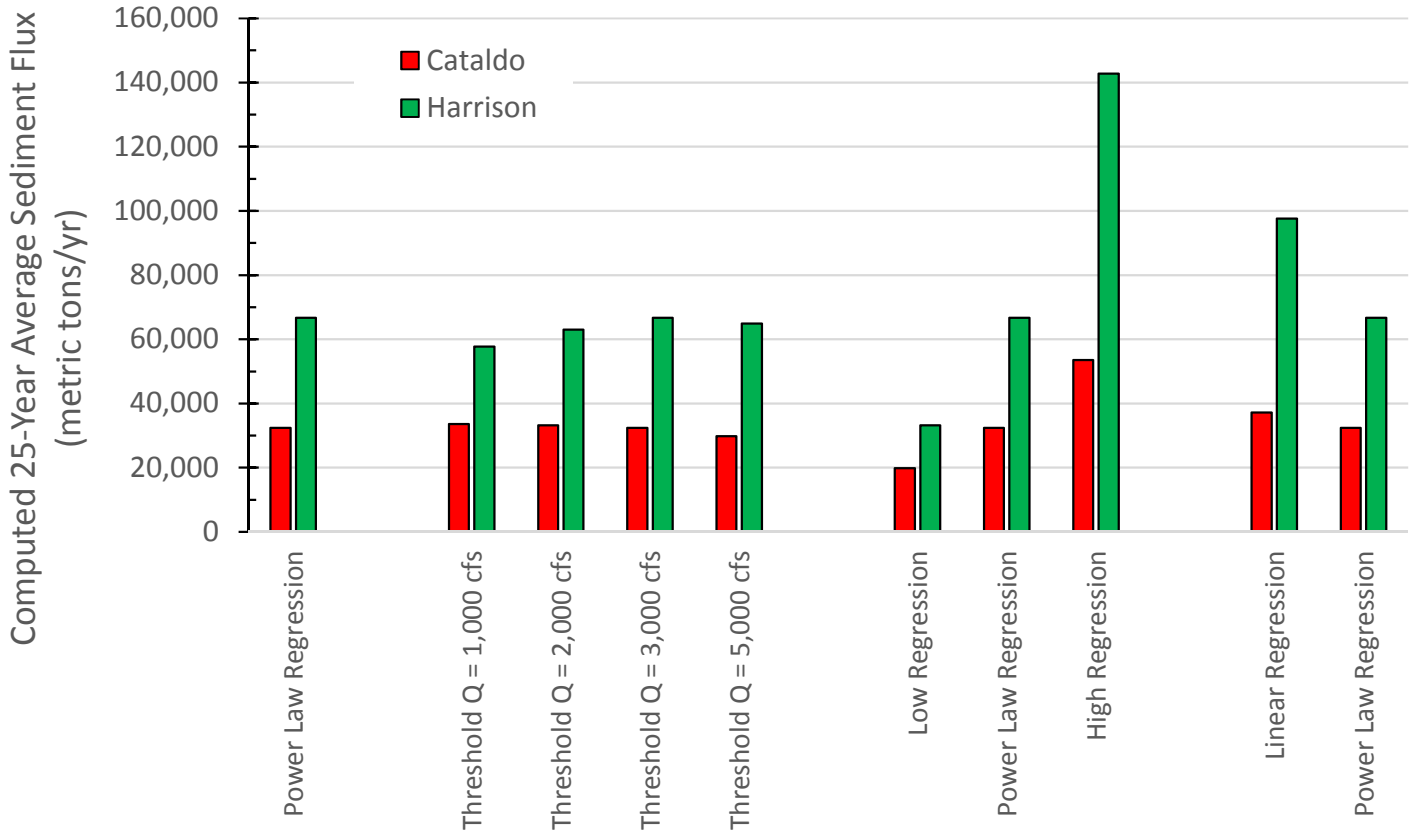

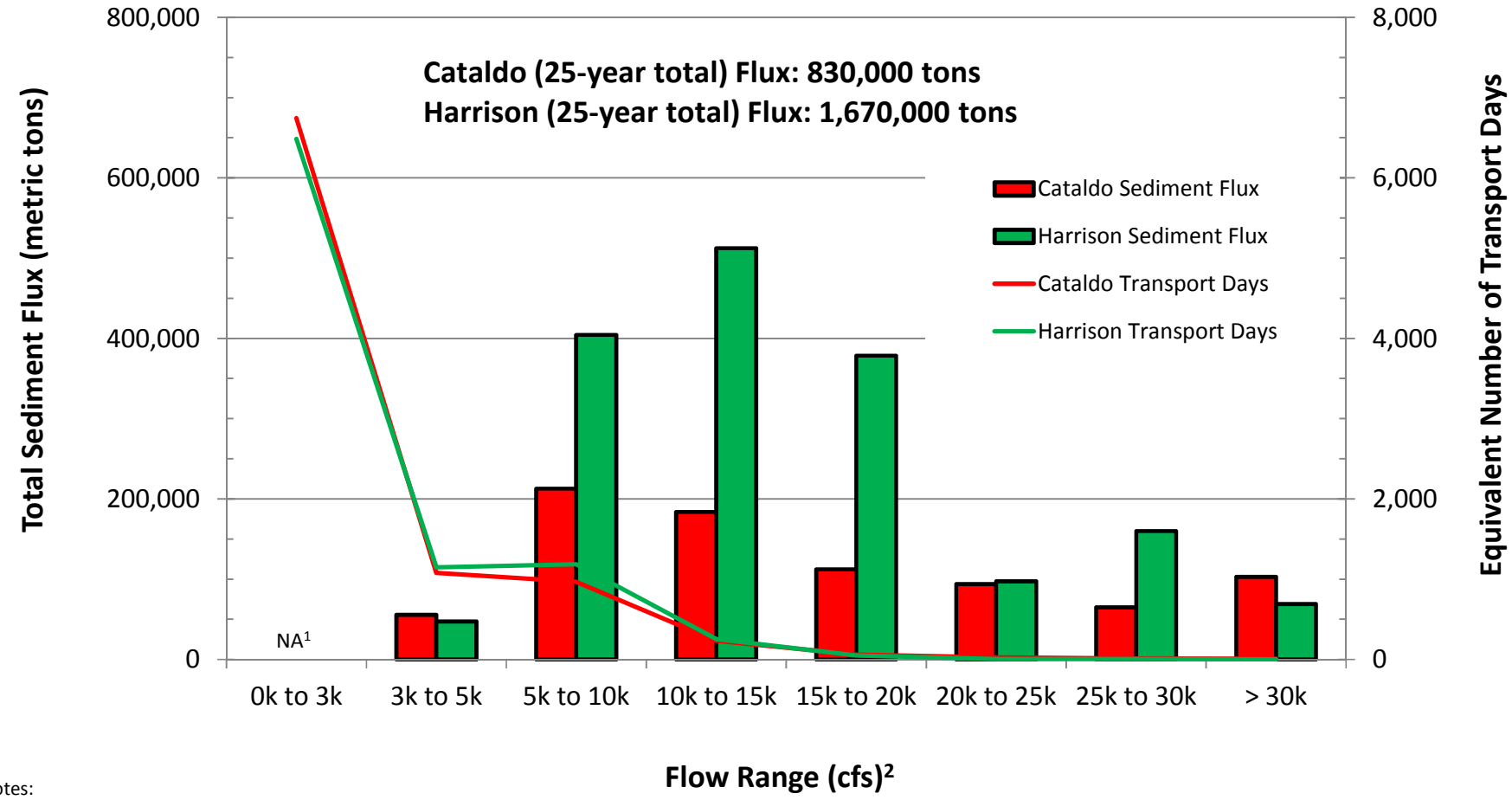

Notes:
[1]Flow range is below threshold.
[2]Measured at Cataldo and Harrison gaging stations, respectively.

Exhibit 25. **Frequency and Magnitude of Sediment Fluxes at Harrison and Cataldo**
Processes of Sediment and Lead Transport, Erosion, and Deposition
Lower Basin Coeur d'Alene River (OU3)

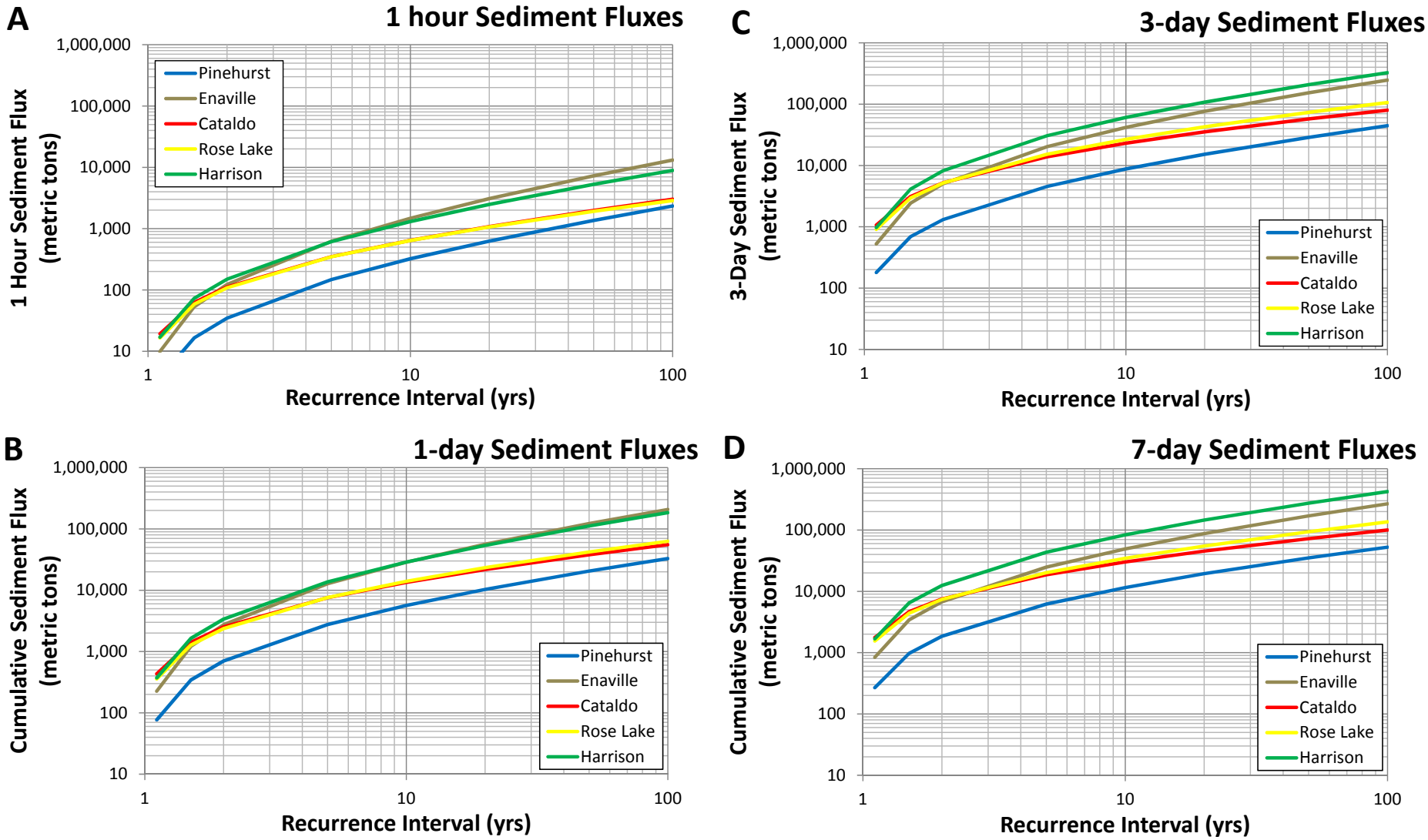

Exhibit 26. **Frequency/Magnitude/Duration Plots for Sediment Transport in the Lower Basin**
Processes of Sediment and Lead Transport, Erosion, and Deposition
Lower Basin Coeur d'Alene River (OU3)

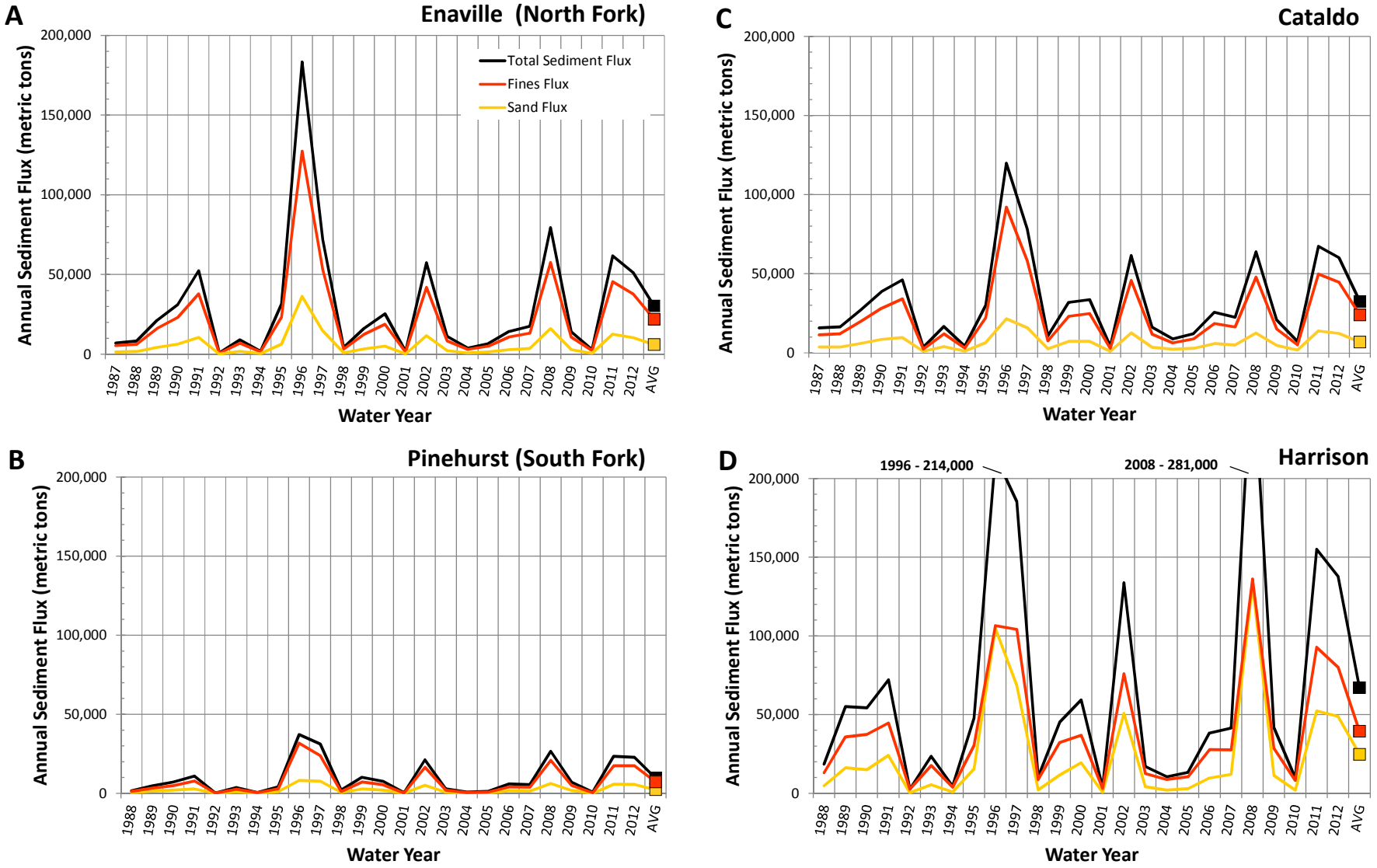

Exhibit 27. **Annual Sediment Fluxes By Grain Size**
Processes of Sediment and Lead Transport, Erosion, and Deposition
Lower Basin Coeur d'Alene River (OU3)

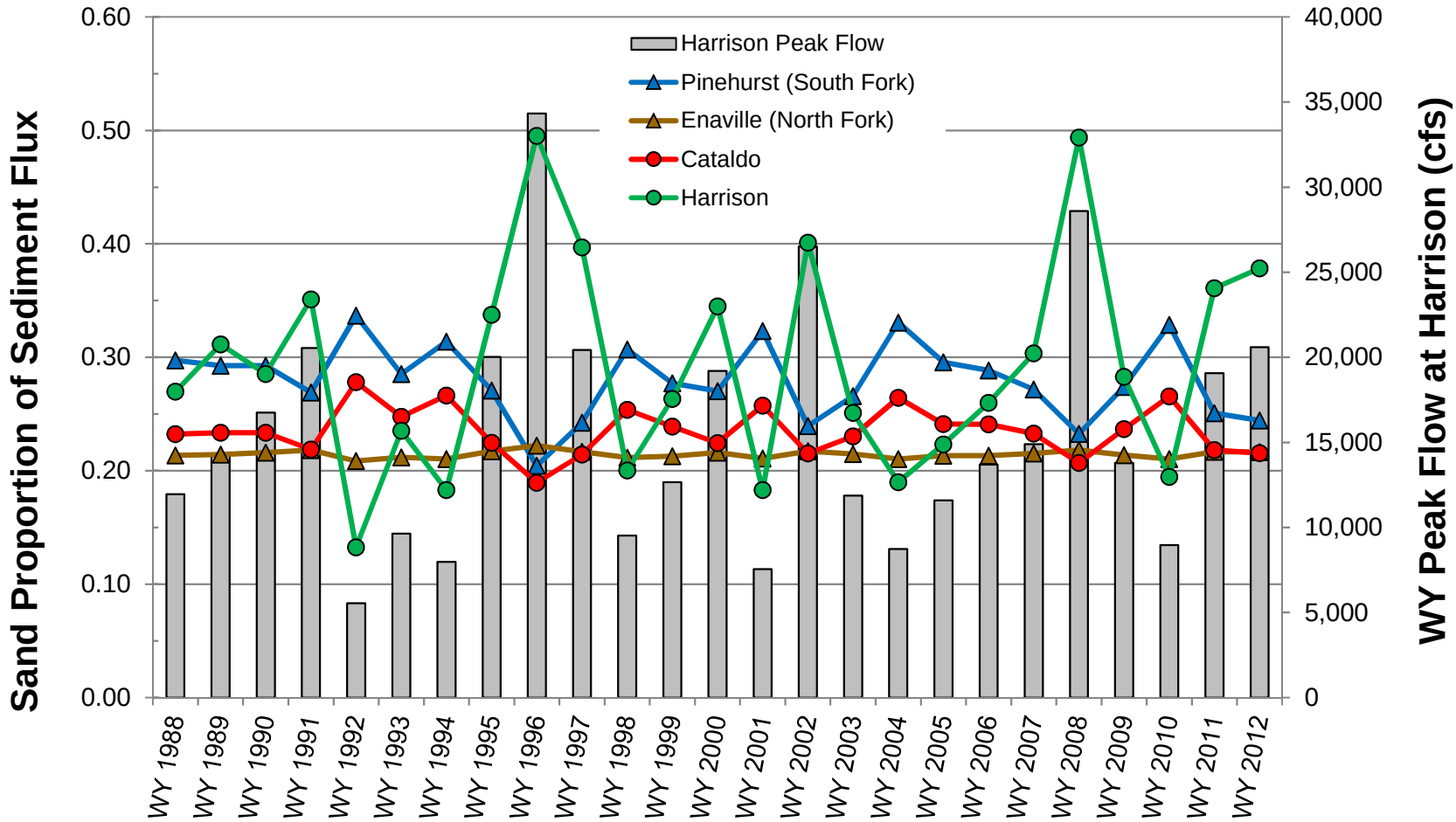

Note: Colored symbols and lines indicate the percent sand in the annual sediment fluxes (left vertical axis) based on using separate rating curves for sand and fines to compute the flux of each fraction (see text for additional explanation).

Exhibit 28. **Computed Sand Proportion of Annual Sediment Flux at Four Gaging Stations**
Processes of Sediment and Lead Transport, Erosion, and Deposition
Lower Basin Coeur d'Alene River (OU3)

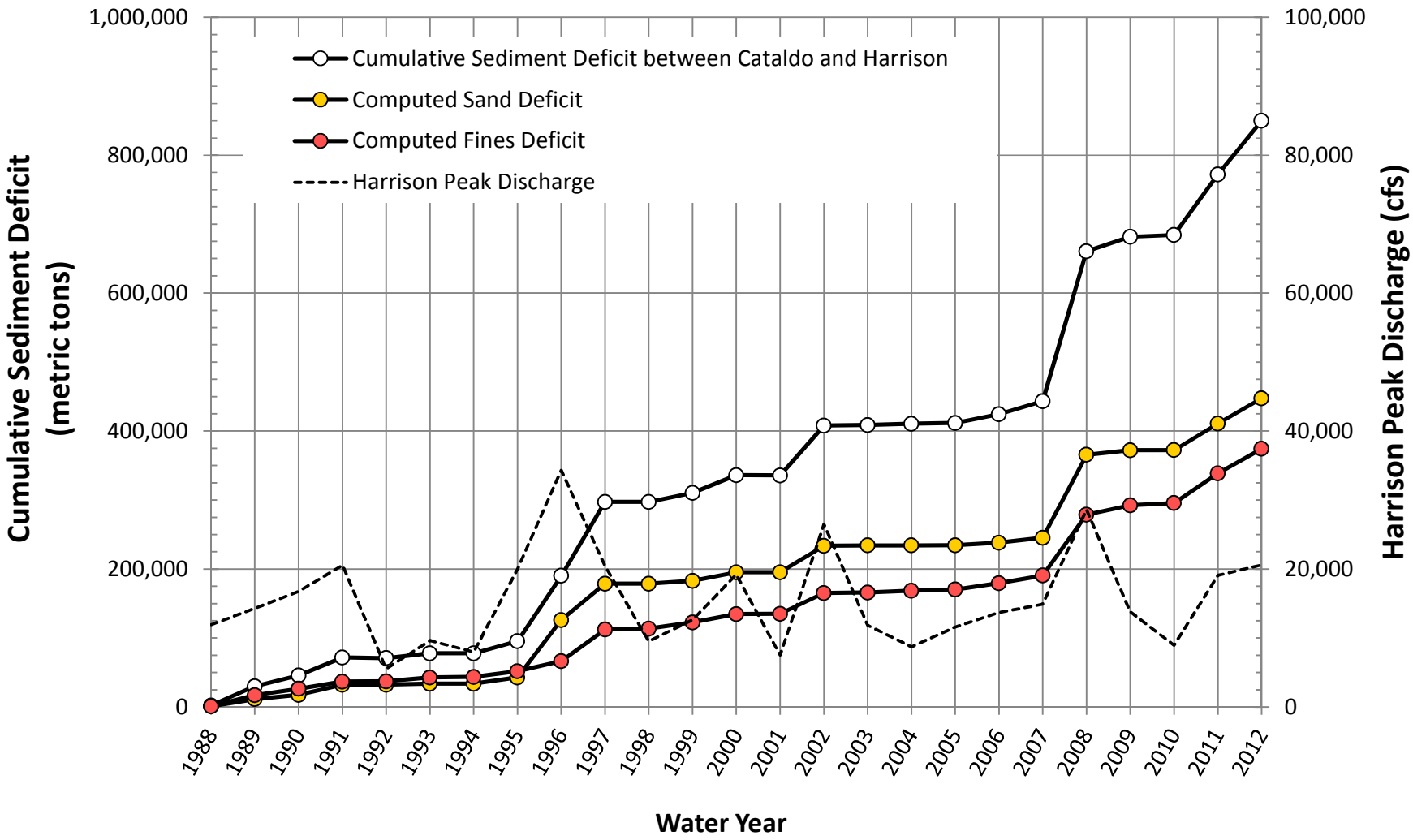

Exhibit 29. **Sand and Fines Contributions to the Net Sediment Deficit between Cataldo and Harrison**
Processes of Sediment and Lead Transport, Erosion, and Deposition
Lower Basin Coeur d'Alene River (OU3)

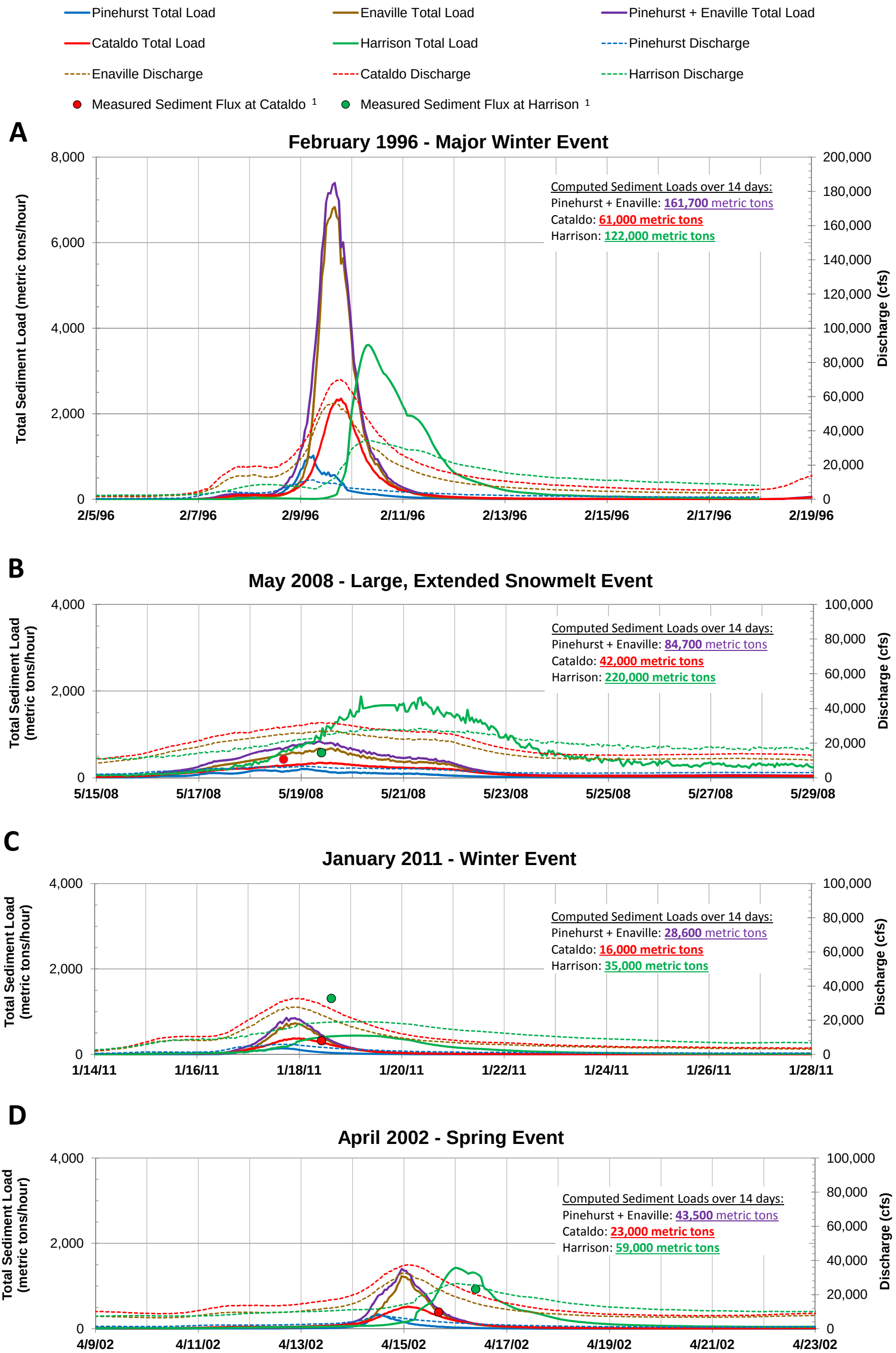

Note:
1. Instantaneous Sediment Flux Computed from SSC Measurement and Gage Discharge

Exhibit 30. **Flow and Sediment Transport in Four High Flow Events**
Processes of Sediment and Lead Transport, Erosion, and Deposition
Lower Basin Coeur d'Alene River (OU3)

Exhibit 31. **Measurements of Lead in Suspended Sediment**
Processes of Sediment and Lead Transport, Erosion, and Deposition
Lower Basin Coeur d'Alene River (OU3)

Date	Time	Discharge (cfs)	SSC (mg/L)	Pb_{BULK} (mg/kg)	$Pb_{63\text{-}250\mu m}$ (mg/kg)	$Pb_{<63\mu m}$ (mg/kg)
Harrison						
5/19/2008	9:30	22,700	249	4,080	--	--
5/20/2009	12:30	11300	9.294	3,930	--	--
12/13/2010	15:00	7,040	35.9	4,870	--	4,490
12/15/2010	15:00	13,300	240	4,480	4,100	5,290
1/18/2011	15:00	19,500	658	4,900	2,890	6,280
5/17/2011	18:00	17,300	105	3,220	2,170	4,320
4/1/2012	16:00	17,400	283	1,550	2,970	5,210
4/13/2012		10,300	22	3,580	--	--
4/24/2012	15:00	17,500	102	3,710	2,700	4,770
4/27/2012	15:00	21,300	240	2,390	2,220	2,390
4/7/2013	16:30	12,800	158	4,290	3,880	5,050
			Average	3,727	2,990	4,725
			Standard Deviation	1,027	751	1,118
Rose Lake						
5/17/2011	13:00	21,800	185	2,510	3,980	2,180
4/1/2012	11:00	25,900	94	1,740	3,050	3,350
4/27/2012	10:30	25,531	49	2,980	3,170	2,470
4/7/2013		no data	53	3,320	4,830	3,550
			Average	2,638	3,758	2,888
			Standard Deviation	684	826	665
Cataldo						
5/18/2008	15:45	29,600	140	1,130	--	--
12/14/2010	14:00	18,500	26.8	966	--	888
1/18/2011	10:30	28,800	108	790	983	651
5/16/2011	12:00	22,300	59.5	662	1,040	754
3/31/2012	10:45	28,900	95	886	1,230	748
4/12/2012	14:00	11,200	13	1,400	--	--
4/24/2012	12:00	24500	73	1,030	1,540	1,070
4/26/2012	9:30	22,800	37	1,840	--	1,690
4/6/2013	17:00	17,400	44	784	1,080	874
			Average	1,054	1,175	954
			Standard Deviation	367	224	351
Pinehurst						
5/18/2008	12:00	6,210	270	2,660	--	--
5/19/2009	17:30	3,430	26	3,440	--	--
12/14/2010	10:00	1,900	23	2,730	3,030	2,170
1/17/2011	16:00	5,840	164	1,440	--	1,480
5/16/2011	12:00	4,660	97	2,940	3,360	2,610
3/31/2012	11:45	5,360	189	1,410	2,000	1,380
4/26/2012		4,250	34	2,490	--	--
4/6/2013	10:00	2,640	33	2,340	--	--
			Average	2,431	2,797	1,910
			Standard Deviation	703	709	584
Enaville						
5/18/2008	13:45	25,100	132	146	--	--
12/15/2010	10:00	12,900	19.7	122	--	135
1/17/2011	14:00	25,900	257	192	205	241
5/16/2011	16:00	18,000	71.6	338	525	365
3/31/2012	14:00	21,400	80	147	--	--
4/26/2012	13:30	16,900	38	362	--	413
4/6/2013	14:00	13,500	83	123	318	238
			Average	204	349	278
			Standard Deviation	102	162	111

Note:
Only data from BEMP samples collected through WY 2013 are shown. Data from USGS samples use different methodology and are not comparable at low flows (see text and Exhibit 32). Lead data from USGS samples and BEMP samples after WY 2013 are provided in Exhibit 32.

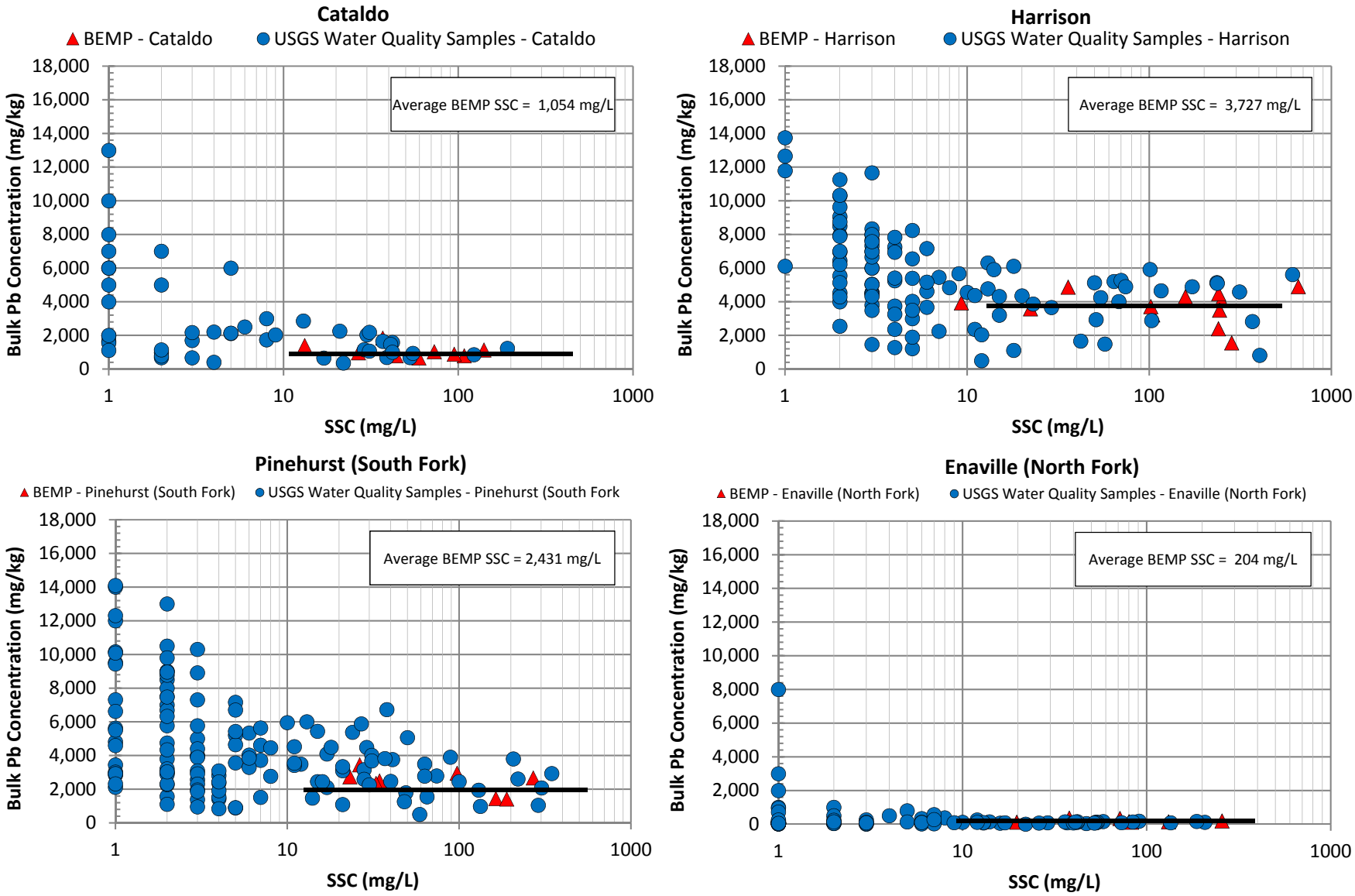

Exhibit 32. **Comparison of Bulk Lead on Sediment between USGS and BEMP Samples**
Processes of Sediment and Lead Transport, Erosion, and Deposition
Lower Basin of the Coeur d'Alene River (OU3)

A. Suspended Sediment Concentration

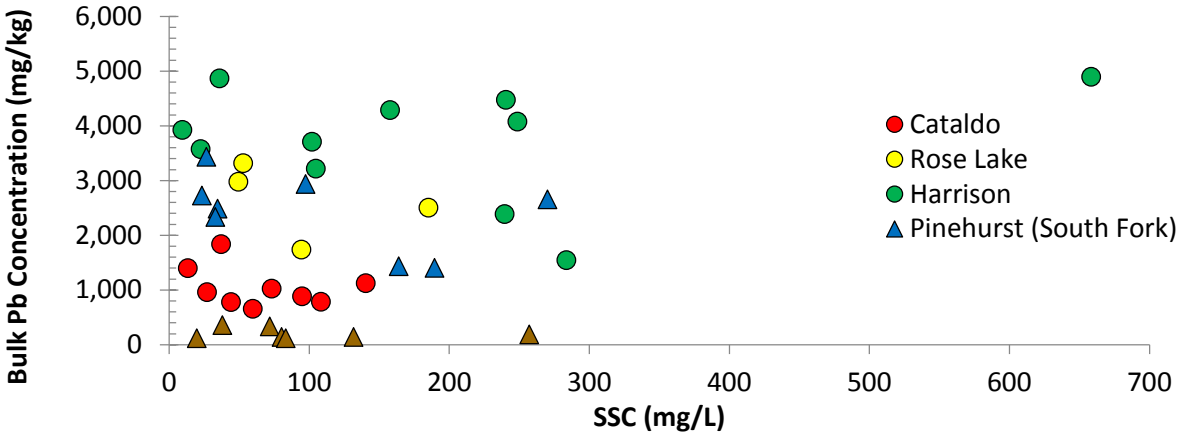

B. Discharge

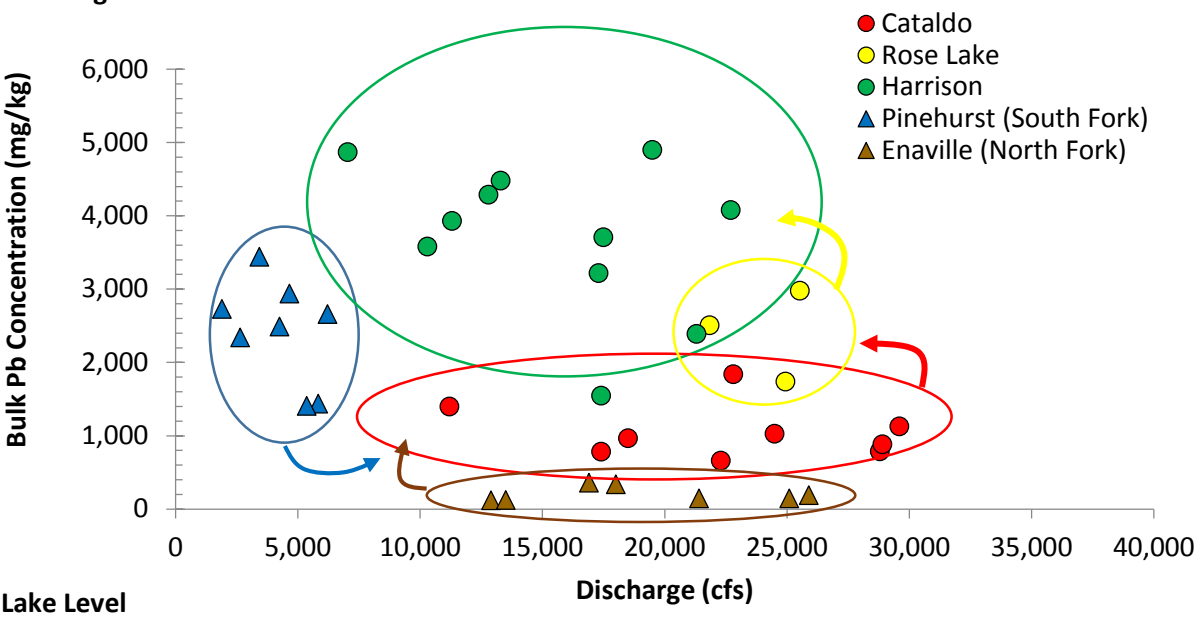

C. Lake Level

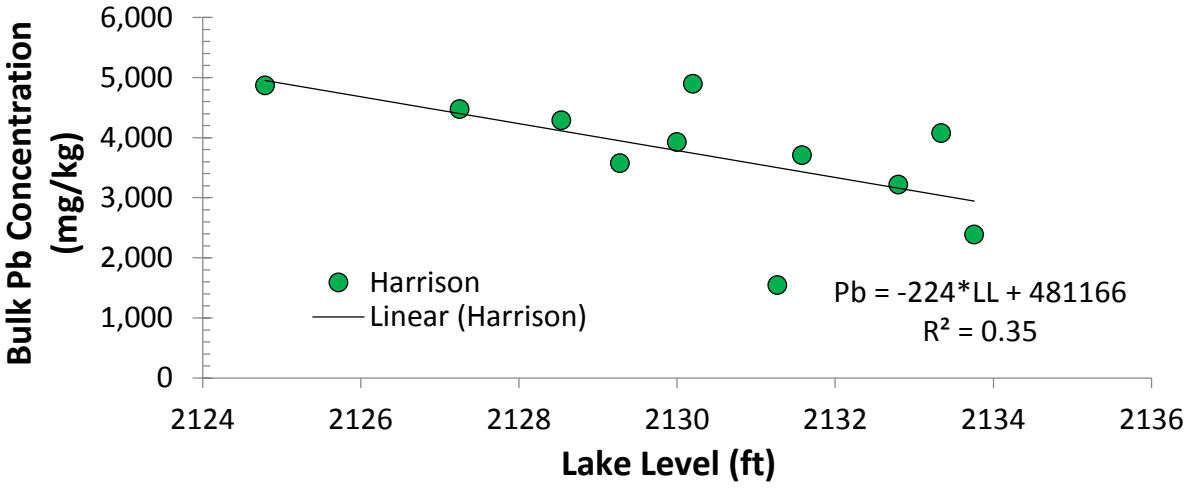

Exhibit 33. **Lead Concentration on Suspended Sediment**
Processes of Sediment and Lead Transport, Erosion, and Deposition
Lower Basin Coeur d'Alene River (OU3)

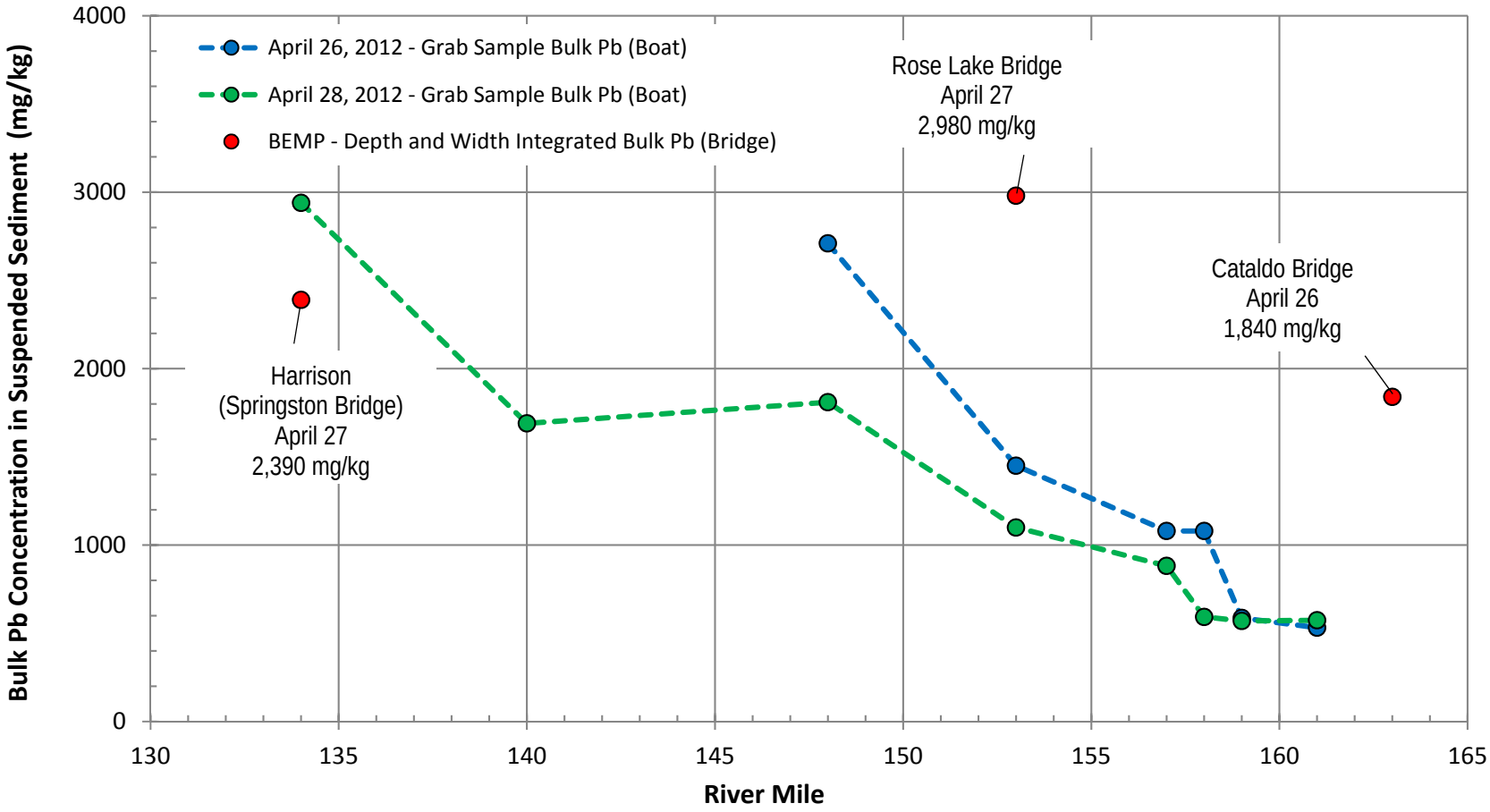

Exhibit 34. **Downstream Distribution of Bulk Lead Concentration on Suspended Sediment in the April 2012 Flood Event**
Processes of Sediment and Lead Transport, Erosion, and Deposition
Lower Basin Coeur d'Alene River (OU3)

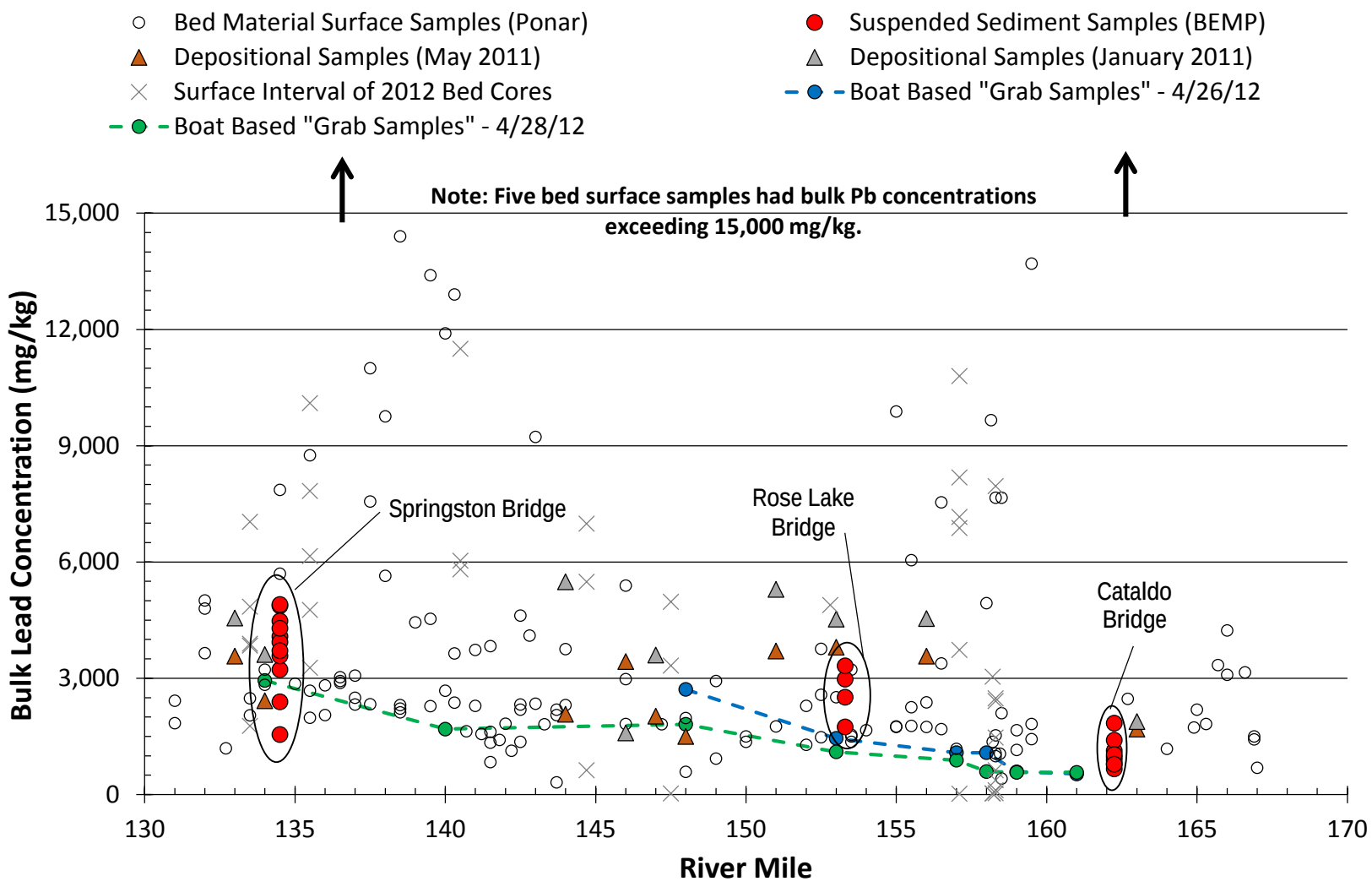

Exhibit 35. **Downstream Distribution of Bulk Lead Concentration in Recent Suspended Sediment, Depositional Sediment, and Riverbed Surface Samples**
Processes of Sediment and Lead Transport, Erosion, and Deposition
Lower Basin Coeur d'Alene River (OU3)

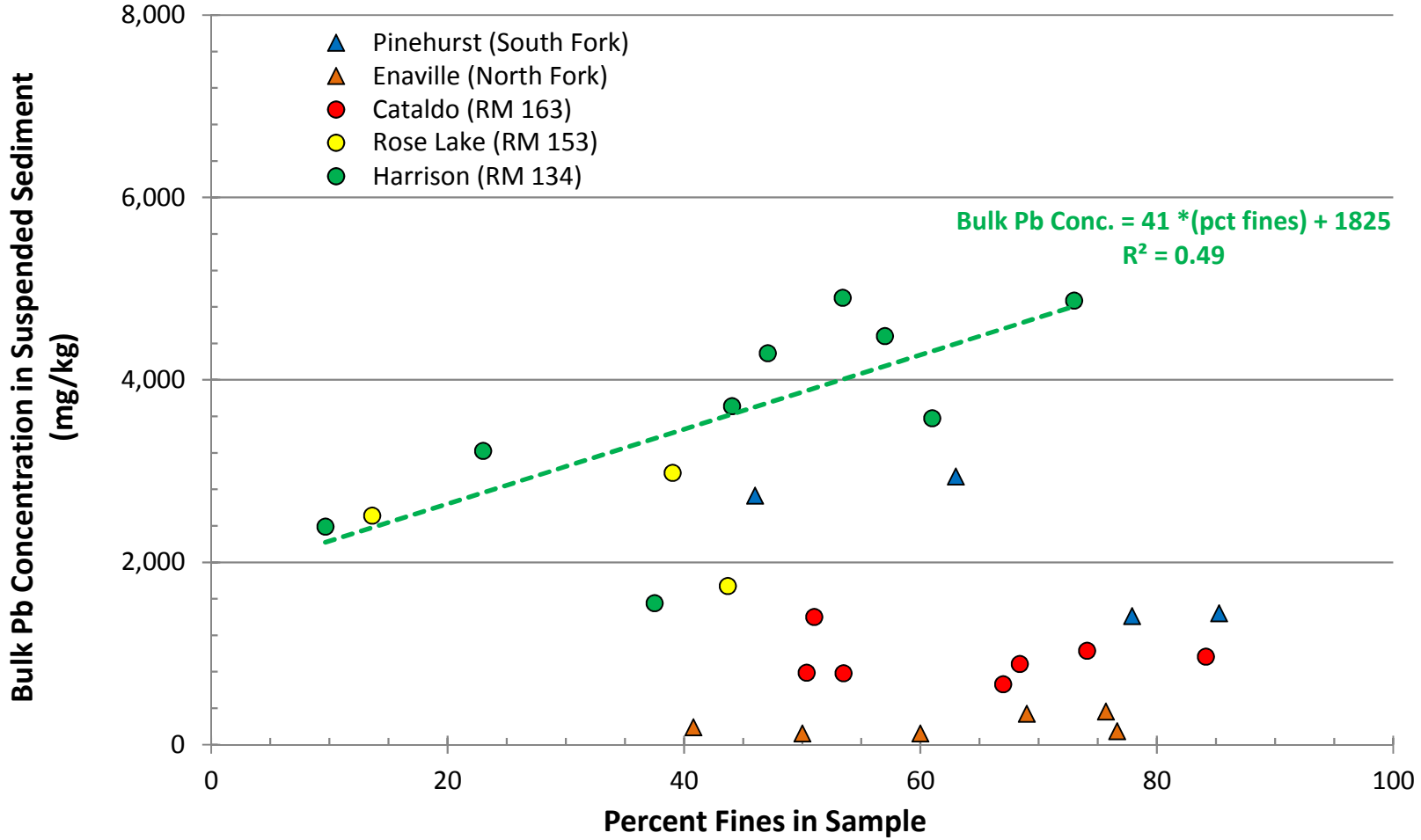

Exhibit 36. **Relationship between Bulk Lead Concentration and Percent Fines in Suspended Sediment**
Processes of Sediment and Lead Transport, Erosion, and Deposition
Lower Basin Coeur d'Alene River (OU3)

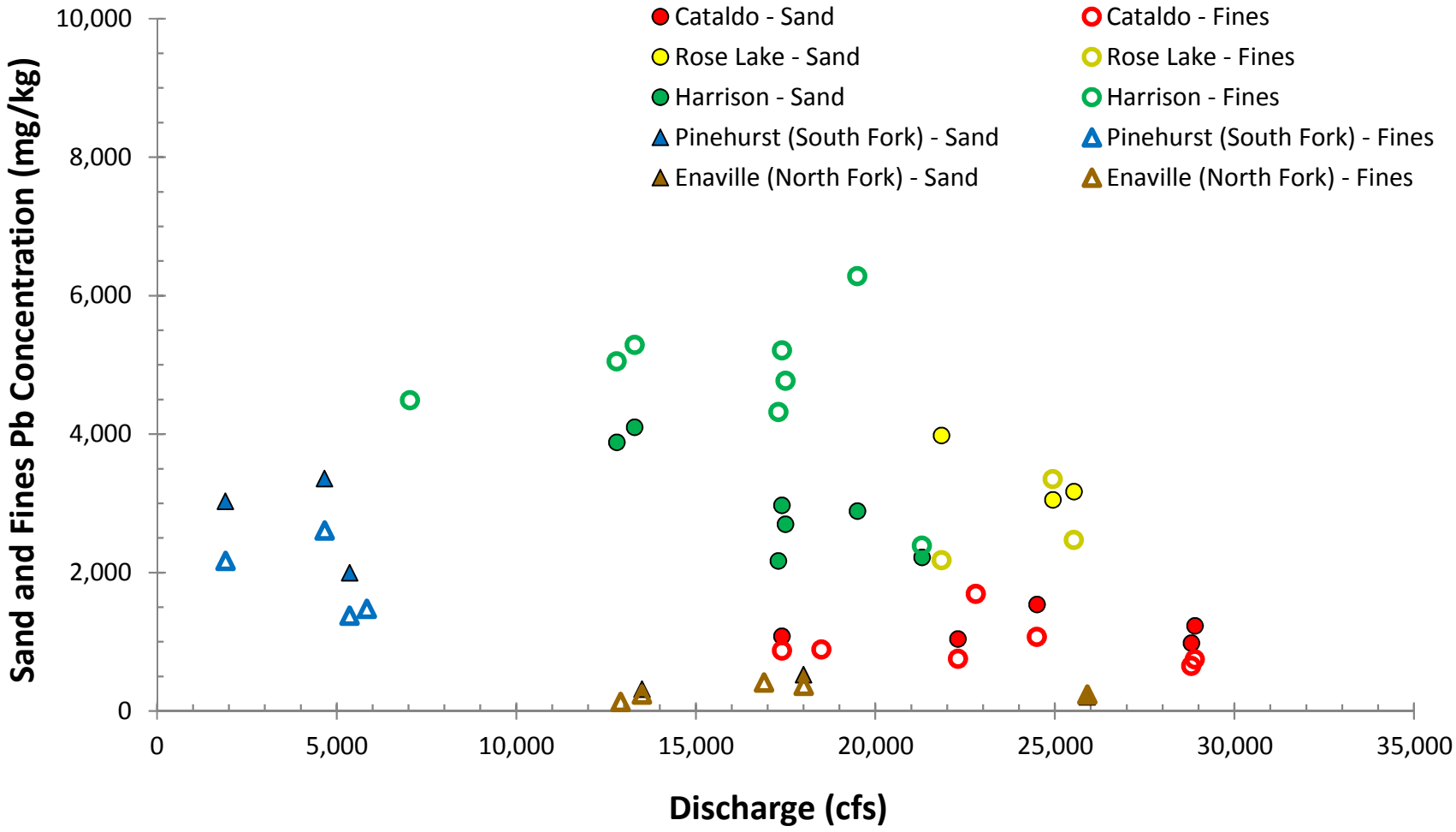

Exhibit 37. **Lead Concentrations in Different Sample Subfractions of Suspended Sediment Samples**
Processes of Sediment and Lead Transport, Erosion, and Deposition
Lower Basin Coeur d'Alene River (OU3)

Exhibit 38. **Computed Lead Fluxes, by Water Year, for Lower Basin Gaging Stations**

Processes of Sediment and Lead Transport, Erosion, and Deposition

Lower Basin Coeur d'Alene River (OU3)

	Total Lead Flux, by Water Year (metric tons)						Peak Flow at	Peak Flow at
Water Year	Pinehurst	Enaville	Cataldo	Rose Lake	Harrison[1]	Cataldo *minus* Harrison[1]	Cataldo (cfs)	Harrison (cfs)
WY 1987	-	1.4	16.6	-	-	-	14,300	-
WY 1988	4.4	1.7	17.2	32.4	69.3	-52.0	17,000	11,948
WY 1989	11.8	4.4	28.6	77.4	205.3	-176.6	17,700	14,314
WY 1990	17.7	6.4	40.7	95.4	202.1	-161.4	28,300	16,750
WY 1991	26.7	10.7	48.6	120.1	269.0	-220.3	33,700	20,551
WY 1992	0.7	0.2	3.7	7.7	9.8	-6.1	7,090	5,543
WY 1993	9.4	1.8	17.6	42.3	87.7	-70.1	11,500	9,633
WY 1994	1.6	0.4	4.5	11.1	16.7	-12.2	9,238	7,977
WY 1995	10.4	6.4	31.7	80.1	177.9	-146.2	32,400	20,014
WY 1996	90.5	37.5	126.3	264.7	799.4	-673.1	69,898	34,322
WY 1997	76.0	14.7	82.5	226.3	690.8	-608.4	26,400	20,425
WY 1998	4.9	0.8	11.1	23.4	38.8	-27.7	14,300	9,523
WY 1999	25.0	3.3	33.7	78.3	168.8	-135.1	17,300	12,656
WY 2000	18.8	5.2	35.5	83.0	221.3	-185.7	28,900	19,192
WY 2001	1.1	0.3	4.3	9.2	13.8	-9.5	11,000	7,547
WY 2002	51.6	11.7	64.8	163.1	498.7	-433.9	37,600	26,509
WY 2003	6.8	2.3	17.0	37.4	63.3	-46.3	23,700	11,872
WY 2004	2.0	0.8	9.4	20.7	39.1	-29.8	9,820	8,740
WY 2005	3.1	1.4	12.8	28.4	49.9	-37.1	20,200	11,600
WY 2006	14.6	2.9	27.1	61.7	142.9	-115.8	20,600	13,700
WY 2007	13.4	3.6	23.7	58.8	154.7	-131.0	24,200	14,900
WY 2008	64.6	16.2	67.2	214.1	1,047.4	-980.1	31,900	28,600
WY 2009	17.3	2.9	21.9	59.0	156.0	-134.1	19,700	13,800
WY 2010	1.9	0.6	7.6	18.9	36.3	-28.8	9,160	8,970
WY 2011	56.8	12.6	70.9	197.7	578.1	-507.2	32,900	19,074
WY 2012	55.5	10.4	63.3	170.5	513.6	-450.3	28,900	20,600
Average	**23.5**	**6.2**	**34.2**	**87.3**	**250.0**	**-215.2**		

Note:

[1] A revised time series of predicted annual sediment and lead fluxes for Harrison is available based on a multiple regression equation approach. See Attachment C.

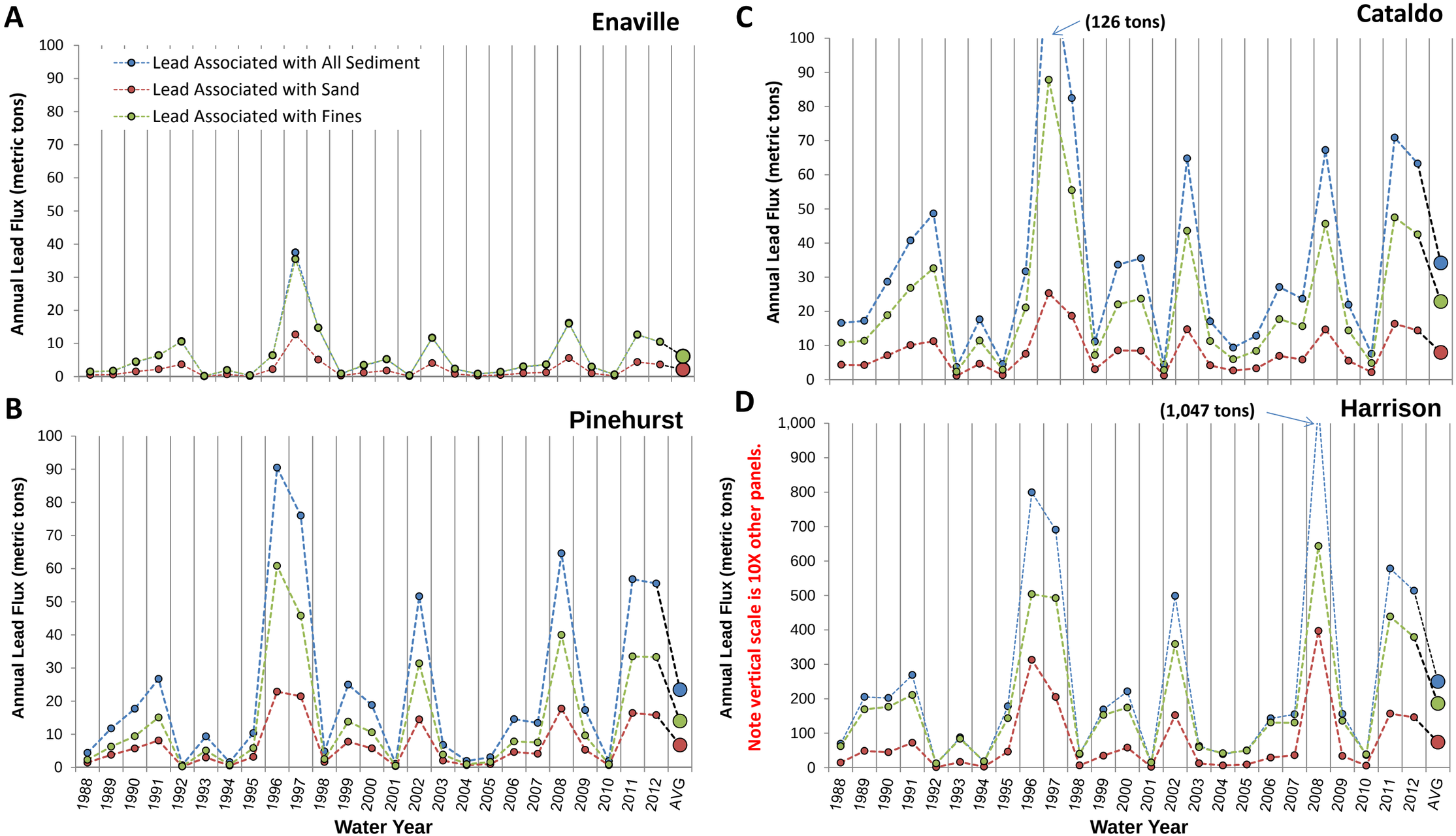

Exhibit 39. **Annual Lead Fluxes Associated with Sediment at Four Stations in Lower Basin**
Processes of Sediment and Lead Transport, Erosion, and Deposition
Lower Basin Coeur d'Alene River (OU3)

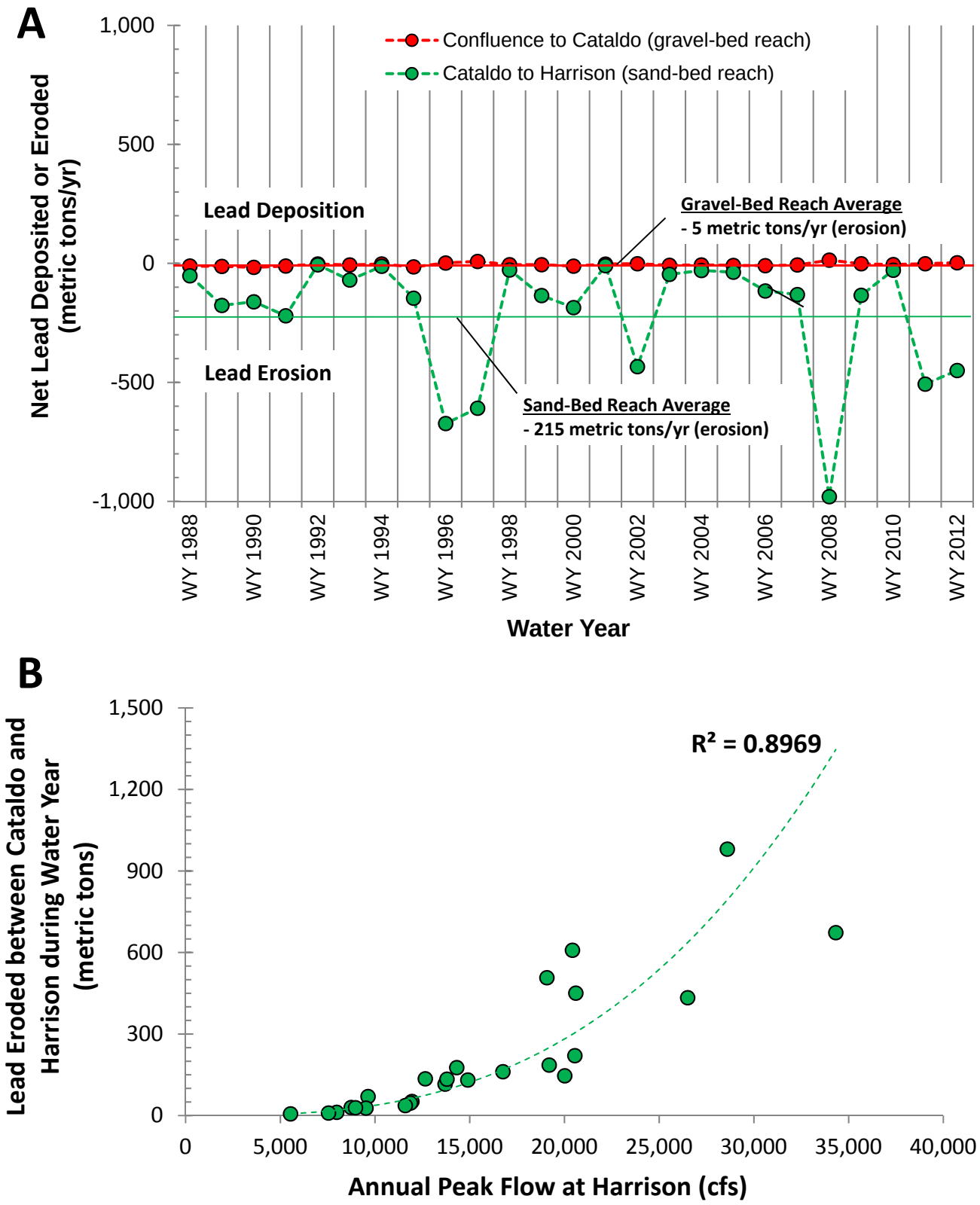

Exhibit 40. **Annual Net Lead Erosion in the Lower Basin**
Processes of Sediment and Lead Transport, Erosion, and Deposition
Lower Basin Coeur d'Alene River (OU3)

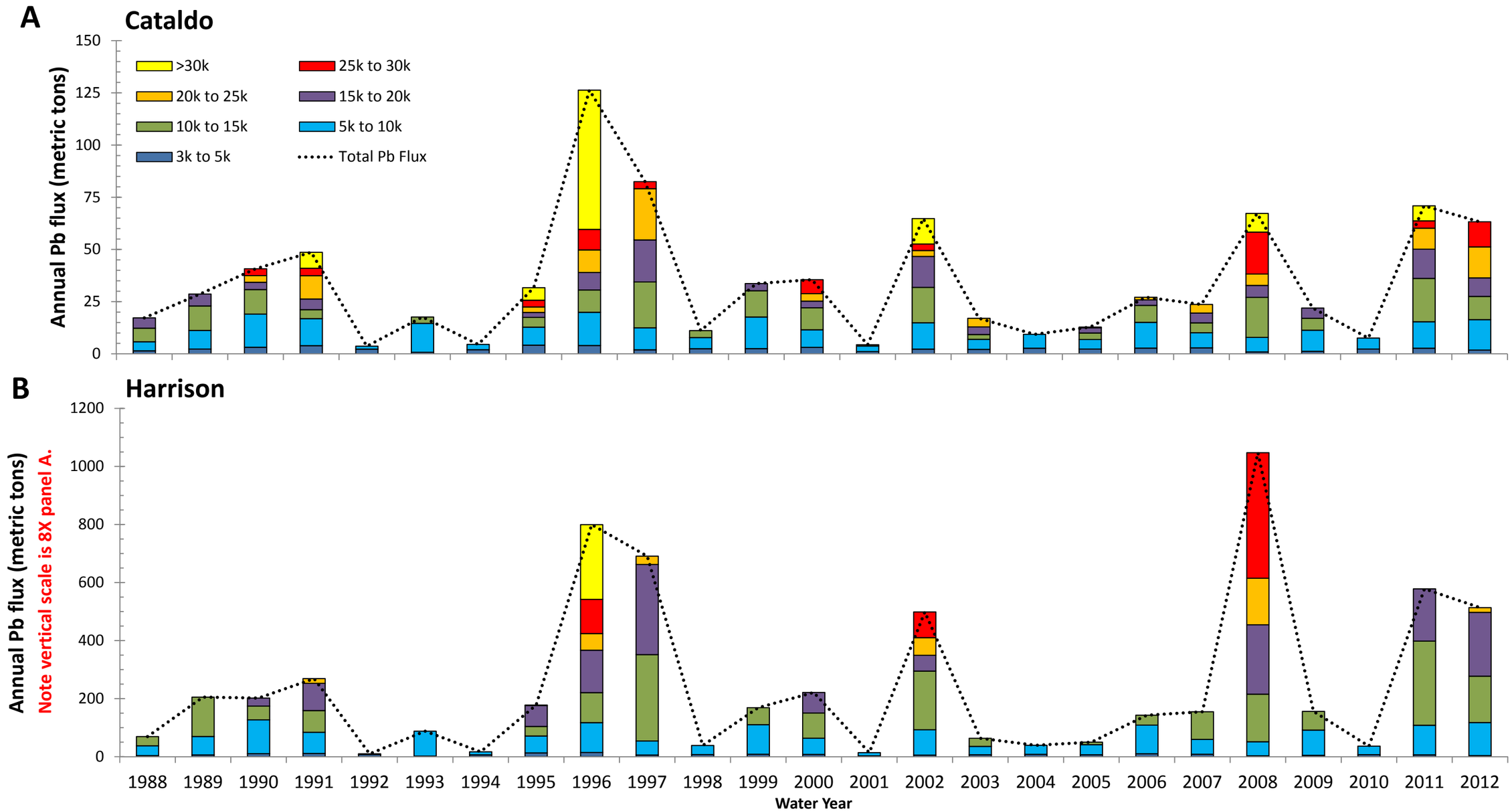

Exhibit 41. **Lead Fluxes Contributed by Flows of Different Magnitude and Frequency**
Processes of Sediment and Lead Transport, Erosion, and Deposition
Lower Basin Coeur d'Alene River (OU3)

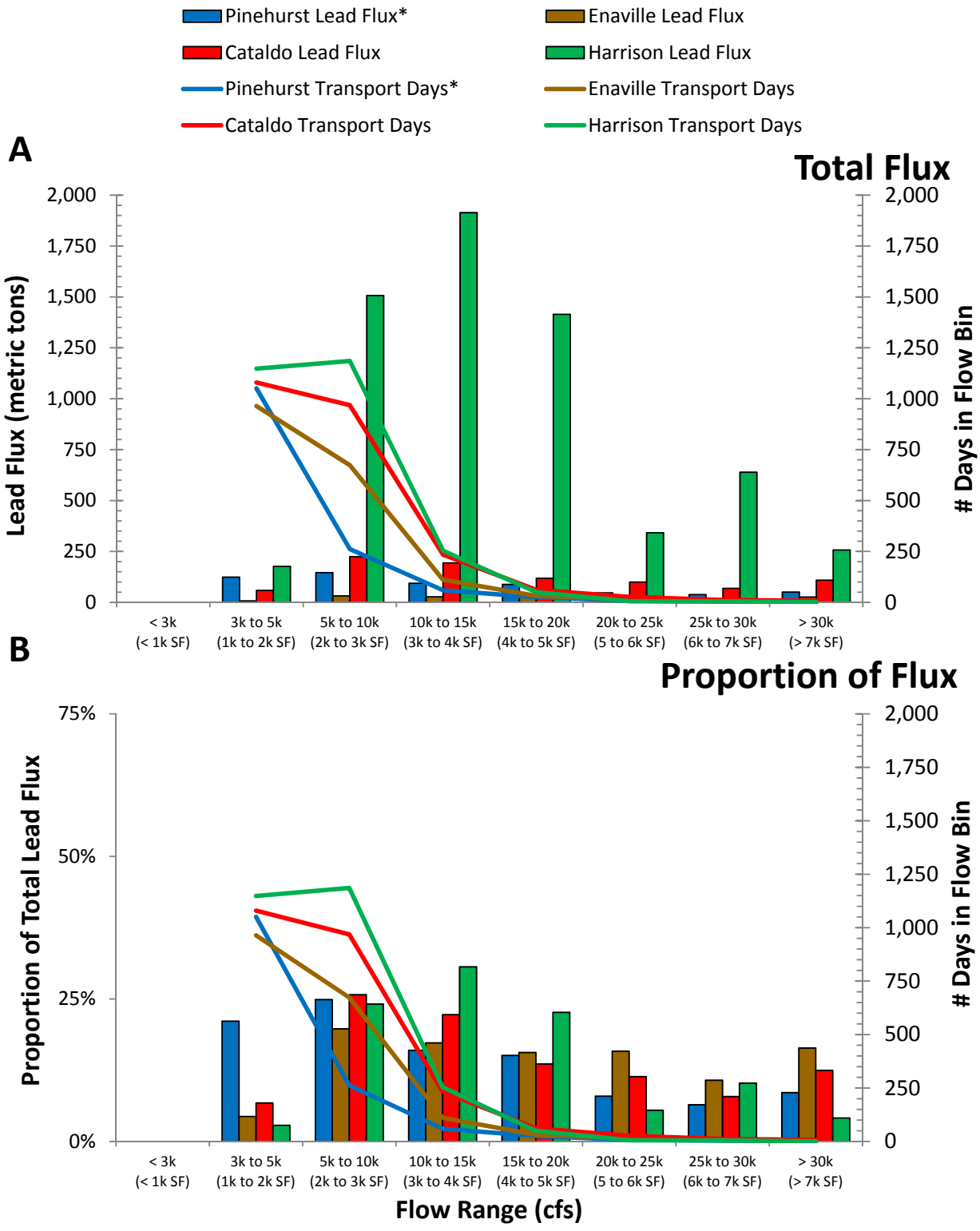

Note:
*The flow bins for the Pinehurst gage (shown in parentheses) are different from those in the other gages to account for the fact that the South Fork has a smaller drainage basin and lower flows.

Exhibit 42. **Relative Proportion of Lead Transported by Different Size Flows**
Processes of Sediment and Lead Transport, Erosion, and Deposition
Lower Basin Coeur d'Alene River (OU3)

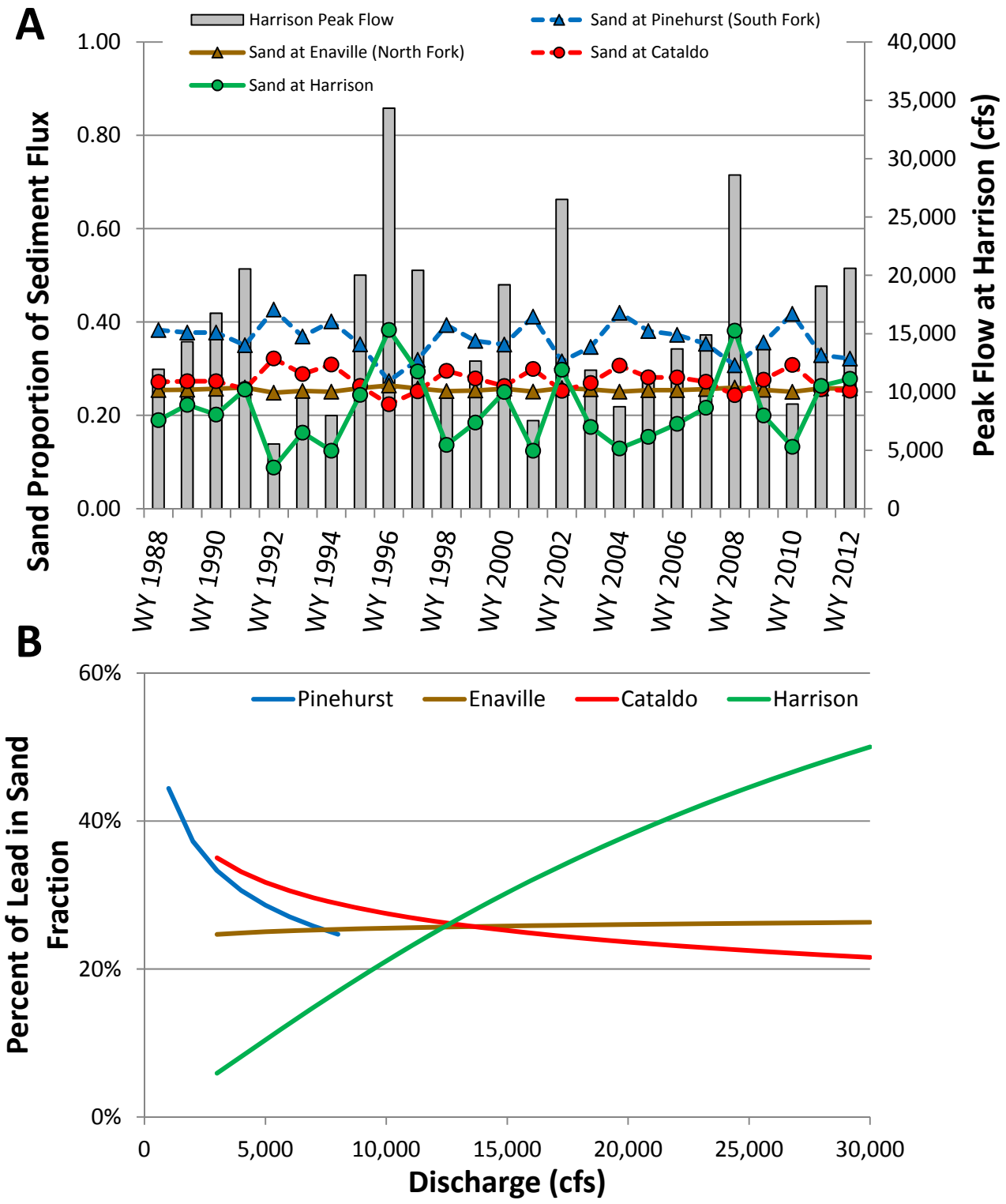

Note: The proportion of lead associated with sand was computed using sediment rating curves for sand and fines rating curves for each station (Exhibits 14 and 15) along with the the average lead concentrations in fines and sands in suspended sediment samples at each station (Exhibit 31).

Exhibit 43. **Sand and Fines Contribution to Annual Lead Transport**
Processes of Sediment and Lead Transport, Erosion, and Deposition
Lower Basin Coeur d'Alene River (OU3)

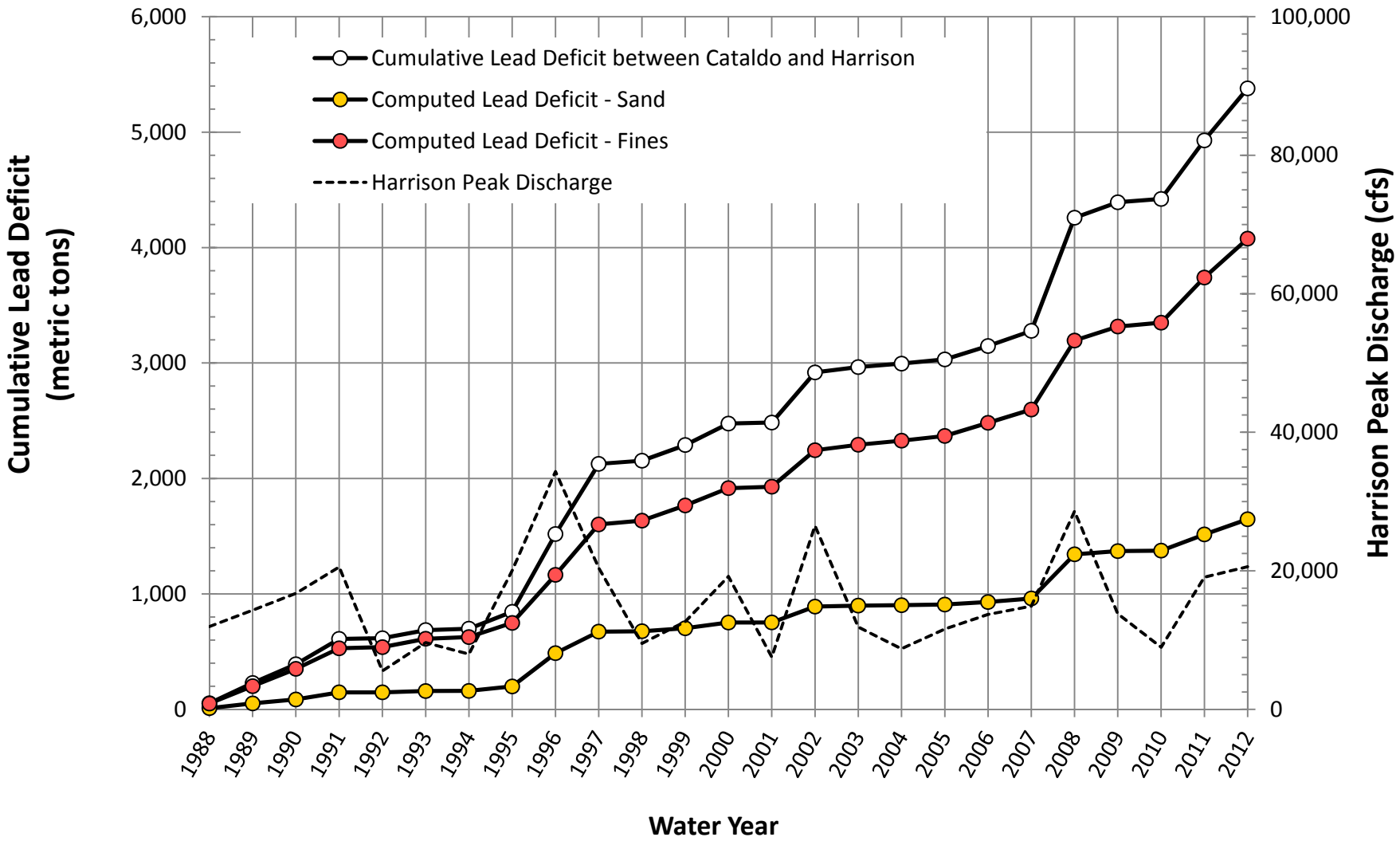

Exhibit 44. **Sand and Fines Contributions to the Net Lead Deficit between Cataldo and Harrison**

Processes of Sediment and Lead Transport, Erosion, and Deposition

Lower Basin Coeur d'Alene River (OU3)

A

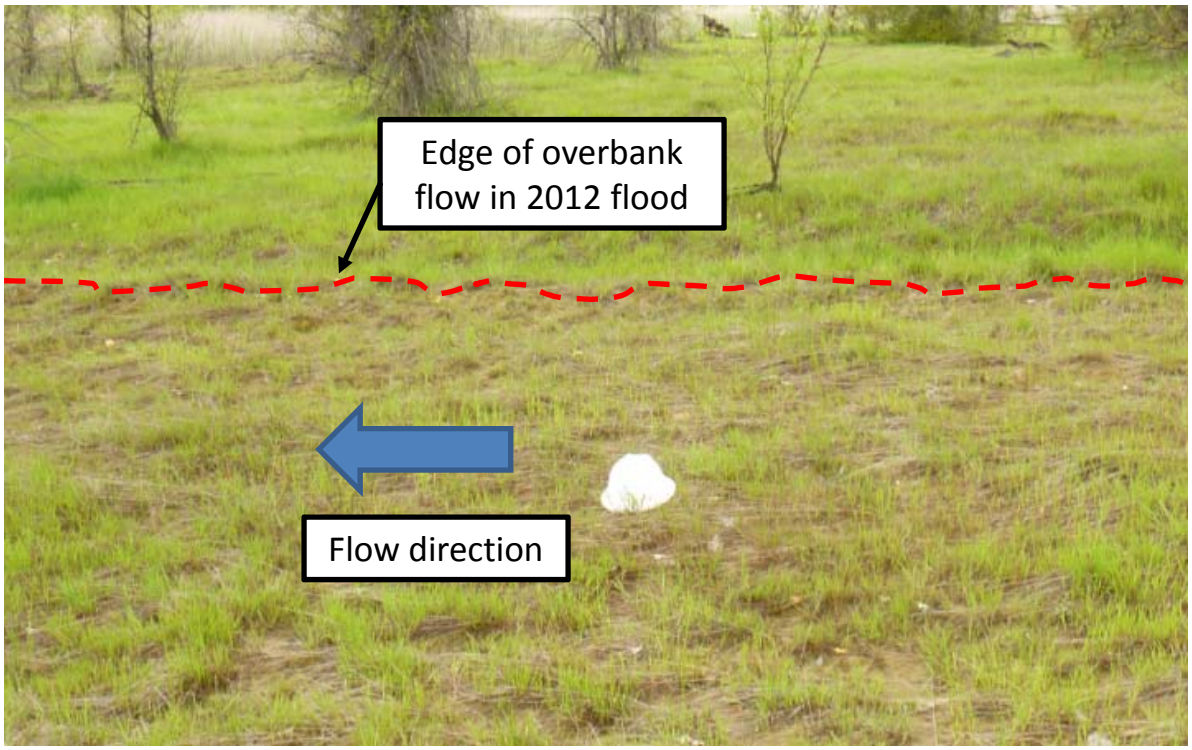

Minimal evidence of floodplain surface erosion at the entrance to Strobl Marsh, where about 50% of the flood flow enters the floodplain (CH2M HILL, 2013d). Photo was taken shortly after the April 2012 overbank flow event.

B

Overbank flooding, April 28, 2012 in Cave Lake, showing mostly standing or slow-moving water at one of the locations in the Lower Basin where overbank flooding is most extensive.

Exhibit 45. **Evidence that Floodplain Surface Erosion is not a Primary Process Moving Sediment in the Lower Basin**

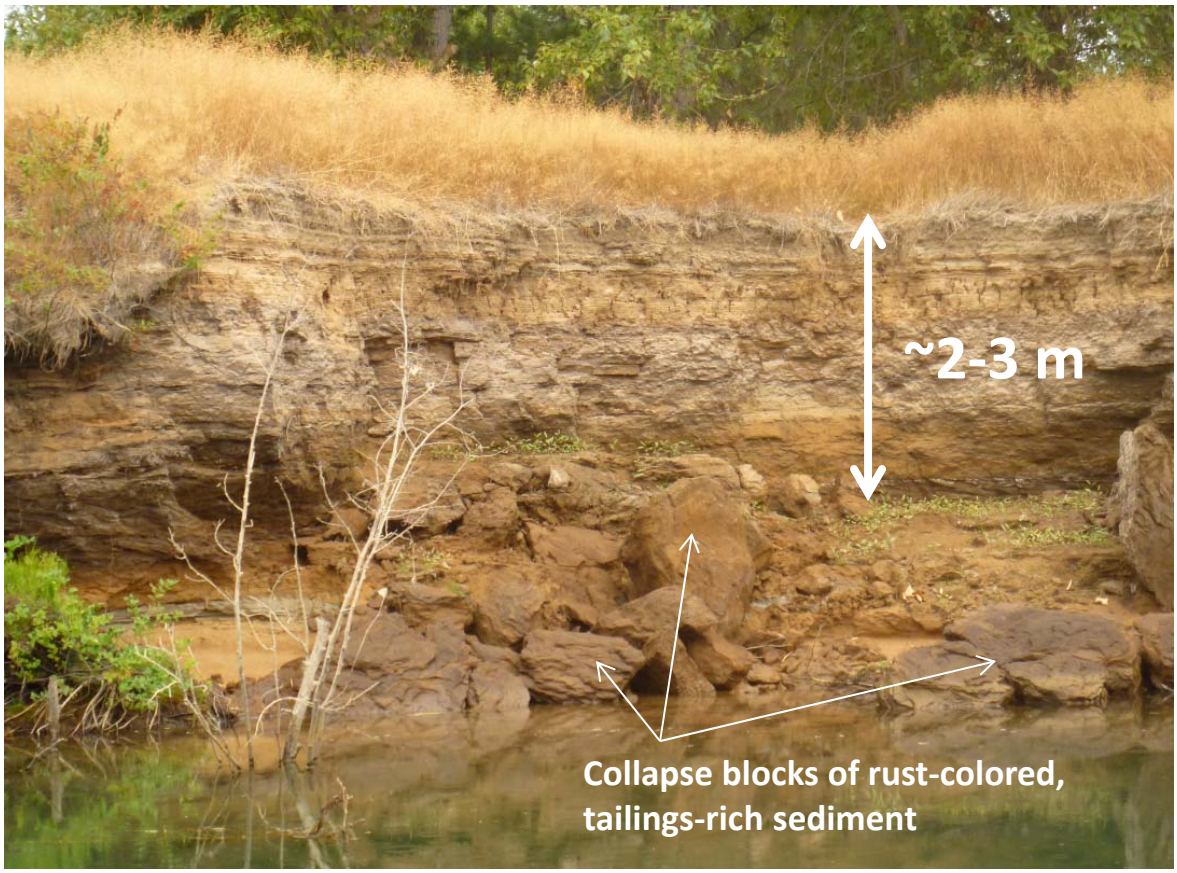

Exhibit 46. **Photograph of Bank Erosion of Tailings-Rich Sediment in Lower Basin**
Processes of Sediment and Lead Transport, Erosion, and Deposition
Lower Basin Coeur d'Alene River (OU3)

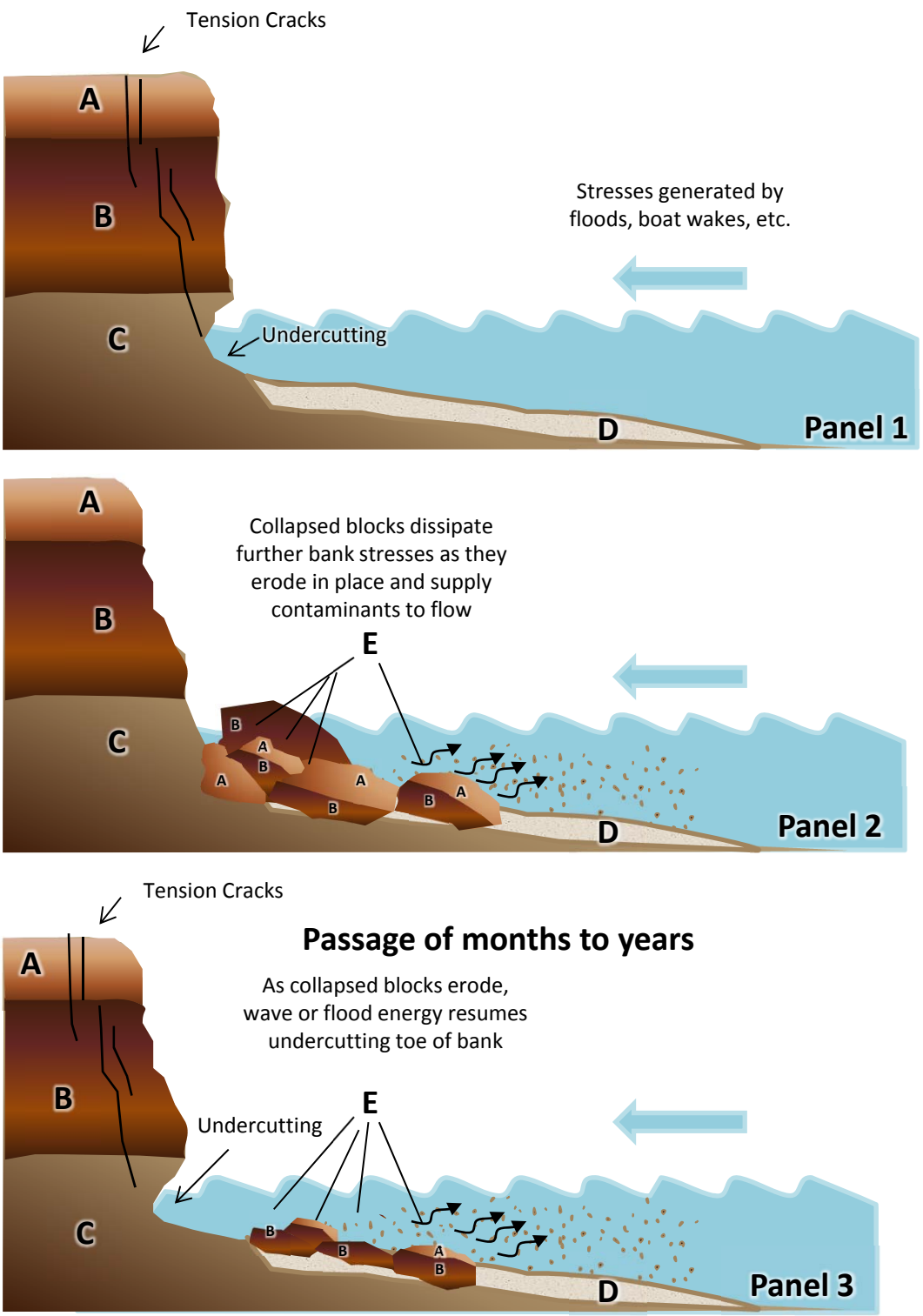

Exhibit 47. **Process of Bank Erosion and Lead Release in the Lower Basin**
Processes of Sediment and Lead Transport, Erosion, and Deposition
Lower Basin Coeur d'Alene River (OU3)

Exhibit 48. **Summary of Calculation of Sediment and Lead Contributed by Bank Erosion in the Lower Basin**

Processes of Sediment and Lead Transport, Erosion, and Deposition
Lower Basin Coeur d'Alene River (OU3)

Parameter	Minimum Estimate[1]	Maximum Estimate[1]	Best Available Estimate[2]
Length of banks (m)[3]	93,200	93,200	93,200
Proportion of banks that are *not* eroding [4]	0.7	0.4	0.63
Rate of bank erosion (m per yr)[5]	0.04	0.15	0.08
Average thickness of banks (m)[6]	1.5	2	1.85
Thickness of contaminated banks (m)[7]	0.9	1.3	1.18
Bulk density of bank material (tons/m^3)[8]	1.4	1.6	1.51
Average concentration of lead in contaminated banks (mg Pb/kg sediment)[9]	4,000	7,000	6,500
Mass of **sediment** contributed by bank erosion (tons/yr) =	2,349	26,842	7,706
Mass of **contaminated sediment** by bank erosion (tons/yr) =	1,409	17,447	**4,915**
Mass of **lead** by bank erosion (tons/yr) =	6	122	**32**

Notes:

1. Minimum and maximum values made for the purpose of reasonably bracketing the maximum and minimum values of lead contribution. These bracketing values are subjectively determined and not used for any calculations beyond what is shown on this table.
2. Best available estimate given the data presented in Technical Memorandum E-1 (CH2M HILL, 2015) or in others. Details in the following notes.
3. Based on digitization of the banklines in 2009 air photos. No minimum and maximum values are given because it is assumed that this value is fairly accurate
4. Best available estimate of 0.63 is total bankline minus the estimated proportion of banks that are armored with riprap (28 percent), heavily vegetated (27 percent), or lined with gently sloping beach deposits not prone to bank collapse (6 percent). Percentages are based on bank mapping as presented in KSSWCD (2009) and may not be current. Maximum and minimum values based on subjective judgement based on field observations in Lower Basin.
5. Based on multiple sources of monitoring data - erosion pins, stakes, and repeat terrestrial LiDAR surveys supported by repeat map/air photo analysis. Maximum and minimum values are bounding estimates from different data sources, as explained in Section 5.3 of TM E-1 (CH2M HILL, 2015).
6. Total average height of banks, including both contaminated and noncontaminated sediments. Values are based on stratigraphic measurements summarized in Exhibit 12 of TM E-1 (CH2M HILL, 2015). Note that average is for the sections measured between the Cataldo and Harrison gages (the area over which the lead contribution is being computed); three sites upstream of Cataldo gage are not included. Maximum and minimum values are subjective based on data shown in Exhibit 12 of TM E-1 (CH2M HILL, 2015) and general field observations.
7. Average thickness of contaminated sediment in the exposed banks measured in Exhibit 12 of TM E-1 (CH2M HILL, 2015). Does not include noncontaminated layer (Unit C). Maximum and minimum values are subjective based on data shown in Exhibit 12 of TM E-1 (CH2M HILL, 2015) and general field observations.
8. Dry bulk density for bank material estimated to be 1.51 tons/m3 by Bookstrom et al. (2001) using from data provided by EPA (1998).
9. Average lead concentration in the contaminated portion of the banks was estimated by simple averaging of all the samples from Units A and B; data in Attachment C of TM E-1 (CH2M HILL, 2015). Minimum and maximum bounding values subjective estimates based on data variability.

U.S. DEPARTMENT OF THE INTERIOR
U.S. GEOLOGICAL SURVEY

Prepared in Cooperation with the Coeur d'Alene Tribe

Open-File Report 2004-1211
Plate 1

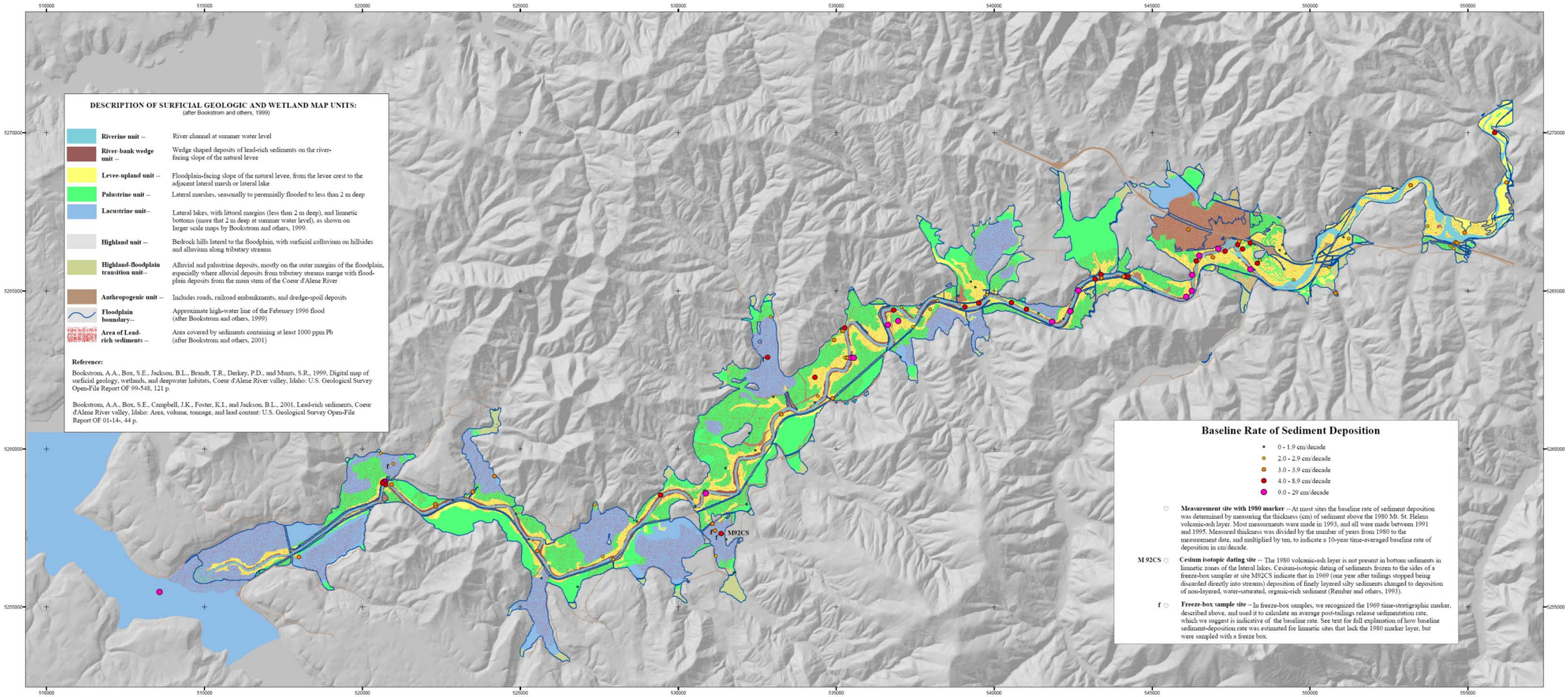

DESCRIPTION OF SURFICIAL GEOLOGIC AND WETLAND MAP UNITS:
(after Bookstrom and others, 1999)

Riverine unit --	River channel at summer water level
River-bank wedge unit --	Wedge shaped deposits of lead-rich sediments on the river-facing slope of the natural levee
Levee-upland unit --	Floodplain-facing slope of the natural levee, from the levee crest to the adjacent lateral marsh or lateral lake
Palustrine unit --	Lateral marshes, seasonally to perennially flooded to less than 2 m deep
Lacustrine unit--	Lateral lakes, with littoral margins (less than 2 m deep), and limnetic bottoms (more that 2 m deep at summer water level), as shown on larger scale maps by Bookstrom and others, 1999.
Highland unit --	Bedrock hills lateral to the floodplain, with surficial colluvium on hillsides and alluvium along tributary streams
Highland-floodplain transition unit--	Alluvial and palustrine deposits, mostly on the outer margins of the floodplain, especially where alluvial deposits from tributary streams merge with flood-plain deposits from the main stem of the Coeur d'Alene River
Anthropogenic unit --	Includes roads, railroad embankments, and dredge-spoil deposits
Floodplain boundary--	Approximate high-water line of the February 1996 flood (after Bookstrom and others, 1999)
Area of Lead-rich sediments --	Area covered by sediments containing at least 1000 ppm Pb (after Bookstrom and others, 2001)

Reference:

Bookstrom, A.A., Box, S.E., Jackson, B.L., Brandt, T.R., Derkey, P.D., and Munts, S.R., 1999, Digital map of surficial geology, wetlands, and deepwater habitats, Coeur d'Alene River valley, Idaho: U.S. Geological Survey Open-File Report OF 99-548, 121 p.

Bookstrom, A.A., Box, S.E., Campbell, J.K., Foster, K.I., and Jackson, B.L., 2001, Lead-rich sediments, Coeur d'Alene River valley, Idaho: Area, volume, tonnage, and lead content: U.S. Geological Survey Open-File Report OF 01-14-, 44 p.

Baseline Rate of Sediment Deposition

- 0 - 1.9 cm/decade
- 2.0 - 2.9 cm/decade
- 3.0 - 3.9 cm/decade
- 4.0 - 8.9 cm/decade
- 9.0 - 29 cm/decade

Measurement site with 1980 marker --At most sites the baseline rate of sediment deposition was determined by measuring the thickness (cm) of sediment above the 1980 Mt. St. Helens volcanic-ash layer. Most measurements were made in 1993, and all were made between 1991 and 1995. Measured thickness was divided by the number of years from 1980 to the measurement date, and multiplied by ten, to indicate a 10-year time-averaged baseline rate of deposition in cm/decade.

M 92CS **Cesium isotopic dating site** -- The 1980 volcanic-ash layer is not present in bottom sediments in limnetic zones of the lateral lakes. Cesium-isotopic dating of sediments frozen to the sides of a freeze-box sampler at site M92CS indicate that in 1969 (one year after tailings stopped being discarded directly into streams) deposition of finely layered silty sediments changed to deposition of non-layered, water-saturated, organic-rich sediment (Rember and others, 1993).

f **Freeze-box sample site** -- In freeze-box samples, we recognized the 1969 time-stratigraphic marker, described above, and used it to calculate an average post-tailings release sedimentation rate, which we suggest is indicative of the baseline rate. See text for full explanation of how baseline sediment-deposition rate was estimated for limnetic sites that lack the 1980 marker layer, but were sampled with a freeze box.

Map Projection and 5,000-meter grid
UTM zone 11, 1927 North American Datum

The digital elevation model (DEM) base map was compiled using the following 7.5 minute USGS 10 meter DEMs: Black Lake, Cataldo, Harrison, Lane, Mica Bay, Medimont, Mount Coeur d'Alene, Rockat Peak, Rose Lake, and Twin Crags.

Baseline Deposition Rates for Sediments Deposited after 1980 on the Floodplain of the Coeur d'Alene River, Idaho

By
Arthur A. Bookstrom, Stephen E. Box, John C. Wallis, and Berne L. Jackson

Kilometers
0 1 2 3 4 5
Scale 1:50,000

N W E S

Dimensional calibration may vary between electronic plotters and between X and Y directions on the same plotter, and paper may change in size due to atmospheric conditions: therefore, scale and proportions may not be true on plots of this map.

BASELINE AND HISTORIC DEPOSITIONAL RATES AND LEAD CONCENTRATIONS, FLOODPLAIN SEDIMENTS, LOWER COEUR D'ALENE RIVER, IDAHO

By
Arthur A. Bookstrom, Stephen E. Box, Robert S. Fousek, John C. Wallis, Helen Z. Kayser, and Berne L. Jackson

Exhibit 49. **Coring Locations and Mapping by Bookstrom et al. (2004)**
Processes of Sediment and Lead Transport, Erosion, and Deposition
Lower Basin Coeur d'Alene River (OU3)

Exhibit 50. **Average Annual Sedimentation in USGS Cores**
Processes of Sediment and Lead Transport, Erosion, and Deposition
Lower Basin Coeur d'Alene River (OU3)

River Mile	Sedimentation Analysis Area ID	Core ID	Year Collected	Depositional Setting	Distance to River (m)	Depth to St. Helens Layer (cm)	Average Annual Deposition Rate (mm/year)	Average Annual Deposition Rate from 1D Sedimentation Model (mm/year)	1D Annual Sedimentation as Percent of USGS Core (percent)
132.8	1245	H934.2	1993	Lacustrine - Littoral	170	5.1	3.9	0.2	5%
135.1	135_L	94xb19	1994	Riverbank	0	10	7.1	1.0	14%
135.2	1244	T91A	1991	Lacustrine - Limnetic	603	3	2.7	0.5	17%
135.2	1244	BL9323	1993	Palustrine	911	3.2	2.5	0.5	18%
136.4	1246	93SBB22	1993	Palustrine	81	4	3.1	0.6	19%
137.1	1240	BL9339	1993	Upland	264	5.1	3.9	0.8	21%
137.6	1240	BL9347	1993	Lacustrine - Littoral	912	5.1	3.9	0.8	21%
138.1	1239	BL9346	1993	Upland	32	1.9	1.5	11.0	735%
138.7	139_L	BL9345	1993	Riverbank	19	1.9	1.5	0.7	47%
139.1	139_L	BL9354	1993	Riverbank	0	5.1	3.9	0.7	18%
139.6	1241	BL9355	1993	Lacustrine - Littoral	307	1.6	1.2	0.1	11%
140.2	1266	BL9360	1993	Palustrine	454	1.9	1.5	0.0	1%
140.8	1265	BL9370	1993	Upland	119	3.8	2.9	2.2	**77%**
141.5	1265	BL9369	1993	Lacustrine - Littoral	1377	3.8	2.9	2.2	**77%**
143.7	144_L	93ABM4	1993	Upland	15	12	9.2	1.0	11%
143.9	1262 & 1264	M9395	1993	Upland	669	4.5	3.4	0.5	15%
144	1262 & 1264	M91A	1991	Lacustrine - Littoral	897	4	3.6	0.5	14%
144	1262 & 1264	M9394	1993	Lacustrine - Littoral	1647	3.8	2.9	0.5	17%
144	1262 & 1264	M93109	1993	Palustrine	2330	1.3	1	0.5	50%
144.1	1262 & 1264	M92CS	1992	Lacustrine - Limnetic	1235	5.2	4.3	0.5	12%
144.2	1262 & 1264	M93108	1993	Lacustrine - Littoral	1410	0.6	0.5	0.5	**100%**
144.3	1262 & 1264	M93107	1993	Palustrine	434	1.3	1	0.5	50%
144.8	1259	M93106	1993	Palustrine	260	2.5	1.9	2.5	**134%**
145.4	1261 & 1260	T98M-43	1998	Upland	150	2	1.1	0.9	**84%**
145.9	1261 & 1260	M93104	1993	Palustrine	574	0	0	0.9	
146.4	146_L	L93118	1993	Upland	10	5.1	3.9	0.1	1%
146.5	1261 & 1260	L93119	1993	Upland	488	2.5	1.9	0.9	49%
147.2	147_R	L93128	1993	Upland	19	2.5	1.9	0.0	3%
147.4	147_R	93SBL32	1993	Upland	114	3	2.3	0.0	2%
147.5	1238	L93135	1993	Palustrine	103	5.1	3.9	0.1	2%
147.8	1257	93SBL31	1993	Upland	333	6	4.6	1.6	35%
147.9	1261 & 1260	91SBKF2	1991	Lacustrine - Limnetic	1693	5	4.5	0.9	21%
148.6	1258	96K178E	1996	Upland	240	18	11.3	0.2	2%
148.6	1258	96K114E	1996	Upland	209	33	20.6	0.2	1%
148.6	1257	94GID3	1994	Upland	43	3	2.1	1.6	**77%**

Notes:

Values in table are provided in or are computed from Bookstrom et al. (2001) and Bookstrom et al. (2004)
Highlighted cells with bold text are within +/- 50% of USGS core deposition rate.

Exhibit 50 (continued). **Average Annual Sedimentation in USGS Cores**
Processes of Sediment and Lead Transport, Erosion, and Deposition
Lower Basin Coeur d'Alene River (OU3)

River Mile	Sedimentation Analysis Area ID	Core ID	Year Collected	Depositional Setting	Distance to River (m)	Depth to St. Helens Layer (cm)	Average Annual Deposition Rate (mm/year)	Average Annual Deposition Rate from 1D Sedimentation Model (mm/year)	1D Annual Sedimentation as Percent of USGS Core (percent)
148.6	1257	94GID5	1994	Palustrine	67	5	3.6	1.6	45%
148.6	1257	94GID6	1994	Palustrine	103	3	2.1	1.6	**77%**
148.9	1257	93SBL30	1993	Upland	366	4	3.1	1.6	**52%**
149.1	1257	93SBL27B	1993	Upland	57	4	3.1	1.6	**52%**
149.1	1257	L93137	1993	Palustrine	122	2.5	1.9	1.6	**85%**
149.2	1257	93SBL27	1993	Riverbank	0	7	5.4	1.6	30%
149.2	1261 & 1260	L93121	1993	Palustrine	2373	3.8	2.9	0.9	32%
150.3	1255	L93154	1993	Lacustrine - Littoral	457	1.6	1.2	0.3	28%
150.7	151_L	94xl13	1994	Riverbank	1	15	10.7	1.8	17%
151.2	151_L	T98L-36	1998	Upland	330	16.5	9.2	1.8	20%
151.2	151_L	94xl04	1994	Riverbank	4	10	7.1	1.8	25%
151.4	152_R	L93156	1993	Upland	35	2.9	2.2	2.9	**132%**
151.7	151_L	L93162	1993	Upland	126	3.8	2.9	1.8	**62%**
152.1	1255	T98R-30	1998	Upland	200	4	2.2	0.3	15%
152.7	9651	T98R-28	1998	Upland	230	2.5	1.4	0.0	0%
152.9	153_R	94xra21	1994	Riverbank	1	10	7.1	1.9	27%
153.3	153_R	94xra15	1994	Riverbank	3	12	8.6	1.9	22%
153.4	9651	RL93178	1993	Upland	437	1.6	1.2	0.0	0%
153.4	9651	RL93177	1993	Upland	667	1	0.8	0.0	0%
153.5	153_R	94xr98	1994	Riverbank	0	4	2.9	1.9	**65%**
154.5	1251	RL93193	1993	Upland	56	2.5	1.9	0.2	12%
154.9	1251	93SBR13	1993	Riverbank	9	15	11.5	0.2	2%
156.6	1249	RL93206	1993	Palustrine	1450	1.6	1.2	0.2	21%
157.3	158_R	RL93213	1993	Riverbank	0	1.6	1.2	0.7	**56%**
158.2	158_R	94xr30	1994	Riverbank	1	13	9.3	0.7	7%
158.4	158_R	94xr25	1994	Riverbank	1	22	15.7	0.7	4%
158.7	158_R	94xr17	1994	Riverbank	1	17	12.1	0.7	6%
159.3	159_L	T98R-31	1998	Upland	120	5.5	3.1	1.7	**55%**
159.6	159_L	C93236	1993	Riverbank	6	11.4	8.8	1.7	19%
159.9	160_R	C93235	1993	Upland	37	5.1	3.9	1.8	45%
160	160_R	93CSC03	1993	Riverbank	1	6	4.6	1.8	39%
160.1	160_R	T98C-17	1998	Upland	45	8	4.4	1.8	40%
160.1	160_R	T98C-21	1998	Palustrine	440	14	7.8	1.8	23%
160.2	160_R	C93244	1993	Upland	414	2.2	1.7	1.8	**104%**
160.5	160_R	T98C-16	1998	Upland	240	9.9	5.5	1.8	32%

Notes:

Values in table are provided in or are computed from Bookstrom et al. (2001) and Bookstrom et al. (2004)
Highlighted cells with bold text are within +/- 50% of USGS core deposition rate.

Exhibit 50 (continued). **Average Annual Sedimentation in USGS Cores**
Processes of Sediment and Lead Transport, Erosion, and Deposition
Lower Basin Coeur d'Alene River (OU3)

River Mile	Sedimentation Analysis Area ID	Core ID	Year Collected	Depositional Setting	Distance to River (m)	Depth to St. Helens Layer (cm)	Average Annual Deposition Rate (mm/year)	Average Annual Deposition Rate from 1D Sedimentation Model (mm/year)	1D Annual Sedimentation as Percent of USGS Core (percent)
160.6	159_L	93SBC15	1993	Upland	4	15	11.5	1.7	15%
160.9	9646	T98C-18	1998	Upland	1025	3	1.7	1.1	**64%**
160.9	9646	C93249	1993	Upland	1033	0	0	1.1	
161.5	160_R	93SBC10	1993	Riverbank	8	3	2.3	1.8	**77%**
161.5	9646	C93250	1993	Upland	825	0	0	1.1	
162.2	1247 & 9648	T98C-25	1998	Upland	450	5	2.8	0.5	17%
162.4	163_L	T98C-8	1998	Upland	125	3	1.7	10.3	605%

Notes:

Values in table are provided in or are computed from Bookstrom et al. (2001) and Bookstrom et al. (2004)
Highlighted cells with bold text are within +/- 50% of USGS core deposition rate.

Exhibit 51. **Estimated Mass of Lead-Rich Sediments in the Floodplain, and Modern-Era (post-1980) Rates of Deposition**
Processes of Sediment and Lead Transport, Erosion, and Deposition
Lower Basin Coeur d'Alene River (OU3)

	Depositional Setting[1]					
	Riverbank	Upland	Palustrine	Lacustrine Littoral	Lacustrine Limnetic	**Entire Floodplain**
Estimated Values (Bookstrom et al., 2004)						
Number of Samples Containing Ash Layer	47	49	18	7	4	125
Area[2] (km^2)	2.1	11.8	17.9	5.0	8.1	45.0
Median Sediment Deposition Rate (cm/decade)	6.4	2.8	2.2	2.9	4.0	3.0
Median Density of Dry Lead-Rich Sediments[3] (metric tons/m^3)	1.51	1.34	1.00	1.13	1.07	1.13
Median Lead Concentration in Sediments[4] (ppm)	3,300	3,800	1,900	2,100	4,400	2,940
Computed Deposition Rates (Revised from Bookstrom et al., 2004)						
Sediment Volumetric Deposition Rate[5] (Mm^3/decade)	0.14	0.33	0.39	0.15	0.33	1.33
Sediment Mass Deposition Rate (metric tons/yr)	2.0E+04	4.4E+04	3.9E+04	1.6E+04	3.5E+04	**156,000**
Lead Deposition Rate (metric tons/year)	67	169	75	34	153	**499**
Calculation of Mass of Contaminated Sediment[6]						
1903 - 1980 (Mm^3)	1.63	3.25	5.49	1.26	3.66	15.3
1980 - 2013 (Mm^3)	0.45	1.09	1.30	0.48	1.08	1.73
1903 - 2013 (Mm^3)						17.0
1903 - 2013 (metric tons)						**19,200,000**
Deposited Lead (Updated from Bookstrom et al., 2004)						
1903 - 1980 (metric tons; from Bookstrom, 2004)	11,107	25,379	34,504	4,045	30,055	**105,000**
1980 - 2013 (metric tons)	2,226	5,567	2,472	1,138	5,062	**6,000**
1903 - 2013 (metric tons)						**111,000**

Notes:

Mm^3 = million cubic meters

[1]Types of Depositional Settings as mapped by Bookstrom et al. (2004)

[2]Areas truncated to match the boundaries of the current study, which are the Cataldo (upstream) and Harrison (downstream) USGS river gages.

[3]Dry Bulk Densities provided by Bookstrom et al. (2001).

[4]Median concentration of lead in sediment overlying the Mt. St. Helens ash layer in all samples reported by Bookstrom et al. (2004). See text for further explanation.

[5]Median sedmient thickness above the ash layer, divided by the time between 1980 and the date the core was collected.

[6]A more detailed explanation of the derivation of these values is found in Bookstrom et al. (2004). The actual values in this table are modified from the original sources as discussed in the text and in the notes above.

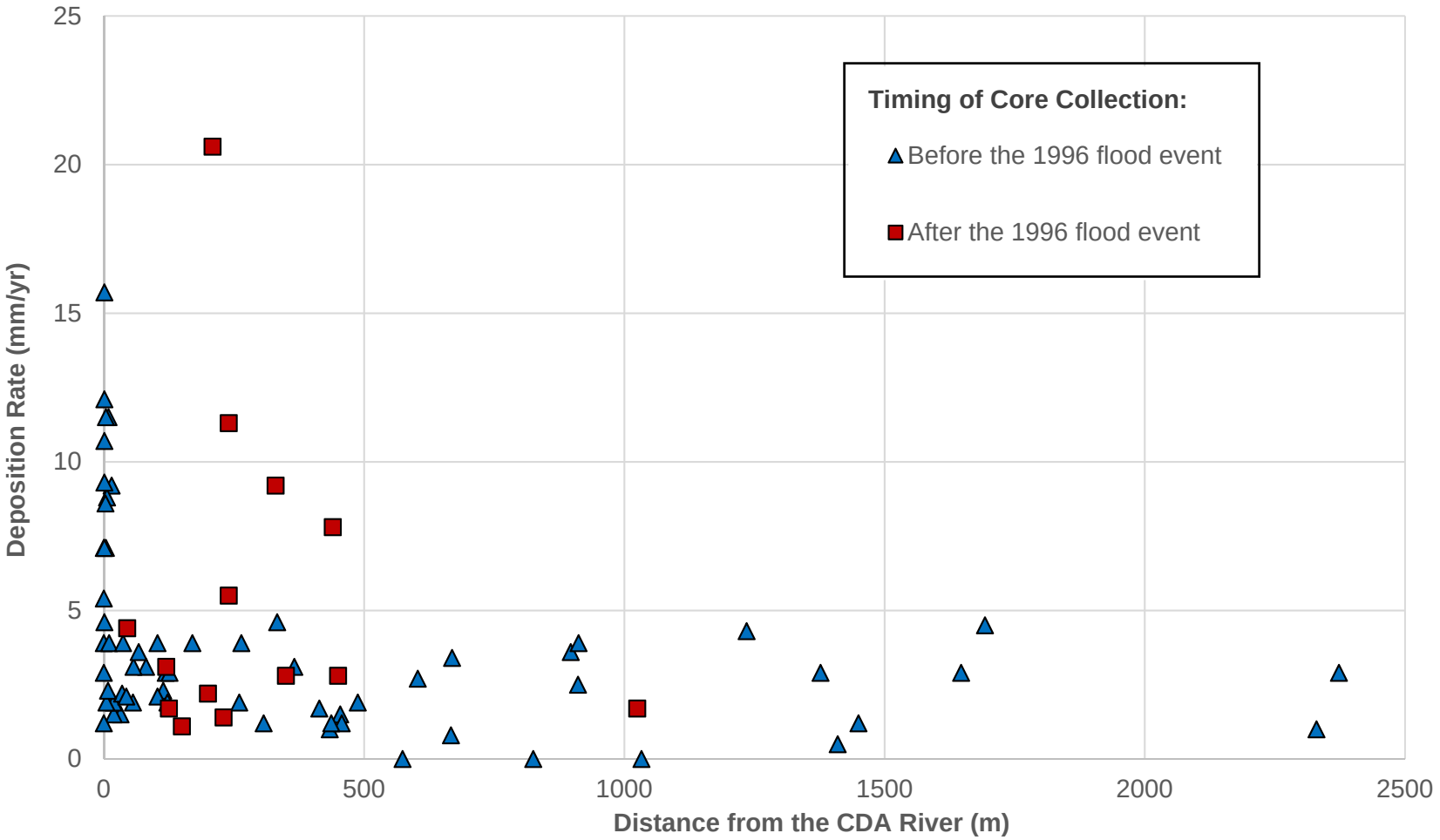

Notes:
n = 79 ; Data from Bookstrom et al. (2004) set of n = 125, reduced to include only cores within the area of 1D sediment deposition analysis.

Exhibit 52. **Average Annual Sedimentation Rate in USGS Cores Versus Distance From the River**
Processes of Sediment and Lead Transport, Erosion and Deposition
Lower Basin Coeur d'Alene River (OU3)

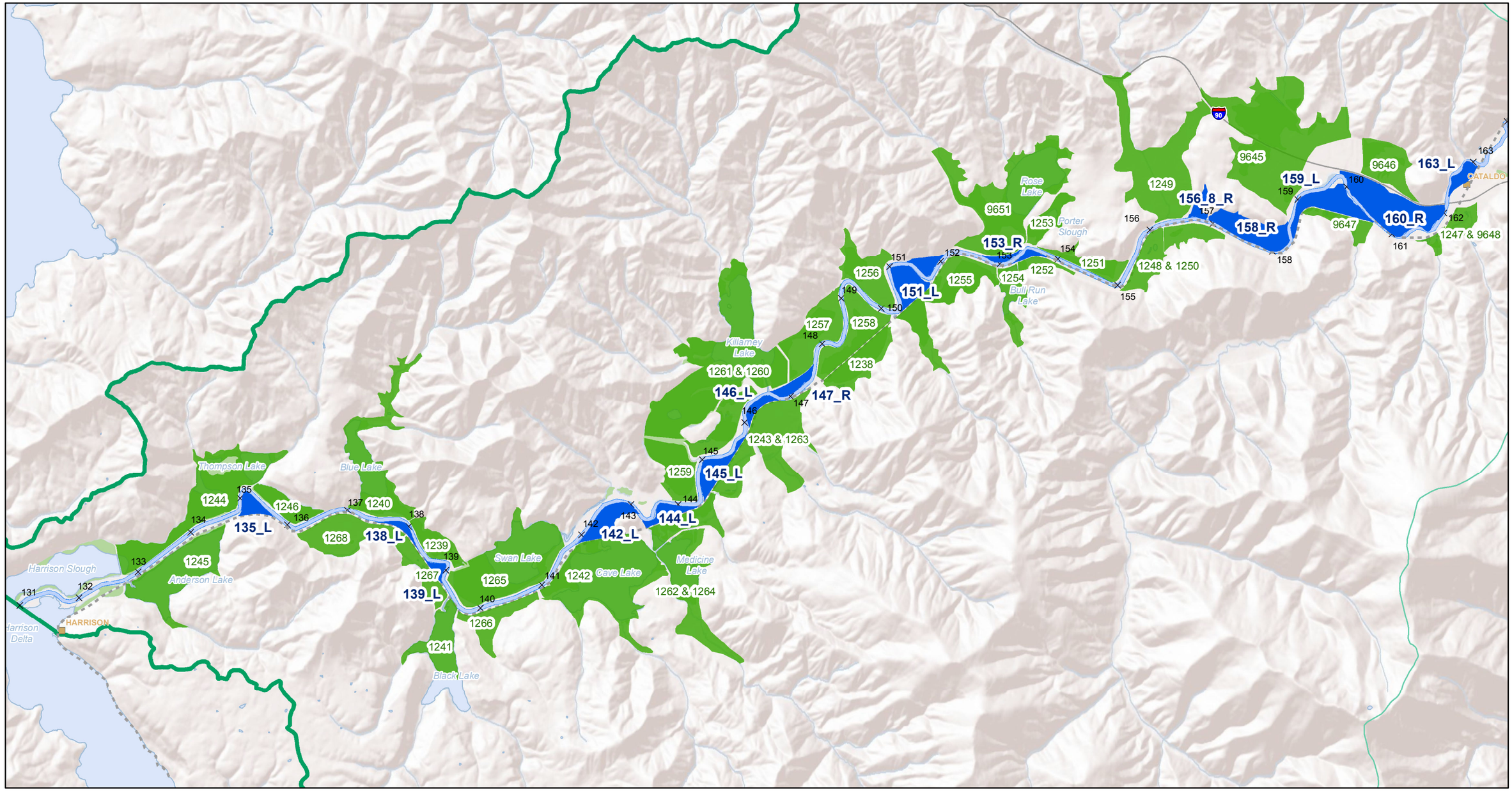

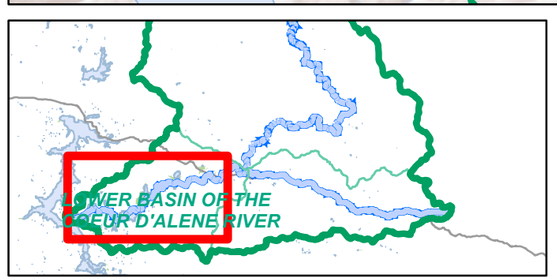

LEGEND

- Trail of the Coeur d'Alenes
- River Mile Marker
- City
- Coeur d'Alene Watershed
- Interstate Highway
- Waterbody
- Marsh or Slough
- Model Overbank Flow Areas (River Mile and Location - Channel Left [L] or Right [R])
- Model Off-Channel Storage Areas (Storage Area Identification Number)

N

0 1 2 4 Kilometers

Source: Shaded Relief (ESRI Online Catalog); Coeur d'Alene River Miles (USEPA); NHD (USGS).

Exhibit 53. **1D Model Areas Used for Sedimentation Analysis**
Processes of Sediment and Lead Transport, Erosion, and Deposition
Lower Basin of the Coeur d'Alene River (OU3)

ch2m

C:\USERS\TJANTZEN\DOCUMENTS\PROJECTS\CDRB\MODELINGTASK\1D\RESULTS\SEDIMENTATIONRATES\EXHIBIT45_1DMODELAREAS.MXD TJANTZEN 1/14/2014 10:22:37 AM

Exhibit 54. **Uncertainty Analysis Summary**
Processes of Sediment and Lead Transport, Erosion, and Deposition
Lower Basin Coeur d'Alene River (OU3)

Uncertainty Factors	Detailed Exhibit (number)*	Report Section (number)*	% Change in Average Annual Sedimentation, relative to Best Estimate	
			Low	High
SSC Rating Curve - Varied Power-Law Regression	23	4.1	-49%	125%
SSC Rating Curve - Varied Regression Models	24	4.1	-48%	39%
SSC Rating Curve - Varied Threshold Discharge	25	4.1	-17%	7%
1D vs. 2D	26	4.2	-28%	none
Updated 1D Model	27	4.3	-4%	none
Varied Representative Flow Lengths	28	4.4	-4%	5%
Exclusion of Tributary Inflows	29	4.5	none	6%
Representative Cross Section	30	4.6	-26%	11%
Varied Representative Sediment Sizes	31	4.7	-5%	6%
Turbulent Flow Correction Factor	32	4.8	-49%	none
SSC uniform in vertical water column		4.1	-?? model likely overestimates; not quantified	none

Notes:
* Exhibit and Section numbers refer to the floodplain sedimentation TM (TM E-5, CH2M HILL 2015).
See the floodplain sedimentation TM (TM E-5, CH2M HILL 2015) for additional details an analysis on specific sources of uncertainty.
See the applicable report section for additional information and background behind each uncertainty type.
The change in average annual sedimentation was calculated for between 1 and 9 of the 48 floodplain areas. Each area has unique hydraulics and sedimentation characteristics, and may not be representative of average or typical basin sedimentation.
The uncertainties presented here are not necessarily independent and/or additive.
These values should be used to guide understanding of overall and relative uncertainty magnitude.

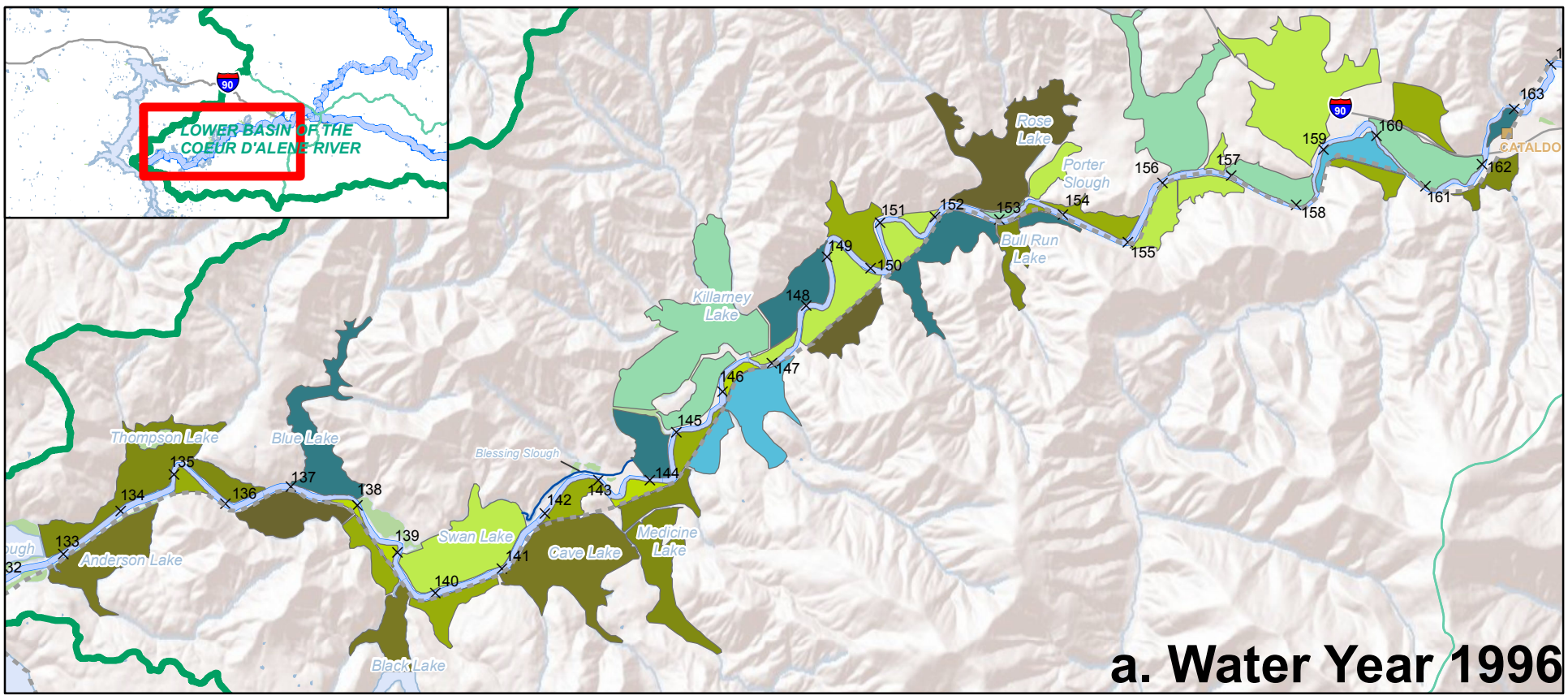

Source: Shaded Relief (ESRI Online Catalog); Coeur d'Alene River Miles (USEPA); NHD (USGS).

LEGEND

- Trail of the Coeur d'Alenes
- River Mile Marker
- City
- Coeur d'Alene Watershed
- Interstate Highway
- Waterbody
- Marsh or Slough

Trapping Efficiency (percent)

- 12
- 13 - 20
- 21 - 30
- 31 - 40
- 41 - 50
- 51 - 60
- 61 - 70
- 71 - 80
- 81 - 90
- 91 - 100

0 1 2 4 Kilometers

N

Exhibit 55. **Floodplain Sediment Trapping Efficiency**
Processes of Sediment and Lead Transport, Erosion, and Deposition
Lower Basin of the Coeur d'Alene River (OU3)

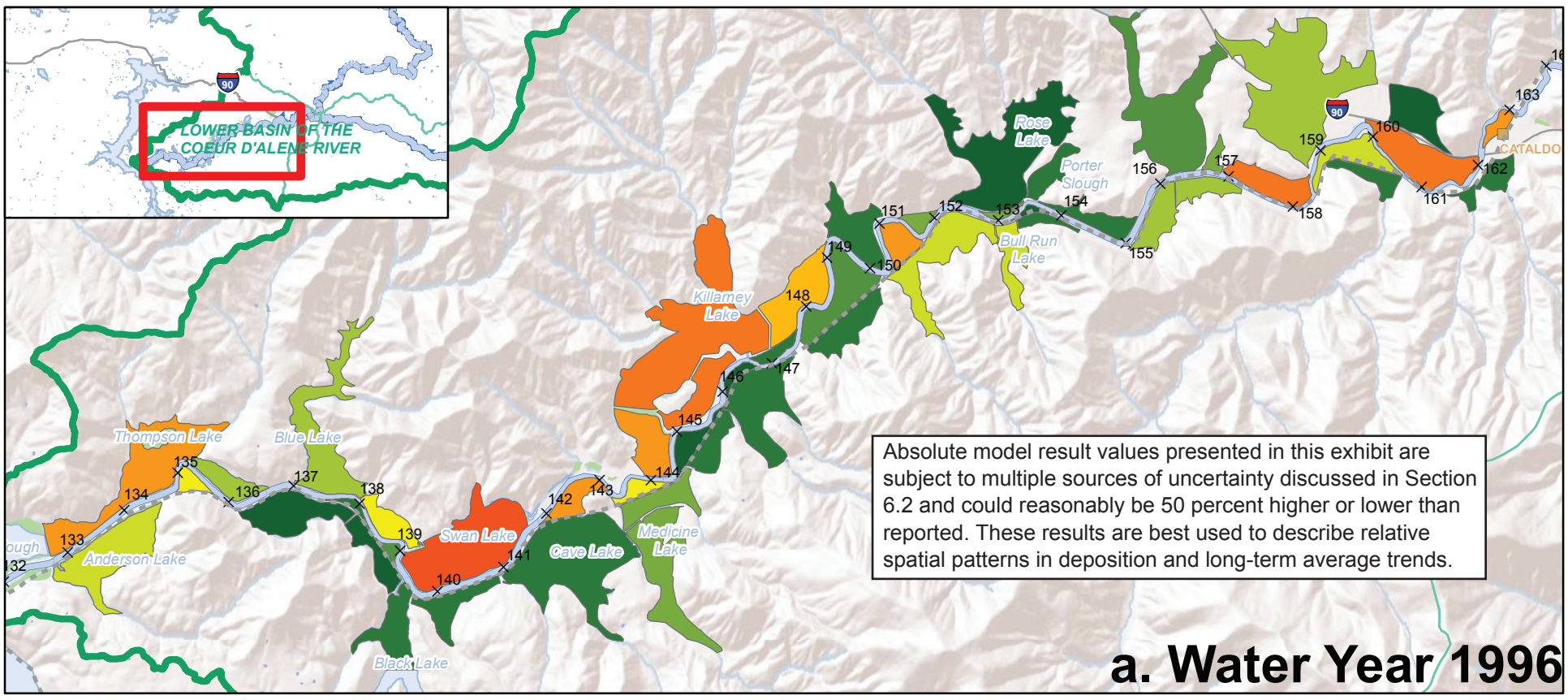

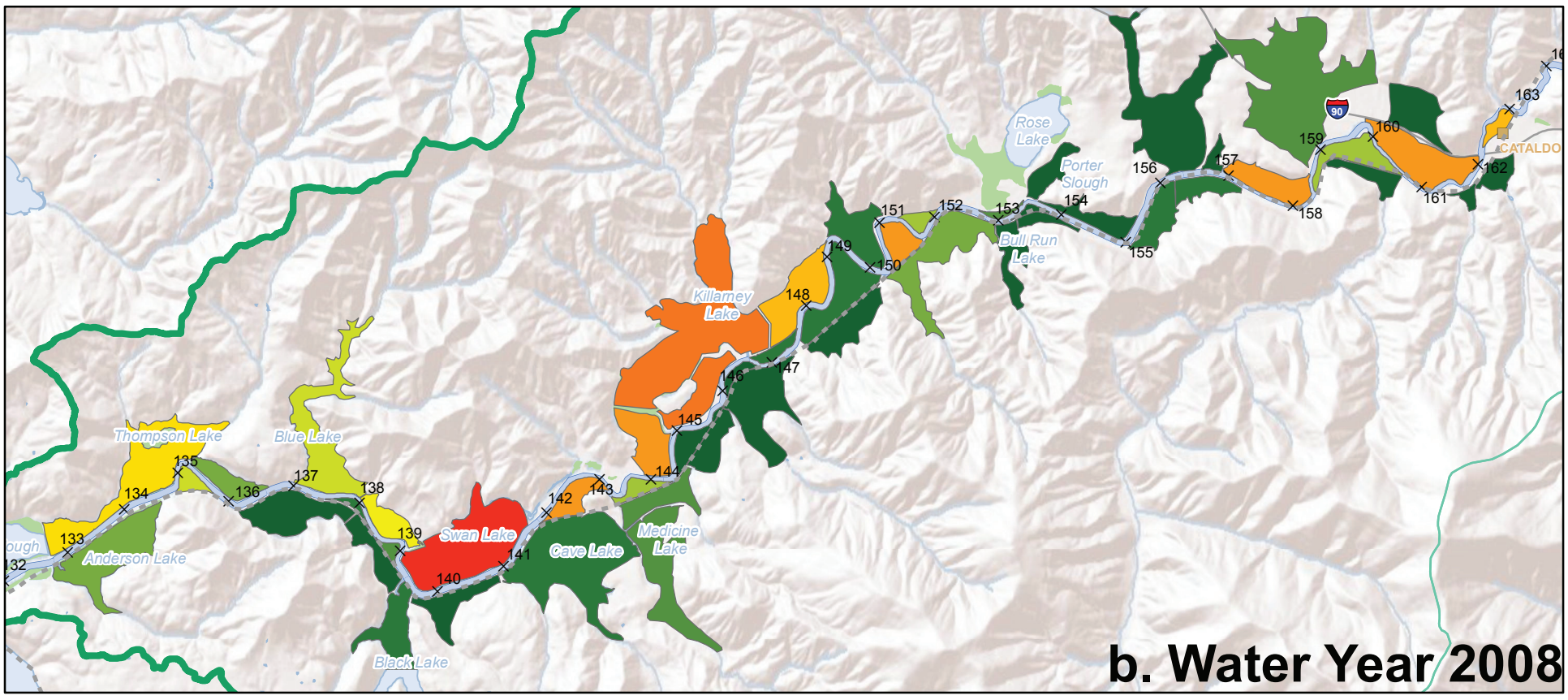

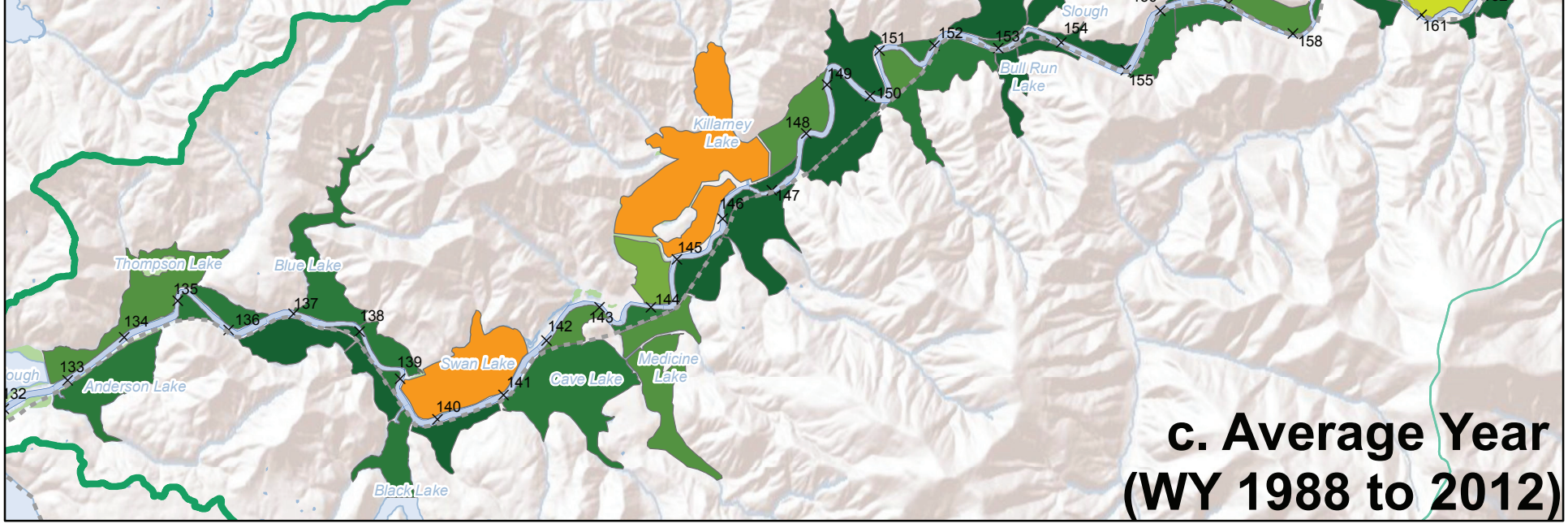

LEGEND

- Trail of the Coeur d'Alenes
- River Mile Marker
- City
- Coeur d'Alene Watershed
- Interstate Highway
- Waterbody
- Marsh or Slough

Sediment Trapped (metric tons per year)

- 0 - 100
- 101 - 500
- 501 - 1000
- 1001 - 1500
- 1501 - 2000
- 2001 - 2500
- 2501 - 3000
- 3001 - 3500
- 3501 - 4000
- 4001 - 10000
- 10001 - 20000
- 20001 - 30000
- 30001 - 70000

Source: Shaded Relief (ESRI Online Catalog); Coeur d'Alene River Miles (USEPA); NHD (USGS).

0 1 2 4 Kilometers

N

Exhibit 56. **Floodplain Sedimentation Mass**

Processes of Sediment and Lead Transport, Erosion, and Deposition
Lower Basin of the Coeur d'Alene River (OU3)

ch2m

C:\USERS\TJANTZEN\DOCUMENTS\PROJECTS\CDRB\MODELINGTASK\1D\RESULTS\SEDIMENTATIONRATES\EXHIBIT47_SEDIMENTMASS_3MAPS.MXD TJANTZEN 4/15/2014 12:23:47 PM

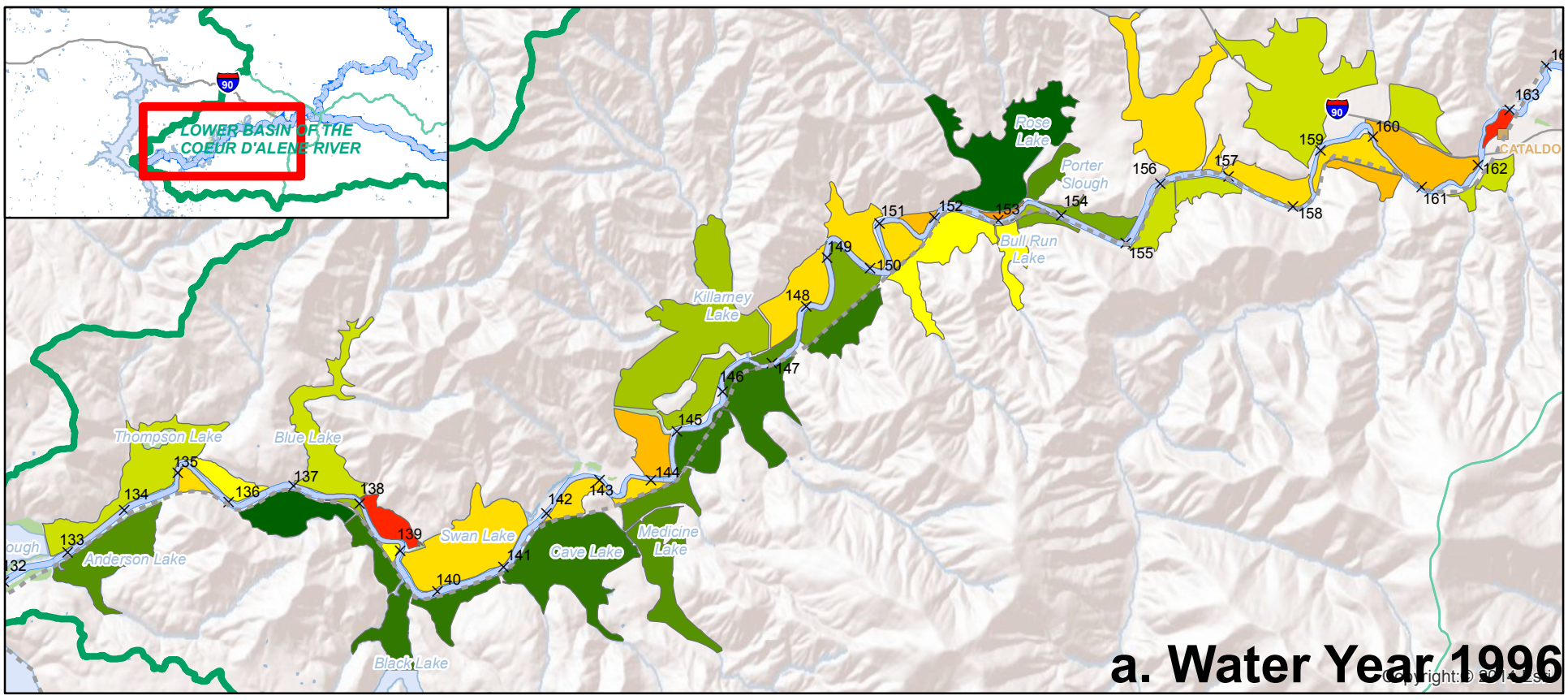

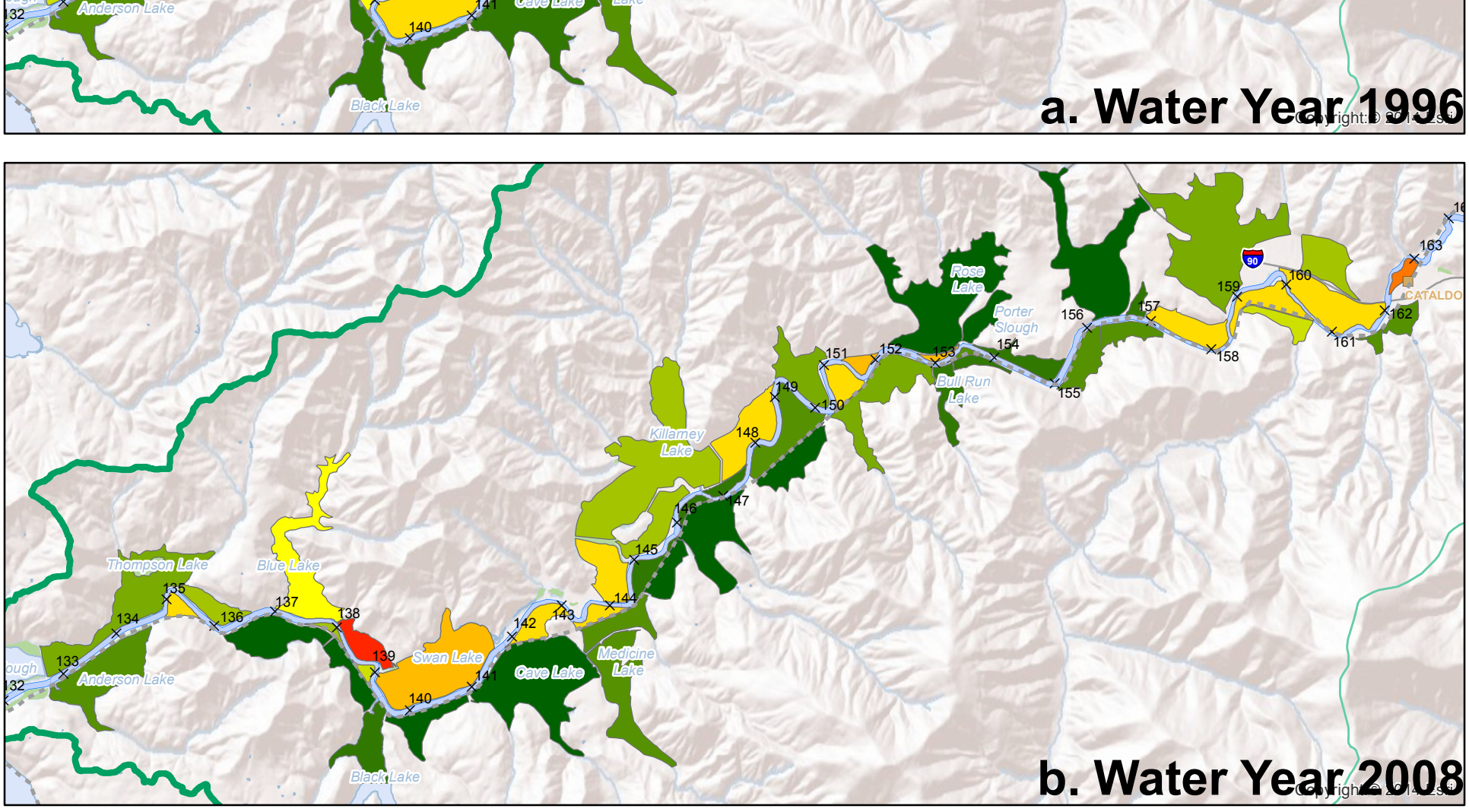

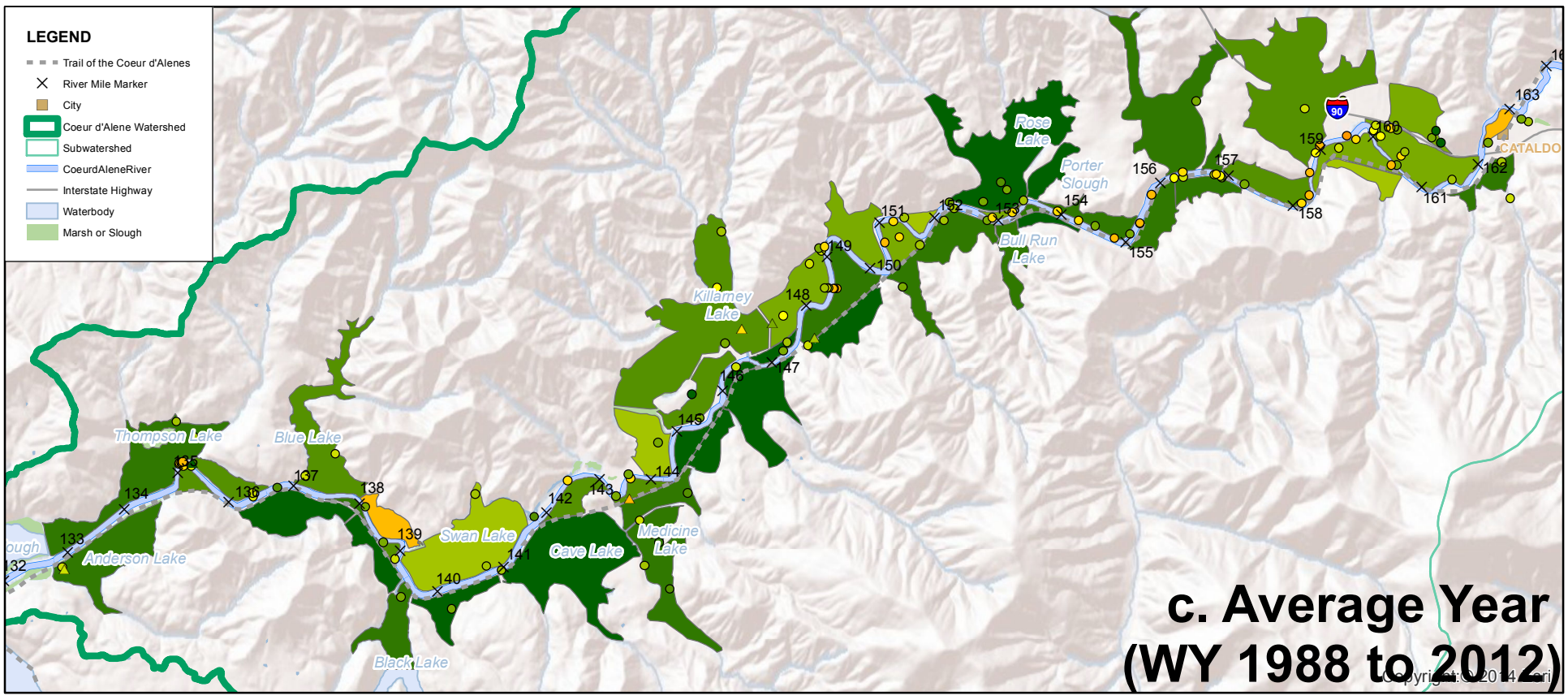

LEGEND - CONTINUED

Sediment Tiles (mm/year)
- 0.3
- 0.4 - 0.5
- 0.6 - 1.0
- 1.1 - 2.0
- 2.1 - 3.0
- 3.1 - 4.0
- 4.1 - 5.0
- 5.1 - 10.0
- 10.1 - 20.0
- 20.1 - 30.0
- 30.1 - 40.0
- 40.1 - 50.0
- 50.1 - 70.0

USGS Cores (mm/year)
- 0.0 - 0.1
- 0.2 - 0.5
- 0.6 - 1.0
- 1.1 - 2.0
- 2.1 - 3.0
- 3.1 - 4.0
- 4.1 - 5.0
- 5.1 - 10.0
- 10.1 - 20.0
- 20.1 - 30.0
- 30.1 - 40.0
- 40.1 - 50.0
- 50.1 - 70.0

Sedimentation Rates (mm/year)
- 0.0 - 0.1
- 0.2 - 0.5
- 0.6 - 1.0
- 1.1 - 2.0
- 2.1 - 3.0
- 3.1 - 4.0
- 4.1 - 5.0
- 5.1 - 10.0
- 10.1 - 20.0
- 20.1 - 30.0
- 30.1 - 40.0
- 40.1 - 50.0
- 50.1 - 70.0

Source: Shaded Relief (ESRI Online Catalog); Coeur d'Alene River Miles (USEPA); NHD (USGS).

0 1 2 4 Kilometers

N

Exhibit 57. **Floodplain Sedimentation Rates**
Processes of Sediment and Lead Transport, Erosion, and Deposition
Lower Basin of the Coeur d'Alene River (OU3)

Exhibit 58. **Average Annual Sedimentation**
Processes of Sediment and Lead Transport, Erosion, and Deposition
Lower Basin Coeur d'Alene River (OU3)

Off-Channel Storage Area Name	Area ID	River Mile	Average Inundated Area (hectares)	Cumulative Sediment Flux into the Floodplain 1988-2012 (metric tons)	Average Trapping Efficiency (%)	Cumulative Mass Deposited 1988-2012 (metric tons)	Average Annual Deposition Mass (metric tons/year)	Average Annual Lead Deposition Mass (metric tons/year)	Average Annual Deposition Rate (mm/year)	Sediment Mass Percent of Basin Total (%)	Lead Mass Percent of Basin Total (%)
Anderson Lake	1245	132.9	186	12,000	90%	10,000	420	1.6	0.2	1.7%	2.3%
Thompson Lake	1244	135.2	190	31,000	81%	25,000	990	3.7	0.5	4.1%	5.4%
Bare Marsh	1246	135.3	31	6,600	79%	5,200	210	0.8	0.6	0.9%	1.1%
Lamb Peak 2	1268	137	148	140	99%	140	5	0.0	0.0	0.0%	0.0%
Blue	1240	137.1	43	32,000	30%	10,000	390	1.5	0.8	1.6%	2.1%
Blue Marsh	1239	138.1	3	88,000	12%	11,000	420	1.6	11.0	1.7%	2.3%
Lamb Peak 1	1267	138.5	64	220	70%	160	6	0.0	0.0	0.0%	0.0%
Swan	1265	139	237	270,000	56%	150,000	6000	22.2	2.2	24.5%	32.7%
Black Lake 2	1241	139.6	104	4,300	93%	4,000	160	0.6	0.1	0.7%	0.9%
Black Lake 1	1266	140.9	56	250	73%	180	7	0.0	0.0	0.0%	0.0%
Cave	1242	141.1	290	4,400	86%	3,800	150	0.6	0.0	0.6%	0.8%
Medicine	1262 & 1264	143.4	124	22,000	80%	17,000	700	1.8	0.5	2.9%	2.7%
Moffit	1259	145.1	47	210,000	16%	30,000	1400	3.6	2.5	5.6%	5.3%
Schlepp	1243 & 1263	145.8	21	540	32%	170	7	0.0	0.0	0.0%	0.0%
Killarney	1261 & 1260	146.6	416	210,000	53%	110,000	4400	11.5	0.9	17.9%	16.9%
Strobl	1257	147.9	41	110,000	17%	20,000	750	2.0	1.6	3.1%	2.9%
Lane 1	1258	148.7	38	5,200	42%	2,200	87	0.2	0.2	0.4%	0.3%
Lane 2	1238	148.7	72	1,200	100%	1,200	49	0.1	0.1	0.2%	0.2%
Strobl Field	1256	149.4	7	3,000	67%	2,000	80	0.2	1.1	0.3%	0.3%
Black Rock Slough	1255	151.6	50	17,000	46%	4,700	190	0.5	0.3	0.8%	0.7%
Rose Lake	9651	152.8	53	0	67%	0	0	0.0	0.0	0.0%	0.0%
Bull Run 2	1254	153.1	45	2,900	27%	2,300	91	0.2	0.2	0.4%	0.4%
Potter Slough	1253	153.6	41	660	100%	290	12	0.0	0.0	0.0%	0.0%
Bull Run 1	1252	154	22	2,400	43%	340	14	0.0	0.1	0.1%	0.1%
Orling Slough	1251	154.2	16	1,500	44%	1,100	42	0.1	0.2	0.2%	0.2%
Upper Marsh 1 & 2	1248 & 1250	156.2	33	6,300	69%	3,300	130	0.3	0.3	0.5%	0.5%
Canyon Marsh	1249	156.3	10	1,900	40%	710	28	0.1	0.2	0.1%	0.1%
Mission Slough	9645	158.8	42	20,000	37%	10,000	390	0.4	0.8	1.6%	0.6%
Dudley Marsh	9647	159.1	1	1,000	38%	700	28	0.0	2.1	0.1%	0.0%
Whiteman's Slough	9646	160.5	2	970	67%	650	26	0.0	1.1	0.1%	0.0%
Skeel Gulch and South Cataldo	1247 & 9648	161.5	5	990	38%	700	28	0.0	0.5	0.1%	0.0%
Off-Channel Storage Areas Subtotal			**2,438**	**1,100,000**	**41%**	**430,000**	**17,000**	**54**	**0.6**	**70.3%**	**79.3%**
Overbank Flow Area ID											
135-L		135.2	27	10,000	74%	7,400	300	1.1	1.0	1.2%	1.6%
138-L		138	12	2,000	59%	1,200	47	0.2	0.3	0.2%	0.3%
139-L		138.9	13	4,300	58%	2,500	100	0.4	0.7	0.4%	0.6%
142-L		142.6	57	20,000	73%	14,000	570	2.1	0.9	2.4%	3.2%
144-L		143.7	25	11,000	64%	7,000	280	0.7	1.0	1.2%	1.1%
145-L		145	49	450	75%	330	13	0.0	0.0	0.1%	0.1%
146-L		146.4	18	390	71%	280	11	0.0	0.1	0.0%	0.0%
147-R		147.2	26	610	57%	350	14	0.0	0.0	0.1%	0.1%
151-L		151	41	41,000	42%	21,000	830	2.2	1.8	3.4%	3.2%
152-R		151.7	9	16,000	51%	7,500	300	0.8	2.9	1.2%	1.2%
153-R		153.1	6	7,600	78%	3,300	130	0.3	1.9	0.5%	0.5%
153.5-L		153.5	4	260	14%	170	7	0.0	0.2	0.0%	0.0%
156.8-R		156.8	13	2,700	51%	1,200	49	0.1	0.3	0.2%	0.2%
158-R		157.8	96	45,000	45%	18,000	730	1.9	0.7	3.0%	2.8%
159-L		159.1	26	33,000	55%	12,000	500	0.5	1.7	2.1%	0.8%
160-R		160	115	150,000	67%	58,000	2300	2.4	1.8	9.5%	3.6%
163-L		162.7	9	100,000	70%	26,000	1000	1.1	10.3	4.3%	1.6%
Overbank Flow Area Subtotal			**545**	**450,000**	**40%**	**180,000**	**7,200**	**14**	**1.2**	**29.7%**	**20.7%**
System Floodplain Total			**2,983**	**1,600,000**	**40%**	**610,000**	**24,000**	**68**	**0.7**	**100.0%**	**100.0%**

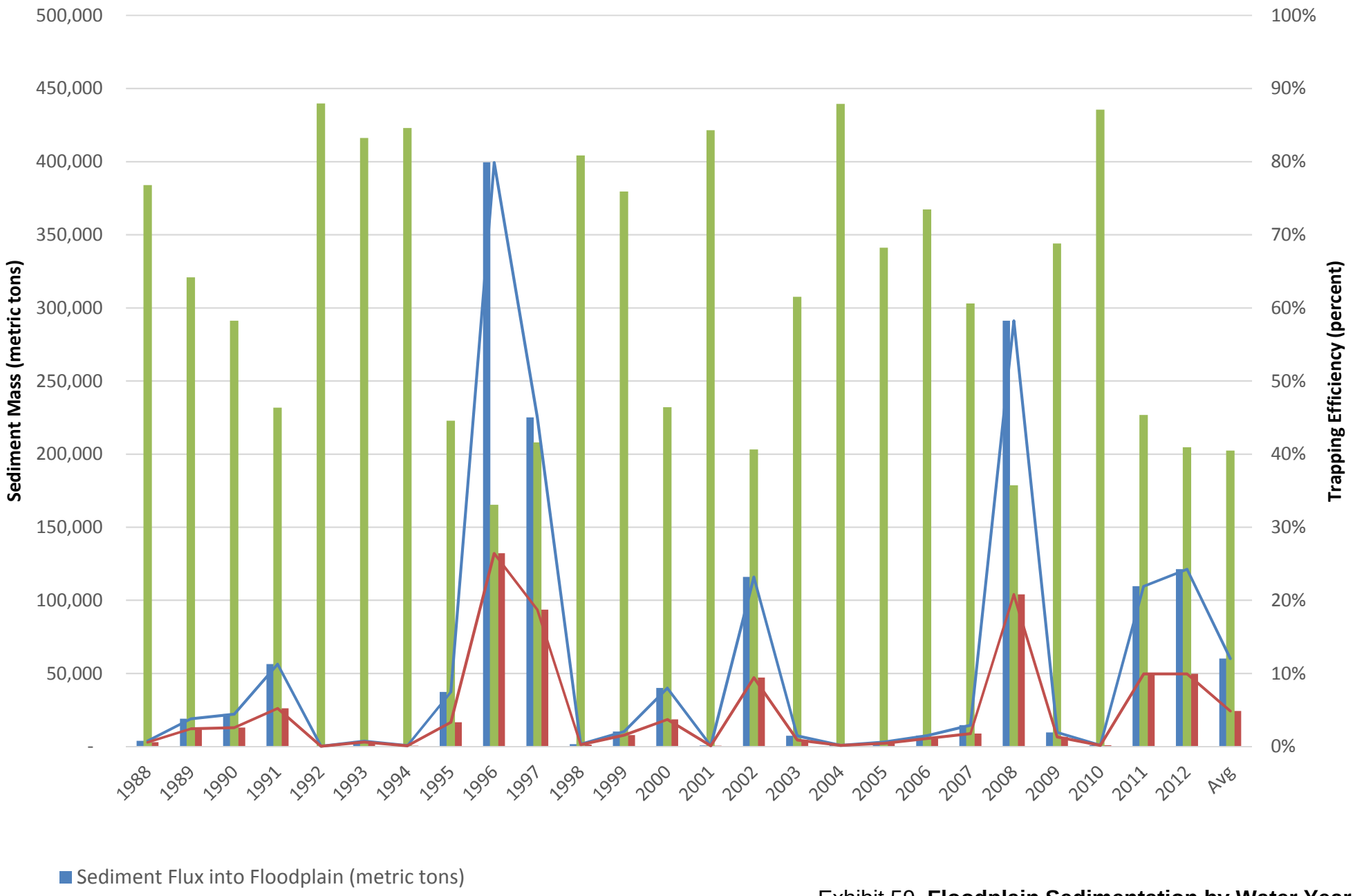

Exhibit 59. **Floodplain Sedimentation by Water Year for the Entire Lower Basin**
Processes of Sediment and Lead Transport, Erosion, and Deposition
Lower Basin Coeur d'Alene River (OU3)

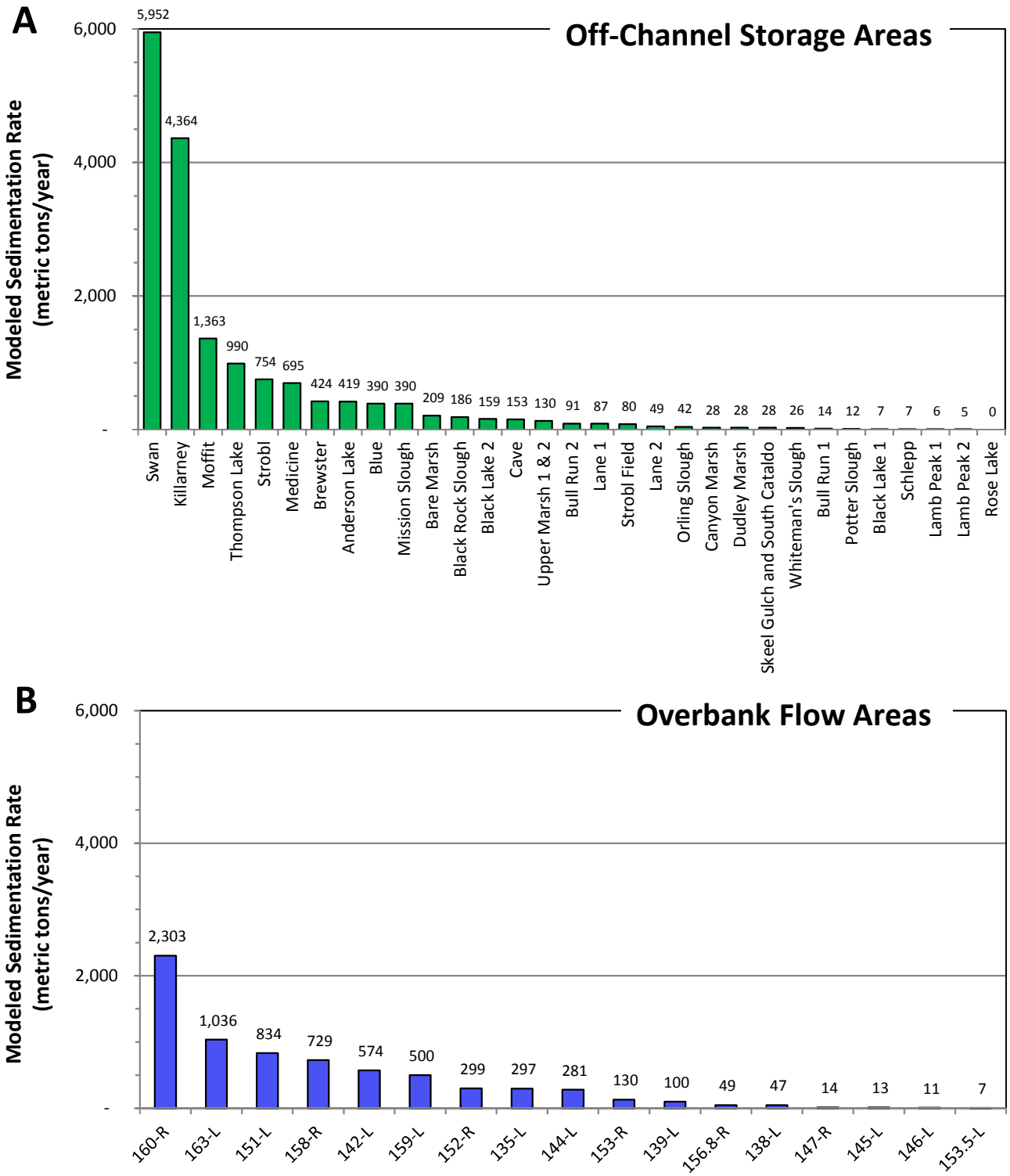

Note: Locations of off-channel storage areas and overbank flow areas shown in these graphs are shown in Exhibit 53.

Exhibit 60. **Annual Sediment Deposition in Lower Basin Floodplain (from CH2M HILL, 2014)**

Processes of Sediment and Lead Transport, Erosion, and Deposition

Lower Basin Coeur d'Alene River (OU3)

Exhibit 61. **Estimation of Mass of Contaminated Channel Bed Sediment by Bookstrom et al. (2001)**

Compiled from Bookstrom et al. (2001), Tables 2, 3, 4, 11, and 12.

Processes of Sediment and Lead Transport, Erosion, and Deposition

Lower Basin Coeur d'Alene River (OU3)

Riverbed Sediment Estimation Unit	R1	R2	R3	R4	R5	R6	Total, Estimation Units R1-R6 (Cataldo Dredge Pool to Coeur d'Alene Lake)	Total, Estimation Units R1-R5 (Approximates sediment budget in this report - indicated by red outline)
Thickness of Pb-Rich Sediments, Summary Statistics (from Bookstrom et al., 2001, Table 2)								
Number of Thickness Measurements in Each Reach	56	69	63	53	48	47	336	289
Minimum Thickness of Pb-Rich Sediments (cm)	128	0	0	0	0	0		
Maximum Thickness of Pb-Rich Sediments (cm)	714	836	531	514	604	397		
Median Thickness of Pb-Rich Sediments (cm)	300	384	321	284	226	162		
Mean Thickness of Pb-Rich Sediments (cm)	337	378	273	251	198	158		
Estimated Area, Thickness, and Volume of Lead-Rich Sediments (from Bookstrom et al., 2001, Table 4)								
Area of Pb-Rich Sediments (km^2)	0.16	0.88	0.87	0.58	0.72	0.61	3.82	3.21
Median Thickness, Pb-Rich Sediments (m)	3	3.84	3.21	2.84	2.26	1.62		
Mean Thickness, Pb-Rich Sediments (m)	3.37	3.78	2.73	2.51	1.98	1.58		
Median-based Estimate of Volume, Pb-Rich Sediments (Mm^3)	0.49	3.37	2.78	1.64	1.63	0.98	10.9	9.91
Mean-based Estimate of Volume, Pb-Rich Sediments (Mm^3)	0.55	3.32	2.36	1.45	1.43	0.96	10.1	9.11
Estimated Tonnage of Dry Lead-Rich Sediments (from Bookstrom et al., 2001, Table 11)								
Median Density, Dry Pb-Rich Sediments (t/m^3)	1.61	1.61	1.61	1.61	1.61	1.61		
Median-based Estimate of Tonnage, Dry Pb-Rich Sediments (Mt)	0.79	5.43	4.47	2.64	2.62	1.58	17.5	16.0
Mean-based Estimate of Tonnage, Dry Pb-Rich Sediments (Mt)	0.83	5.02	3.57	2.19	2.16	1.45	15.2	13.8
Estimated Lead in Contaminated Sediments (from Bookstrom et al., 2001, Tables 3 and 12)								
Median Thickness Weighted Average Concentration (mg/kg)	2,315	9,221	5,286	9,138	6,608	7,404		
Mean Thickness Weighted Average Concentration (mg/kg)	2,362	9,919	5,650	10,060	7,136	7,446		
Median-based Estimate of Tonnage, Pb in Pb-Rich Sediments (kt Pb)	1.8	50.1	23.6	24.1	17.3	11.7	129	117

Note:

Cataldo gage is just upstream of Estimation Unit R-1 and Harrison gage is close to the boundary between R-5 and R-6. Thus, the channel bed sediment reservoir included here is approximately equivalent to the R-1 through R-5 (as indicated by red outline), or, about 16 million metric tons, based on the median values preferred by Bookstrom et al. (2001).

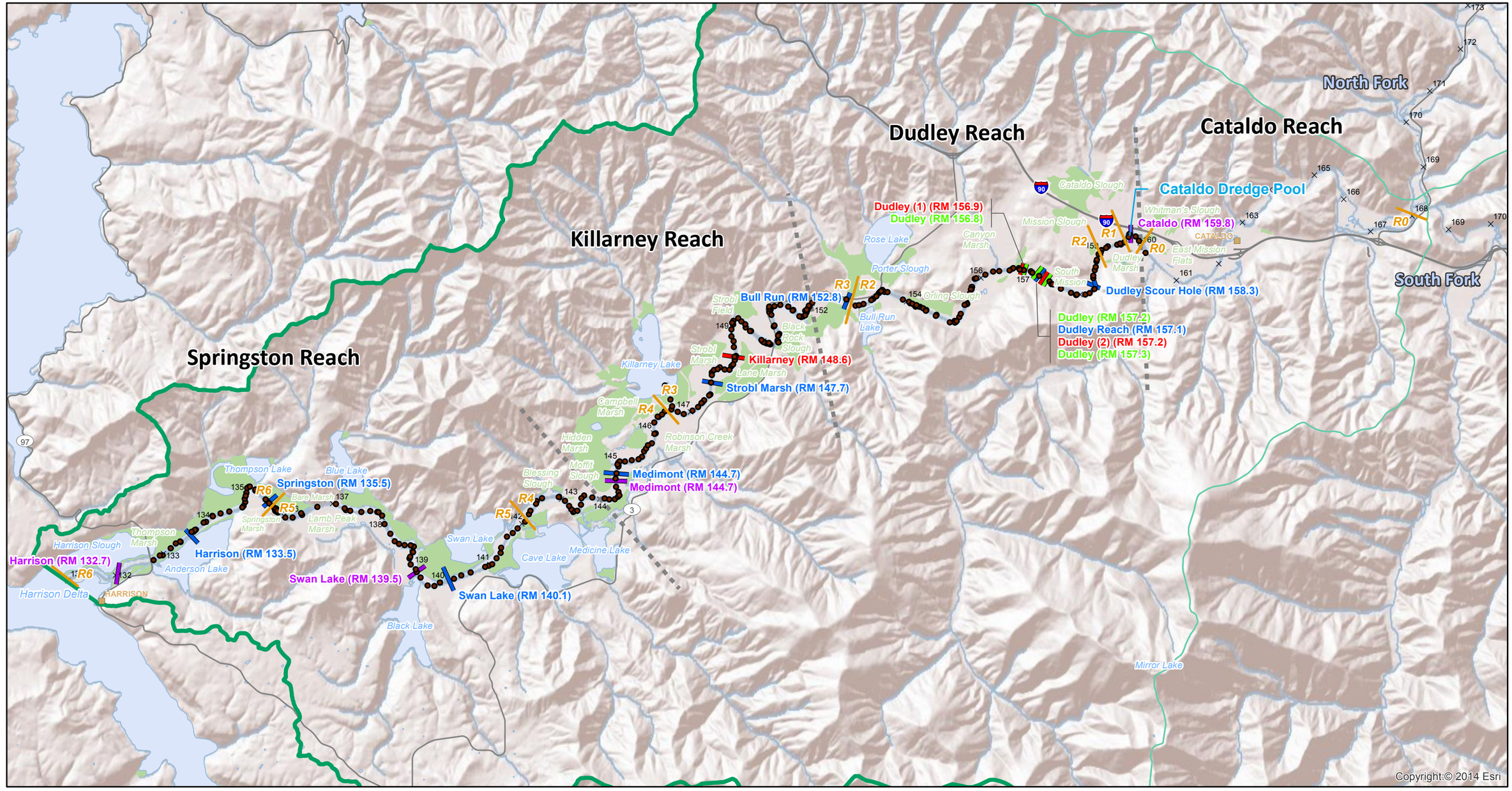

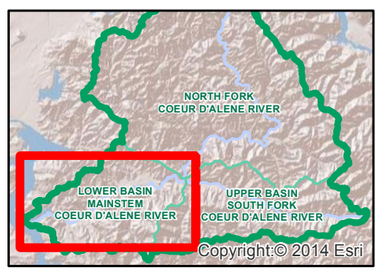

LEGEND

- 2012 Sonic Cores
- 2012 Vibracore Transects (CH2M HILL, 2012)
- EPA Coring Transects (CH2M HILL and URS, 2002)
- USGS Coring Transects (Box et al., 2001)
- 2013 Shallow Vibracore Location
- R6/R5 Estimation Unit (Bookstrom et al., 2001)
- Reach Divide
- City
- River Mile Marker
- Road
- Waterbody
- Marsh or Slough

N

0 1 2 4 Miles

Exhibit 62. **Locations of Cores and Core Transects**

Processes of Sediment and Lead Transport, Erosion, and Deposition
Lower Basin of the Coeur d'Alene River (OU3)

ch2m

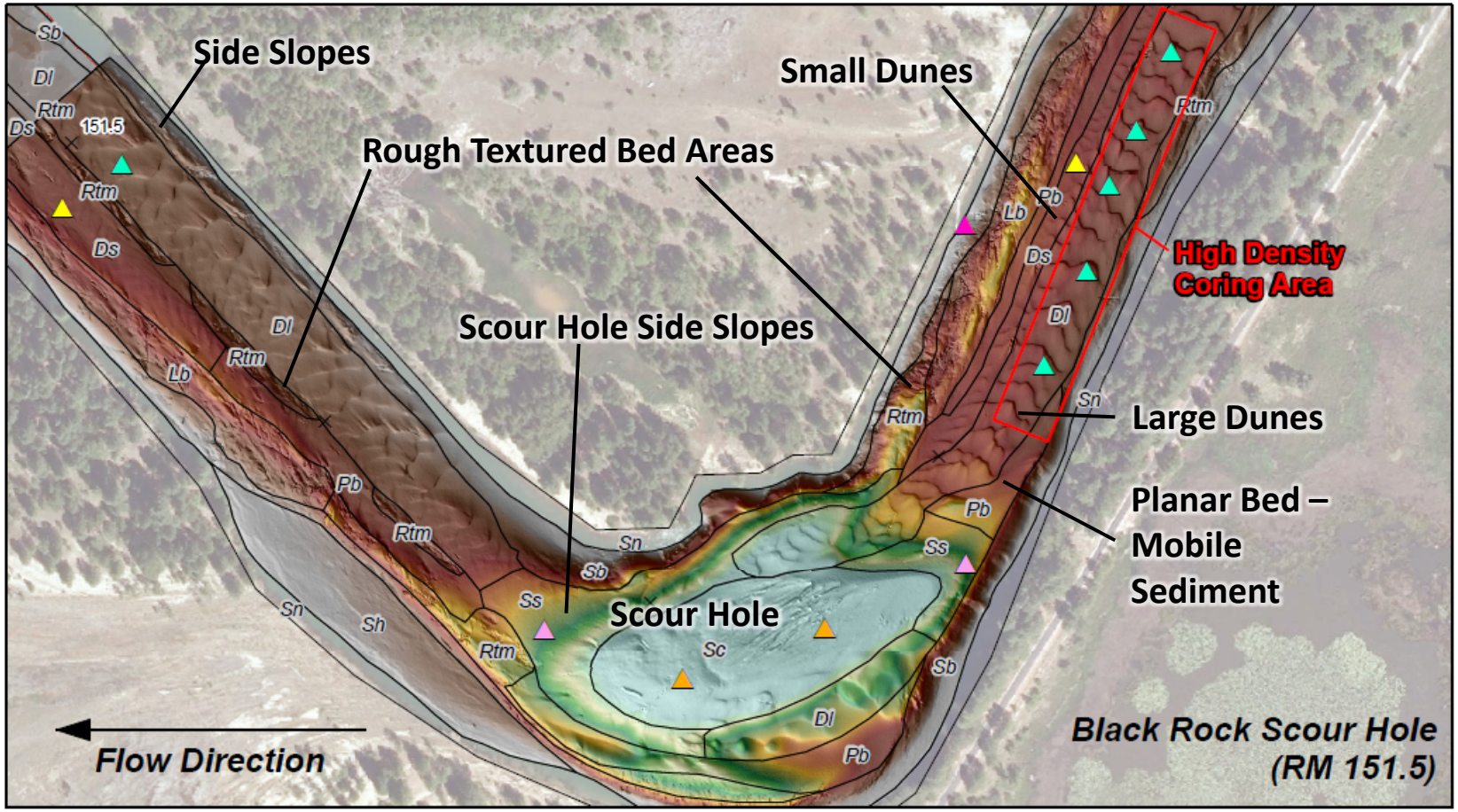

Exhibit 63. **Example of Geomorphic Mapping and Coring (Triangles) Used in 2013 Shallow Vibracore Investigation**
Processes of Sediment and Lead Transport, Erosion, and Deposition
Lower Basin Coeur d'Alene River (OU3)

A

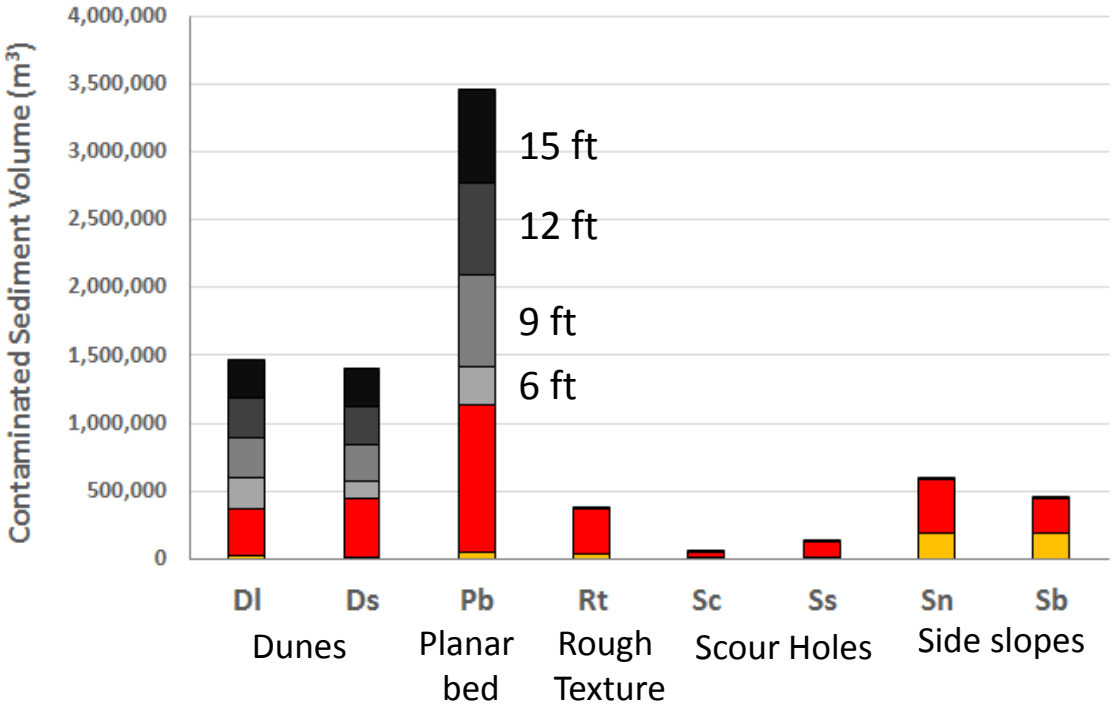

LEGEND

Sediment volume based on cores that reached the base of contamination.

Sediment volume based on cores that did not reach base of contamination.

Gray and black portions of columns show volumes of unsampled sediment below cores that did not reach base of contamination . Different volumes are based on different assumptions about the thickness of unsampled sediments below cores.

B

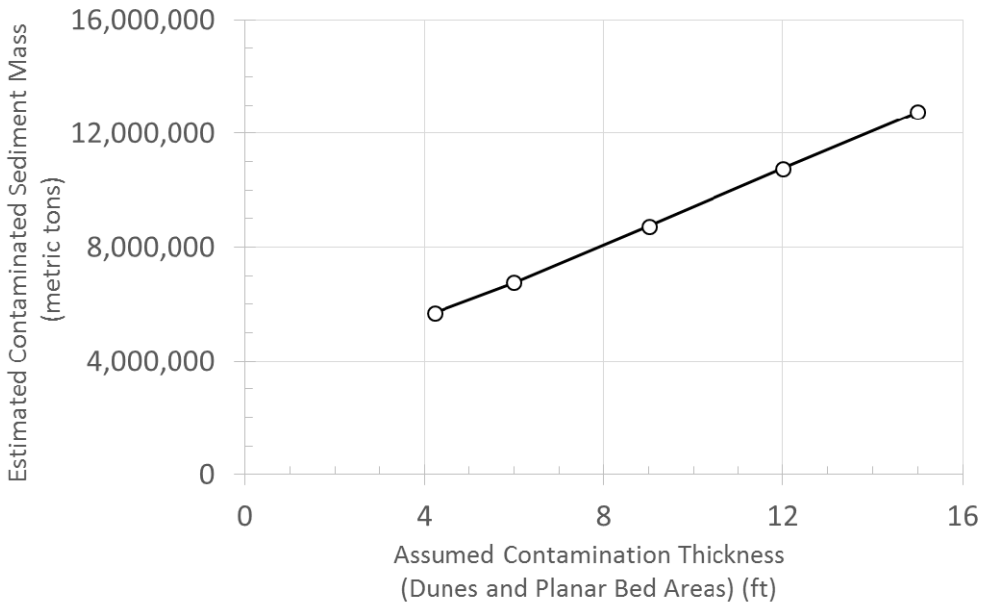

Exhibit 64 **Estimate of the Volumes and Masses of Contaminated Sediment in the Riverbed Based on Geomorphic Mapping and 2013 Shallow Vibracore Sampling**

(A) Contaminated sediment volume by geomorphic unit type (B) Total sediment mass as a function of assumed sediment thickness in dunes and planar bed areas (based on assumed dry bulk density of 1.61 metric tons per m^3).

Processes of Sediment and Lead Transport, Erosion, and Deposition

Lower Basin Coeur d'Alene River (OU3)

ch2m

Exhibit 65. **Sediment and Lead Budgets for the Lower Basin (Cataldo to Harrison Gages)**
Processes of Sediment and Lead Transport, Erosion, and Deposition
Lower Basin Coeur d'Alene River (OU3)

(all values rounded to two significant digits unless otherwise specified)

	Mass of Contaminated Sediment Transfer (metric tons/yr)[1]	Percent of Source/Sink	Mass Lead Transfer (metric tons/yr)	Percent of Source/Sink
Sediment and Lead Sources				
Bed Erosion Rate[2]	54,000	59%	250	79%
Flux in at Cataldo[3]	32,000	35%	34	11%
Bank Erosion[4]	4,900	5%	32	10%
Sediment and Lead Sinks				
Flux out at Harrison[3]	67,000	74%	250	79%
Floodplain Deposition[5]	24,000	26%	68	21%

	Mass of Contaminated Sediment Stored (metric tons)		Mass of Lead Stored (metric tons)	
Sediment and Lead Storage Reservoirs				
Channel Bed[6]	12,000,000		60,000	
Floodplain[7]	19,000,000		110,000	

Notes

All values rounded to two significant digits unless otherwise noted.

1. Values refer to the amount of post-mining sediment contaminated with lead within the valley between the Cataldo and Harrison gaging stations, as shown in Exhibit 1. For the purpose of this report contaminated sediment includes sediments with lead concentrations above 1,000 mg/kg, well above background lead content, and consistent with the value used by Bookstrom et al. (2004) to distinguish contaminated sediment.

2. Back calculated from the other elements in the sediment and lead budgets.

3. Bulk sediment and lead fluxes computed using rating curves, suspended sediment lead concentrations, and flow history, averaged over the 25-year modeling period including water years 1987-2012, as described in Sections 3.6 and 4.3 of this report.

4. Bank erosion rate of contaminated portion of riverbank only; total bank erosion rate of sediment estimated to be 7,800 metric tons/yr. See Section 5.2 for summary, and CH2M HILL (2013d) for detailed explanation of data and analysis.

5. Estimated using floodplain deposition modeling based on 1-dimensional hydraulic model and sediment rating curves as summarized in Section 6.2. Alternate estimate based on the total deposition rate since 1980, as measured in cores compiled by Bookstrom et al. (2004) and adjusted to the spatial and temporal boundaries referred to in this report, are much higher - 156,000 tons of sediment and 500 tons of lead (Section 6.1). CH2M HILL favors the model-based estimate for reasons explained in the text.

6. Channel mass is the amount of contaminated sediment stored in channel bed between Cataldo and Harrison USGS gages. These are considered provisional values, an estimate based on results of evaluations of three independent data sets: (a) coring and geophysical data compiled and summarized by Bookstrom et al. (2001); (b) analyses of 8 coring transects collected in summer 2012; and (c) analysis of 315 shallow vibracores collected in September 2013. The results of the three different approaches are provisional, as summarized in Section 7.1 of this addendum. A more thorough reporting on riverbed characterization will be reported in an upcoming technical memorandum, anticipated in 2016.

7. Floodplain mass is the estimated amount of contaminated (post-1903) sediment in floodplain storage between the Cataldo and Harrison USGS gages, based on reanalysis of data presented by Bookstrom et al. (2004), as described in Section 7.2 of this addendum.

Sediment

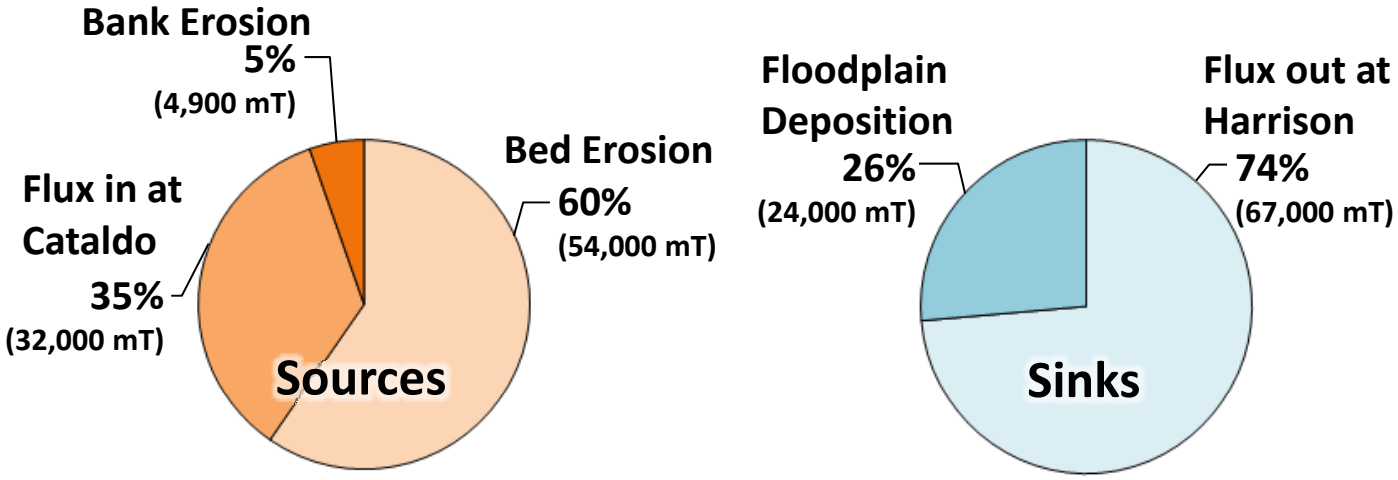

Lead

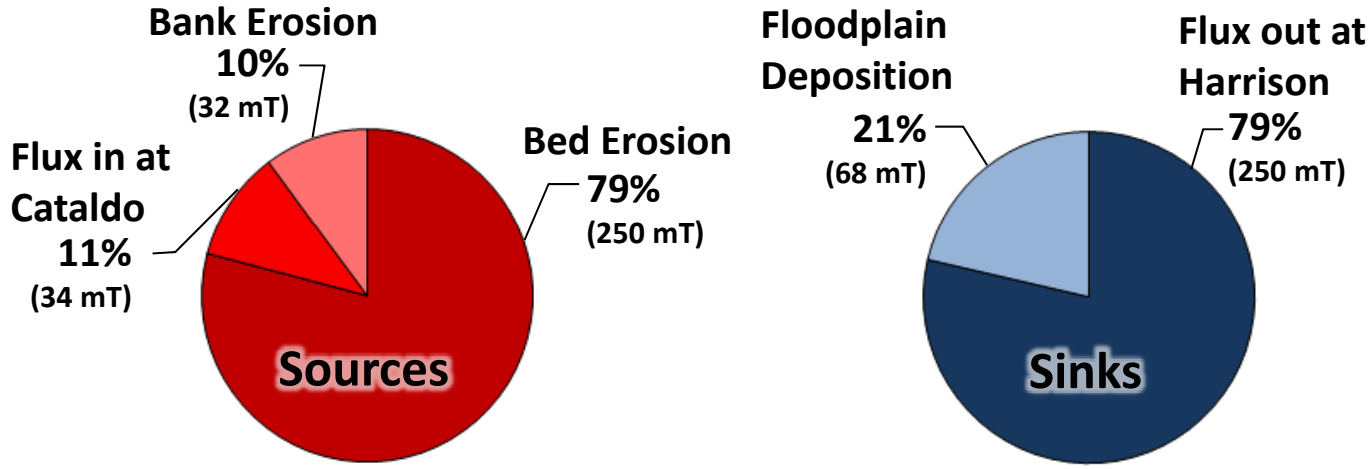

Exhibit 66. **Relative Sources and Sinks of Contaminated Sediment and Lead in the Lower Basin**
Processes of Sediment and Lead Transport, Erosion, and Deposition
Lower Basin Coeur d'Alene River (OU3)

Attachment A
Compilation of Suspended Sediment Data from Five Gages in the North Fork, South Fork, and Main Stem Coeur d'Alene River

Attachment A. **Summary of BEMP and USGS Sample Data (Suspended Sediment Concentration, Grain Size, and Lead Concentrations)**
Processes of Sediment and Lead Transport, Erosion, and Deposition
Lower Basin Coeur d'Alene River (OU3)

Sampler	Station	Date	Time	Discharge (cfs)	SSC (mg/L)	Percent Fines	SSC - sand (mg/L)	SSC - fines (mg/L)	Lake Level (ft NAVD88)	Flow, day before measurement (cfs)	Mean Flow, day of measurement (cfs)	Flow, day after measurement (cfs)	Rising, Falling,Peak, or Steady[a]	$Pb_{FILTERED}$ (µg/L)	$Pb_{UNFILTERED}$ (µg/L)	Pb^{c}_{BULK} (mg/kg)	$Pb_{63\text{-}250µm}$ (mg/kg)	$Pb_{<63µm}$ (mg/kg)
HARRISON DATA																		
BEMP (USGS)	Harrison	05/19/08	9:30	22,700	249				2133.34	19,600	24,300	27,200	Rising			4,080		
BEMP (USGS)	Harrison	05/20/09	12:30	11300	9.294				2130	11,000	11,300	10,300	Peak			3,930		
BEMP (CH2M HILL)	Harrison	12/13/10	15:00	7,040	35.9	73	9.7	26.2	2124.79	2,230	6,250	11,700	Rising			4,870		4,490
BEMP (CH2M HILL)	Harrison	12/15/10	15:00	13,300	240	57	103.4	137.1	2127.25	11,700	13,000	10,900	Peak			4,480	4,100	5,290
BEMP (CH2M HILL)	Harrison	01/18/11	15:00	19,500	658	53	306.7	351.6	2130.2	13,800	18,000	18,800	Rising			4,900	2,890	6,280
BEMP (CH2M HILL)	Harrison	05/17/11	18:00	17,300	105	23	80.5	24.0	2132.8	15,600	17,100	16,500	Peak			3,220	2,170	4,320
BEMP (CH2M HILL)	Harrison	4/1/12	16:00	17,400	283	38	177.1	106.3	2131.27	14,000	16,900	16,300	Peak			1,550	2,970	5,210
BEMP (CH2M HILL)	Harrison	4/13/12		10,300	22	61	8.7	13.6	2129.28	8,350	10,100	10,600	Rising			3,580		
BEMP (CH2M HILL)	Harrison	4/24/12	15:00	17,500	102	44	57.0	44.9	2131.58	15,500	17,900	19,300	Rising			3,710	2,700	4,770
BEMP (CH2M HILL)	Harrison	4/27/12	15:00	21,300	240	10	216.4	23.1	2133.76	19,300	19,300	18,500	Peak			2,390	2,220	2,390
BEMP (CH2M HILL)	Harrison	4/7/13	16:30	12,800	158	47	83.5	74.2	2128.54	10,500	12,700	13,000	Rising			4,290	3,880	5,050
BEMP (CH2M HILL)	Harrison	3/11/14		18,100	243	30	170.1	72.9								3,500	3,350	5,420
NWIS (USGS)	12413860	02/16/93	13:30	789	13	70	3.9	9.1	2122.57	767	640	554	Steady		82	6308		
NWIS (USGS)	12413860	03/10/93	15:30	1,970	5	69	1.6	3.5	2123.07	1,530	1,530	1,490	Steady		27	5400		
NWIS (USGS)	12413860	04/12/93	14:00	9,680	20	62	7.6	12.4	2129.28	8,920	7,770	6,770	Falling		87	4350		
NWIS (USGS)	12413860	04/20/93	13:50	9,100	18	72	5.0	13.0	2128.57	8,140	8,170	7,110	Steady		110	6111		
NWIS (USGS)	12413860	05/05/93	13:00	8,720	42	39	25.6	16.4	2129.7	8,830	8,610	8,860	Steady		70	1667		
NWIS (USGS)	12413860	05/17/93	16:00	8,590	13	78	2.9	10.1	2130.55	7,910	6,930	6,130	Falling		62	4769		
NWIS (USGS)	12413860	06/02/93	12:00	3,250	3	83	0.5	2.5	2128.51	2,820	2,670	2,590	Steady		21	7000		
NWIS (USGS)	12413860	06/21/93	14:00	1,400	4	98	0.1	3.9	2128.7	1,310	1,320	1,390	Steady		29	7250		
NWIS (USGS)	12413860	07/22/93	16:35	1,900	2	64	0.7	1.3	2128.59	1,620	1,570	1,540	Steady		17	8500		
NWIS (USGS)	12413860	08/17/93	18:50	1,010	11	15	9.4	1.7	2128.74	777	777	766	Steady		26	2364		
NWIS (USGS)	12413860	09/20/93	14:45	626	4	59	1.6	2.4	2128.11	495	483	482	Steady		21	5250		
NWIS (USGS)	12413860	11/16/93	13:40	465	3	90	0.3	2.7	2124.99	367	365	369	Steady		24	8000		
NWIS (USGS)	12413860	11/20/93	10:15	800[b]	7	67	2.3	4.7	2124.87	380	377	372	Steady					
NWIS (USGS)	12413860	12/13/93	15:24	877	3	89	0.3	2.7	2124.25	802	776	740	Steady		35	11667		
NWIS (USGS)	12413860	01/18/94	10:45	1,800	5	69	1.6	3.5	2123.34	1,610	1,500	1,360	Steady		15	3000		
NWIS (USGS)	12413860	02/23/94	10:30	820	15	95	0.8	14.3	2122.16	574	577	581	Steady		48	3200		
NWIS (USGS)	12413860	03/09/94	13:12	2,980	3	95	0.2	2.9	2124.12	3,030	2,590	2,340	Steady					
NWIS (USGS)	12413860	03/14/94	13:20	2,080	18	78	4.0	14.0	2124.12	1,870	1,890	2,040	Steady		20	1111		
NWIS (USGS)	12413860	04/06/94	13:10	4,750	9	57	3.9	5.1	2125.56	4,950	4,600	4,320	Steady		51	5667		
NWIS (USGS)	12413860	04/20/94	12:15	7,780	51	78	11.2	39.8	2127.09	8,610	9,180	8,720	Steady		150	2941		
NWIS (USGS)	12413860	05/11/94	9:14	2,760	3	96	0.1	2.9	2128.41	3,370	3,120	2,930	Steady		18	6000		
NWIS (USGS)	12413860	05/11/94	11:04	3,000[b]	3	96	0.1	2.9	2128.41	3,370	3,120	2,930	Steady		18	6000		
NWIS (USGS)	12413860	06/14/94	14:55	1,280	3	92	0.2	2.8	2128.72	992	999	1,000	Steady		20	6667		
NWIS (USGS)	12413860	07/20/94	9:30	648	3	87	0.4	2.6	2128.68	444	437	431	Steady		25	8333		
NWIS (USGS)	12413860	08/15/94	17:20	346	3	90	0.3	2.7	2128.58	312	310	301	Steady		23	7667		
NWIS (USGS)	12413860	09/20/94	14:35	221	3	93	0.2	2.8	2128.01	255	255	249	Steady		24	8000		
NWIS (USGS)	12413860	04/16/02	9:30	24,700	368	54	169.3	198.7	2133.24	33,000	19,800	12,800	Falling	20.4	1060	2825		
NWIS (USGS)	12413860	04/18/02	9:00	14,500	57	35	37.1	20.0	2133.12	12,800	9,610	8,220	Falling	6.22	90.9	1486		
NWIS (USGS)	12413860	10/09/03	9:35	436	5				2127.29	260	268	272	Steady	2.46	22.6	4028		
NWIS (USGS)	12413860	12/09/03	9:45	1,900	1				2124.43	2,050	1,600	1,330	Steady	3.15	16.9	13750		
NWIS (USGS)	12413860	03/03/04	14:15	2,920	5				2124.59	2,890	2,790	2,650	Steady					
NWIS (USGS)	12413860	04/07/04	12:40	7,350	14				2127.34	6,810	7,420	7,780	Rising	5.69	88.5	5915		
NWIS (USGS)	12413860	04/27/04	10:00	4,380	2				2126.53	4,230	4,100	5,000	Steady					
NWIS (USGS)	12413860	05/10/04	9:40	3,820	2				2126.92	4,180	4,090	3,870	Steady	4.5	12.5	4000		

Attachment A. **Summary of BEMP and USGS Sample Data (Suspended Sediment Concentration, Grain Size, and Lead Concentrations)**
Processes of Sediment and Lead Transport, Erosion, and Deposition
Lower Basin Coeur d'Alene River (OU3)

Sampler	Station	Date	Time	Discharge (cfs)	SSC (mg/L)	Percent Fines	SSC - sand (mg/L)	SSC - fines (mg/L)	Lake Level (ft NAVD88)	Flow, day before measurement (cfs)	Mean Flow, day of measurement (cfs)	Flow, day after measurement (cfs)	Rising, Falling,Peak, or Steady[a]	$Pb_{FILTERED}$ (µg/L)	$Pb_{UNFILTERED}$ (µg/L)	Pb^{c}_{BULK} (mg/kg)	$Pb_{63\text{-}250µm}$ (mg/kg)	$Pb_{<63µm}$ (mg/kg)
HARRISON DATA (continued)																		
NWIS (USGS)	12413860	06/08/04	12:40	3,130	2				2128.63	3,750	3,250	3,030	Steady	3.33	8.43	2550		
NWIS (USGS)	12413860	07/19/04	14:00	792	2				2128.78	800	790	760	Steady	4.11	24.7	10295		
NWIS (USGS)	12413860	09/01/04	13:15	155	2				2128.72	620	580	550	Steady	2.65	11.7	4525		
NWIS (USGS)	12413860	10/12/04	14:05	657	2				2127.01	650	529	508	Steady	4.09	18	6955		
NWIS (USGS)	12413860	12/13/04	14:45	10,900	64				2127.65	10,500	10,800	9,080	Peak	13.6	347	5209		
NWIS (USGS)	12413860	02/08/05	10:00	2,840	2	94	0.1	1.9	2125.39	3,140	2,980	2,850	Steady	4.12	12.7	4290		
NWIS (USGS)	12413860	03/14/05	14:00	1,180	8	57	3.4	4.6	2123.21	1,450	1,420	1,390	Steady	11	49.7	4838		
NWIS (USGS)	12413860	03/30/05	14:50	8,160	29	84	4.6	24.4	2127.23	8,850	8,160	6,840	Falling	7.93	114	3658		
NWIS (USGS)	12413860	05/12/05	15:30	2,550	4	54	1.8	2.2	2128.41	2,970	2,870	2,700	Steady	3.49	8.62	1283		
NWIS (USGS)	12413860	06/28/05	10:00	738	2	89	0.2	1.8	2128.76	960	954	1,010	Steady	4.79	20.7	7955		
NWIS (USGS)	12413860	07/18/05	13:40	570	4	81	0.8	3.2	2128.81	645	658	636	Steady	3.76	25.4	5410		
NWIS (USGS)	12413860	08/25/05	12:45	139	5	52	2.4	2.6	2128.68	395	397	391	Steady	1.73	7.79	1212		
NWIS (USGS)	12413860	10/18/05	12:00	502	2	92	0.2	1.8	2126.48	653	654	659	Steady	5.21	21	7895		
NWIS (USGS)	12413860	01/09/06	12:30	3,870	1	92	0.1	0.9	2125.98	3,840	3,900	4,460	Steady	3.14	15.8	12660		
NWIS (USGS)	12413860	01/12/06	10:40	8,750	68	92	5.4	62.6	2127.77	7,350	8,780	8,180	Peak	9.16	282	4012		
NWIS (USGS)	12413860	02/15/06	13:00	2,220	6	91	0.5	5.5	2124.83	2,520	2,320	2,400	Steady	11.9	54.9	7167		
NWIS (USGS)	12413860	04/08/06	13:25	9,140	54	81	10.3	43.7	2127.77	7,760	8,970	9,330	Rising	6.73	236	4246		
NWIS (USGS)	12413860	05/20/06	14:00	8,100	10	89	1.1	8.9	2128.96	8,000	7,880	7,630	Steady	4.64	50.2	4556		
NWIS (USGS)	12413860	06/15/06	13:15	3,390	1	91	0.1	0.9	2128.81	2,790	3,390	3,760	Steady	2.57	8.68	6110		
NWIS (USGS)	12413860	07/13/06	14:55	891	2	78	0.4	1.6	2128.72	940	890	860	Steady	7.01	19.9	6445		
NWIS (USGS)	12413860	08/16/06	12:55	468	3	79	0.6	2.4	2128.78	520	490	470	Steady	3.2	16.8	4533		
NWIS (USGS)	12413860	11/09/06	13:50	4,720	12	96	0.5	11.5	2127.91	6,690	4,820	3,360	Falling	4.82	29.3	2040		
NWIS (USGS)	12413860	02/12/07	13:30	1,960	5	79	1.1	4.0	2123.16	1,620	1,890	2,060	Steady	2.63	20.1	3494		
NWIS (USGS)	12413860	03/14/07	11:50	14,400	235	80	47.0	188.0	2128.71	12,700	14,400	13,000	Peak	21.4	1230	5143		
NWIS (USGS)	12413860	05/09/07	15:30	4,330	4	69	1.2	2.8	2127.11	4,110	4,340	4,820	Steady	4.14	13.6	2365		
NWIS (USGS)	12413860	06/11/07	13:45	1,630	3	67	1.0	2.0	2128.7	1,600	1,540	1,400	Steady	4.04	8.44	1467		
NWIS (USGS)	12413860	08/07/07	11:15	310	2	78	0.4	1.6	2128.65	325	321	318	Steady	0.91	12	5545		
NWIS (USGS)	12413860	10/09/07	14:45	639	3	73	0.8	2.2	2127.39	614	583	554	Steady	3.79	15.2	3803		
NWIS (USGS)	12413860	12/05/07	10:00	4,000	6	80	1.2	4.8	2124.89	2,500	3,750	3,350	Steady	6.39	34.1	4618		
NWIS (USGS)	12413860	05/08/08	15:00	14,000	70	82	12.6	57.4	2129.57	11,900	13,200	12,800	Peak	17.2	386	5269		
NWIS (USGS)	12413860	05/19/08	8:50	22,400	404	55	181.8	222.2	2135.48		24,300			29	358	814		
NWIS (USGS)	12413860	06/30/08	14:45	3,540	4	92	0.3	3.7	2128.17	3,960	3,530	3,150	Steady	12	27	3750		
NWIS (USGS)	12413860	08/05/08	10:55	586	2	94	0.1	1.9	2128.71	723	705	685	Steady	7.38	29.9	11260		
NWIS (USGS)	12413860	09/08/08	15:10	565	1	92	0.1	0.9	2128.7	498	491	481	Steady	3.81	15.6	11790		
NWIS (USGS)	12413860	10/15/08	11:45	516	3	73	0.8	2.2	2126.73	493	501	486	Steady	5.89	19.5	4537		
NWIS (USGS)	12413860	11/14/08	12:45	1,100	4	84	0.6	3.4	2126.25	1,500	1,210	1,020	Steady	9.51	37.3	6948		
NWIS (USGS)	12413860	01/10/09	10:05	10,500	74	89	8.1	65.9	2127.58	12,000	9,700	7,000	Falling	18.6	381	4897		
NWIS (USGS)	12413860	02/26/09	11:20	2,770	3	43	1.7	1.3	2123.79	1,630	2,630	3,260	Steady	9	31	7333		
NWIS (USGS)	12413860	05/20/09	12:15	11,100	23	83	3.9	19.1	2130	11,000	11,300	10,300	Peak	9.45	98.4	3867		
NWIS (USGS)	12413860	06/18/09	12:50	2,230	5	71	1.5	3.6	2128.67	2,270	2,230	2,070	Steady	5.69	15.2	1902		
NWIS (USGS)	12413860	08/11/09	14:50	650	3	71	0.9	2.1	2128.61	681	648	605	Steady	1.46	16.6	5047		
NWIS (USGS)	12413860	10/27/09	11:30	1,100	3	65	1.1	2.0	2126.94	736	1,140	1,080	Steady	8.77	22.1	4443		
NWIS (USGS)	12413860	01/26/10	10:00	1,320	2	100	0.0	2.0	2123.19	1,580	1,390	1,290	Steady	7.36	19.8	6220		
NWIS (USGS)	12413860	03/31/10	11:43	6,850	50	95	2.5	47.5	2124.32	5,530	6,870	5,560	Steady	10.3	267	5134		
NWIS (USGS)	12413860	04/23/10	15:55	6,060	15	92	1.2	13.8	2126.17	6,350	5,940	5,090	Steady	6.47	71.2	4315		
NWIS (USGS)	12413860	07/15/10	11:30	1,210	3	81	0.6	2.4	2128.62	1,250	1,210	1,160	Steady	6.94	17.4	3487		
NWIS (USGS)	12413860	10/12/10	11:15	641	2	81	0.4	1.6	2127.2	635	660	709	Steady	2.38	20.5	9060		

Attachment A. **Summary of BEMP and USGS Sample Data (Suspended Sediment Concentration, Grain Size, and Lead Concentrations)**
Processes of Sediment and Lead Transport, Erosion, and Deposition
Lower Basin Coeur d'Alene River (OU3)

Sampler	Station	Date	Time	Discharge (cfs)	SSC (mg/L)	Percent Fines	SSC - sand (mg/L)	SSC - fines (mg/L)	Lake Level (ft NAVD88)	Flow, day before measurement (cfs)	Mean Flow, day of measurement (cfs)	Flow, day after measurement (cfs)	Rising, Falling,Peak, or Steady[a]	$Pb_{FILTERED}$ (µg/L)	$Pb_{UNFILTERED}$ (µg/L)	Pb^{c}_{BULK} (mg/kg)	$Pb_{63\text{-}250µm}$ (mg/kg)	$Pb_{<63µm}$ (mg/kg)
HARRISON DATA (continued)																		
NWIS (USGS)	12413860	12/14/10	10:40	11,700	236	89	26.0	210.0	2126.14	6,250	11,700	13,000	Rising	37	1240	5097		
NWIS (USGS)	12413860	01/18/11	14:45	19,000	611	68	195.5	415.5	2130.2	13,800	18,000	18,800	Rising	48	3480	5617		
NWIS (USGS)	12413860	02/15/11	12:55	2,690	3	104		3.0	2125.02	2,420	2,400	2,430	Steady	8.82	23.9	5027		
NWIS (USGS)	12413860	06/09/11	13:15	9,270	7	80	1.4	5.6	2131.56	10,300	9,730	9,010	Falling	5.06	20.8	2249		
NWIS (USGS)	12413860	07/19/11	12:10	1,350	2	90	0.2	1.8	2128.62	1,420	1,300	1,340	Steady	9.2	23.2	7000		
NWIS (USGS)	12413860	10/04/11	11:25	290	2	93	0.1	1.9	2127.77	355	402	414	Steady	2.73	22	9635		
NWIS (USGS)	12413860	02/08/12	12:30	1,210	7	94	0.4	6.6	2122.66	1,310	1,280	1,190	Falling	13.6	51.8	5457		
NWIS (USGS)	12413860	02/27/12	11:00	2,640	6	89	0.7	5.3	2123.96	2,910	2,540	2,290	Falling	7.04	29.1	3677		
NWIS (USGS)	12413860	03/17/12	14:00	10,000	172	86	24.1	147.9	2126.58	7,290	9,860	9,300	Peak	21.4	864	4899		
NWIS (USGS)	12413860	04/28/12	15:50	19,700	103	24	78.3	24.7	2134.04	20,500	19,900	17,000	Falling	11.8	309	2885		
NWIS (USGS)	12413860	06/28/12	9:45	3,240	12	45	6.6	5.4	2128.5	4,010	3,620	3,390	Falling	6.56	12.6	503		
NWIS (USGS)	12413860	10/10/12	11:20	545	2	56	0.9	1.1	2127.44	575	582	546	Steady	2.94	23.6	10330		
NWIS (USGS)	12413860	11/21/12	11:55	5,070	5	83	0.9	4.2	2125.83	2,460	5,030	5,030	Peak	4.73	37.5	6554		
NWIS (USGS)	12413860	02/04/13	11:20	2,080	3	72	0.8	2.2	2123.59	2,090	1,639	1,522	Falling	5.94	18.9	4320		
NWIS (USGS)	12413860	03/19/13	14:05	6,700	11	83	1.9	9.1	2126.24	7,460	6,780	6,030	Falling	4.95	53.1	4377		
NWIS (USGS)	12413860	04/08/13	11:35	13,500	101	67	33.3	67.7	2129.02	12,900	13,300	12,200	Peak	17.8	616	5923		
NWIS (USGS)	12413860	07/01/13	12:45	1,120	2	87	0.3	1.7	2131.62		1,660			5.02	15.3	5140		
NWIS (USGS)	12413860	10/18/13	11:55	850	3	68	1.0	2.0	2130.3		788			3.39	0.43	-987		
NWIS (USGS)	12413860	12/03/13	11:50	2,760	3	83	0.5	2.5	2128.73		2,600			7.25	28.2	6983		
NWIS (USGS)	12413860	02/05/14	12:00	603	5	87	0.7	4.4	2125.15		699			16.3	57.5	8240		
NWIS (USGS)	12413860	03/11/14	10:45	18,300	313	62	118.9	194.1	2133.24		17,900			34.7	1470	4586		
NWIS (USGS)	12413860	05/19/14	15:15	7,620	4	87	0.5	3.5	2131.85		7,910			3.75	16.8	3263		
NWIS (USGS)	12413860	07/16/14	11:30	1,220	3	91	0.3	2.7	2131.61		1,120			3.76	26.5	7580		
NWIS (USGS)	12413860	02/07/15	13:30	5,730	6	82	1.1	4.9	2129.07		5,790			3.7	34.7	5167		
NWIS (USGS)	12413860	03/16/15	13:30	10,500	116	69	36.0	80.0	2127.91		9,570			18.6	558	4650		
NWIS (USGS)	12413860	06/08/15	10:45	549	4	90	0.4	3.6	2131.21		781			6.46	37.8	7835		
NWIS (USGS)	12413860	10/01/15	11:15	197	2	71	0.6	1.4	2130.28		275			1.71	19.2	8745		
ROSE LAKE DATA																		
BEMP (CH2M HILL)	Rose Lake	05/17/11	13:00	*21,844*	185	14	159.9	25.2	2132.80				Peak			2,510	3,980	2,180
BEMP (CH2M HILL)	Rose Lake	4/1/12	11:00	24,942	94	44	53.1	41.2	2131.27				Peak			1,740	3,050	3,350
BEMP (CH2M HILL)	Rose Lake	4/27/12	10:30	25,531	49	39	30.0	19.2	2133.76				Falling			2,980	3,170	2,470
BEMP (CH2M HILL)	Rose Lake	4/7/13			53	49.9	26.5	26.4	2128.54							3,320	4,830	3,550
BEMP (CH2M HILL)	Rose Lake	3/11/14		25,583	70	29	49.8	20.3								3,410	4,480	4,070
NWIS (USGS)	12413810	03/05/94	10:56	5,240	30				2123.40	3,980	5,120	4,680	Steady		160	5333		
NWIS (USGS)	12413810	03/17/94	11:47	3,800	7				2124.35	2,850	3,670	4,160	Steady		24	3429		
NWIS (USGS)	12413810	04/07/94	11:20	4,800	3				2125.62	4,710	4,470	4,180	Steady		14	4667		
NWIS (USGS)	12413810	04/12/94	13:54	3,840	4				2125.68	3,830	4,120	4,790	Steady					
NWIS (USGS)	12413810	04/19/94	17:02	8,170	36				2126.65	7,400	9,780	10,200	Rising		200	5556		
NWIS (USGS)	12413810	05/10/94	12:45	3,820	2				2128.27	3,580	3,580	3,390	Steady		12	6000		
NWIS (USGS)	12413810	06/16/94	9:18	990	1				2128.72	1,080	1,060	1,030	Steady		7	7000		
NWIS (USGS)	12413810	07/20/94	15:40	538	4				2128.68				Steady		19	4750		
NWIS (USGS)	12413810	08/16/94	14:15	373	3				2128.56				Steady		32	10667		
NWIS (USGS)	12413810	09/19/94	17:21	253	1				2128.07				Steady		10	10000		
NWIS (USGS)	12413810	04/21/99	14:30	13,200	30				2128.16	10,983[b]	11,619[b]	10,277[b]	Peak	2	66.8	2160		
NWIS (USGS)	12413810	02/07/15	10:30	7,430	11	84	1.8	9.2	2129.05					1.67	33.4	2885		
NWIS (USGS)	12413810	03/16/15	10:55	15,000	85	70	25.5	59.5	2127.78					7.23	132	1468		
NWIS (USGS)	12413810	06/08/15	8:10	837	2	80	0.4	1.6	2131.19					3.98	9.82	2920		
NWIS (USGS)	12413810	10/01/15	8:15	250	1	92	0.1	0.9	2130.29					1.47	9.92	8450		

Attachment A. **Summary of BEMP and USGS Sample Data (Suspended Sediment Concentration, Grain Size, and Lead Concentrations)**
Processes of Sediment and Lead Transport, Erosion, and Deposition
Lower Basin Coeur d'Alene River (OU3)

Sampler	Station	Date	Time	Discharge (cfs)	SSC (mg/L)	Percent Fines	SSC - sand (mg/L)	SSC - fines (mg/L)	Lake Level (ft NAVD88)	Flow, day before measurement (cfs)	Mean Flow, day of measurement (cfs)	Flow, day after measurement (cfs)	Rising, Falling,Peak, or Steady[a]	$Pb_{FILTERED}$ (µg/L)	$Pb_{UNFILTERED}$ (µg/L)	Pb^{c}_{BULK} (mg/kg)	$Pb_{63\text{-}250µm}$ (mg/kg)	$Pb_{<63µm}$ (mg/kg)
ROSE LAKE DATA (continued)																		
NWIS (USGS)	12413810	04/23/16	9:40	7,550	5	86	0.7	4.3	2130.61					1.24	15	2752		
NWIS (USGS)	12413810	05/23/16	11:15	2,950	2	68	0.6	1.4	2131.68					1.17	4.85	1840		
NWIS (USGS)	12413810	05/25/16	17:15	3,400	20	24	15.2	4.8	2131.72					1.06	48.5	2372		
CATALDO DATA																		
BEMP (USGS)	Cataldo	05/18/08	15:45	29,600	140				2132.14	24,400	28,400	31,200	Rising			1,130		
BEMP (CH2M HILL)	Cataldo	12/14/10	14:00	18,500	26.8	84	4.3	22.6	2126.14	10,000	17,900	15,500	Peak			966		888
BEMP (CH2M HILL)	Cataldo	01/18/11	10:30	28,800	108	50	53.8	54.6	2130.20	27,800	27,800	16,200	Peak			790	983	651
BEMP (CH2M HILL)	Cataldo	05/16/11	12:00	22,300	59.5	67	19.6	39.9	2132.00	20,000	22,200	19,900	Peak			662	1,040	754
BEMP (CH2M HILL)	Cataldo	3/31/12	10:45	28,900	95	68	30.0	64.9	2130.20	13,800	27,300	20,400	Peak			886	1230	748
BEMP (CH2M HILL)	Cataldo	4/12/12	14:00	11,200	13	51	6.5	6.7	2129.05	6,110	10,300	12,300	Rising			1400		
BEMP (CH2M HILL)	Cataldo	4/24/12	12:00	24,500	73	74	18.9	54.1	2131.58	19,000	24,000	25,700	Rising			1030	1540	1070
BEMP (CH2M HILL)	Cataldo	4/26/12	9:30	22,800	37				2133.20	25,700	22,700	22,000	Falling			1840		1690
BEMP (CH2M HILL)	Cataldo	4/6/13	17:00	17,400	44	53	20.5	23.6	2127.92	11,000	16,300	18,100	Rising			784	1080	874
NWIS (USGS)	12413500	11/12/86	12:00	451	3	49	1.5	1.5	2124.24	442	451	440	Steady					
NWIS (USGS)	12413500	01/27/87	10:30	598	2	50	1.0	1.0	2122.08	602	602	616	Steady					
NWIS (USGS)	12413500	03/31/87	11:00	2,310	2	53	0.9	1.1	2126.06	2,360	2,290	2,340	Steady					
NWIS (USGS)	12413500	05/15/87	10:30	2,630	3	52	1.4	1.6	2127.87	2,880	2,590	2,360	Steady					
NWIS (USGS)	12413500	07/07/87	10:00	722	1	76	0.2	0.8	2128.67	757	719	667	Steady					
NWIS (USGS)	12413500	09/02/87	10:30	312	1	82	0.2	0.8	2128.66	322	309	305	Steady					
NWIS (USGS)	12413500	11/24/87	9:00	362	1	89	0.1	0.9	2125.20	357	366	370	Steady					
NWIS (USGS)	12413500	01/13/88	11:00	339	1	72	0.3	0.7	2122.00	343	340	359	Steady					
NWIS (USGS)	12413500	03/24/88	11:00	3,070	7	67	2.3	4.7	2124.15	2,760	3,250	3,210	Steady					
NWIS (USGS)	12413500	05/25/88	11:00	2,420	1	76	0.2	0.8	2128.80	2,440	2,270	2,020	Steady					
NWIS (USGS)	12413500	07/13/88	10:30	604	3	65	1.1	2.0	2128.69	606	606	703	Steady					
NWIS (USGS)	12413500	11/29/88	11:00	903	1	87	0.1	0.9	2125.36	995	906	854	Steady					
NWIS (USGS)	12413500	01/20/89	11:30	1,580	2	89	0.2	1.8	2122.91	1,660	1,570	1,440	Steady					
NWIS (USGS)	12413500	03/09/89	11:30	1,500	4	86	0.6	3.4	2123.05	1,330	1,510	3,770	Rising					
NWIS (USGS)	12413500	06/01/89	10:30	3,930	2	83	0.3	1.7	2128.61	4,270	4,020	4,110	Steady					
NWIS (USGS)	12413500	07/06/89	11:00	915	1	82	0.2	0.8	2128.74	922	901	870	Steady					
NWIS (USGS)	12413500	08/31/89	12:00	572	1	76	0.2	0.8	2128.66	613	574	543	Steady					
NWIS (USGS)	12413500	11/02/89	13:00	492	1	75	0.3	0.8	2125.56	509	493	493	Steady					
NWIS (USGS)	12413500	01/16/90	13:00	4,470	4	82	0.7	3.3	2128.56	5,130	4,490	4,010	Falling					
NWIS (USGS)	12413500	03/08/90	11:00	4,090	7	80	1.4	5.6	2125.76	3,370	3,960	4,320	Rising					
NWIS (USGS)	12413500	05/22/90	10:00	4,240	2	80	0.4	1.6	2127.53	4,300	4,260	4,980	Steady					
NWIS (USGS)	12413500	07/13/90	10:30	1,080	1	86	0.1	0.9	2128.66	1,150	1,100	1,060	Steady					
NWIS (USGS)	12413500	09/05/90	11:00	449	3	39	1.8	1.2	2128.57	454	450	443	Steady					
NWIS (USGS)	12413500	11/01/90	14:30	1,520	9	75	2.3	6.8	2126.03	1,080	1,530	1,260	Steady					
NWIS (USGS)	12413500	01/04/91	11:30	1,090	2	80	0.4	1.6	2124.58	1,310	1,170	1,110	Steady					
NWIS (USGS)	12413500	03/11/91	10:00	3,780	7	81	1.3	5.7	2127.97	3,940	3,630	3,300	Steady					
NWIS (USGS)	12413500	05/08/91	9:00	5,690	8	67	2.6	5.4	2127.74	4,720	6,030	8,650	Rising					
NWIS (USGS)	12413500	07/16/91	11:00	1,280	1	16	0.8	0.2	2128.64	1,280	1,240	1,220	Steady					
NWIS (USGS)	12413500	09/11/91	11:30	473	2	84	0.3	1.7	2128.59	462	457	455	Steady					
NWIS (USGS)	12413500	11/08/91	8:45	472	3	35	2.0	1.1	2125.57	470	471	521	Steady					
NWIS (USGS)	12413500	01/15/92	8:30	466	3	13	2.6	0.4	2122.67	476	464	482	Steady					
NWIS (USGS)	12413500	03/25/92	10:00	2,480	6	70	1.8	4.2	2125.56	2,620	2,460	2,420	Steady					
NWIS (USGS)	12413500	05/20/92	9:30	1,540	3	72	0.8	2.2	2128.72	1,420	1,490	1,470	Steady					
NWIS (USGS)	12413500	07/09/92	9:00	615	2	40	1.2	0.8	2128.68	615	622	644	Steady					

Attachment A. **Summary of BEMP and USGS Sample Data (Suspended Sediment Concentration, Grain Size, and Lead Concentrations)**
Processes of Sediment and Lead Transport, Erosion, and Deposition
Lower Basin Coeur d'Alene River (OU3)

Sampler	Station	Date	Time	Discharge (cfs)	SSC (mg/L)	Percent Fines	SSC - sand (mg/L)	SSC - fines (mg/L)	Lake Level (ft NAVD88)	Flow, day before measurement (cfs)	Mean Flow, day of measurement (cfs)	Flow, day after measurement (cfs)	Rising, Falling,Peak, or Steady[a]	$Pb_{FILTERED}$ (µg/L)	$Pb_{UNFILTERED}$ (µg/L)	Pb^{c}_{BULK} (mg/kg)	$Pb_{63\text{-}250µm}$ (mg/kg)	$Pb_{<63µm}$ (mg/kg)
CATALDO DATA (continued)																		
NWIS (USGS)	12413500	09/10/92	17:00	408	1	76	0.2	0.8	2128.75	403	409	407	Steady					
NWIS (USGS)	12413500	11/17/92	12:00	636	1	65	0.4	0.7	2126.08	644	627	627	Steady					
NWIS (USGS)	12413500	01/20/93	11:00	391	1	75	0.3	0.8	2121.78	379	396	443	Steady		6	6000		
NWIS (USGS)	12413500	09/22/93	8:35	465	2	77	0.5	1.5	2127.97	482	482	482	Steady		10	5000		
NWIS (USGS)	12413500	10/21/93	10:20	481					2126.15	506	486	473	Steady		6			
NWIS (USGS)	12413500	11/19/93	9:44	386	1	74	0.3	0.7	2124.91	384	380	377	Steady		8	8000		
NWIS (USGS)	12413500	12/14/93	8:10	739	1	83	0.2	0.8	2124.27	776	740	702	Steady		10	10000		
NWIS (USGS)	12413500	01/19/94	10:10	1,360	1	78	0.2	0.8	2123.31	1,500	1,360	1,230	Steady		6	6000		
NWIS (USGS)	12413500	02/15/94	12:00	612	1	93	0.1	0.9	2122.28	628	607	598	Steady		4	4000		
NWIS (USGS)	12413500	03/06/94	9:30	4,630	8	74	2.1	5.9	2123.76	5,130	4,520	3,670	Falling		24	3000		
NWIS (USGS)	12413500	03/16/94	9:10	2,490	22	33	14.7	7.3	2124.22	2,040	2,590	3,490	Rising		8	364		
NWIS (USGS)	12413500	04/05/94	12:30	5,040	6	73	1.6	4.4	2125.40	4,870	4,950	4,600	Steady		15	2500		
NWIS (USGS)	12413500	04/13/94	13:15	4,610	5	76	1.2	3.8	2125.77	3,970	4,770	5,110	Rising		30	6000		
NWIS (USGS)	12413500	04/19/94	13:05	8,270	30	74	7.8	22.2	2126.65	6,840	8,610	9,180	Rising		61	2033		
NWIS (USGS)	12413500	05/11/94	17:00	3,120	2	72	0.6	1.4	2128.41	3,370	3,120	2,930	Falling		14	7000		
NWIS (USGS)	12413500	06/15/94	13:45	1,000					2128.71	999	1,000	978	Steady		5			
NWIS (USGS)	12413500	07/21/94	12:40	429	1	64	0.4	0.6	2128.68	437	431	418	Steady		5	5000		
NWIS (USGS)	12413500	08/17/94	11:44	278	1	59	0.4	0.6	2128.55	301	301	301	Steady		13	13000		
NWIS (USGS)	12413500	09/21/94	8:30	263	1	73	0.3	0.7	2127.95	255	249	244	Steady		7	7000		
NWIS (USGS)	12413500	04/15/02	16:15	3,100	123	94	7.4	115.6	2132.26	27,900	33,000	19,800	Peak	1.74	107	856		
NWIS (USGS)	12413500	04/17/02	8:15	13,300	29	88	3.5	25.5	2133.39	19,800	12,800	9,610	Falling	1.11	34.7	1158		
NWIS (USGS)	12413500	10/17/07	9:40	323	2	58	0.8	1.2	2126.93	310	321	338	Steady	0.961	2.92	980		
NWIS (USGS)	12413500	12/05/07	8:00	4,480	21	68	6.7	14.3	2124.89	3,090	4,350	3,190	Steady	0.838	48.1	2251		
NWIS (USGS)	12413500	01/29/08	14:00	654	1	71	0.3	0.7	2122.23	631	632	617	Steady		1.65	1650		
NWIS (USGS)	12413500	05/07/08	13:45	15,500	42	84	6.7	35.3	2129.19	14,000	16,300	15,200	Peak	0.947	67.4	1582		
NWIS (USGS)	12413500	05/18/08	15:15	29,000	191	93	13.4	177.6	2132.14	24,400	28,400	31,200	Rising	2.82	238	1231		
NWIS (USGS)	12413500	06/26/08	13:30	3,490	4	71	1.2	2.8	2128.73	3,870	3,500	3,240	Steady	1.9	10.7	2200		
NWIS (USGS)	12413500	08/11/08	12:30	578	2	43	1.1	0.9	2128.72	613	602	593	Steady	1.86	3.21	675		
NWIS (USGS)	12413500	09/15/08	10:30	407	1	83	0.2	0.8	2128.41	415	407	399	Steady	1.99	3.97	1980		
NWIS (USGS)	12413500	03/30/10	14:31	8,360	37	89	4.1	32.9	2123.86	2,890	7,200	6,870	Peak	0.792	61.9	1652		
NWIS (USGS)	12413500	04/22/10	12:20	7,720	31	47	16.4	14.6	2125.78	6,670	7,220	6,250	Peak	0.513	68.2	2183		
NWIS (USGS)	12413500	07/06/10	12:00	1,610	2	57	0.9	1.1	2128.69	1,760	1,680	1,570	Steady	0.753	2.32	784		
NWIS (USGS)	12413500	10/07/10	14:15	401	1	56	0.4	0.6	2127.45	420	402	418	Steady	0.755	2.31	1555		
NWIS (USGS)	12413500	01/16/11	15:15	13,500	41	73	11.1	29.9	2126.63	9,690	13,100	27,800	Rising	1.2	61.2	1463		
NWIS (USGS)	12413500	06/08/11	15:10	9,740	8	76	1.9	6.1	2131.55	10,800	9,880	8,640	Falling	0.999	14.9	1738		
NWIS (USGS)	12413500	07/13/11	13:00	1,960	3	50	1.5	1.5	2128.63	1,950	1,960	1,900	Steady	1.23	6.34	1703		
NWIS (USGS)	12413500	02/24/12	13:20	2,790	3	80	0.6	2.4	2123.77	3,550	2,870	2,540	Falling	0.67	7.19	2173		
NWIS (USGS)	12413500	04/27/12	14:15	22,500	39	94	2.3	36.7	2133.76	22,700	22,000	17,200	Falling	1.21	28.1	689		
NWIS (USGS)	12413500	06/27/12	11:30	3,660	17	28	12.2	4.8	2128.47	3,450	3,630	3,200	Peak	1.35	12.5	656		
NWIS (USGS)	12413500	10/01/12	14:45	351	4	64	1.4	2.6	2127.84	351	351	349	Steady	0.918	2.53	403		
NWIS (USGS)	12413500	03/18/13	11:50	7,620	5	75	1.3	3.8	2126.1	8,540	7,670	6,160	Falling	0.552	11.1	2110		
NWIS (USGS)	12413500	04/06/13	18:30	17,900	53	86	7.4	45.6	2127.92	11,100	16,300	18,100	Rising	0.65	37.1	688		
NWIS (USGS)	12413500	06/26/13	14:20	1,840	1	67	0.3	0.7	2131.59		1,860			0.95	2.95	2000		
NWIS (USGS)	12413500	10/22/13	13:00	401	1	62	0.4	0.6	2129.91		401			0.535	1.65	1115		
NWIS (USGS)	12413500	03/07/14	11:40	14,800	42	77	9.7	32.3	2128.74		14,400			0.832	43	1004		
NWIS (USGS)	12413500	05/17/14	10:25	8,850	9	81	1.7	7.3	2131.62		8,710			0.781	19.1	2035		
NWIS (USGS)	12413500	07/07/14	12:30	1,100	2	53	0.9	1.1	2131.59		781			0.972	3.26	1144		
NWIS (USGS)	12413500	10/06/14	11:45	328	< 0.5	67			2130.14		327			0.583	1.79			
NWIS (USGS)	12413500	02/07/15	8:45		13	75	3.3	9.8	2129.03		7,900			0.747	37.9	2858		
NWIS (USGS)	12413500	03/16/15	8:30	15,800	55	84	8.8	46.2	2127.68		16,200			1.38	52.8	935		
NWIS (USGS)	12413500	06/02/15	13:20	1,040	3	62	1.1	1.9	2131.27		1,020			1.12	3.12	667		
NWIS (USGS)	12413500	02/16/16	11:05	14,800	31	81	5.9	25.1	2128.61		14,500			0.939	34.1	1070		
NWIS (USGS)	12413500	04/23/16	14:08	6,930	5	69	1.6	3.5	2130.64		6,830			0.535	11.2	2133		

Attachment A. **Summary of BEMP and USGS Sample Data (Suspended Sediment Concentration, Grain Size, and Lead Concentrations)**
Processes of Sediment and Lead Transport, Erosion, and Deposition
Lower Basin Coeur d'Alene River (OU3)

Sampler	Station	Date	Time	Discharge (cfs)	SSC (mg/L)	Percent Fines	SSC - sand (mg/L)	SSC - fines (mg/L)	Lake Level (ft NAVD88)	Flow, day before measurement (cfs)	Mean Flow, day of measurement (cfs)	Flow, day after measurement (cfs)	Rising, Falling,Peak, or Steady[a]	$Pb_{FILTERED}$ (µg/L)	$Pb_{UNFILTERED}$ (µg/L)	Pb^{c}_{BULK} (mg/kg)	$Pb_{63\text{-}250µm}$ (mg/kg)	$Pb_{<63µm}$ (mg/kg)
CATALDO DATA (continued)																		
NWIS (USGS)	12413500	05/23/16	13:15	2,820	2	86	0.3	1.7	2131.68		2,840							
PINEHURST DATA																		
BEMP (USGS)	Pinehurst	05/18/08	12:00	6,210	270					5,310	6,190	6,020	Peak			2,660		
BEMP (USGS)	Pinehurst	05/19/09	17:30	3,430	26					2,430	3,310	2,780	Peak			3,440		
BEMP (CH2M HILL)	Pinehurst	12/14/10	10:00	1,900	23	46	12.5	10.7		1,110	1,890	1,380	Peak			2,730	3,030	2,170
BEMP (CH2M HILL)	Pinehurst	01/17/11	16:00	5,840	164	85	24.1	139.6		2,640	5,420	4,030	Peak			1,440		1,480
BEMP (CH2M HILL)	Pinehurst	05/16/11	12:00	4,660	97	63	36.0	61.3		4,370	4,540	3,520	Peak			2,940	3,360	2,610
BEMP (CH2M HILL)	Pinehurst	3/31/12	11:45	5,360	189	78	41.9	147.6		4,270	5,390	3,730	Peak			1,410	2,000	1,380
BEMP (CH2M HILL)	Pinehurst	4/26/12		4,250	34					4,710	4,250	3,930	Falling			2,490		
BEMP (CH2M HILL)	Pinehurst	4/6/13	10:00	2,640	33					2,260	2,780	2,620	Steady			2,340		
NWIS (USGS)	12413470	07/12/89	10:15	211	3					215	205	218	Steady					
NWIS (USGS)	12413470	08/10/89	12:00	153	11	90	1.1	9.9		160	140	130	Steady					
NWIS (USGS)	12413470	09/20/89	14:00	130	6					146	128	115	Steady					
NWIS (USGS)	12413470	11/20/89	14:00	406	3					401	415	427	Steady					
NWIS (USGS)	12413470	03/22/90	11:00	1,290	13					1,220	1,290	1,150	Peak					
NWIS (USGS)	12413470	05/17/90	10:00	867	3					918	902	925	Steady					
NWIS (USGS)	12413470	09/18/90	11:00	136	5					135	134	129	Steady					
NWIS (USGS)	12413470	11/14/90	12:00	468	8	91	0.7	7.3		457	472	411	Steady					
NWIS (USGS)	12413470	03/19/91	12:00	548	2					553	558	593	Steady					
NWIS (USGS)	12413470	05/21/91	13:30	2,540	144					2,610	2,590	2,310	Falling					
NWIS (USGS)	12413470	09/11/91	14:30	125	4					126	123	122	Steady					
NWIS (USGS)	12413470	11/07/91	10:20	117	24					145	128	125	Steady					
NWIS (USGS)	12413470	03/24/92	15:30	452	3					475	455	449	Steady					
NWIS (USGS)	12413470	05/19/92	15:30	526	3					506	527	571	Steady					
NWIS (USGS)	12413470	09/09/92	16:30	103	6					118	118	108	Steady					
NWIS (USGS)	12413470	09/09/92	17:15	103	6					118	118	108	Steady					
NWIS (USGS)	12413470	11/18/92	11:00	85	3					147	145	142	Steady					
NWIS (USGS)	12413470	01/19/93	11:50	88	7	84	1.1	5.9		89	84	102	Steady					
NWIS (USGS)	12413470	01/21/93	8:20	139	13	76	3.1	9.9		102	136	131	Steady			78	6000	
NWIS (USGS)	12413470	03/23/93		852	41					703	1,110	1,960	Rising	6		160	3756	
NWIS (USGS)	12413470	09/21/93	13:30	123	2					119	122	116	Steady	1		22	10500	
NWIS (USGS)	12413470	10/18/93	13:43	130	2	62	0.8	1.2		126	125	120	Steady			18	9000	
NWIS (USGS)	12413470	10/28/93	16:45	101	10	40	6.0	4.0		101	101	100	Steady					
NWIS (USGS)	12413470	11/17/93	9:55	96	2	62	0.8	1.2		92	96	98	Steady			14	7000	
NWIS (USGS)	12413470	12/14/93	11:20	175	2	66	0.7	1.3		169	166	161	Steady			18	9000	
NWIS (USGS)	12413470	01/19/94	10:10	223	2	74	0.5	1.5		246	227	215	Steady			17	8500	
NWIS (USGS)	12413470	02/15/94	16:05	120	2	91	0.2	1.8		120	117	119	Steady			15	7500	
NWIS (USGS)	12413470	03/06/94	12:00	698	6	64	2.2	3.8		846	693	580	Falling			32	5333	
NWIS (USGS)	12413470	03/16/94	11:30	483	3	79	0.6	2.4		388	484	552	Steady	5		17	4000	
NWIS (USGS)	12413470	04/05/94	9:40	672	5	58	2.1	2.9		713	675	632	Steady			26	5200	
NWIS (USGS)	12413470	04/20/94	16:30	1,840	29	54	13.3	15.7		1,710	1,810	1,840	Rising			130	4483	
NWIS (USGS)	12413470	05/12/94	9:20	1,070	7	48	3.6	3.4		1,080	1,060	958	Falling			26	3714	
NWIS (USGS)	12413470	05/26/94	10:30	488	1	55	0.5	0.6		497	486	471	Steady	7		19	12000	
NWIS (USGS)	12413470	06/15/94	8:30	268	1	46	0.5	0.5		272	266	257	Steady			14	14000	
NWIS (USGS)	12413470	07/19/94	9:55	119	2	63	0.7	1.3		120	120	116	Steady			16	8000	
NWIS (USGS)	12413470	08/18/94	13:06	79	2	69	0.6	1.4		79	78	73	Steady			26	13000	
NWIS (USGS)	12413470	09/23/94	8:20	75	3	60	1.2	1.8		71	75	77	Steady	9		24	5000	
NWIS (USGS)	12413470	11/21/94	13:45	124	1	72	0.3	0.7		127	120	106	Steady	5				
NWIS (USGS)	12413470	03/29/95	12:30	741	3	89	0.3	2.7		788	743	708	Steady	9				
NWIS (USGS)	12413470	05/08/95	12:40	1,120	6	65	2.1	3.9		1,020	1,050	1,100	Steady	8				

Attachment A. **Summary of BEMP and USGS Sample Data (Suspended Sediment Concentration, Grain Size, and Lead Concentrations)**
Processes of Sediment and Lead Transport, Erosion, and Deposition
Lower Basin Coeur d'Alene River (OU3)

Sampler	Station	Date	Time	Discharge (cfs)	SSC (mg/L)	Percent Fines	SSC - sand (mg/L)	SSC - fines (mg/L)	Lake Level (ft NAVD88)	Flow, day before measurement (cfs)	Mean Flow, day of measurement (cfs)	Flow, day after measurement (cfs)	Rising, Falling,Peak, or Steady[a]	$Pb_{FILTERED}$ (µg/L)	$Pb_{UNFILTERED}$ (µg/L)	Pb^{c}_{BULK} (mg/kg)	$Pb_{63\text{-}250µm}$ (mg/kg)	$Pb_{<63µm}$ (mg/kg)
PINEHURST DATA (continued)																		
NWIS (USGS)	12413470	09/20/95	13:15	134	6	96	0.2	5.8		129	133	131	Steady	2				
NWIS (USGS)	12413470	04/15/96	12:55	909	9					1,680	1,400	1,160	Falling					
NWIS (USGS)	12413470	05/16/96	11:45	1,820	38					1,860	1,800	1,690	Falling					
NWIS (USGS)	12413470	06/13/96	11:45	691	4					726	687	666	Steady					
NWIS (USGS)	12413470	07/15/96	12:00	254	4					258	250	245	Steady					
NWIS (USGS)	12413470	08/13/96	13:00	150	2					144	150	150	Steady					
NWIS (USGS)	12413470	09/06/96	8:00	142	18					129	138	128	Steady					
NWIS (USGS)	12413470	04/10/97	11:15	710	5	99	0.1	5.0		740	721	690	Steady	4	39.8	7160		
NWIS (USGS)	12413470	05/21/97	10:45	2,550	100					2,650	2,520	2,320	Falling	1	246	2450		
NWIS (USGS)	12413470	06/12/97	12:00	1,790	50					1,890	1,790	1,580	Falling	5	258	5060		
NWIS (USGS)	12413470	07/22/97	12:30	344	5					352	342	325	Steady	12	29.8	3560		
NWIS (USGS)	12413470	08/20/97	13:20	179	9					185	178	173	Steady					
NWIS (USGS)	12413470	09/17/97	12:25	172	24					185	185	199	Steady	5	134	5375		
NWIS (USGS)	12413470	04/21/98	7:30	589	2	100		2.0		548	595	813	Rising	4	23.6	9800		
NWIS (USGS)	12413470	05/18/98	14:00	670	7	100		7.0		763	700	650	Falling	5	37.3	4614		
NWIS (USGS)	12413470	06/11/98	8:45	561	3	100		3.0		574	549	521	Steady					
NWIS (USGS)	12413470	07/07/98	12:15	249	3	100		3.0		252	244	239	Steady	11	22.8	3933		
NWIS (USGS)	12413470	08/19/98	9:30	120	7	100		7.0		120	119	121	Steady					
NWIS (USGS)	12413470	09/15/98	11:40	100	5					101	99	96	Steady					
NWIS (USGS)	12413470	11/04/98	12:00	105	38					98	96	101	Steady	11.6	267	6721		
NWIS (USGS)	12413470	12/09/98	12:10	275	3					317	276	249	Steady	3	33.9	10300		
NWIS (USGS)	12413470	02/03/99	11:00	322	1					320	314	310	Steady					
NWIS (USGS)	12413470	03/17/99	10:00	748	2	72	0.6	1.4		787	726	664	Steady	2.46	20	8770		
NWIS (USGS)	12413470	03/23/99	13:30	1,610	15	70	4.5	10.5		1,770	1,700	1,660	Falling	3.41	85	5439		
NWIS (USGS)	12413470	04/13/99	7:30	610	3					570	608	614	Steady	4	21.3	5767		
NWIS (USGS)	12413470	04/20/99	12:00	2,060	27	68	8.6	18.4		1,960	2,100	1,950	Peak	5.34	164	5876		
NWIS (USGS)	12413470	05/06/99	13:30	1,160	7	100		7.0		1,300	1,180	1,220	Falling	4.96	44.4	5634		
NWIS (USGS)	12413470	05/25/99	12:45	4,190	207	80	41.4	165.6		3,130	4,050	3,740	Peak	4.62	790	3794		
NWIS (USGS)	12413470	05/27/99	12:45	2,730	89	79	18.7	70.3		3,740	2,790	2,740	Falling	2.78	350	3901		
NWIS (USGS)	12413470	06/02/99	7:45	2,160	31					2,150	2,130	2,000	Falling	3.63	128	4012		
NWIS (USGS)	12413470	06/29/99	13:00	983	7	70	2.1	4.9		1,070	973	939	Falling					
NWIS (USGS)	12413470	07/15/99	12:00	508	3					535	501	464	Steady	6.68	28.6	7307		
NWIS (USGS)	12413470	07/26/99	13:15	326	2	69	0.6	1.4		335	318	304	Steady	8.72	22.1	6690		
NWIS (USGS)	12413470	08/09/99	14:15	237	2					297	237	220	Steady	7.89	25.8	8955		
NWIS (USGS)	12413470	09/07/99	14:30	140	1					140	140	135	Steady	4.5	18.6	14100		
NWIS (USGS)	12413470	10/19/99	14:00	107	1	67	0.3	0.7		107	105	105	Steady	6.29	18.6	12310		
NWIS (USGS)	12413470	01/11/00	14:30	237	1	75	0.3	0.8		249	241	239	Steady	3.79	13.3	9510		
NWIS (USGS)	12413470	02/28/00	11:00	596	1	75	0.3	0.8		543	604	680	Steady	2.74	12.9	10160		
NWIS (USGS)	12413470	03/27/00	13:20	700	2	55	0.9	1.1		746	737	960	Rising	3.75	18.7	7475		
NWIS (USGS)	12413470	03/28/00	11:00	948	59					737	960	980	Rising	3.14	32.6	499		
NWIS (USGS)	12413470	04/10/00	13:15	1,290	5	77	1.2	3.9		915	1,150	1,590	Rising	2.6	25.8	4640		
NWIS (USGS)	12413470	04/14/00	13:15	4,890	302	74	78.5	223.5		2,370	4,630	3,560	Peak	3.13	630	2076		
NWIS (USGS)	12413470	04/17/00	13:15	2,360	17	76	4.1	12.9		2,740	2,380	2,380	Neither	3.23	72.8	4092		
NWIS (USGS)	12413470	05/02/00	11:45	1,890	11	68	3.5	7.5		1,390	1,840	2,040	Rising	3.79	53.6	4528		
NWIS (USGS)	12413470	05/10/00	13:20	1,340	9	100		9.0		1,250	1,340	1,260	Peak					
NWIS (USGS)	12413470	05/18/00	10:00	1,890	8	75	2.0	6.0		1,500	1,660	1,610	Peak	3.84	39.5	4458		
NWIS (USGS)	12413470	06/02/00	9:30	1,110	3	65	1.1	2.0		1,120	1,040	1,030	Falling	4.39	17.6	4403		
NWIS (USGS)	12413470	06/15/00	9:55	934	4	100		4.0		974	920	846	Falling					
NWIS (USGS)	12413470	06/29/00	11:30	446	2	83	0.3	1.7		407	390	377	Steady	5.57	17.1	5765		
NWIS (USGS)	12413470	07/19/00	12:30	202	2					206	198	191	Steady					
NWIS (USGS)	12413470	07/24/00	13:00	241	1	67	0.3	0.7		180	179	174	Steady	5.77	15.2	9430		
NWIS (USGS)	12413470	08/08/00	12:00	134	1					137	134	132	Steady					
NWIS (USGS)	12413470	08/31/00	12:15	110	4	88	0.5	3.5		110	109	118	Steady	6.16	17.4	2810		

Attachment A. **Summary of BEMP and USGS Sample Data (Suspended Sediment Concentration, Grain Size, and Lead Concentrations)**
Processes of Sediment and Lead Transport, Erosion, and Deposition
Lower Basin Coeur d'Alene River (OU3)

Sampler	Station	Date	Time	Discharge (cfs)	SSC (mg/L)	Percent Fines	SSC - sand (mg/L)	SSC - fines (mg/L)	Lake Level (ft NAVD88)	Flow, day before measurement (cfs)	Mean Flow, day of measurement (cfs)	Flow, day after measurement (cfs)	Rising, Falling,Peak, or Steady[a]	$Pb_{FILTERED}$ (µg/L)	$Pb_{UNFILTERED}$ (µg/L)	Pb^{c}_{BULK} (mg/kg)	$Pb_{63\text{-}250µm}$ (mg/kg)	$Pb_{<63µm}$ (mg/kg)
PINEHURST DATA (continued)																		
NWIS (USGS)	12413470	09/07/00	7:35	115	10					117	114	117	Steady					
NWIS (USGS)	12413470	11/06/00	13:30	120	1	75	0.3	0.8		134	120	113	Steady	5.61	15.7	10090		
NWIS (USGS)	12413470	12/18/00	12:00	94	2	82	0.4	1.6		104	92	91	Steady	4.45	17.1	6325		
NWIS (USGS)	12413470	01/23/01	14:30	86	1	75	0.3	0.8		95	92	88	Steady	5.19	12.5	7310		
NWIS (USGS)	12413470	03/14/01	11:45	247	5	81	1.0	4.1		206	247	233	Steady	4.36	31.5	5428		
NWIS (USGS)	12413470	04/10/01	11:00	260	2	71	0.6	1.4		264	259	255	Steady	5.11	14.6	4745		
NWIS (USGS)	12413470	04/10/01	11:15	260	4					264	259	255	Steady	5.11	14.6	2373		
NWIS (USGS)	12413470	05/01/01	14:00	1,470	21					1,120	1,460	1,170	Peak	2.98	68.1	3101		
NWIS (USGS)	12413470	05/03/01	13:00	909	3	81	0.6	2.4		1,170	922	806	Falling	3.16	29.9	8913		
NWIS (USGS)	12413470	06/12/01	12:30	385	2	86	0.3	1.7		368	384	377	Steady	4.9	12.5	3800		
NWIS (USGS)	12413470	06/25/01	15:45	251	1					252	251	239	Steady	6.78	13.4	6620		
NWIS (USGS)	12413470	07/24/01	10:40	133	2					138	132	131	Steady					
NWIS (USGS)	12413470	08/06/01	15:05	108	2					115	111	109	Steady	6.82	15.5	4340		
NWIS (USGS)	12413470	09/10/01	11:15	81	4					81	80	76	Steady					
NWIS (USGS)	12413470	04/02/02	9:45	867	4					797	857	823	Steady					
NWIS (USGS)	12413470	04/15/02	13:45	4,650	220	85	33.0	187.0		6,390	4,750	2,840	Falling	2.8	576	2605		
NWIS (USGS)	12413470	04/16/02	16:45	2,560	74	76	17.8	56.2		4,750	2,840	1,920	Falling	2.54	209	2790		
NWIS (USGS)	12413470	05/01/02	10:30	1,540	18					1,160	1,530	1,710	Rising					
NWIS (USGS)	12413470	06/11/02	16:00	1,180	12					1,280	1,190	1,220	Steady	6.07	47.9	3486		
NWIS (USGS)	12413470	07/08/03	14:20	195	2					184	187	181	Steady					
NWIS (USGS)	12413470	08/18/03	14:45	102	2					105	101	100	Steady	6.28	12.7	3210		
NWIS (USGS)	12413470	09/08/03	12:10	97	3					86	97	112	Steady					
NWIS (USGS)	12413470	10/08/03	9:20	88	5					84	87	89	Steady	5.17	9.61	888		
NWIS (USGS)	12413470	12/06/03	12:47	470	28					242	445	439	Steady	1.25	89.7	3159		
NWIS (USGS)	12413470	01/21/04	14:05	164	5					166	166	163	Steady	2.56	7.07	902		
NWIS (USGS)	12413470	03/31/04	15:35	904	5					650	871	861	Steady	3.3	36.8	6700		
NWIS (USGS)	12413470	05/05/04	10:00	1,260	6					1,360	1,250	1,090	Falling	1.64	25.8	4027		
NWIS (USGS)	12413470	06/10/04	15:30	679	1					692	671	663	Steady	3.49	8.3	4810		
NWIS (USGS)	12413470	07/27/04	14:15	177						169	166	164	Steady	3.95	8.4			
NWIS (USGS)	12413470	09/07/04	14:00	145	1					147	142	139	Steady	4.22	7.66	3440		
NWIS (USGS)	12413470	10/13/04	14:10	133	2					140	134	131	Steady	3.3	6.43	1565		
NWIS (USGS)	12413470	12/12/04	13:30	1,890	17					2,000	2,020	1,270	Peak	0.888	36.7	2107		
NWIS (USGS)	12413470	02/24/05	14:35	268	1	60	0.4	0.6		269	264	260	Steady	3.15	6.17	3020		
NWIS (USGS)	12413470	03/29/05	12:23	1,620	14	60	5.6	8.4		2,480	1,690	1,260	Falling	1.36	22	1474		
NWIS (USGS)	12413470	05/17/05	14:30	860	7	29	5.0	2.0		779	855	800	Steady	2.58	13.2	1517		
NWIS (USGS)	12413470	06/21/05	15:00	277	1	67	0.3	0.7		274	263	250	Steady	3.32	6.16	2840		
NWIS (USGS)	12413470	08/10/05	15:00	114	2	62	0.8	1.2		113	111	111	Steady	4.18	6.39	1105		
NWIS (USGS)	12413470	10/19/05	13:15	114	1	85	0.2	0.9		110	111	118	Steady	2.89	5	2110		
NWIS (USGS)	12413470	01/05/06	11:00	646	1	82	0.2	0.8		725	642	588	Steady	1.92	7.54	5620		
NWIS (USGS)	12413470	02/15/06	8:45	368	2	69	0.6	1.4		395	374	361	Steady	1.61	7.61	3000		
NWIS (USGS)	12413470	04/07/06	8:30	2,060	31	78	6.8	24.2		1,660	2,070	1,930	Peak	2.05	116	3676		
NWIS (USGS)	12413470	05/18/06	10:15	3,000	63	82	11.3	51.7		2,840	2,930	2,880	Peak	2.88	223	3494		
NWIS (USGS)	12413470	06/14/06	11:00	852	3	77	0.7	2.3		747	860	908	Steady	2.63	14.3	3890		
NWIS (USGS)	12413470	07/12/06	10:45	282	1	68	0.3	0.7		287	278	271	Steady	3.53	8.12	4590		
NWIS (USGS)	12413470	08/15/06	14:50	155	4	80	0.8	3.2		153	148	145	Steady	3.2	8.89	1423		
NWIS (USGS)	12413470	11/08/06	15:45	1,270	21	73	5.7	15.3		2,880	1,640	799	Falling	1.26	24.2	1092		
NWIS (USGS)	12413470	02/08/07	8:45	259	4	88	0.5	3.5		235	282	342	Steady	1.8	7.92	1530		
NWIS (USGS)	12413470	03/12/07	15:00	3,640	289	80	57.8	231.2		1,060	2,930	3,870	Rising	0.98	304	1049		
NWIS (USGS)	12413470	04/23/07	14:15	705	1					717	714	817	Steady					
NWIS (USGS)	12413470	05/03/07	14:15	1,520	6	65	2.1	3.9		1,530	1,530	1,310	Steady	1.83	21.6	3295		
NWIS (USGS)	12413470	05/21/07	10:35	980	1	82	0.2	0.8		1,120	977	833	Falling					
NWIS (USGS)	12413470	06/14/07	12:45	394	1	68	0.3	0.7		413	394	377	Steady	3.34	6.26	2920		
NWIS (USGS)	12413470	06/14/07	12:50	394	1					413	394	377	Steady	3.34	6.26	2920		

Attachment A. **Summary of BEMP and USGS Sample Data (Suspended Sediment Concentration, Grain Size, and Lead Concentrations)**
Processes of Sediment and Lead Transport, Erosion, and Deposition
Lower Basin Coeur d'Alene River (OU3)

Sampler	Station	Date	Time	Discharge (cfs)	SSC (mg/L)	Percent Fines	SSC - sand (mg/L)	SSC - fines (mg/L)	Lake Level (ft NAVD88)	Flow, day before measurement (cfs)	Mean Flow, day of measurement (cfs)	Flow, day after measurement (cfs)	Rising, Falling,Peak, or Steady[a]	$Pb_{FILTERED}$ (µg/L)	$Pb_{UNFILTERED}$ (µg/L)	Pb^{c}_{BULK} (mg/kg)	$Pb_{63\text{-}250µm}$ (mg/kg)	$Pb_{<63µm}$ (mg/kg)
PINEHURST DATA (continued)																		
NWIS (USGS)	12413470	07/23/07	11:00	151	2					154	150	147	Steady					
NWIS (USGS)	12413470	08/09/07	14:20	125	3					121	122	120	Steady	3.81	11.5	2563		
NWIS (USGS)	12413470	08/21/07	12:20	139	4					123	135	119	Steady					
NWIS (USGS)	12413470	09/10/07	11:50	99	2					95	94	92	Steady					
NWIS (USGS)	12413470	10/17/07	13:40	104	3	75	0.8	2.3		99	102	103	Steady	2.55	6.7	1383		
NWIS (USGS)	12413470	12/04/07	12:15	1,300	21	87	2.7	18.3		415	1,260	1,060	Peak	1.44	71.6	3341		
NWIS (USGS)	12413470	02/04/08	15:40	161	2	82	0.4	1.6		175	168	161	Steady	1.6	7.57	2985		
NWIS (USGS)	12413470	05/06/08	14:45	2,690	37	73	10.0	27.0		2,200	2,700	3,040	Rising	5.77	147	3817		
NWIS (USGS)	12413470	05/18/08	11:30	6,170	346	92	27.7	318.3		5,310	6,190	6,020	Peak	5.77	1020	2931		
NWIS (USGS)	12413470	06/26/08	9:20	1,290	6	69	1.9	4.1		1,370	1,260	1,180	Falling	3.9	27	3850		
NWIS (USGS)	12413470	09/11/08	14:40	138	3	91	0.3	2.7		133	133	132	Steady	5.42	14.7	3093		
NWIS (USGS)	12413470	10/20/08	11:05	109	1	45	0.6	0.5		109	109	115	Steady	3.96	9.47	5510		
NWIS (USGS)	12413470	11/13/08	12:15	483	10	80	2.0	8.0		190	478	312	Steady	3.91	63.4	5949		
NWIS (USGS)	12413470	01/09/09	9:00	2,310	130	69	40.3	89.7		3,680	2,190	1,150	Falling	1.51	254	1942		
NWIS (USGS)	12413470	02/24/09	13:50	375	8	74	2.1	5.9		188	353	646	Steady	2.24	24.4	2770		
NWIS (USGS)	12413470	05/19/09	16:30	3,440	63	56	27.7	35.3		2,430	3,310	2,780	Peak	3.17	178	2775		
NWIS (USGS)	12413470	06/18/09	8:30	694	3	76	0.7	2.3		718	689	655	Steady	3.86	12.6	2913		
NWIS (USGS)	12413470	08/05/09	14:25	160	3	64	1.1	1.9		161	158	158	Steady	3.5	10.4	2300		
NWIS (USGS)	12413470	10/19/09	13:30	113	3	71	0.9	2.1		110	107	105	Steady	3.81	9.68	1957		
NWIS (USGS)	12413470	03/30/10	17:15	971	11	79	2.3	8.7		569	1,020	760	Peak	1.55	39.1	3414		
NWIS (USGS)	12413470	04/21/10	17:00	1,100	18	88	2.2	15.8		841	1,100	1,080	Steady	1.48	82.3	4490		
NWIS (USGS)	12413470	07/08/10	14:45	333	2	50	1.0	1.0		367	340	321	Steady	2.75	7.3	2275		
NWIS (USGS)	12413470	10/07/10	11:30	119	3	88	0.4	2.6		121	123	129	Steady	1.75	7.36	1870		
NWIS (USGS)	12413470	01/16/11	9:45	1,910	65	52	31.2	33.8		1,330	2,640	5,420	Rising	1.37	102	1548		
NWIS (USGS)	12413470	06/07/11	16:35	3,040	28	71	8.1	19.9		2,960	3,060	2,810	Peak	2.14	74.6	2588		
NWIS (USGS)	12413470	07/12/11	16:05	666	4	73	1.1	2.9		674	667	677	Steady	3.43	15.8	3093		
NWIS (USGS)	12413470	10/14/11	14:20	131	2	75	0.5	1.5		135	132	141	Steady	1.98	7.74	2880		
NWIS (USGS)	12413470	02/24/12	8:45	623	4	68	1.3	2.7		820	605	548	Falling	1.52	9.18	1915		
NWIS (USGS)	12413470	04/26/12	16:20	4,170	49	79	10.3	38.7		4,710	4,250	3,930	Falling	3.27	91	1790		
NWIS (USGS)	12413470	06/26/12	14:35	1,220	15	54	6.9	8.1		1,020	1,090	1,010	Peak	2.81	39.6	2453		
NWIS (USGS)	12413470	10/04/12	13:30	104	4	48	2.1	1.9		100	103	103	Steady	2.07	11.8	2433		
NWIS (USGS)	12413470	03/15/13	16:10	1,170	16	68	5.1	10.9		754	1,120	1,340	Rising	1.35	40.5	2447		
NWIS (USGS)	12413470	04/06/13	15:30	2,650	40	52	19.2	20.8		2,260	2,780	2,620	Peak	1.55	100	2461		
NWIS (USGS)	12413470	06/26/13	11:45	480	2	60	0.8	1.2			480			2.94	7.58	2320		
NWIS (USGS)	12413470	10/24/13	8:25	113	4	71	1.16	2.84			111			1.24	4.61	843		
NWIS (USGS)	12413470	03/06/14	15:30	3,570	133	58	55.86	77.14			3,380			2.06	132	977		
NWIS (USGS)	12413470	05/16/14	13:30	2,310	30	39	18.3	11.7			2,250			1.35	69.2	2262		
NWIS (USGS)	12413470	07/10/14	8:30	326	2	62	0.76	1.24			318			1.95	8.01	3030		
NWIS (USGS)	12413470	02/10/15	14:00	3,920	48	59	19.68	28.32			3,810			2.31	62.6	1256		
NWIS (USGS)	12413470	03/18/15	12:00	1,700	11	45	6.05	4.95			1,700			1.73	40.7	3543		
NWIS (USGS)	12413470	06/04/15	15:10	299	3	56	1.32	1.68			304			2.82	5.67	950		
NWIS (USGS)	12413470	10/09/15	9:30	77	1	91	0.09	0.91			78			1.23	3.55	2320		
ENAVILLE DATA																		
BEMP (USGS)	Enaville	05/18/08	13:45	25,100	132					20,100	24,100	26,300	Rising			146		
BEMP (CH2M HILL)	Enaville	12/15/10	10:00	12,900	19.7	60	7.9	11.8		14,900	12,300	7,160	Falling			122		135
BEMP (CH2M HILL)	Enaville	01/17/11	14:00	25,900	257	41	152.2	104.9		10,400	23,300	22,100	Peak			192	205	241
BEMP (CH2M HILL)	Enaville	05/16/11	16:00	18,000	71.6	69	22.2	49.4		15,800	17,400	15,300	Peak			338	525	365
BEMP (CH2M HILL)	Enaville	3/31/12	14:00	21,400	80	77	18.7	61.5		10,500	20,900	14,900	Peak			147		
BEMP (CH2M HILL)	Enaville	4/26/12	13:30	16,900	38	76	9.2	28.8		20,100	17,400	16,900	Falling			362		413
BEMP (CH2M HILL)	Enaville	4/6/13	14:00	13,500	83	50	41.5	41.5		8,700	12,900	14,200	Rising			123	318	238
NWIS (USGS)	12413000	05/21/80	13:30	2,150	18					2,120	2,080	2,010	Steady					

Attachment A. **Summary of BEMP and USGS Sample Data (Suspended Sediment Concentration, Grain Size, and Lead Concentrations)**
Processes of Sediment and Lead Transport, Erosion, and Deposition
Lower Basin Coeur d'Alene River (OU3)

Sampler	Station	Date	Time	Discharge (cfs)	SSC (mg/L)	Percent Fines	SSC - sand (mg/L)	SSC - fines (mg/L)	Lake Level (ft NAVD88)	Flow, day before measurement (cfs)	Mean Flow, day of measurement (cfs)	Flow, day after measurement (cfs)	Rising, Falling,Peak, or Steady[a]	$Pb_{FILTERED}$ (µg/L)	$Pb_{UNFILTERED}$ (µg/L)	Pb^{c}_{BULK} (mg/kg)	$Pb_{63\text{-}250µm}$ (mg/kg)	$Pb_{<63µm}$ (mg/kg)
ENAVILLE DATA (continued)																		
NWIS (USGS)	12413000	11/21/89	11:00	1,980	3					1,520	1,610	1,670	Steady					
NWIS (USGS)	12413000	03/21/90	12:30	4,270	5					3,180	4,090	4,760	Rising					
NWIS (USGS)	12413000	05/16/90	15:00	2,850	2					2,880	2,820	2,950	Steady					
NWIS (USGS)	12413000	09/19/90	10:00	268	1					255	250	242	Steady					
NWIS (USGS)	12413000	11/18/92	9:15	494	1					474	480	535	Steady					
NWIS (USGS)	12413000	01/19/93	14:45	248	2	83	0.3	1.7		258	250	264	Steady					
NWIS (USGS)	12413000	03/24/93	9:15	8,320	91					3,400	8,100	7,510	Peak	1	17	176		
NWIS (USGS)	12413000	04/06/93	8:15	7,310	12					8,600	7,040	5,710	Falling		3	250		
NWIS (USGS)	12413000	04/20/93	12:20	6,860	16	78	3.5	12.5		7,100	6,930	5,900	Falling		1	63		
NWIS (USGS)	12413000	05/04/93	9:55	6,830	8	70	2.4	5.6		6,960	6,940	6,730	Steady		3	375		
NWIS (USGS)	12413000	05/20/93	8:35	3,450	5	67	1.7	3.4		3,640	3,430	3,230	Steady		4	800		
NWIS (USGS)	12413000	06/03/93	11:25	1,780	2	76	0.5	1.5		1,790	1,750	1,590	Steady		2	1000		
NWIS (USGS)	12413000	06/22/93	14:52	868	1	82	0.2	0.8		820	873	884	Steady					
NWIS (USGS)	12413000	08/25/93	12:45	421	1	42	0.6	0.4		460	443	428	Steady					
NWIS (USGS)	12413000	09/21/93	9:45	342	1	84	0.2	0.8		324	330	332	Steady					
NWIS (USGS)	12413000	10/18/93	17:10	425	1	39	0.6	0.4		419	420	388	Steady					
NWIS (USGS)	12413000	11/17/93	9:05	252	1	72	0.3	0.7		249	251	261	Steady		2	2000		
NWIS (USGS)	12413000	12/16/93	10:00	442	47	79	9.9	37.1		469	431	367	Steady		2	43		
NWIS (USGS)	12413000	01/19/94	13:10	1,040	1	95	0.1	1.0		1,110	1,020	925	Steady		1	1000		
NWIS (USGS)	12413000	02/15/94	14:30	421	< 1	77				449	432	427	Steady		1			
NWIS (USGS)	12413000	03/06/94	15:40	3,390	4	77	0.9	3.1		3,970	3,490	2,820	Steady		2	500		
NWIS (USGS)	12413000	03/15/94	13:35	1,570	1	80	0.2	0.8		1,450	1,590	2,070	Steady		3	3000		
NWIS (USGS)	12413000	04/04/94	16:25	4,140	6	70	1.8	4.2		3,530	4,030	4,110	Steady		2	333		
NWIS (USGS)	12413000	04/21/94	15:22	6,650	11	79	2.3	8.7		7,090	6,660	6,080	Falling					
NWIS (USGS)	12413000	05/10/94	10:25	2,260	2	65	0.7	1.3		2,170	2,150	2,010	Steady		1	500		
NWIS (USGS)	12413000	06/15/94	10:37	701	< 1	48				653	674	650	Steady		1			
NWIS (USGS)	12413000	07/21/94	10:20	272	1	87	0.1	0.9		282	276	267	Steady					
NWIS (USGS)	12413000	08/17/94	15:47	175	1	71	0.3	0.7		174	173	172	Steady		8	8000		
NWIS (USGS)	12413000	09/20/94	14:35	173	< 1	87				172	168	163	Steady		2			
NWIS (USGS)	12413000	04/16/96	7:30	4,450	4					4,580	4,480	5,160	Steady					
NWIS (USGS)	12413000	05/14/96	9:15	2,770	3					2,260	3,120	5,220	Rising					
NWIS (USGS)	12413000	06/13/96	8:15	1,400	2					1,470	1,400	1,340	Steady					
NWIS (USGS)	12413000	07/15/96	14:15	574	< 1					574	565	548	Steady					
NWIS (USGS)	12413000	09/06/96	10:50	255	2					235	253	256	Steady					
NWIS (USGS)	12413000	04/20/98	12:45	2,460	1	100		1.0		2,400	2,450	2,600	Steady					
NWIS (USGS)	12413000	05/19/98	12:45	1,690	1	100		1.0		1,840	1,710	1,630	Steady					
NWIS (USGS)	12413000	06/11/98	12:45	1,580	1	83	0.2	0.8		1,710	1,590	1,490	Steady					
NWIS (USGS)	12413000	07/07/98	17:45	675	1	78	0.2	0.8		727	686	659	Steady					
NWIS (USGS)	12413000	08/19/98	14:45	304	1	69	0.3	0.7		306	304	300	Steady					
NWIS (USGS)	12413000	09/15/98	7:50	248	< 1	82				253	249	247	Steady					
NWIS (USGS)	12413000	03/02/99	11:30	4,450	4	57	1.7	2.3		5,290	4,630	3,920	Falling					
NWIS (USGS)	12413000	03/23/99	10:00	6,880	14	76	3.4	10.6		6,700	7,210	7,040	Steady		2	143		
NWIS (USGS)	12413000	04/13/99	10:30	2,740	2	100		2.0		2,550	2,720	2,820	Steady					
NWIS (USGS)	12413000	04/20/99	11:20	9,680	37	72	10.4	26.6		7,600	9,720	9,680	Peak		3	81		
NWIS (USGS)	12413000	05/06/99	10:10	5,180	3	100		3.0		5,860	5,120	5,200	Steady		0.78	260		
NWIS (USGS)	12413000	05/20/99	10:00	6,400	7	93	0.5	6.5		6,190	6,840	6,700	Steady		4	571		
NWIS (USGS)	12413000	05/25/99	9:30	11,100	84	76	20.2	63.8		8,960	11,300	11,200	Peak		11.3	135		
NWIS (USGS)	12413000	06/02/99	10:15	5,810	5	71	1.5	3.6		5,840	5,750	5,180	Steady		0.67	134		
NWIS (USGS)	12413000	06/29/99	10:00	1,370	1	60	0.4	0.6		1,610	1,500	1,420	Steady					
NWIS (USGS)	12413000	07/13/99	7:40	902	< 1	100				927	898	867	Steady		0.17			
NWIS (USGS)	12413000	07/26/99	10:00	522	1	86	0.1	0.9		618	596	573	Steady					
NWIS (USGS)	12413000	08/10/99	7:45	504	22	0	22.0			569	495	465	Steady		0.14	6		
NWIS (USGS)	12413000	12/01/99	11:45	1,560	1	80	0.2	0.8		1,870	1,730	1,740	Steady					

Attachment A. **Summary of BEMP and USGS Sample Data (Suspended Sediment Concentration, Grain Size, and Lead Concentrations)**
Processes of Sediment and Lead Transport, Erosion, and Deposition
Lower Basin Coeur d'Alene River (OU3)

Sampler	Station	Date	Time	Discharge (cfs)	SSC (mg/L)	Percent Fines	SSC - sand (mg/L)	SSC - fines (mg/L)	Lake Level (ft NAVD88)	Flow, day before measurement (cfs)	Mean Flow, day of measurement (cfs)	Flow, day after measurement (cfs)	Rising, Falling,Peak, or Steady[a]	$Pb_{FILTERED}$ (µg/L)	$Pb_{UNFILTERED}$ (µg/L)	Pb^{c}_{BULK} (mg/kg)	$Pb_{63\text{-}250µm}$ (mg/kg)	$Pb_{<63µm}$ (mg/kg)
ENAVILLE DATA (continued)																		
NWIS (USGS)	12413000	01/11/00	11:00	931	1	75	0.3	0.8		910	879	875	Steady					
NWIS (USGS)	12413000	02/16/00	8:20	1,550						1,700	1,530	1,420	Steady					
NWIS (USGS)	12413000	02/29/00	8:00	2,020	2	69	0.6	1.4		1,980	2,260	2,420	Steady					
NWIS (USGS)	12413000	03/27/00	9:45	3,290	2	84	0.3	1.7		3,800	3,650	4,420	Steady					
NWIS (USGS)	12413000	03/28/00	8:05	4,180	3	100		3.0		3,650	4,420	4,980	Steady					
NWIS (USGS)	12413000	04/10/00	9:45	4,680	4	77	0.9	3.1		4,560	5,190	6,780	Steady					
NWIS (USGS)	12413000	04/14/00	9:45	18,200	207	90	20.7	186.3		9,390	18,800	20,000	Rising		23.9	115		
NWIS (USGS)	12413000	04/17/00	9:45	10,900	29	89	3.2	25.8		13,600	11,100	10,500	Falling		2.5	86		
NWIS (USGS)	12413000	05/02/00	9:00	5,080	6	87	0.8	5.2		4,820	5,730	6,800	Rising					
NWIS (USGS)	12413000	05/10/00	9:45	4,000	4	100		4.0		3,750	3,990	3,910	Steady					
NWIS (USGS)	12413000	05/18/00	7:30	3,770	3	74	0.8	2.2		3,840	4,160	4,040	Steady					
NWIS (USGS)	12413000	06/02/00	7:15	1,970	3	74	0.8	2.2		2,410	2,140	2,040	Steady					
NWIS (USGS)	12413000	06/15/00	7:40	2,010	2	100		2.0		1,990	2,000	1,920	Steady					
NWIS (USGS)	12413000	06/29/00	8:00	954	1	80	0.2	0.8		1,010	972	933	Steady					
NWIS (USGS)	12413000	07/19/00	9:15	532	1					540	528	511	Steady					
NWIS (USGS)	12413000	07/24/00	10:30	440	1	60	0.4	0.6		473	460	451	Steady					
NWIS (USGS)	12413000	08/08/00	15:15	327	< 1					334	326	321	Steady					
NWIS (USGS)	12413000	08/31/00	9:15	236	1	82	0.2	0.8		249	249	265	Steady					
NWIS (USGS)	12413000	09/07/00	11:00	285	1	100	0.0	1.0		282	283	286	Steady					
NWIS (USGS)	12413000	11/06/00	10:30	341	1	67	0.3	0.7		319	337	307	Steady					
NWIS (USGS)	12413000	12/13/00	11:00	149	1	67	0.3	0.7		160	150	170	Steady					
NWIS (USGS)	12413000	01/23/01	10:00	216	1	75	0.3	0.8		212	213	201	Steady	0.05	1	950		
NWIS (USGS)	12413000	03/14/01	8:45	590	1	88	0.1	0.9		504	608	672	Steady					
NWIS (USGS)	12413000	04/10/01	8:15	1,110	1	75	0.3	0.8		1,140	1,110	1,110	Steady					
NWIS (USGS)	12413000	05/01/01	11:00	6,610	13					5,940	6,540	6,000	Steady	0.058	1.08	79		
NWIS (USGS)	12413000	05/03/01	10:15	4,870	3	90	0.3	2.7		6,000	4,840	4,080	Falling	0.087				
NWIS (USGS)	12413000	06/12/01	9:30	880	1	75	0.3	0.8		867	894	925	Steady					
NWIS (USGS)	12413000	06/25/01	13:00	590	< 1					589	587	571	Steady					
NWIS (USGS)	12413000	07/24/01	8:00	304	1					309	303	296	Steady					
NWIS (USGS)	12413000	08/06/01	13:00	248	1					253	247	241	Steady					
NWIS (USGS)	12413000	09/17/01	16:00	166	1					161	166	164	Steady					
NWIS (USGS)	12413000	04/16/02	8:30	15,700	58	90	5.8	52.2		26,500	14,800	9,920	Falling	0.221	9.26	156		
NWIS (USGS)	12413000	10/09/03	12:20	182	2					171	176	179	Steady		0.08	40		
NWIS (USGS)	12413000	12/06/03	9:20	1,300	1					1,030	1,440	2,140	Steady	0.079	0.18	101		
NWIS (USGS)	12413000	01/22/04	9:40	476	0					478	469	489	Steady		0.04			
NWIS (USGS)	12413000	04/01/04	12:30	6,250	10					5,440	6,210	5,260	Peak	0.079	1.23	115		
NWIS (USGS)	12413000	05/05/04	13:00	3,780	2					4,050	3,780	3,320	Steady	0.088	0.35	131		
NWIS (USGS)	12413000	06/07/04	11:00	2,360	1					2,540	2,350	2,090	Steady	0.166	0.2	34		
NWIS (USGS)	12413000	07/26/04	11:45	371	0					381	369	361	Steady	0.168	0.1			
NWIS (USGS)	12413000	09/08/04	11:00	278	1					289	281	275	Steady	0.043	0.09	47		
NWIS (USGS)	12413000	10/14/04	10:00	295	0					310	298	291	Steady	0.043	0.06			
NWIS (USGS)	12413000	12/12/04	15:30	13,100	53					8,680	13,600	8,210	Peak	0.172	6.38	117		
NWIS (USGS)	12413000	02/25/05	10:40	961	1	79	0.2	0.8		1,050	1,030	1,010	Steady		0.07	70		
NWIS (USGS)	12413000	03/29/05	14:22	8,820	17	84	2.7	14.3		7,790	8,180	6,130	Peak	0.054	1.48	84		
NWIS (USGS)	12413000	05/18/05	10:45	1,730	2	71	0.6	1.4		1,750	1,760	1,720	Steady	0.07	0.26	95		
NWIS (USGS)	12413000	06/20/05	9:30	801	1	71	0.3	0.7		934	835	774	Steady		0.11	110		
NWIS (USGS)	12413000	08/11/05	11:25	265	1	53	0.5	0.5		271	267	276	Steady	0.046	0.09	44		
NWIS (USGS)	12413000	10/17/05	12:05	292	< 1	75				300	291	283	Steady	0.742	0.05			
NWIS (USGS)	12413000	01/03/06	12:30	3,390	2	89	0.2	1.8		3,900	3,400	2,980	Steady	0.054	0.53	238		
NWIS (USGS)	12413000	02/13/06	10:15	1,640	1	58	0.4	0.6		1,620	1,620	1,550	Steady	0.081	0.09	9		
NWIS (USGS)	12413000	04/07/06	10:45	8,630	42	83	7.1	34.9		6,710	8,570	8,900	Rising	0.129	4.84	112		
NWIS (USGS)	12413000	06/12/06	8:20	1,720	1	82	0.2	0.8		1,800	1,690	1,600	Falling	0.14	0.21	70		
NWIS (USGS)	12413000	07/10/06	13:30	688	1	73	0.3	0.7		712	687	668	Falling	0.09	0.29	200		

Attachment A. **Summary of BEMP and USGS Sample Data (Suspended Sediment Concentration, Grain Size, and Lead Concentrations)**
Processes of Sediment and Lead Transport, Erosion, and Deposition
Lower Basin Coeur d'Alene River (OU3)

Sampler	Station	Date	Time	Discharge (cfs)	SSC (mg/L)	Percent Fines	SSC - sand (mg/L)	SSC - fines (mg/L)	Lake Level (ft NAVD88)	Flow, day before measurement (cfs)	Mean Flow, day of measurement (cfs)	Flow, day after measurement (cfs)	Rising, Falling,Peak, or Steady[a]	$Pb_{FILTERED}$ (µg/L)	$Pb_{UNFILTERED}$ (µg/L)	Pb^{c}_{BULK} (mg/kg)	$Pb_{63\text{-}250µm}$ (mg/kg)	$Pb_{<63µm}$ (mg/kg)
ENAVILLE DATA (continued)																		
NWIS (USGS)	12413000	08/14/06	9:30	332	< 1	100				350	331	319	Falling	0.15	0.09			
NWIS (USGS)	12413000	10/02/06	10:45	223	< 0.5	50				224	221	219	Falling	0.16	0.06			
NWIS (USGS)	12413000	11/07/06	10:00	6,100	36	84	5.8	30.2		1,800	6,390	6,360	Peak	0.23	5.38	143		
NWIS (USGS)	12413000	02/08/07	10:30	843	1	61	0.4	0.6		805	846	931	Steady	0.07	0.2	130		
NWIS (USGS)	12413000	03/12/07	16:05	10,700	135	80	27.0	108.0		3,680	9,510	19,000	Rising	0.08	11.7	86		
NWIS (USGS)	12413000	05/02/07	14:00	4,520	3	81	0.6	2.4		4,510	4,490	4,570	Steady	0.26	0.47	70		
NWIS (USGS)	12413000	06/13/07	10:50	829	2	53	0.9	1.1		882	824	789	Steady					
NWIS (USGS)	12413000	08/08/07	9:00	231	1	71	0.3	0.7		232	232	235	Steady	0.06	0.09	30		
NWIS (USGS)	12413000	10/11/07	11:45	244	1	33	0.7	0.3		242	242	237	Steady	0.08	0.07	-10		
NWIS (USGS)	12413000	12/04/07	14:40	2,450	7	85	1.1	6.0		507	2,220	3,280	Rising	0.064	0.64	82		
NWIS (USGS)	12413000	01/29/08	11:00	428	1	67	0.3	0.7		458	464	457	Steady		0.06	60		
NWIS (USGS)	12413000	05/07/08	9:30	13,100	54	78	11.9	42.1		11,200	13,100	12,100	Peak	0.154	6.44	116		
NWIS (USGS)	12413000	05/18/08	13:15	24,300	187	90	18.7	168.3		20,100	24,100	26,300	Rising	0.569	31	163		
NWIS (USGS)	12413000	06/23/08	13:40	3,220	3	83	0.5	2.5		3,410	3,230	2,850	Steady	0.116	0.46	115		
NWIS (USGS)	12413000	08/08/08	8:45	432	1	80	0.2	0.8		434	427	421	Steady	0.049	0.08	31		
NWIS (USGS)	12413000	09/10/08	9:15	296	1	71	0.3	0.7		293	290	285	Steady	0.124	0.09	-34		
NWIS (USGS)	12413000	10/14/08	12:05	255	< 0.5	75				253	255	260	Steady	0.07	0.12			
NWIS (USGS)	12413000	11/13/08	14:20	1,190	2	95	0.1	1.9		727	1,190	850	Steady	0.086	0.33	122		
NWIS (USGS)	12413000	01/09/09	14:40	10,600	42	83	7.1	34.9		12,000	11,800	5,900	Falling	0.239	6.41	147		
NWIS (USGS)	12413000	02/23/09	8:45	524	6	93	0.4	5.6		500	535	674	Steady	0.062	0.15	15		
NWIS (USGS)	12413000	05/18/09	8:45	7,150	9	70	2.7	6.3		6,690	7,280	8,700	Rising	0.088	0.93	94		
NWIS (USGS)	12413000	06/16/09	9:10	1,410	1	54	0.5	0.5		1,380	1,370	1,220	Steady	0.116	0.84	724		
NWIS (USGS)	12413000	08/03/09	8:50	339	2	58	0.8	1.2		346	338	329	Steady	0.115	0.22	53		
NWIS (USGS)	12413000	10/20/09	15:20	257	3	73	0.8	2.2		269	258	245	Steady	0.08	0.09	3		
NWIS (USGS)	12413000	03/30/10	12:39	6,520	40	89	4.4	35.6		2,660	6,120	5,610	Peak	0.197	3.4	80		
NWIS (USGS)	12413000	04/22/10	9:20	5,780	13	73	3.5	9.5		5,400	5,730	4,890	Steady	0.074	1.37	100		
NWIS (USGS)	12413000	07/06/10	9:00	1,250	2	37	1.3	0.7		1,310	1,250	1,170	Steady	0.053	0.16	54		
NWIS (USGS)	12413000	10/04/10	8:30	270	1	60	0.4	0.6		254	277	303	Steady	0.046	0.1	54		
NWIS (USGS)	12413000	01/16/11	12:40	9,410	26	75	6.5	19.5		7,800	10,400	23,300	Rising	0.12	2	72		
NWIS (USGS)	12413000	06/08/11	12:55	6,650	6	72	1.7	4.3		7,220	6,620	5,920	Falling	0.084	0.77	114		
NWIS (USGS)	12413000	07/13/11	9:25	1,310	3	52	1.4	1.6		1,310	1,310	1,280	Steady	0.088	0.19	34		
NWIS (USGS)	12413000	10/11/11	8:45	310	1	40	0.6	0.4		309	322	396	Steady	0.026	0.09	64		
NWIS (USGS)	12413001	02/24/12	11:30	2,130	2	67	0.7	1.3		2,560	2,120	1,880	Falling	0.08	0.36	140		
NWIS (USGS)	12413002	04/27/12	9:30	17,300	53	91	4.8	48.2		17,400	16,900	13,000	Falling	0.257	4.84	86		
NWIS (USGS)	12413003	06/27/12	9:15	2,490	7	57	3.0	4.0		2,240	2,420	2,110	Peak	0.091	0.27	26		
NWIS (USGS)	12413004	10/01/12	12:25	238	1	38	0.6	0.4		241	237	233	Steady	0.082	0.1	18		
NWIS (USGS)	12413005	03/18/13	9:00	5,940	6	72	1.7	4.3		6,700	5,990	4,780	Falling	0.078	0.67	99		
NWIS (USGS)	12413006	04/06/13	17:00	13,900	73	78	16.1	56.9		8,700	12,900	14,200	Rising	0.178	6.77	90		
NWIS (USGS)	12413006	06/24/13	9:00	1,500	1	62	0.38	0.62			1,480			0.049	0.13	81		
NWIS (USGS)	12413006	10/17/13	14:10	305	< 0.5	50					305			0.043	0.05			
NWIS (USGS)	12413006	03/07/14	9:05	10,700	52	81	9.88	42.12			10,300			0.196	3.61	66		
NWIS (USGS)	12413006	05/17/14	8:20	6,180	7	87	0.91	6.09			6,110			0.164	2.09	275		
NWIS (USGS)	12413006	07/07/14	10:30	722	1	71	0.29	0.71			718			0.062	0.12	58		
NWIS (USGS)	12413006	10/06/14	9:10	229	1	80	0.2	0.8			228				0.1	100		
NWIS (USGS)	12413006	02/06/15	10:15	2,730	1	92	0.08	0.92			2,880			0.045	0.3	255		
NWIS (USGS)	12413006	03/18/15	9:00	8,050	12	87	1.56	10.44			7,830			0.148	1.51	114		
NWIS (USGS)	12413006	06/02/15	8:45	629	1	62	0.38	0.62			653			0.112	0.14	28		
NWIS (USGS)	12413006	10/09/15	11:45	166	1	50	0.5	0.5			165			0.049	0.1	51		
NWIS (USGS)	12413006	02/16/16	9:00	11,800	41	80	8.2	32.8			11,600			0.311	5.79	134		
NWIS (USGS)	12413006	04/23/16	10:52	4,930	3	80	0.6	2.4			4,850			0.07	0.33	87		
NWIS (USGS)	12413006	06/13/16	9:10	722	1	60	0.4	0.6			718							

Notes

[a] Subjective grouping based on trend of the 3 day mean daily flow; clear trends in higher flow measurements denoted; steady generally refers to ambiguous classification at lower flow.

[b] Discharge at time of sampling estimated from HEC-RAS.

[c] Bulk Lead on sediment in USGS samples was computed by subtracting the filtered lead value from the unfiltered lead value, and dividing by the SSC.

Attachment B
Summary of Laser In-Situ Scattering and Transmissivity (LISST) Data from April 2012 High-Flow Event

EPA Contract No. EP-W-06-021
Task Order 85

Summary of Laser In-Situ Scattering and Transmissometry (LISST) and Data from April 2012 High Flow Event

Lower Basin of the Coeur d'Alene River (OU3)

PREPARED FOR: U.S. Environmental Protection Agency, Region 10

PREPARED BY: CH2M

DATE: February 17, 2016

1.0 Introduction and Scope

This Attachment is a supplement to *Technical Memorandum (TM) Addendum D-3: Processes of Sediment and Lead Transport, Erosion, and Deposition (*CH2M HILL, 2016), reporting work not discussed in the main body of the report.

In late April 2012, CH2M HILL and subcontractors conducted intensive monitoring of flow, sediment and lead transport, and river bed topography during an overbank flood in the Lower Basin of the Coeur d'Alene River (Lower Basin). This attachment documents a portion of that 2012 flood sampling effort by presenting initial data and analyses of suspended sediment concentration (SSC) and grain size distribution (GSD) information obtained using a Laser In-Situ Scattering and Transsmissometry (LISST) instrument (manufactured by Sequoia Scientific, Inc.) deployed from a work boat during the 2012 flood. In addition to the LISST, the same boat collected 20 liter (L) water samples using a hydrostatic pressure-activated sampler (Go Flo product from General Oceanics); samples were filtered on board and the resulting sediment samples were analyzed for lead concentration in sediments.

The boat-based high flow sampling event was planned following the identification of important data gaps in the original ECSM (CH2M HILL, 2010). For the past several years, CH2M HILL has collected high volume isokinetic sediment samples at bridge locations during floods as part of EPA's monitoring program (BEMP). The data from this program have provided critical information regarding sediment and metals transport at peak flows during floods, leading to the conceptual site models (CSM) described in the main body of the report (CH2M HILL, 2016). However, the BEMP measurements are confined to bridge locations, which are relatively few and widely spaced, and thus only generally represent the range of conditions in the Lower Basin during floods. In addition, a single measurement of flow and suspended sediment concentration at a gage site requires several hours to complete, so represents a "snapshot" of conditions, and one that is averaged over several hours of non-steady flow and sediment transport. More detailed measurements of the spatial and temporal variability of flow and sediment dynamics during floods are required to better understand and predict the redistribution of lead and sediment in the Lower Basin.

To begin to address the data gap, in 2012 CH2MHILL planned and implemented a focused high flow monitoring effort aimed at collecting detailed measurements of flow, sediment transport, and river bed

dynamics during a flood event[1]. The sampling effort included two boats containing instrumentation, in addition to three bridge sampling teams collecting traditional data at the BEMP locations (Exhibit B1; sampling map at end of this Attachment). The sampling was conducted during the spring 2012 snowmelt flood. The sampling plan, updated following the 2012 event, has remained in place but no viable flood events have yet occurred that have triggered subsequent sampling.

This Attachment provides the results of the LISST measurements. The lead concentration measurements from this sampling event are provided in the main report (Exhibit 34), and are not discussed further here.

2.0 High Flow Sampling Event

2.1 April 2012 Flood Event

In late April 2012, a period of unseasonably warm weather caused an above-average snowpack to begin to melt. Following this, a large, warm frontal storm was forecast to deliver substantial rain to the watershed on April 26, causing a peak flow of more than 33,000 cfs on April 27, much higher than bankfull (Exhibit B2A). In anticipation of the second, larger flood peak, the team mobilized on April 25, before the 2nd forecast flood peak. The plan called for sampling on the rising part of the hydrograph, at its peak, and during the falling limb.

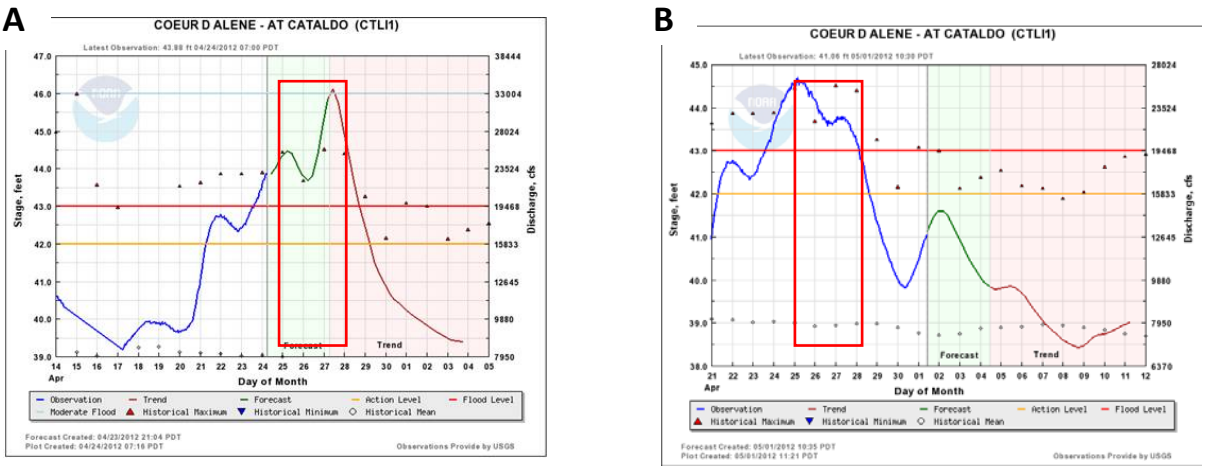

FORECAST HYDROGRAPH **ACTUAL HYDROGRAPH**

Exhibit B2. Forecast and Measured Hydrograph Trends at Cataldo during April 26–29, 2012, Sampling Event, from National Weather Service Website

Red boxes shows the sampling period April 26–28, 2012. (A) Forecast hydrograph. Blue line is measured flow, and green and red are forecasted flows (downloaded on April 24, 2012). (B) Measured hydrograph at Cataldo (downloaded May 1, 2012). Hydrographs downloaded from: http://www.nwrfc.noaa.gov/river/station/flowplot/flowplot.cgi?id=CTLI1.

The event that occurred differed substantially from what was predicted (Exhibit B2B). The frontal storm predicted for April 26 largely missed the watershed, and the resulting second peak turned out to be smaller than the first peak. Therefore, the sampling period bracketed not a large flood peak, but a temporary halt during the falling limb of the hydrograph (Exhibit B3). Still, the mobilization event offered

[1] Defined for the purpose of this study as flow exceeding bankfull capacity (approximately 20,000 cfs), the point at which flow spreads onto the floodplain.

the opportunity to collect observations and data in the river during a large overbank flood event. The BEMP program collected manual samples at both flood peaks, on April 24 and 27.

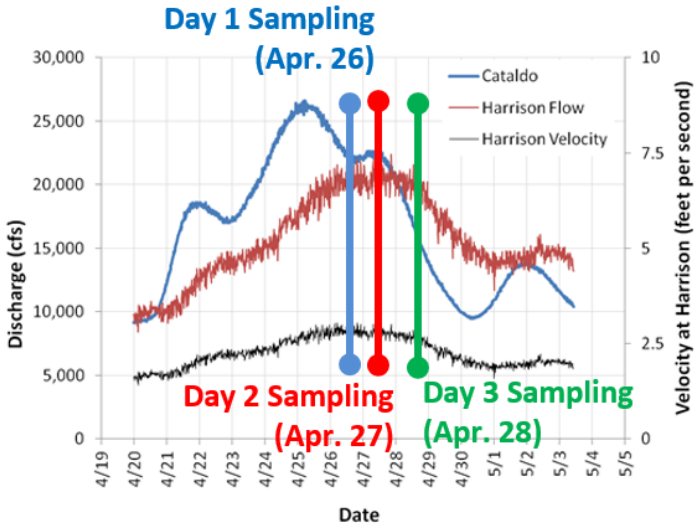

Exhibit B3. Timing of LISST Sampling in Context of 2012 Flood Event

2.2 LISST Casting and Data Processing

The following bullet points summarize the field data collection and subsequent data processing procedures:

- A LISST-100X (Sequoia Scientific, Inc.) was "cast" (lowered to the bottom and raised at a uniform rate) off the back of the work boat (Exhibit B4).
- For each measurement, water depth was logged along with computed *volumetric* SSC in 32 size fractions (using a Sequoia proprietary algorithm).
- Data were recorded ten times per second during each 2–3 minute cast.
- Data reduction included conversion from volumetric to mass concentration using an assumed particle density of 2.85 grams per cubic centimeter (g/cm^3) (based on measurements of particle density in four bed material samples, which ranged from 2.8 to 3.2 g/cm^3). Variability of particle density in the Lower Basin has not been well documented but appears to vary based on lead content and other factors.

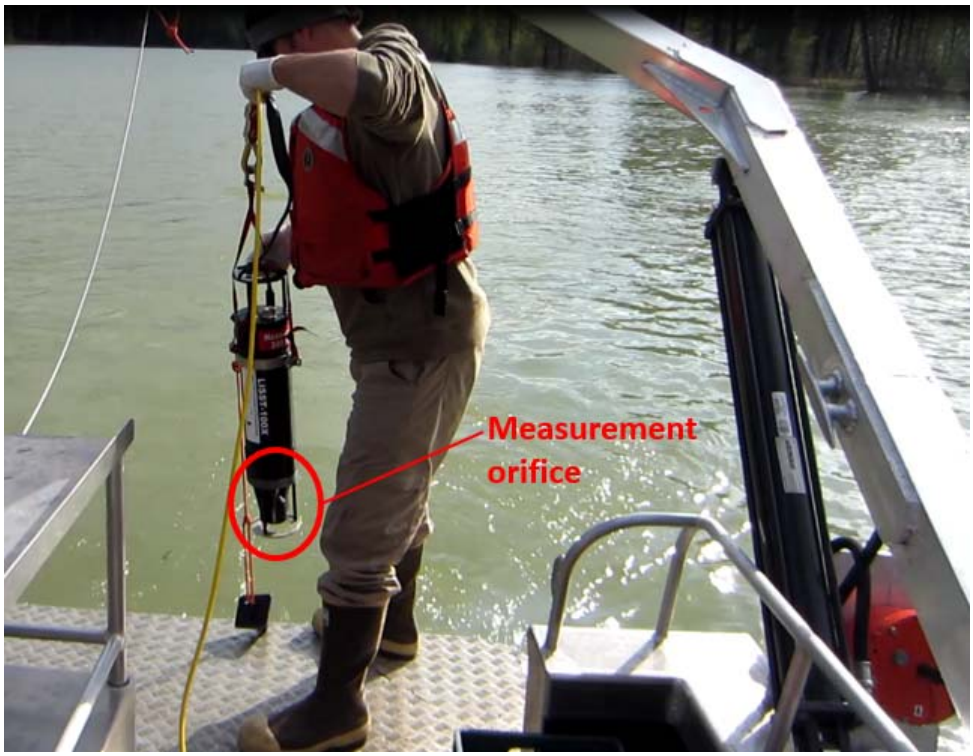

Exhibit B4. Photograph of LISST Casting from the Back of Work Boat

3.0 Results of LISST Measurements

LISST sampling occurred over 3 days (April 26–April 28, 2012), and included 60 LISST casts collected throughout the Lower Basin as shown in Exhibit B1 (included at the end of this attachment). This section summarizes observations of the results and provides graphs that support and lead to the interpretations.

3.1 Example Vertical Profiles

Exhibit B5 provides selected examples of the type of data that was obtained from the LISST castings and subsequent data postprocessing. The following observations summarize general interpretations of the SSC profiles in the LISST castings:

- Vertical sediment profiles varied significantly by location and by day of sampling.
- The sand profile varies significantly between locations. Variability in the sand concentration accounts for most of the measured variability in total SSC throughout the Lower Basin.
- Silt and clay are vertically well-mixed at all locations and show comparatively little spatial variability in concentrations.

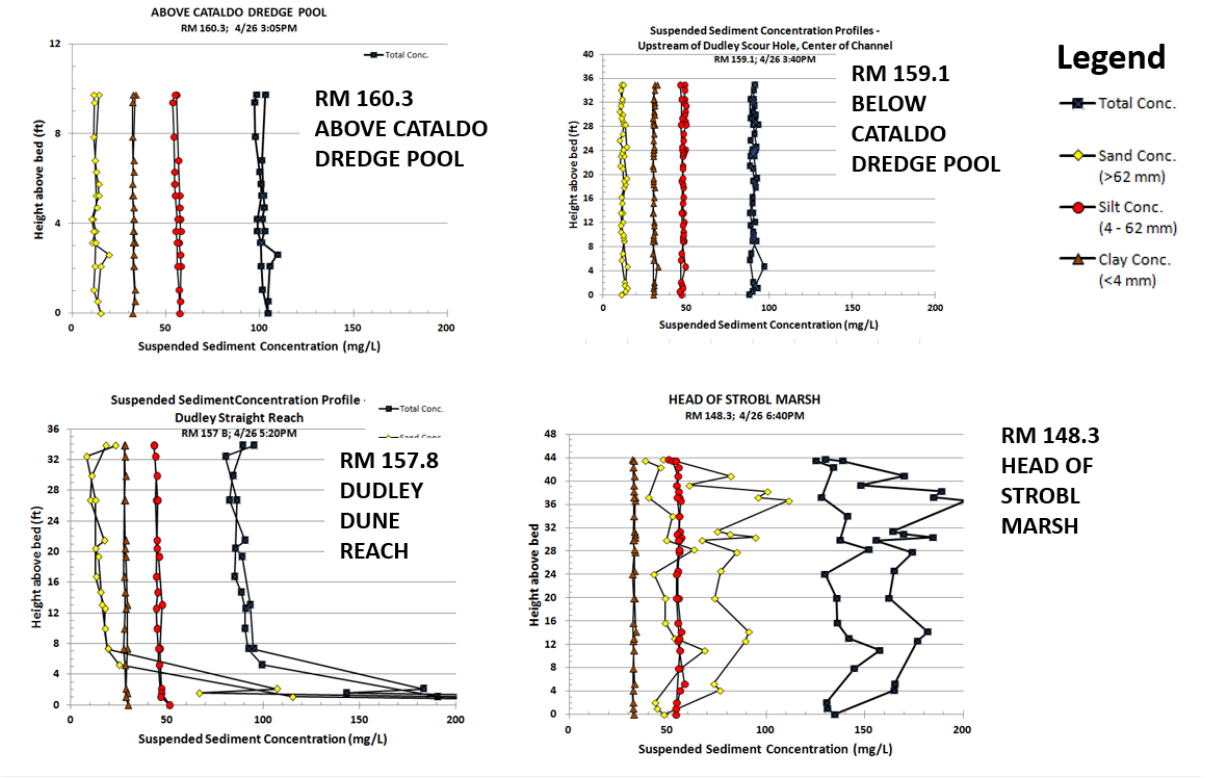

Exhibit B5. Selected Examples of Postprocessed LISST Casting Data from Throughout the Lower Basin

Each of the four panels shows the results from a single cast recording during lowering, then raising.

3.2 Transect Through the Dudley Scour Hole

One of the questions the high-flow sampling was designed to begin to answer is whether the numerous "scour holes" in the Lower Basin could be responsible for supplying large amounts of sediment to the flow. These features have, at some point, eroded more quickly than surrounding areas, leading to the development of deep scour features. As these features have also been shown to contain high levels of lead contamination close to the bed surface, the LISST sampling attempted to measure whether SSC and GSD changed significantly across one of these features. Exhibits B6 and B7 show the longitudinal LISST transects across the Dudley Scour Hole (River Mile [RM] 158.3) on Day 1 (April 26) and Day 3 (April 28) of sampling, respectively. The following points summarize the interpretations of the data shown in these graphs:

Day 1 of Sampling (Exhibit B6)

- Sediment concentrations and vertical profiles do not show obvious major changes longitudinally across the upstream-most scour hole in the Lower Basin.
- Some sand transport is seen near the bed upstream of scour hole, but not below. This may be attributable to local hydraulics or a lack of near-bed sand supply locally at the downstream sample location (about 0.5 mile below the scour hole). It could also indicate that sand transport was generally low during the falling limb of the hydrograph that was sampled.
- Similarity in duplicate profiles measured at upstream scour hole demonstrate the repeatability of LISST casts.

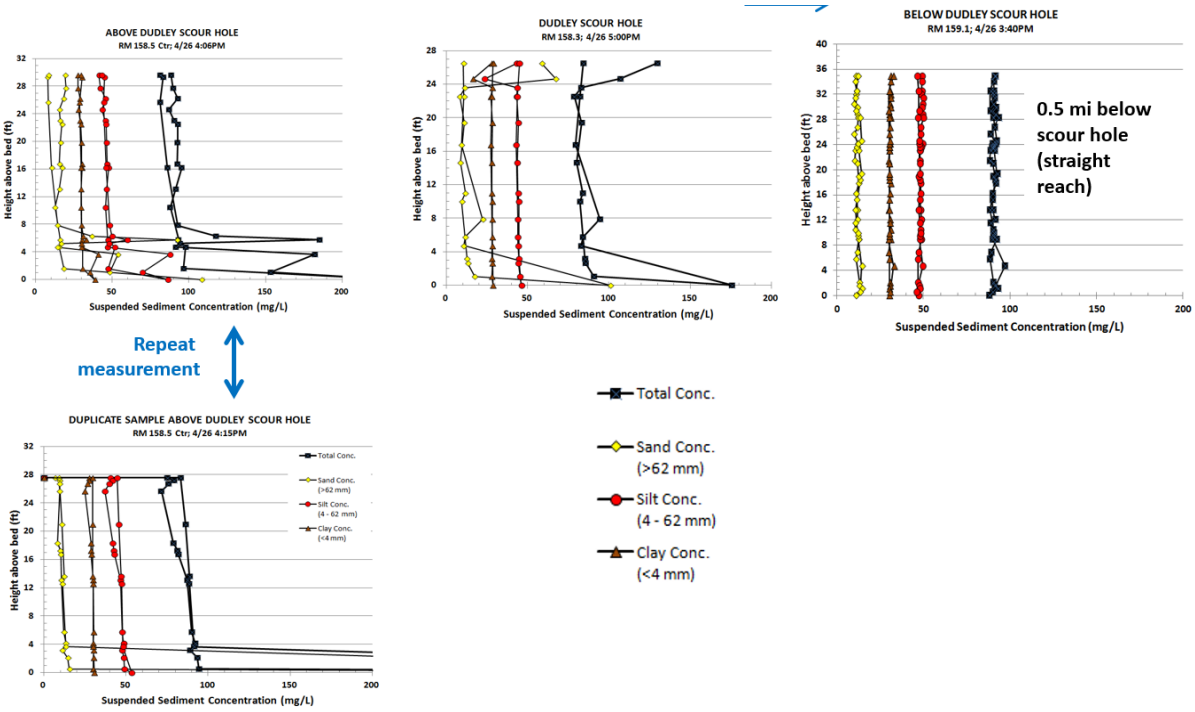

Exhibit B6. LISST Transect through Dudley Scour Hole (RM 158), Sampling Day 1 (April 26, 2015)

Day 3 of Sampling (Exhibit B7)

- Little vertical or downstream variability in any size class is noted through Dudley scour hole on Day 3.
- Silt and clay concentrations have dropped by about a third compared with Day 1 (Exhibit B6): concentrations dropped from ~ 50 parts per million (ppm) to ~35 ppm for silt, and ~30 ppm to ~ 20 ppm for clay, between Day 1 and Day 3.
- Flow near the Dudley Scour Hole (as measured at the Cataldo gage) was lower during Day 3 compared with Day 1, which could partially explain reductions in sand transport at Dudley, and(or) the amount of mobilization of fines from the bed. Note that this was not the case near Harrison, where flows were more similar throughout the entire sampling period (Exhibit B3).

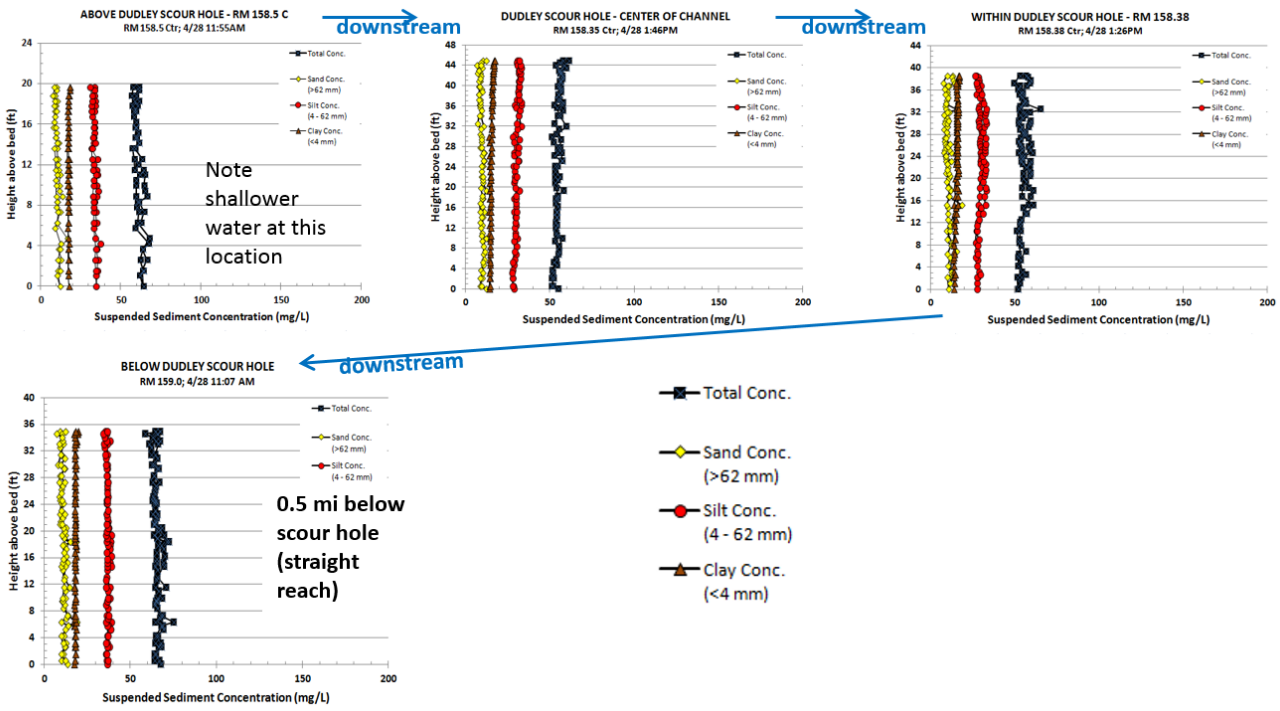

Exhibit B7. LISST Transect through Dudley Scour Hole (RM 158), Sampling Day 3 (April 28, 2015)

3.3 LISST Cross Section Transects

On Day 2 of LISST sampling, the effort concentrated on sampling at cross sections near two bridges: Rose Lake and Springston. Both bridges have U.S. Geological Survey (USGS) stream gages and were sampled concurrently using standard isokinetic methods used by the BEMP program. The across-stream profiles measured with LISST are shown in Exhibit B8. The following points summarize observations of results of the LISST cross section transects. The comparison between the LISST and BEMP sampling on April 27 is discussed in Section 3.7 below.

- Vertical profiles are more well -mixed at Rose Lake Bridge than at Springston Bridge. At Rose Lake Bridge, most of the sand is vertically fairly well mixed (the exception being the second profile from the left, which has some stratification of sand. By contrast, at Springston Bridge, sand is stratified at all five verticals, and most of the sand is concentrated in the lowest 8 to 10 feet of the flow.
- At Springston, the sand profile varies across the channel—the least sand transport was occurring near the left bank and the most in the center and center-right parts of the channel.

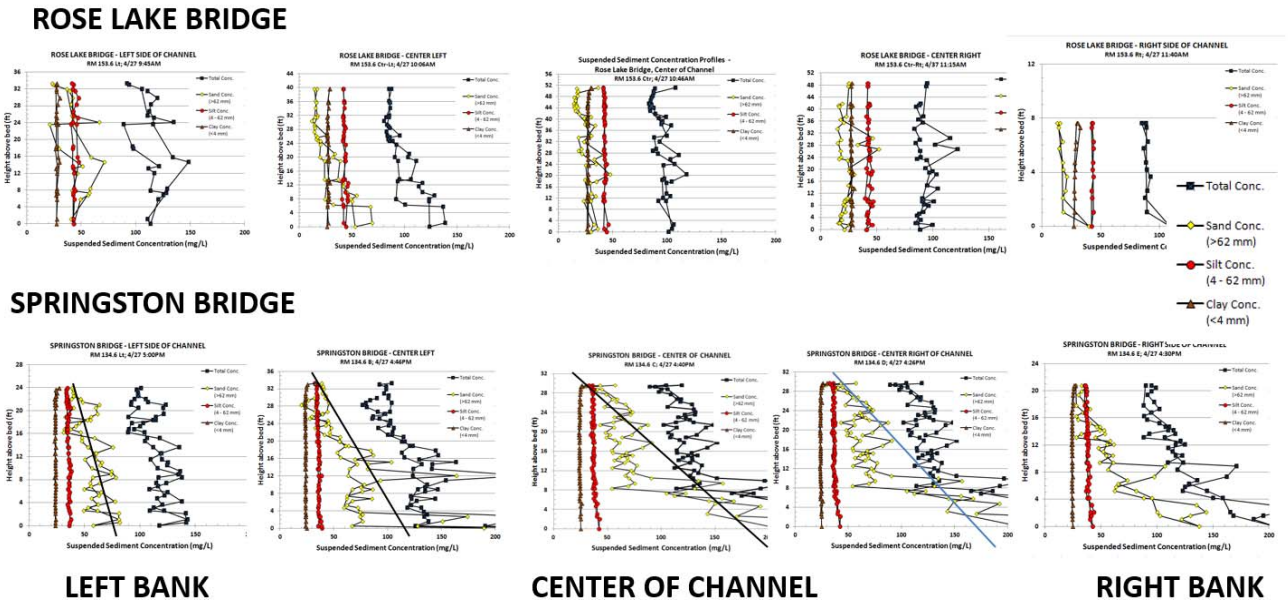

Exhibit B8. LISST Transects Across Channel at Rose Lake and Springston Bridges (Locations of USGS Gages)

3.4 Vertical Sediment Profile in Killarney Tie Channel

On Day 3 of LISST sampling (April 28, 2012), one vertical sediment profile was measured in the tie channel connecting Killarney Lake to the main stem Coeur d'Alene River (Exhibit B9). The Killarney Lake tie channel is understood, based on modeling, to convey a significant portion of flow and its associated sediment load, into Killarney Lake during floods, especially during the rising limb. (The sampling was conducted during the falling limb of the April 2012 flood.) The following points summarize observations in the Killarney tie channel:

- Flow was continuing to enter Killarney Lake on Day 3, though river levels were dropping (this condition was determined by visual observation and measurements of water velocity using an Acoustic Doppler Current Profiler, not LISST).
- Sediment concentration and particle size distribution in the connecting channel were similar to most other LISST measurements in the Lower Basin on Day 3, which represents the waning stages of the flood event.
- Sand, silt, and clay, though relatively low in concentrations, were all relatively well mixed vertically in the tie channel at the time of sampling.
- Additional LISST measurements in tie channels could be very useful. Future measurements may include comparative rising limb-falling limb samples to compare with in-channel profiles and to assess sediment flux into and out of off-channel water bodies.

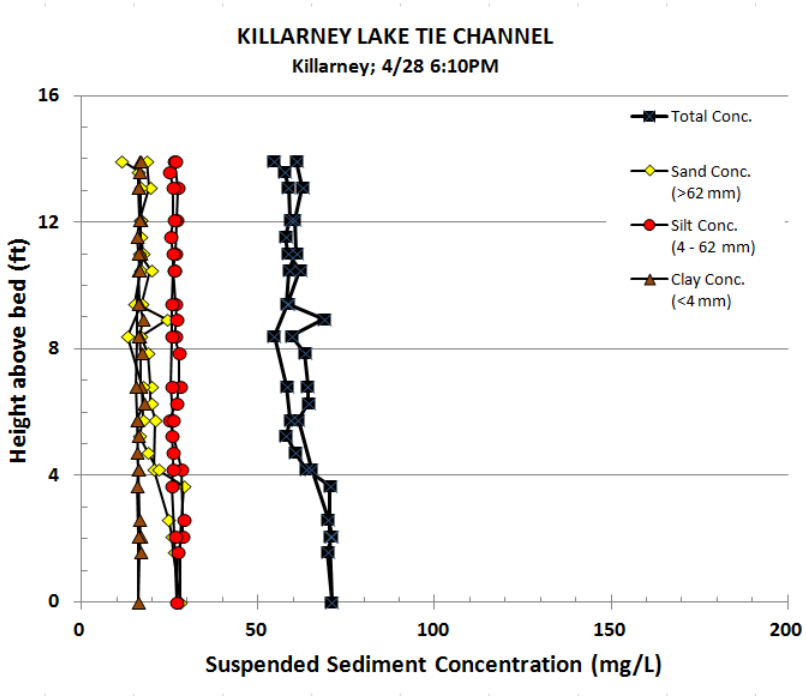

Exhibit B9. Vertical Sediment Concentration Profiles in Killarney Tie Channel as Measured by LISST in the Falling Limb of April 2012 Flood

3.5 Changes over Time During the Falling Limb

Exhibit B10 compares the vertical profiles of SSC and grain size between Day 1 and Day 3 of sampling at three locations in the Lower Basin. The following points summarize the interpretation of the data in Exhibit B10:

- Data suggest a reduction in the upstream sediment supply between Day 1 and Day 3 (see top panels showing the data from above the Cataldo Dredge Pool, RM 160.8); at this location total concentration dropped by about one third from > 100 ppm (Day 1) to ~ 70 ppm (Day 3).
- Vertical stratification in sediment concentration (notably sand) appears to be less on Day 3 than on Day 1, indicating a reduction in sand mobilization on Day 3.
- More sand was in the water column at the head of Strobl Marsh (RM 148.3) on Day 1 than Day 3. Sand higher in the water column is more likely to enter the floodplain where flow overtops the bank (at this locality, into the Strobl-Killarney complex).
- There is a “hysteresis” pattern on the Day 1 Strobl cast (bottom left panel), with higher sand concentrations on the lowering cast than on the raising cast. This may be attributable to temporary or localized turbulence; the river is sinuous in this reach with complex bed features, which may be creating more turbulent flow.

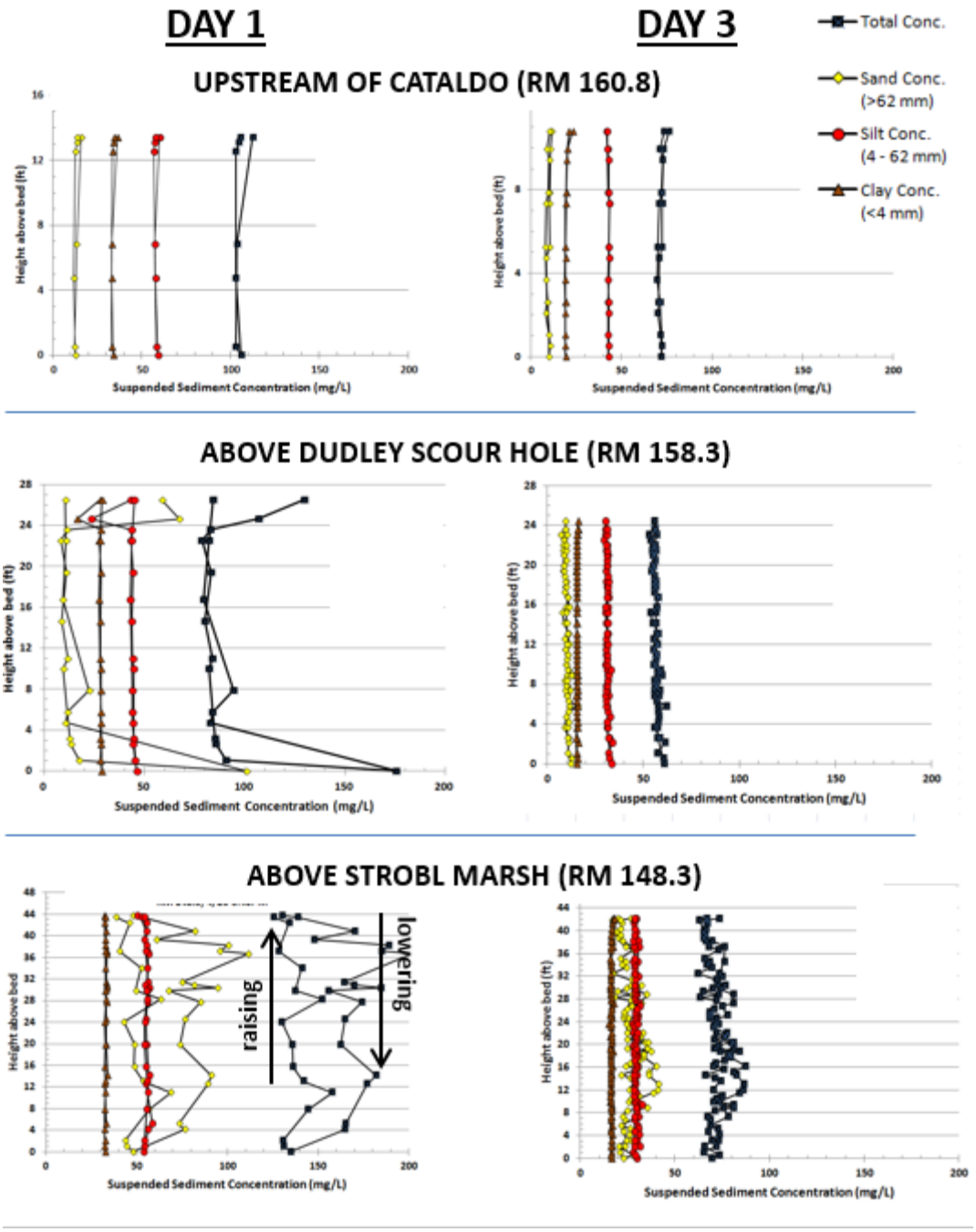

Exhibit B10. Comparison of LISST-Measured Sediment Concentration Profiles at Selected Locations on Two Different Days

3.6 Downstream Patterns in Sediment Transport from LISST Data

Exhibits B11 and B12 show longitudinal, rather than vertical, profiles in lead and sand concentrations measured with LISST. In those plots, each data point represents the depth-averaged concentration of the casts measured at each location.

3.6.1 Downstream Pattern in SSC and Sand

The following points summarize information about downstream trends in SSC and sand shown in Exhibit B11:

- Longitudinal patterns of SSC (top panel) and sand content (bottom panel) in the downstream direction compare closely, indicating that SSC patterns are largely driven by differences in local mobilization of sand, which in turn is driven by local hydraulics.
- Sand content follows distinctive longitudinal patterns that may provide clues to local hydraulics. For example, a dip in SSC and sand concentration around RM 148 at Strobl Marsh (April 28) may reflect flow exiting channel and a resulting decrease in the ability of the flow to suspend sand.
- An apparent step increase in SSC and sand at RM 157 (April 26) may pinpoint a location where sand was being mobilized from the bed.
- The step increase in SSC and sand at Harrison (RM 135 on April 28) may similarly reflect a threshold increase in shear stress sufficient to mobilize more sand. Modeling will help to further evaluate this hypothesis and allow predictions of where sand mobilization is likely to occur under different hydraulic conditions.

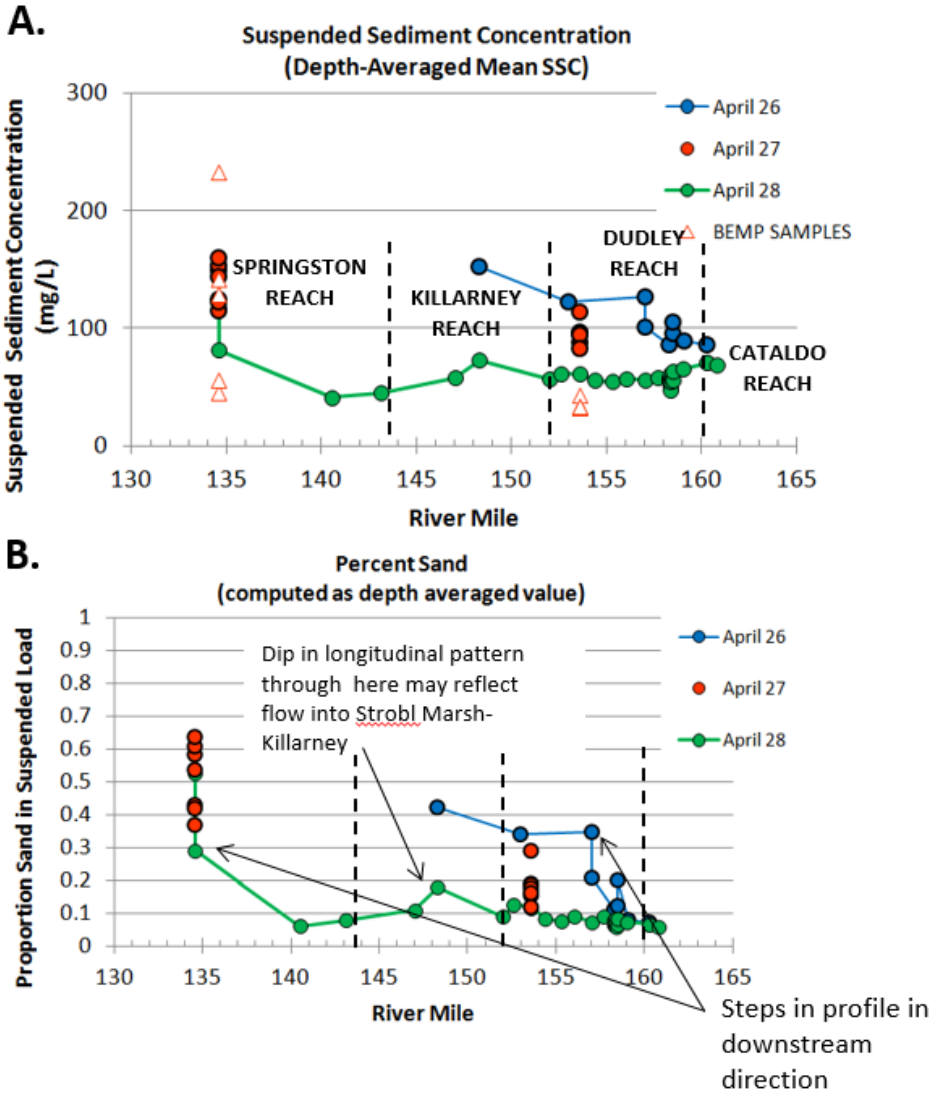

Exhibit B11. Downstream Patterns in the Depth-Averaged Suspended Sediment Concentration (A) and in the Percent Sand in Suspension (B) as Measured by LISST

3.6.2 Downstream Patterns in Grain Size Distribution

The following points summarize information about downstream trends in sand, silt, and clay concentrations shown in Exhibit B12:

- Both silt and clay concentrations were higher on Day 1 (April 26) sampling, at higher flows, compared with Day 3 (April 28).
- The concentration of silt in the flow on Day 3 shows a slight decrease in the downstream direction; this may reflect silt settling out in the Lower Basin. A slight decrease in silt is noted occurring near RM 148 at Strobl Marsh.
- Clay and silt concentrations remain relatively constant throughout the Lower Basin, but decrease over time during the 3 days of sampling. Because it occurs to a similar degree throughout the Lower Basin, the drop in silt and clay concentration is attributed to changes over time in the supply from upstream.
- Spatial variability in total SSC is most strongly influenced by the sand fraction and is assumed to be affected on two factors:
    1. Available sand supply locally (i.e., sand concentration will decrease in areas where less mobile sand is available).
    2. Local hydraulics (sand concentrations will increase locally where there is a spike in the ability of flow to suspend sand size particles).

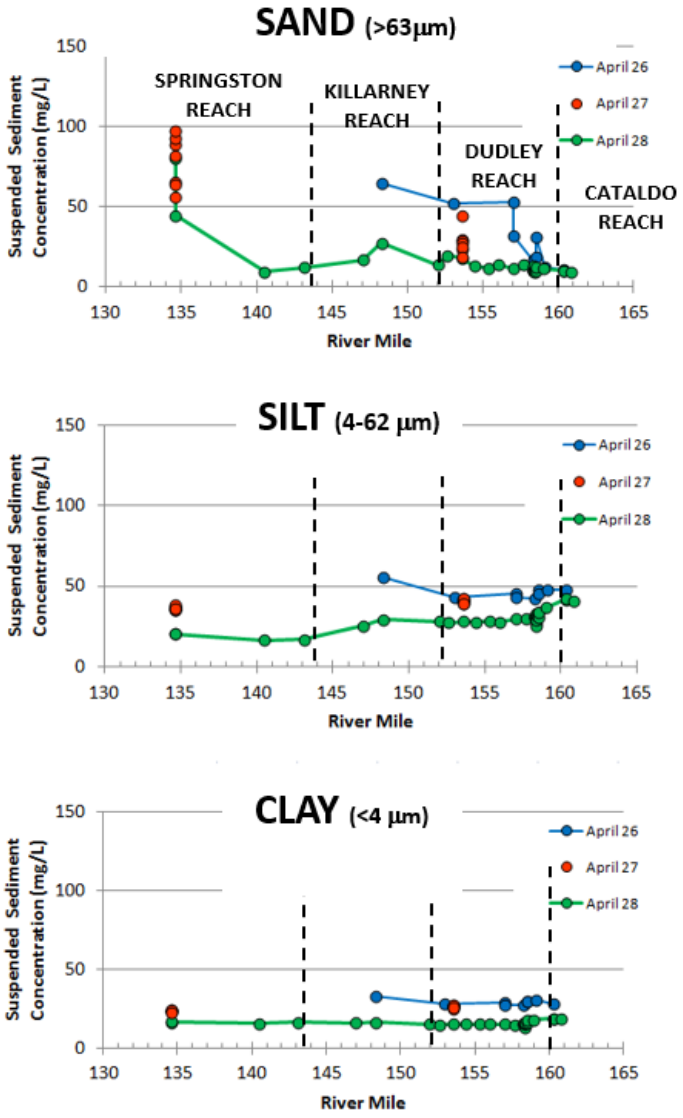

Exhibit B12. Downstream Profiles of the Depth-Averaged Concentrations of Sand, Silt, and Clay as Measured by LISST

3.7 LISST Verification Measurements

On Day 2 of LISST sampling (April 27), a verification study was conducted to better understand the accuracy and related characteristics of the LISST, relative to isokinetic sampling, on the Coeur d'Alene River. This section summarizes the set-up of the verification study and results of the comparison.

3.7.1 Verification Study Set-Up

- Verification was conducted by nearly simultaneously sampling with the LISST and a traditional depth-integrating isokinetic sampler (D-96) at two locations (Springston Bridge and Rose Lake Bridge). Exhibit B13 shows the bridge sampling crew from the vantage of the work boat.
- LISST and isokinetic casts were done near-simultaneously at Rose Lake Bridge. Samples were collected within 1 hour or less of each other at Springston Bridge.
- Five verticals were measured at each bridge using each method; a single lowering/raising cast was conducted for each vertical. SSC was measured for each vertical by each method, for a total of 10 comparisons (Exhibit B14).

- Unlike isokinetic sampling, the boat deploying the LISST was allowed to drift during casts (so that the LISST device would remain vertical in the current and sample the entire water column). Up to 100 feet of drift was noted during casts, both downstream and across-stream.

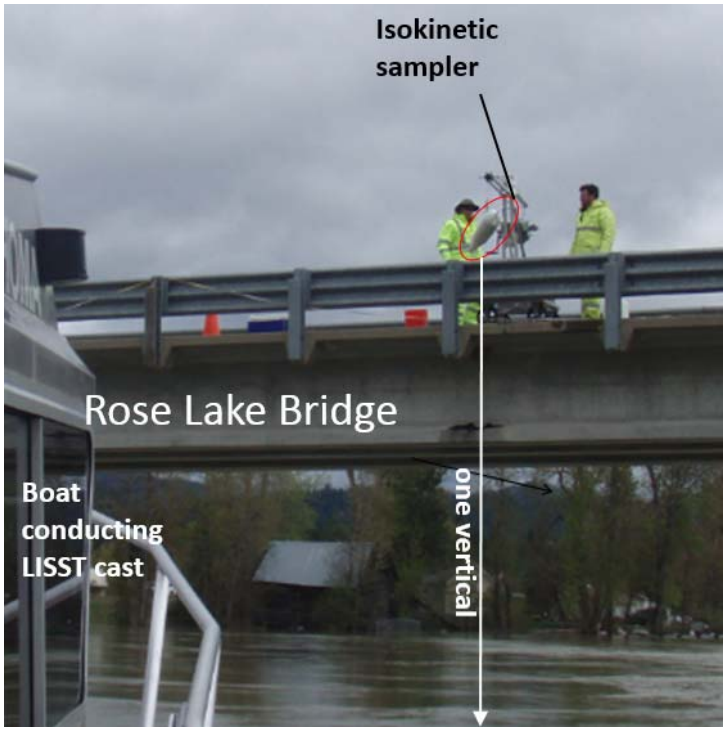

Exhibit B13. Photograph of LISST Verification Study: Concurrent LISST and Bridge Sampling at a Single Vertical at Rose Lake Bridge

3.7.2 LISST Verification Results

The following points summarize the comparison of LISST with isokinetic sampling shown in Exhibits B14 and B15:

- SSC estimates derived from LISST are within a factor of about 2 of isokinetic sampler (BEMP) data, and are generally higher.
- Therefore, LISST may overestimate the mass concentration of sediment in flow compared with the isokinetic samples. The discrepancies may be the result of multiple factors, including conversion algorithms, assumptions of particle density, methodology differences, and temporal and spatial variations of actual conditions during sampling measurements.
- Duplicate LISST casts (sequential casts at same location) show ~30 percent variability, both higher and lower relative to isokinetic (see open triangles), suggesting that temporal fluctuations in SSC occur over a time frame of seconds to minutes. (BEMP samples generally average over longer time periods.)
- The LISST measurements agree with BEMP sampling data in showing a relative increase in SSC from the Rose Lake Bridge to Springston Bridge (see bottom panel).
- Repeat LISST measurements at Springston Bridge suggest more variable agreement with isokinetic (both higher and lower).
- Boat drift of up to ~100 feet during LISST measurements (necessary to keep instrument vertical) may have affected spatial comparability with fixed-transit isokinetic samples.

- Small-scale temporal and spatial variability may affect absolute LISST and isokinetic samples, but relative changes appear to be consistent. More data are needed to better understand comparability.

COMPARISON OF LISST AND BEMP SAMPLING ON APRIL 27, 2012

(data are in mg/L)

		BEMP SSC	LISST SSC	LISST SSC duplicate
	Springston Bridge			
134.6	A	45	115	
134.6	B	56	125	149
134.6	C	129	154	
134.6	D	142	144	160
134.6	E	233	122	
	avg	**121**	**132**	
	Rose Lake Bridge			
153.6	A	32	114	
153.6	B	32	96	96
153.6	C	43	95	88
153.6	D	33	94	
153.6	E	33	83	
	avg	**35**	**97**	

Exhibit B14. Table Comparing BEMP (Isokinetic) and LISST Measurements of SSC at Five Verticals at Two Bridges

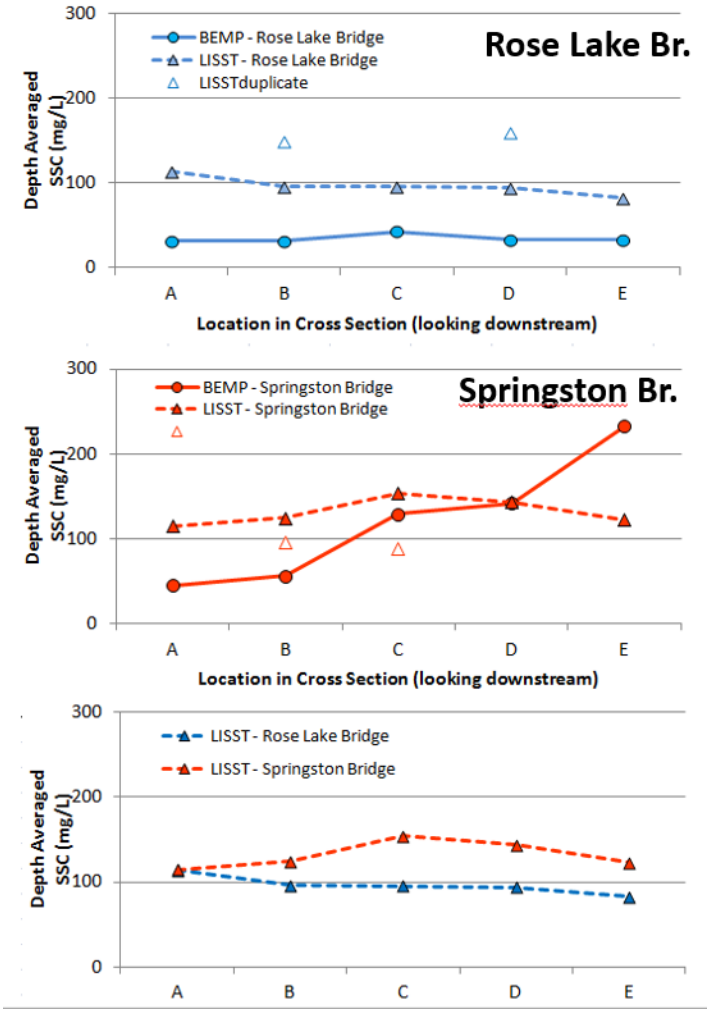

Exhibit B15. Graph Comparing BEMP (Isokinetic) and LISST Measurements of SSC at Five Verticals at Two Bridges

4.0 Interpretations and Conclusions

The following points summarize the preliminary interpretations and conclusions of the LISST deployment in the April 2012 flood. These preliminary conclusions may be refined by subsequent LISST measurements during future flood events.

- Absolute values of in-channel SSC obtained by LISST appear to be within a factor of about 2 of the isokinetic values, and may be closer.
- Relative distribution (vertical and lateral) of sediment, by size class, appears to be accurately represented by LISST casting data.
- Silt and clay size classes are vertically well-mixed in the channel and exhibit little variability through the Lower Basin. They appear to be transported as wash load during flood conditions and have limited interaction with the bed.
- Transport rates for silt and clay on the falling limb of this flood sampling event are interpreted to have been largely controlled by the change in supply from the Upper Basin, and change over a time scale of days. If the sampling had also captured the hydrograph rising limb and peak flow, it is possible that spatial differences in erosion of fines from the bed might have been observed.

- Spatial variability in SSC in this data set is primarily attributed to variability in sand transport. Sand transport is in turn determined by (1) local hydraulics and (2) the available sand supply from the bed.
- The timing and location of vertical sand mixing may be key to determining mobility patterns of contaminants during floods. Where sand is mixed high in the flow during flooding, contaminated bed material may be more likely to be transported into the floodplain; where sand is more stratified in the flow, contaminated sediment will be more confined within the channel.
- LISST data validate isokinetic results showing higher sediment transport rates at the Springston Bridge location. These phenomena may be localized in the area near the Springston Bridge.
- Additional LISST casting during future flooding events will be beneficial for understanding sediment and contaminant dynamics.

5.0 References

CH2M HILL. 2010. *Enhanced Conceptual Site Model for the Lower Basin of the Coeur d'Alene River*. Technical Memorandum Series. Prepared for U.S. Environmental Protection Agency. August.

CH2M HILL. 2016. *Processes of Sediment and Lead Transport, Erosion, and Deposition. Lower Basin of the Coeur d'Alene River (OU3)*. *Technical Memorandum Addendum D-3*. Prepared for U.S. Environmental Protection Agency. February.

Springston Reach

Killarney Reach

Dudley Reach

Cataldo Reach

Dudley Scour Hole

Casting LISST Deployment and Van Dorn Sampling at Dudley Scour Hole during Rising and Falling Limb

0 65 130 260 Feet

LOWER BASIN OF THE COEUR D'ALENE RIVER

LEGEND

- Anchored LISST deployment during the duration of the peak flow event
- Approximate casting LISST deployment location during rising limb and falling limb
- LISST transect location and BEMP sampling stations during peak flow
- Van Dorn sample collection locations during rising and falling limb
- Van Dorn transect locations and BEMP sampling stations during peak flow (5 points on transect)
- Bathymetric Survey Location
- River Mile Marker
- City
- Trail of the Coeur d'Alenes
- Interstate Highway
- Waterbody
- Marsh or Slough

N

0 1 2 4 Miles

EXHIBIT B1
Lower Basin Focused Suspended Sediment Investigation
Lower Basin of the Coeur d'Alene River

ch2m

\\ROSA\PROJ\USEPA\333911\GIS\MAPFILES\2012\BEMP\BASINWIDESUSPENDEDSED_NOMARSHES.MXD GGEE 4/6/2012 7:28:44 AM

Attachment C
Revised Estimates of Sediment Transport at Harrison Using a Multiple Regression Rating Curve Approach

EPA Contract No. EP-W-06-021
Task Order 85

Revised Estimates of Sediment Transport at Harrison Using a Multiple Regression Rating Curve Approach

Lower Basin of the Coeur d'Alene River (OU3)

PREPARED FOR: U.S. Environmental Protection Agency, Region 10

PREPARED BY: CH2M

DATE: February 17, 2016

1.0 Introduction and Scope

This Attachment C supplements *Technical Memorandum (TM) Addendum D-3: Processes of Sediment and Lead Transport, Erosion, and Deposition (*CH2M HILL, 2016), and was produced after completion of the addendum.

In computing the sediment and lead fluxes for the period 1987 to 2013, TM Addendum D-3 (the addendum) estimates the suspended sediment concentration (SSC, in mg/L) at each stream gaging station as a power function of discharge (in cfs) based on the data shown in Exhibit 4. The station-specific SSC rating curves were applied to the measured hydrographs at the four gaging stations in the Lower Basin—Enaville (on the North Fork Coeur d'Alene River), Pinehurst (South Fork), Cataldo, and Harrison (mainstem)—to estimate the historic 25-year sediment flux for each station. This is a standard approach for predicting longer-term suspended sediment fluxes in rivers using empirical data, recognizing that the rating curve approach incorporates significant levels of inherent and largely unavoidable uncertainty.[1]

The analyses and data presented in Section 3 of the addendum, and especially addendum Exhibits 9 through 11, suggest that sediment transport rates at the Harrison gage, at the downstream end of the Coeur d'Alene River, are strongly affected by fluctuations in the elevation of Coeur d'Alene Lake. Following the completion of TM Addendum D-3, CH2M HILL conducted an additional analysis of sediment and lead fluxes at Harrison to evaluate the influence of lake level on sediment transport. This revised analysis uses a multiple regression rating curve, which predicts the SSC using both discharge and lake level as independent variables.

The revised multiple regression approach reduces the residuals between predicted and observed sediment transport rate, and is based on physical processes as suggested by data and basic hydraulics. The revised estimates of the sediment and lead fluxes in this attachment are therefore considered more representative than those shown in the body of the addendum, and the exhibits cited in Sections 3 and 4 of the addendum.

[1] A detailed sensitivity analysis was performed to try to quantify this uncertainty. See Section 3.6.5 of the main report.

2.0 Background

In Exhibit 4 of the addendum, a single-variate power-law regression was empirically fit to paired measurements of discharge and SSC to predict SSC as a function of discharge at the USGS gage near Harrison (Gage 12413860). As explained in addendum Section 3, data collected when discharge was below 3,000 cubic feet per second (cfs) were excluded from the development of the regression because (1) at flows less than 3,000 cfs, there is no statistical relationship between SSC and discharge (addendum Exhibit 4) and (2) including paired measurements of discharge and SSC at low flows, for which there are many measurements, ends up skewing the regression equation to better-fit low discharges and under-predict SSC at higher discharges when nearly all the sediment is transported. A best fit power-law regression was fit to the data for each station and then used to estimate annual fluxes of sediment at each of the gages (addendum Exhibit 17). A sensitivity analysis (addendum Section 3.6.5) examined the influence of the choice of threshold discharges, power-law regression exponents, and the form of regression equation on the annual sediment fluxes and deficits. The sensitivity analysis concluded that the sediment deficit between Cataldo and Harrison, on the order of tens of thousands of metric tons per year, is probably real, and is unlikely to be the result of statistical uncertainty in rating curves.

Although the R^2 value of 0.78 for the regression at Harrison was quite high for the power-law regression (addendum Exhibit 4), there is still a large amount of scatter in the calculated error residuals (addendum Exhibit 6). Data analyses presented in the addendum (Section 3.4) also showed that other factors besides discharge also contribute to the variability of SSC at each station and, at Harrison, the lake level is likely to explain much of the additional scatter not explained by the regression equation. At Harrison, the relationship between discharge and stream power or shear stress (both are frequently used as variables to describe the forces driving sediment transport) is complicated by backwater of Coeur d'Alene Lake: at low lake levels, the water surface slope, shear stress, and stream power are all higher compared with similar discharges that occur when the lake is lower. To account for the impact of Coeur d'Alene Lake on sediment transport capacity at Harrison, a bi-variate regression to estimate SSC as a function of discharge (*Q*) and stage (*H*) was evaluated.

3.0 Methodology

In the analyses, the discharge (*Q*) used in the regression was the instantaneous discharge measurement at the Harrison gage, and the stage variable (*H*) was the daily (midnight) water level on the day of sampling at of Coeur d'Alene Lake at the USGS water level gage at the City of Coeur d'Alene (USGS gage 12415500)[2]. Recorded water surface elevations at that gage are recorded once per day at midnight. For example, today's measurement would be recorded at midnight tonight. Because of the distance between Coeur d'Alene and Harrison (about 20 miles), and the possible lag time between changes in stage at the two gages, the preceding day's measurement was considered to better represent lake levels at the time of measurement than the gage reading at midnight on the day of sampling.

Microsoft Excel 2013 was used to develop the bi-variate regression to estimate SSC as a function of discharge and stage. While several analysis techniques were considered, the adopted approach utilized the "LINEST" function which is a curve-fitting routine that employs a least squares analysis to fit a regression of the form:

$$y = m_1x_1 + \ldots m_{n-1}x_{n-1} + m_nx_n + b$$

[2] It would have been preferable to use the gage height at the Harrison gage as a dependent variable rather than the stage at Coeur d'Alene Lake gage at the City of Coeur d'Alene, more than 20 miles away (measured along the lake). However, the record at Harrison was not sufficiently long to be used in the sediment budget reported here (1987–2012): stage measurements at Harrison began in 1991, whereas at Coeur d'Alene, lake elevation measurements go back to 1903.

Regressions were fit to several combinations of paired measurements of SSC, discharge, water surface elevation, and gage height. Consistent with the single-variate regression developed as part of the addendum, paired measurements for which the instantaneous discharge was less than 3,000 cfs were excluded from the development of the bi-variate regression.

The SSC data used as the dependent variable in the regression included the same depth- and width-integrated measurements of SSC used in the addendum (e.g., Exhibit 4); these data were collected as part of the Coeur d'Alene River Basin Environmental Monitoring Plan (BEMP) and National Water Information System (NWIS) sources, as detailed in Section 3.1 of the addendum. Both "normal" and log-transformed values of the two independent variables (*Q* and *H*) were considered in the development of the multi-variate regression. The resulting bi-variate regressions were evaluated based on (1) goodness-of-fit, as determined from calculated R^2 values, and (2) statistical significance at the 99 percent confidence level, as determined by the statistical "F-test."

4.0 Results

4.1 Regression Evaluation

The bi-variate regression (which has been transformed from log-space to normal-space) recommended for further consideration is provided below:

$$SSC = 0.015 \cdot Q^{3.07} \cdot H^{-6.13}$$

where:

SSC = suspended sediment concentration in mg/L

Q = instantaneous discharge at Harrison, in cfs

H = gage height of Coeur d'Alene Lake for the preceding day, as measured by USGS Gage 12415500, in feet

A statistical F-test of overall significance was performed to assess the statistical significance of the bi-variate regression. The calculated F-statistic for the bi-variate regression is 135, which is greater than the critical F-statistic of 99 for a significance level of 1 percent. Therefore, the developed bi-variate regression was found to be statistically significant with a confidence of 99 percent.

The calculated R2 value of the bi-variate regression model is 0.85, which is comparable to, and slightly better than, the R2 value of the single-variate power-law regression model (0.78). Visual observation of the error residuals in relation to discharge and SSC (Exhibit C1) confirm that the absolute error of the bi-variate regression is generally less than that of the single-variate regression, especially at higher discharges. The plot of residuals against SSC (Exhibit C1B) highlights the tendency of both equations to significantly under-predict the two points with the highest SSC, with measured values greater than 600 milligrams per liter (mg/L). The regression residuals of the univariate regression for these two samples are close to 400 mg/L and close to 300 mg/L for the bi-variate regression. Those two data points were collected close in time in the same flood event in January 2011 by the two different sampling programs (BEMP and USGS), and measured unusually high SSC compared with other SSC samples. One likely cause of the anomalously high SSC in those samples is that lower lake level during the flood led to higher-than-usual shear stresses, which contributed to more erosion of the riverbed in the lower part of the river, and higher SSC in those events. As seen in Exhibit C1, the bi-variate regression still under-predicts these two samples, though not as much as the univariate regression equation.

Exhibit C1. **Comparison of Residuals for Single-Variate Regression and Bi-Variate Regression at Harrison**[1]

Processes of Sediment and Lead Transport, Erosion, and Deposition
Lower Basin Coeur d'Alene River (OU3)

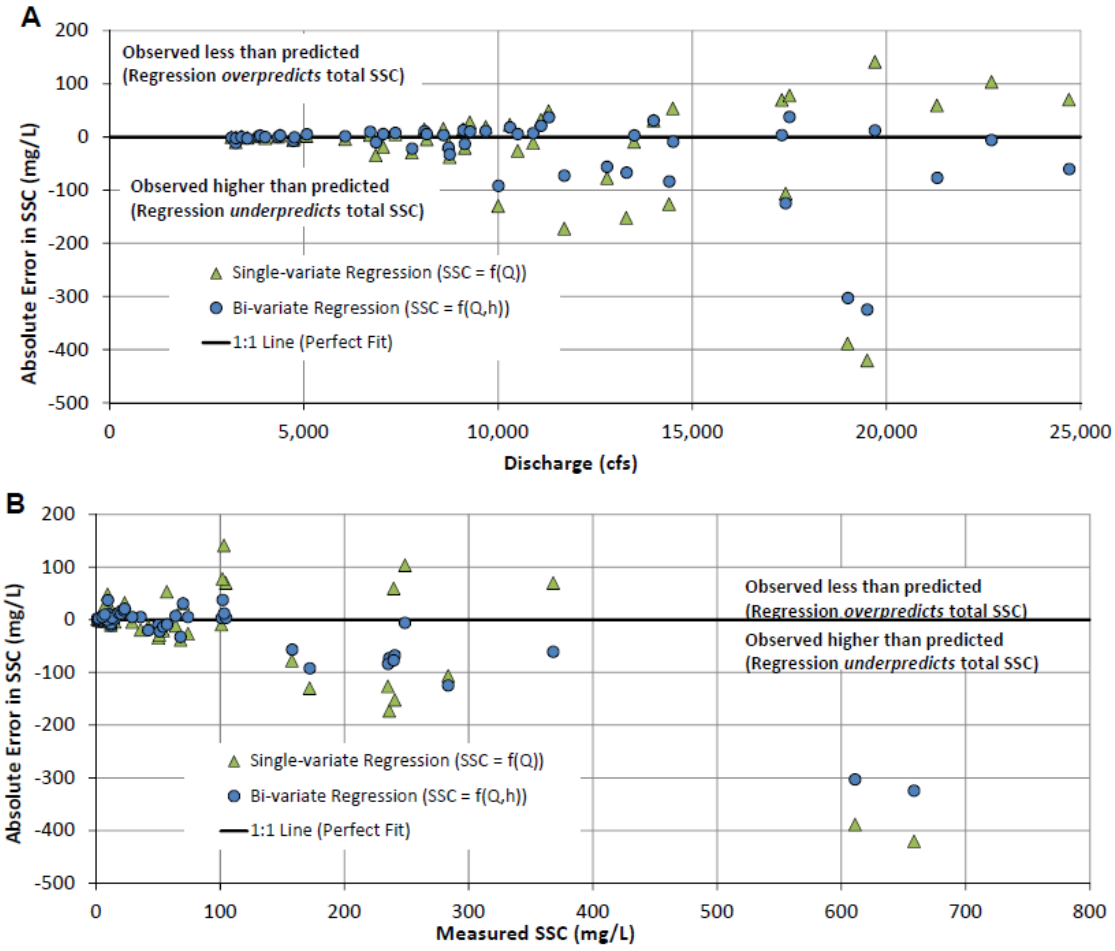

Note
1. Both regressions take the form of power law equations.

4.2 Computed Annual Sediment Fluxes

Computed annual sediment fluxes and annual sediment deficits between Harrison and Cataldo are tabulated by water year (WY) in Exhibit C2, and Exhibit C3 compares the fluxes computed using the bi-variate regression with values computed with the univariate regression equation. Annual sediment fluxes and sediment deficits calculated via both regressions are higher in years in which greater peak discharges occurred. In most years, the difference in the magnitude of annual sediment flux is ± 20 percent. However, during years in which high sediment fluxes were estimated, the difference in annual sediment fluxes between the two regressions is greater. Because of the different predictions of the two models in higher flow years, the average annual sediment flux at Harrison computed using the bi-variate regression (49,000 metric tons per years [mt/yr]) is approximately 25 percent less than that computed using the single-variate regression (67,000 mt/yr).

Exhibit C2. **Computed Sediment and Lead Fluxes and Deficits, by Water Year, for Single-variate and Bi-variate Regressions**

Processes of Sediment and Lead Transport, Erosion and Deposition
Lower Basin Coeur d'Alene River (OU3)

Estimated Sediment Fluxes and Deficits

Water Year	Annual Sediment Flux (mTon/yr)			Annual Sediment Deficit[1] (mTon/yr)		Peak Flow at Harrison (cfs)
	Cataldo	Harrison (Single-variate)[2]	Harrison (Bi-variate)	Single-variate	Bi-variate	
1987	15,737	-	-	-	-	-
1988	16,329	18,471	18,058	-2,142	-1,730	11,948
1989	27,167	54,747	36,983	-27,580	-9,816	14,314
1990	38,640	53,906	50,951	-15,267	-12,311	16,750
1991	46,145	71,731	75,172	-25,585	-29,027	20,551
1992	3,473	2,614	3,223	859	250	5,543
1993	16,722	23,399	17,573	-6,677	-851	9,633
1994	4,302	4,464	5,525	-162	-1,223	7,977
1995	30,057	47,446	41,622	-17,389	-11,565	20,014
1996	119,822	213,181	145,129	-93,359	-25,307	34,322
1997	78,232	184,235	82,056	-106,003	-3,824	20,425
1998	10,551	10,341	11,054	210	-504	9,523
1999	31,926	45,009	38,079	-13,082	-6,153	12,656
2000	33,710	59,011	39,402	-25,301	-5,692	19,192
2001	4,122	3,687	3,011	435	1,111	7,547
2002	61,469	132,996	97,710	-71,527	-36,242	26,509
2003	16,171	16,887	19,568	-716	-3,396	11,872
2004	8,874	10,429	11,187	-1,555	-2,313	8,740
2005	12,163	13,303	17,790	-1,140	-5,627	11,600
2006	25,702	38,121	35,580	-12,419	-9,878	13,700
2007	22,460	41,250	40,042	-18,790	-17,582	14,900
2008	63,780	279,316	152,256	-215,536	-88,476	28,600
2009	20,796	41,605	43,084	-20,808	-22,288	13,800
2010	7,164	9,693	9,324	-2,529	-2,160	8,970
2011	67,249	154,172	122,285	-86,923	-55,037	19,074
2012	60,010	136,965	91,553	-76,955	-31,543	20,600
1988 to 2012 AVERAGE	**32,414**	**66,679**	**48,329**	**-33,598**	**-15,247**	

Estimated Lead Fluxes and Deficits

Water Year	Annual Lead Flux (mTon/yr)			Annual Lead Deficit[1] (mTon/yr)	
	Cataldo	Harrison (Single-variate)[2]	Harrison (Bi-variate)	Single-variate	Bi-variate
1988 to 2012 AVERAGE[3]	**34.2**	**248.5**	**180.1**	**-214.3**	**-146.0**

Notes

[1] Calculated as the annual sediment (or lead) flux at Cataldo minus the annual sediment (or lead) flux at Harrison. Negative values indicate net erosion.

[2] The slight difference between the values in this column and those in Addendum TM D-3 (CH2M HILL, 2016; Exhibits 17 and 38) are due to a rounding difference. The fluxes reported in the addendum (Exhibits 17 and 38) were computed after rounding the rating curve coefficients and exponents to two significant figures prior to computing long term fluxes, whereas the rating curve values for the calculation in this exhibit were not rounded.

[3] Average annual lead flux computed by multiplying Water Year 1988 to 2012 average annual sediment flux by average lead concentration (1,054 mg/kg at Cataldo; 3,727 mg/kg at Harrison - see Exhibit 30 of Addendum TM D-3 (CH2M HILL, 2016).

Exhibit C3. **Comparison of Annual Sediment Flux at Harrison Computed with Single- and Bi-variate Regression**

Processes of Sediment and Lead Transport, Erosion and Deposition
Lower Basin Coeur d'Alene River (OU3)

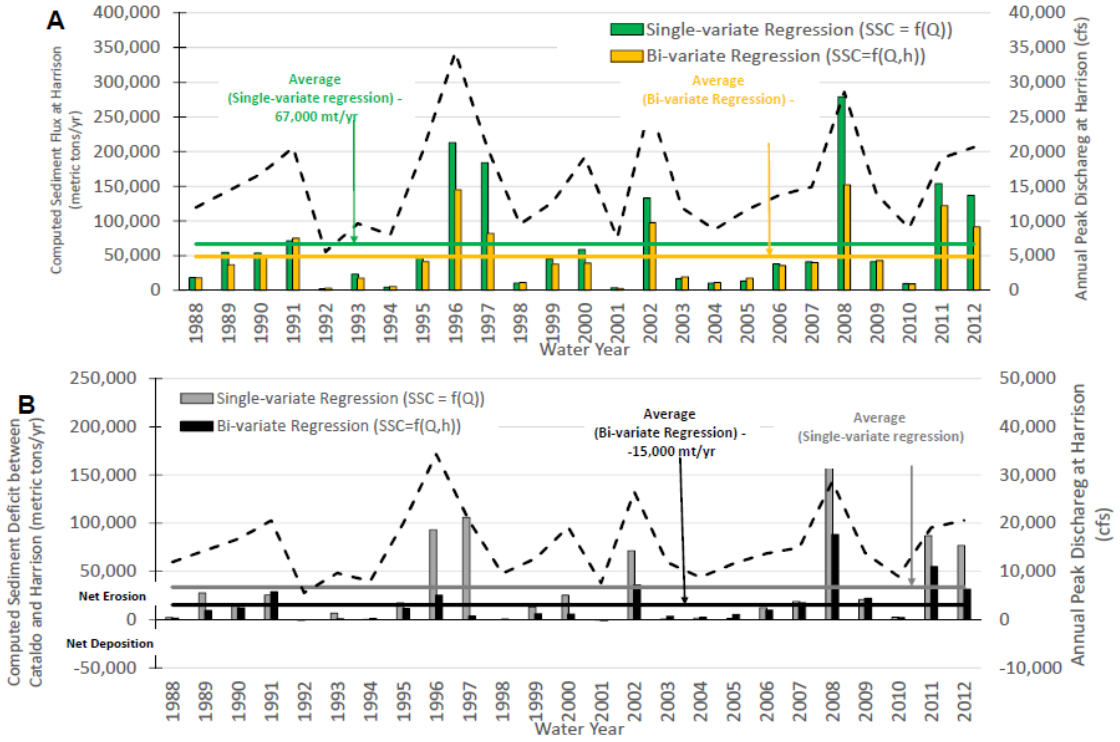

The average annual sediment flux at Harrison calculated via the bi-variate regression is approximately 50 percent greater than the average flux at Cataldo (computed using a univariate regression). By comparison, the difference was approximately 100 percent when the single-variable regression equation was used for both stations. Thus, ignoring for the time being sources and sinks of sediment other than the riverbed, the impact of using the bi-variate regression at Harrison is to reduce the estimated annual average sediment deficit by half: for the single-variate regression, the calculated average annual sediment deficit was 34,000 mt/yr; for the bi-variate regression, 16,000 mt/yr. Converting these sediment deficits to equivalent channel bed degradation rates by dividing by riverbed area, the revised estimate of the spatially averaged channel bed degradation rate is reduced from 1.05 cm/yr (computed using the single variable regression) to 0.48 cm/yr using the revised analysis (Exhibit C4). Cumulatively over the 25-year period analyzed, the total calculated sediment deficit and equivalent channel bed degradation (in parentheses) for the single-variate and bi-variate regressions are 840,000 mt (26 cm) and 380,000 mt (11.7 cm) (Exhibit C5). Thus, although the percent change in the estimated average annual sediment deficit is large, the direction and order of magnitude of channel change is the same.

Exhibit C4. **Sensitivity of Average Annual Sediment Flux to Single-variate and Bi-variate Regression**
Processes of Sediment and Lead Transport, Erosion and Deposition
Lower Basin Coeur d'Alene River (OU3)

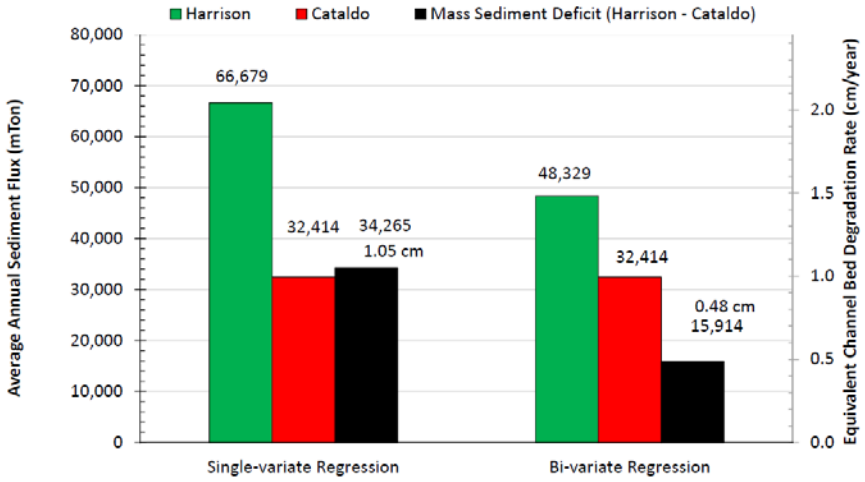

Exhibit C5. **Sensitivity of Cumulative Sediment Deficit between Harrison and Cataldo to Single-variate and Bi-variate Regression**
Processes of Sediment and Lead Transport, Erosion, and Deposition
Lower Basin Coeur d'Alene River (OU3)

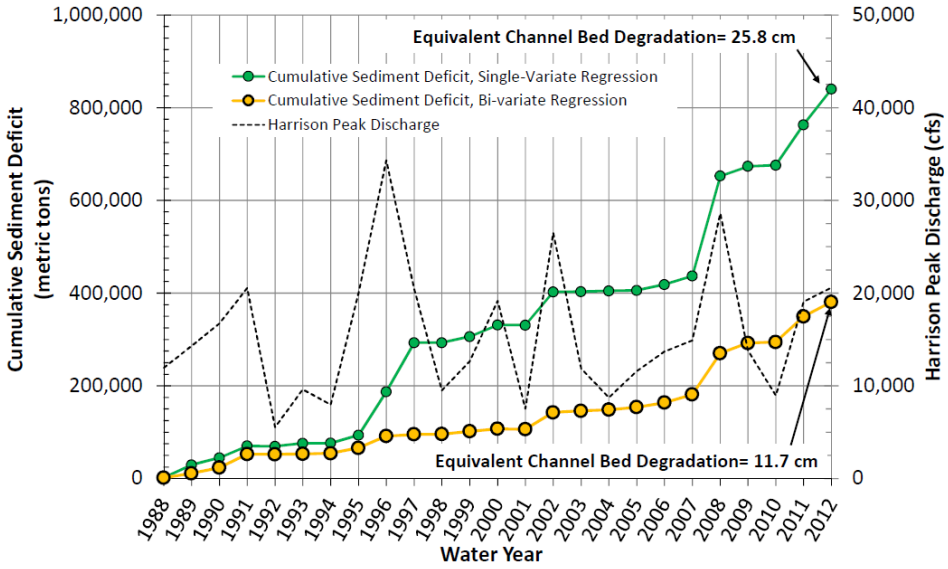

Finally, because the bi-variate regression equation at Harrison moderates the SSC in higher flows compared with the single variable regression used in the addendum, the revised analysis suggests a smaller year-by-year variability in the annual sediment deficit (Exhibit C5). The revised estimated annual sediment deficit between Harrison and Cataldo is, therefore, more consistent over time, and, therefore, the revised analysis suggests that the importance of high flows on net erosion of the riverbed is not as significant as implied in the original analysis of the addendum.

Attachment D
Review Comments from Prof. William Dietrich and Responses from CH2M

To: Kim Prestbo
Remedial Project Manager
Office of Environmental Cleanup
USEPA Region 10, Seattle

Date: May 25, 2016

From: William E. Dietrich
Peer Advisor
Berkeley, California

Re: Comments on Technical Memorandum Addendum D-3 (TM D-3), Processes of Sediment and Lead Transport, Erosion, and Deposition Lower Basin of the Coeur D'Alene River (OU3), dated February 17, 2016

At the request of Kim Prestbo, I am sending comments about the TM D-3. After reading the document I offered initial oral comments during a teleconference and this was followed up by direct discussions with Daniel Malmon of CH2M Hill, the primary author of the report.

The report is thorough and exhaustive in reporting data on sediment transport and implications for sediment sources, erosion and deposition. It is an impressive, useful document about which I have no fundamental disagreement. The absence, however, of an executive summary in the report, which would list primary conclusions, and state what we still don't know and what should be done to reduce the knowledge gaps, made the reading the report challenging. Sections 3.6.10 and 4.3.7 do provide useful summaries of sediment and lead transport analyses. I had to form my own opinion, however, on what were the main points of the report. Subsequent to the release of the TM D-3 document, and recently delivered to me, CH2M Hill provided an Executive Summary that highlights the main findings and comments on future potential work to fill data gaps. I generally agree with the summary of "what we know" and "knowledge gaps" discussion. The "recommendations" for addressing knowledge gaps offered by this summary, however, needs a discussion with EPA staff because the debate of costs and benefits needs to be placed in some context of an overall plan.

I wont offer a detailed review here of TM D-3 as I don't think that was the nature of the request "for comments", but rather focus on main issues for which there is both agreement and differences of interpretation.

The analysis presented in TM D-3 concludes that sediment flux at Harrison is significantly greater than that at Cataldo, which implies net scour of the river bed between the two reaches. There is a large increase in lead in the sediment discharged at Harrison. The data suggest to me that the greatest increase in lead occurs before Rose Lake. TM D-3 report argues that the when the lake level is low, significant lead entrainment may occur in the lower reaches as well. A strong case is made that the source of the lead entrainment and hence recontamination of incoming sediment is the legacy sediment from the mining period during which significant deposition occurred in the channel bed and adjacent floodplain. This puts a spotlight on mapping the pattern of

surface or near surface legacy sediment and on the thickness and contaminant evolution of the post-mining mobile sediment. An important question to ask: is there considerable exposed legacy sediment in the "Springston Reach"?

Our discussion of the report centered on two things: 1) the notion of an "active layer", 2) spatial extent on floodplain contamination and current rates of contaminated sediment across the floodplain. Most of the discussion focused on the "active layer". There was confusion because of the use of this term in sediment transport theory (as introduced by Hirano in 1970 and subsequently widely used in studies of transport and sorting) is different than that employed by CH2M Hill.

The "active layer" concept in sediment transport theory is introduced to recognize that when flows entrain sediment there is a finite distance below the surface where there is active exchange between the advecting sediment and the depositing and eroding sediment. Put succinctly by Parker (2008) in discussion of gravel transport theory involving just bedload transport, the active layer is "the bed layer that exchanges directly with the bed load" (Figure 1). The active layer can be thought of as a probability distribution function of bed elevations, a particularly useful way to think about it when applied to migrating dunes on a sandy (e.g. Blom et al 2008). There is considerable theory and observation to support this active layer concept. Suspended bed material participates in active layer exchange processes.

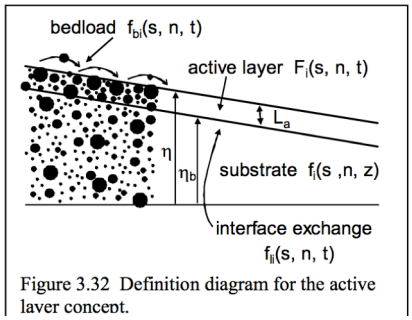

Figure 3.32 Definition diagram for the active layer concept.

Figure 1. Active layer concept. From Parker 2008

As used by CH2M Hill the term "active layer" was assigned to the sediment that has been reworked, introduced (from upstream), and mobilized and lies as a distinct blanket over the legacy sediment. The two figures below, taken from CH2M Hill reports illustrate their use of the term active layer.

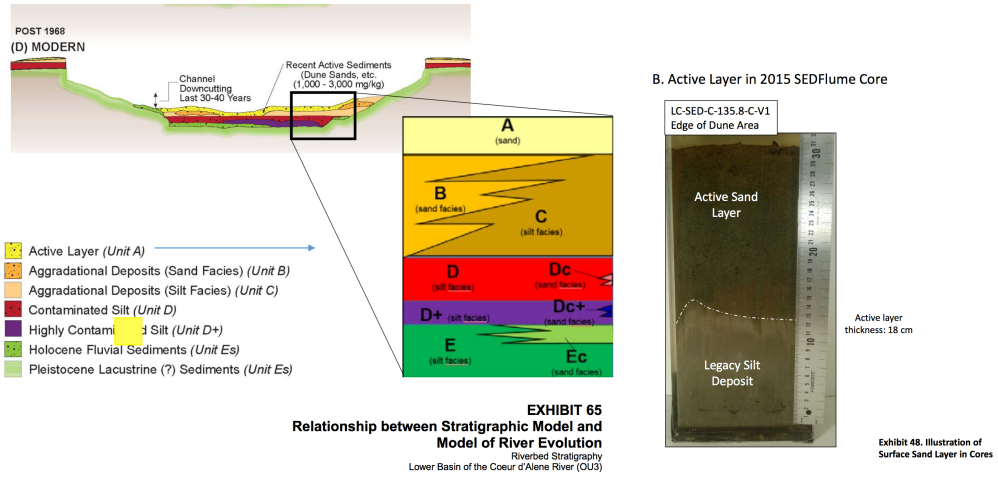

Figure 2. The conceptual cartoon of an "active layer" over mine legacy sediments and a photograph of a core sample.

I suggest that the term "active layer" be replaced for this project by another term in order to avoid confusion, especially to outside readers of reports with knowledge of sediment transport mechanics. One descriptive alternative term is "post-mining mobilized sediment layer". This albeit clumsy term is what the conceptual cartoon of the stratigraphy of the channel implies. Reducing the term to "mobile sediment layer" could be considered, but is less precise and could be confusing. Alternatives can be considered, but "active layer" should be reserved for its original, and quite useful, meaning and application. The implication is that the post-mining mobilized sediment will always be the surface layer if present. The challenge is how, in practice, to map it, i.e what criteria to use to distinguish it from legacy sediment. CH2M Hill proposes low silt

and clay content and lead less than 3000 ppm. The challenge is not to falsely classify by texture and lead content sediment as legacy when it is currently mobile and records currently elevated fines and lead. Is it the case that cohesive, relatively fine bedded and elevated sediment deposits are only legacy sediments? The recently distributed ECSM_TM_Addendum_E-6 will presumably address this issue directly, including what fines load is associated with cohesive behavior.

The post-mining mobilized sediment can vary in thickness from absent to perhaps meters thick, and, importantly it will have an active layer during periods of sediment transport. If the active layer descends through the post-mining layer into the legacy sediment then scour and entrainment may occur, even if on average there is a mantle of less contaminated post-mining sediment. The active layer grain size and lead concentration can be spatially and temporally dynamic and may differ from the underlying post-mining sediment, if that sediment is relatively thick.

This analysis leads to another discussion about the grain size and lead content of the bed material and specifically of the post-mining mobilized sediment. In TM D-3 it is stated several times that silt and clay is "wash load" and is not deposited in or "interact with" the sand bed (Pages 5, 14, 28, 43 and 46). This is a good practical approximation, but is not always correct in a way that matters here. At least three conditions can lead to fines (laden with lead in this case) entering a sand bed: 1) backwater effects, that occurs due to the lake, which reduce water surface slopes, cause deceleration of flows, reduction of boundary shear stresses, and net sediment settling to the bed. Sand bedded rivers have silt and even clay in their beds where backwater effects occur; 2) If sediment concentrations are sufficiently high, fine sediment can be incorporated into the active layer. This was observed on the Fly River in response to elevated fines from mining waste; and 3) Low flow sediment transport may drape less mobile sand beds with fine sediment.

The silt and clay content in the "river bed" increases in the downstream "Springston reach" where backwater effects operate. The possible influence of samples of legacy sediments in this analysis needs to be resolved if possible. How the active layer (as defined by sediment transport theory) is treated in the sediment transport model used here matters and should be discussed. It is through this layer that a contamination or decontamination (exchange with relatively clean sediment) occurs.

The second discussion issue regarding the TM D-3 report has been the spatial extent on floodplain contamination and current rates of contaminated sediment across the floodplain. I was not asked to comment on this topic, but it matters to conclusions drawn in the document. A reanalysis of the Bookstrom et al. (2004) by CH2M Hill was performed, with the conclusion that the modern floodplain deposition rate could be 7 or 8 times lower than that based on the coring results by Bookstrom. This matters greatly to understanding the overall sediment budget including whether the Harrison sediment flux is correct and how much channel bed scour is taking place. It also matters to what the persistent loading would be to floodplain environments and what recontamination potential might be when considering for floodplain restoration or protection measures. I did not attempt to review in detail the analysis of the floodplain sediment deposition rates presented in TM D-3 because it seems the problem is one of limited data such that a wide range of answers is possible. No systematic data have been collected to evaluate current

rates and patterns of elevated lead sedimentation on the floodplain since Bookstrom's report. I suggest that further discussion would be warranted on the value of reducing the large uncertainty in floodplain sedimentation rates.

As a final note, the comments above on the use and meaning of "active layer" and implications for interpreting bed material contamination will also be applicable to the recently released ECSM TM Addendum E-6 Riverbed Characterization by CH2M Hill.

References cited:

Blom, A., Ribberink, J., Parker., G. 2008. Vertical sorting and the morphodynamics of bedform-dominated rivers: A sorting evolution model. *Journal of Geophysical Research Earth Surface*, 113, F01019, doi:10.1029/2006JF000618, 19

Hirano, M. ,1970, On phenomena of river-bed lowering and armouring below reservoirs, paper presented at 14th Hydraulic Lecture Meeting, Civ. Eng. Assoc., Hydraul. Comm., Hatsumei Kaikan, 13 – 14 Feb.

Parker, G. 2008. Transport of Gravel and Sediment Mixtures, Chapter 3, *Sedimentation Engineering: Processes, Measurements, Modeling and Practice*, ASCE Manual of Practice 110, American Society of Civil Engineers, M. H. Garcia, ed., 165-252

EPA Contract No. EP-W-06-021
Task Order 85

Response to written comments from Professor Bill Dietrich on draft version of the report, TM D-3, Processes of Sediment and Lead Transport, Erosion, and Deposition

PREPARED FOR:	U.S. Environmental Protection Agency, Region 10
PREPARED BY:	CH2M
DATE:	July 1, 2016

As requested, this letter provides written responses to comments from Professor Bill Dietrich on the February 2016 draft version of Technical Memorandum Addendum D-3, Processes of Sediment and Lead Transport, Erosion and Deposition. As Professor Dietrich notes in his May 25, 2016 letter, his comments were not meant to be a detailed review of the report, but rather a summary of important conclusions, and related points of clarification, agreement, and differences of interpretation. The main points of his written comments are paraphrased below, followed by CH2M's responses to each of them:

1. **The lack of an Executive Summary stating the main conclusions and remaining data gaps made it difficult to review the report and identify the main points that were being made.**

Response: An Executive Summary was added to the final version of the report, focusing on two separate categories: Primary Findings, and Remaining Data Gaps.

2. **The review generally agrees with the primary conclusions of the technical memorandum with regard to the processes and rates of sediment and lead transfers, and the sources and sinks in the Lower Basin, to the extent that the available data are conclusive. Specifically, the reviewer agrees that the data show the most important lead source in the Lower Basin is erosion of legacy contaminated sediment presently stored in the riverbed.**

Response: No response needed.

3. **The review notes that the finding that the riverbed legacy sediments are the primary contaminant source spotlights the need to understand and map the patterns of surface and near-surface legacy sediment.**

Response: CH2M fully agrees, and because of this understanding, characterization of the riverbed geomorphology and stratigraphy has been a central focus of data collection and analysis on the project for the past several years. EPA has directed extensive sampling and observations of the riverbed composition and characteristics between 2011 and 2015 to fill many data gaps. Data collection was followed by a comprehensive summary and analysis of the relevant data collected from the 1990s through 2015, culminating in the definition of a formal lithostratigraphic model of the riverbed, and a three dimensional map of grain size and lead in the near-surface bed material. This work was submitted to EPA in draft form in April 2016 as Technical Memorandum E-6 (Riverbed Characterization), and is currently in review by EPA and the Peer Advisor group.

4. **The review notes that in previous conversations CH2M has used the term "active layer" to refer to something different from the active layer as used in the literature on sediment transport theory. The term "active layer" should be reserved for its more formal definition as the "bed layer that exchanges directly with the bed load" (Parker, 2008). In previous discussions, the term "active layer" was used to refer to the discontinuous mantle of sand-dominated, post-mining mobile sediments found at the bed surface. The review recommends replacing the term "active layer" with a different term to avoid confusion.**

Response: This suggestion will be implemented. There is only one instance of the term "active layer" in TM D-3 and this was revised as "mobile layer". The draft version of a separate report, TM E-6 (Riverbed Characterization), which discusses the feature in more detail, will also be revised to consistently use the term "mobile layer" or "post-mining mobile sediment layer" to refer to the deposits that have been mobilized since the cessation of mine waste discharges, as distinguished from the more consolidated and silt-rich "legacy" mining era deposits.

5. **The review includes a discussion of the post-mining mobile sediment layer (formerly called the "active layer"), pointing out that it varies in thickness, grain size, and lead concentration, and should be mapped using multiple criteria.**

Response: CH2M agrees with the way in which the mobile sediment layer is characterized in the review and the need for mapping it using multiple criteria. The understanding of this feature is discussed in detail in TM E-6 (Riverbed Characterization), in which the feature is mapped and characterized and the specific criteria for mapping are defined. That report includes a section showing the spatial variation of grain size, thickness, and lead concentrations in the mobile layer.

6. **The review notes that in TM D-3, silt and clay are categorized as wash load, implying that those size classes are not deposited in the sand bed. The review notes that is a good practical approximation but is not always correct because fine sediment can deposit in sand beds when certain conditions cause it, including: (1) backwater effects, (2) elevated fines concentrations in the flow, and (3) draping of fines over the sand bed during low flows.**

Response: For practical purposes, silt and clay are generally considered to behave primarily as wash load in this system under current conditions. Some fines may deposit in the mobile sediment layer during the falling limb of floods due to backwater effects (reason 1 noted above), but these fines are typically a relatively small component of the mobile layer (usually <10%), and of the modern day sediment budget. During the period of mine waste discharges, large quantities of contaminated silt and clay-sized sediment deposited in the bed due to reasons (2) and (3) above, and those legacy deposits are now the primary source of mobile lead in the system. Under present conditions, however, the conditions supporting reasons 2 and 3 do not exist – that is, sediment concentrations are not high enough, even at high flows, to create conditions that cause fines deposition in sand beds (the total SSC is typically between 100 and 500 mg/L, of which about half is fines); and as shown in Section 3 of the report, sediment transport during low flow periods is a minimal fraction of the total load. For the purpose of the current report, which focuses on quantification of sediment fluxes (rather than on the character of sediment in the bed), silt and clay are thus considered to behave dominantly as wash load, which is a useful concept for understanding sediment transfer processes addressed in the current report. The presence of silt and clay in the bed material is important, however, and this topic is evaluated in much more detail in TM E-6.

7. **The review points out that the most significant remaining data gap in understanding the sediment budget is a lack of sufficient field data to estimate the basin-wide floodplain sedimentation rate and its spatial distribution. This data gap bears on the estimate of the bed erosion rate (which is back-calculated from the other elements in the sediment**

budget) and relates to the potential for recontamination in floodplain areas. The review suggests further discussion on the value of reducing the uncertainty in floodplain sedimentation rates.

Response: CH2M and EPA recognize that the basin-wide floodplain sedimentation rate, and spatial patterns of deposition, are important remaining data gaps in this project. The new Executive Summary states this as a key remaining uncertainty. At present, floodplain sampling is being planned to help reduce uncertainty related to this data gap, and EPA has solicited input from Professor Dietrich on the initial proposed sampling plans.